Modules 1-5

Integrated Photonics

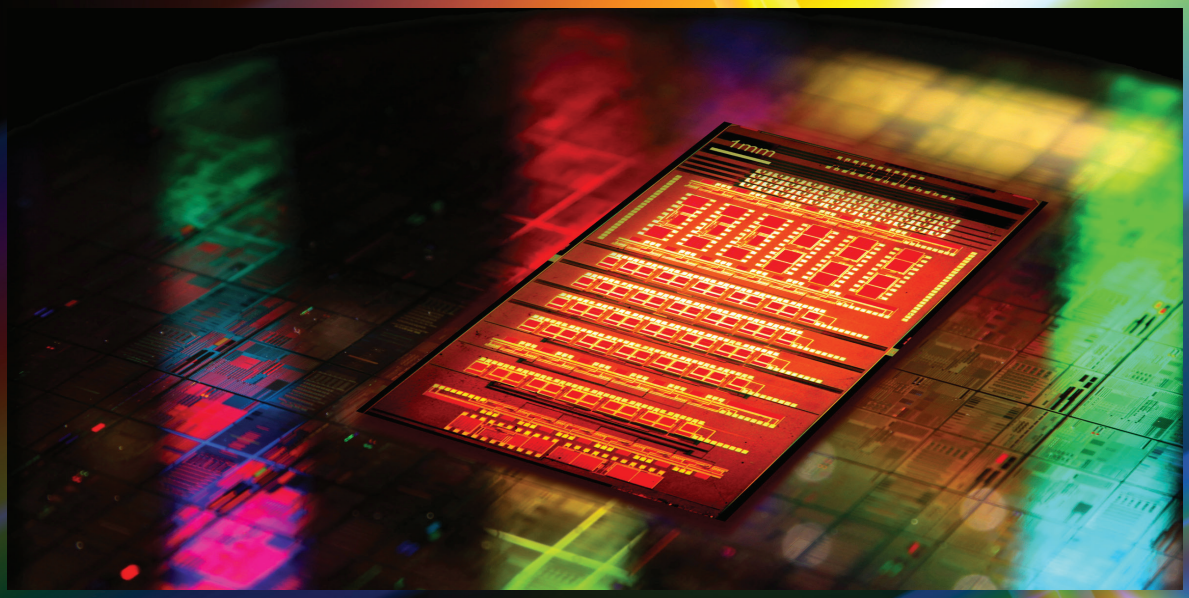

OP-TEC

Optics and Photonics Series

Integrated Photonics

OPTICS AND PHOTONICS SERIES

This text was developed by the National Center for Optics and Photonics Education (OP-TEC), University of Central Florida, under NSF ATE grant 1303732. Any opinions, findings, and conclusions or recommendations expressed in this material are those of the author(s) and do not necessarily reflect the views of the National Science Foundation.

Published and distributed by
OP-TEC
University of Central Florida
http://www.op-tec.org

ISBN 978-0-9858006-6-6

PREFACE

Silicon photonics (SiP) is an emerging field in opto-electronics. In silicon photonics, complementary metal-oxide semiconductor (CMOS) electronics foundries are used to manufacture optical chips, known as photonic integrated circuits *(PICS). Revolutionary new SiP systems are being developed for applications such as optical and wireless communications, bioenvironmental sensing, and computing. Silicon photonics is currently in the early stage of expansion, as electronics was in the 1970–80s, but with a major advantage for chip fabrication:* existing silicon foundries.

The rapidly emerging field of integrated photonics, sometimes called silicon photonics (SiP) requires engineering technicians who work in microchip or nanochip fabrication facilities and in materials R&D fabrication laboratories. These technicians need to understand not only the technology, hardware, and procedures of clean rooms and high-vacuum deposition, but also geometric and wave optics applications and diagnostic equipment, as well as vertical cavity, surface-emitting laser diodes (VCSELs) and nanofabrication equipment, procedures, and inspection techniques. Technicians currently working in chip fabrication facilities require additional education and training in the technologies that support SiP.

Integrated Photonics is a five-module course that provides an overview of the technology, device characteristics, fabrication techniques and equipment, and applications in high-speed computing, telecommunications, biomedicine, and other fields. The contents are:

Module 1. Photonic Integrated Circuits: Materials and Fabrication Technologies

Module 2. Silicon Photonic Integrated Circuits and Devices

Module 3. III-V and Compound Semiconductor Devices

Module 4. Dielectric and Polymer Waveguides and Waveguide Devices

Module 5. Integrated Photonic Circuits and Systems

Prerequisites for this course include knowledge of technical mathematics and solid-state materials, as well as *Fundamentals of Light and Lasers* (OP-TEC Course 1).

Sections in the back of the book after Module 5, contain a glossary of terms and an index.

OP-TEC would appreciate feedback and comments on your use of this material.

Acknowledgments

The author of these materials is Dr. Anca Sala, Dean of Engineering and Computer Technology at Baker College in Michigan. Dr. Sala is an experienced engineer in integrated photonics.

Daniel M. Hull, PI July 2016
OP-TEC

CONTENTS

Photonic Integrated Circuits

Materials and Fabrication Technologies

Module 1

of

Integrated Photonics

OPTICS AND PHOTONICS SERIES

This material was created under Grant # 1303732 from the Advanced Technological Education division of the National Science Foundation. Any opinions, findings, and conclusions or recommendations expressed in this material are those of the author(s) and do not necessarily reflect the views of the National Science Foundation.

For more information about the text or OP-TEC, contact:

Dan Hull
PI, Executive Director, OP-TEC
316 Kelly Drive
Waco, TX 76710
(254) 751-9000
hull@op-tec.org

Taylor Jeffrey
Curriculum Development Engineer
316 Kelly Drive
Waco, TX 76710
(254) 751-9000
tjeffrey@op-tec.org

Published and distributed by
OP-TEC
316 Kelly Drive
Waco, TX 76710
254-751-9000
http://www.op-tec.org/

ISBN 978-0-9903125-5-0

CONTENTS OF MODULE 1

Module 1
Photonic Integrated Circuits

INTRODUCTION

Photonics encompasses the science of light and the technology of using light to generate and control energy and to transmit and detect information. The quantum unit of light is the photon. It is expected that the twenty-first century will depend as much on photonics as the twentieth century depended on electronics. During the last century, tremendous technological advances were made possible by the invention of the electronic integrated circuit (EIC) and its further development.

The rapid pace of advance of EICs is captured by Moore's law, which states, "The number of transistors in an integrated circuit doubles every two years." This has held true for four decades, starting in the 1970s, and has resulted in the now ubiquitous and affordable personal computers, cell phones, tablets, and the myriad other consumer electronic products we are all using today. Figure 1-1 shows the growth in the number of transistors in a microprocessor chip between 1970 and 2010. Today it appears that the expansion predicted by Moore's law is starting to level off. Some limiting factors that come into play as the number of processors per chip increases are *power dissipation, packaging, and communication bottlenecks between chips*. At the same time, the younger field of integrated photonics is now poised for rapid growth and expansion, and it is expected that this field's growth will help sustain the pace of progress we have enjoyed so far. Using photonic integrated circuits (PIC), for example for communication between chip processors and from one chip to another, can mitigate the limitations above.

A photonic integrated circuit is a device that integrates multiple photonic functions, similar to an electronic integrated circuit. Another term that describes such devices is the optoelectronic integrated circuit (OEIC). For example, a photonic interconnection network can route information between the processor and memory chips in a computer. PICs offer many advantages: when replacing a system constructed from bulk or discrete optical components, they allow the system to be much more compact and efficient and to operate at higher speeds.

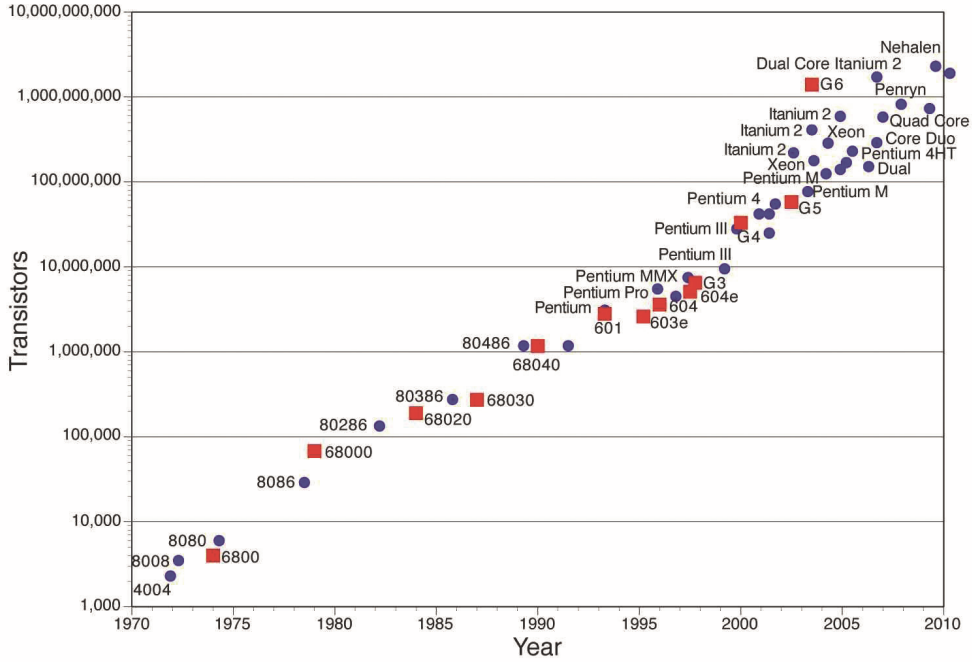

Figure 1-1 *Illustration of Moore's law, which predicts that the number of transistors in a microprocessor chip doubles every two year*

Electronic and photonic integrated circuits are not just analogous terms used to describe electronic vs. optical integrated devices. EICs and PICs are also related in other ways. They are in some cases made from the same materials and using similar fabrication processes. Being able to leverage the very mature technology of fabrication and advanced equipment from the semiconductor industry to produce PICs is very attractive. However, while the EICs today are predominantly made out of silicon and fabricated using the technology of the complementary metal-oxide semiconductor (CMOS), PICs are made from a variety of materials, depending on their functionality. This is due to the fact that no one material platform and technology is currently capable of producing all the required photonic components at high volume, low cost, and the desired level of performance. Certain materials are better suited for the fabrication of semiconductor lasers, others are best for photodetectors, and still others are appropriate for the variety of optical components used in telecommunications and photonic sensors.

The ultimate goal of integrated photonics is to combine together the optical sources, processing, and detection components in one circuit, leading to minimum cost and footprint and avoiding complicated assembly operations. Integrating all devices on the same platform is called *monolithic integration*. Moreover, photonic and electronic circuits could be integrated together in one circuit, resulting in the best performance and cost functionality. These technological advances will fuel the growth and integration of vast, low-power, reliable networks of connected devices that collect, process, communicate, and exchange data. Integrated optical and photonic systems will enable new and emerging networking technologies, sensors, high bandwidth connectivity, and processing and storage technologies. These technologies include athletic wearables with integrated sensors that collect, process, and communicate biometric information; medical devices that use integrated labs-on-chips without drawing blood, thus eliminating needles; and advanced automotive driver-assistance systems, including surrounding sensors, intelligent headlamps, optical car-to-car communications, and heads-up displays, along with

self-driving features. While this level of integration, information collection, processing, and communications does not exist today, groups of scientists and engineers around the world are working to create faster, more compact, and lower-cost components to bring these possibilities closer to reality.

PREREQUISITES

OP-TEC's *Fundamentals of Light and Lasers Course 1*

OBJECTIVES

Upon completion of this module, the student should be able to:

- Define *photonic integrated circuits* (PIC)
- Give examples of PIC and their applications
- Explain monolithic integration and its advantages
- Describe the principle of operation of optical waveguides
- Explain and calculate the refractive index contrast, numerical aperture, and maximum half-acceptance angle of an optical waveguide
- Define modes of optical waveguides
- Explain the electromagnetic field intensity distribution in the cross section of the waveguide
- Describe planar optical waveguides and their geometries
- Determine whether an optical fiber and a slab waveguide are single mode or multimode
- Describe basic characteristics of planar optical waveguides, including dimensions, bend radius, propagation loss, and thermo-optic effect
- Identify the main groups of materials used for PIC and their properties
- Describe the fabrication technologies used to make PIC
- Specify equipment used to fabricate PIC in a clean-room environment, such as deposition, photolithography and etching systems, and direct laser writing systems

SCENARIO

Antonio works as a *wafer fab equipment technician* with a company that designs and manufactures photonic integrated circuit devices. His duties are in maintenance, troubleshooting, upgrades, and installations of clean-room equipment. Antonio starts his day at his computer, where he reads the reports from the previous shift to see what tools are down and reviews charts and maintenance needs. After reviewing the equipment status, he puts on the clean-room *bunny suit* and enters the clean room. He works on equipment that needs maintenance, calibrates tools so they can be put back in production, and addresses urgent problems that show up. When a tool does not perform at the required level or stops working, Antonio gathers information from the process team to help him troubleshoot the problem. He discusses issues with engineers to help him decide if the equipment can be repaired with existing parts or if new parts must be ordered.

Throughout the day, Antonio communicates with other team members through e-mail, page, and text messages. He often needs to multitask and resolve multiple priority issues quickly and efficiently to improve the overall fab performance. He loves solving problems and working to improve the tools and process performance. As new equipment is added to the fab, there is always something new to learn. Antonio's job is challenging and rewarding, and he brings an important contribution to the success of his company.

BASIC CONCEPTS

What are Photonic Integrated Circuits?

A photonic integrated circuit (PIC) is a device that integrates multiple photonic functions to perform certain operations onto a light or optical signal. PICs operate in the visible and near-infrared regions of the electromagnetic spectrum (350–1650 nm). A wide variety of PICs have been developed and commercialized, and many others are in the research-and-development stage. An early example of a PIC is found in semiconductor lasers. Some of these lasers contain structures called distributed Bragg reflectors, which serve as high-quality reflectors for certain wavelengths and are examples of photonic integration. As shown in Figure 1-2, in these lasers the end mirrors have been integrated together with the active medium responsible for the gain of the laser.

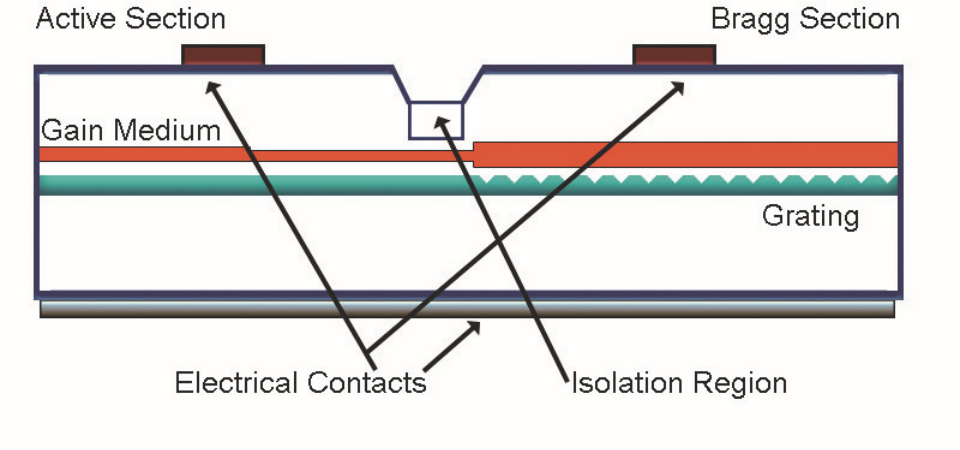

Figure 1-2 *Illustration of distributed Bragg reflector semiconductor laser. The active section and the grating sections serving as mirrors are integrated in the same structure.*

In the telecommunications field, a variety of PICs are used to process the optical signals carried by optical fibers, including devices such as couplers, switches, modulators, and filters. While couplers and switches distribute and route the optical signals from various input ports to various output ports, modulators operate on the phase and power level of the signal, and filters operate on the signal wavelengths. A PIC, which integrates optical sources with a circuit to route the optical signals to various outputs and with photodetectors to convert optical to electrical signals, is shown in Figure 1-3.

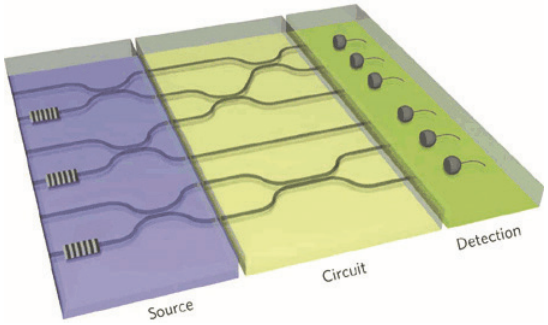

Figure 1-3 *PIC integrating optical sources, a routing circuit, and photodetectors*

PICs are expected to play a growing role in the further development of computers and data servers. They are capable of connecting electronic chips to one another at very high speeds, using low power. Other applications of PICs are in photonic sensors applied in biological and biomedical fields. PIC-based sensors, capable of optically measuring human blood-glucose levels without the need for a blood sample, have been demonstrated. Later modules will describe in detail photonic integrated circuits used in applications such as the ones mentioned above.

Optical Waveguides

The basic element of all PICs is the *optical waveguide*. An optical waveguide is a physical structure that guides and confines light waves. *Optical fibers* are a familiar type of optical waveguide that consist of a cylindrical core surrounded by a cladding. Because the core has a higher index of refraction than the cladding, total internal reflection (TIR) at the interface between core and cladding confines and guides the light traveling down the fiber.

There are two conditions that must be met for total internal reflection to occur. One condition is that the index of refraction of the medium in which the light beam is traveling (in this case, the core) must be greater than the index of refraction of the medium that the beam is moving toward (the cladding). The second condition is that the angle of incidence of the light beam at the interface between core and cladding must be greater than the *critical angle*, which is given by the following equation:

$$\phi_c = \sin^{-1}(n_{clad}/n_{core}) \qquad (1\text{-}1)$$

Where: n_{clad} is the index of refraction for the cladding material and

n_{core} is the index of refraction for the core material

The optical fiber, shown in Figure 1-4, consists of a central glass core of radius “a” surrounded by an outer cladding made of glass with a slightly lower refractive index. The corresponding refractive index distribution in the transverse direction is given by

$$n = n_{core} \text{ for } r < a \qquad (1\text{-}2)$$
$$n = n_{clad} \text{ for } r > a$$

which is known as a step-index distribution.

Figure 1-4 shows a light ray incident on the air-core left interface at an angle θ_i. The ray refracts at angle θ in accordance with Snell's law (the law of refraction) and then strikes the core-cladding interface at angle ϕ. In the drawing shown in Figure 1-4b, the angle ϕ is greater than the critical angle ϕ_c defined in Equation 1-1, thus leading to total internal reflection at *A*. The reflected ray is internally reflected again at *C* and *B* and so on, remaining trapped in the fiber as it propagates along the core axis.

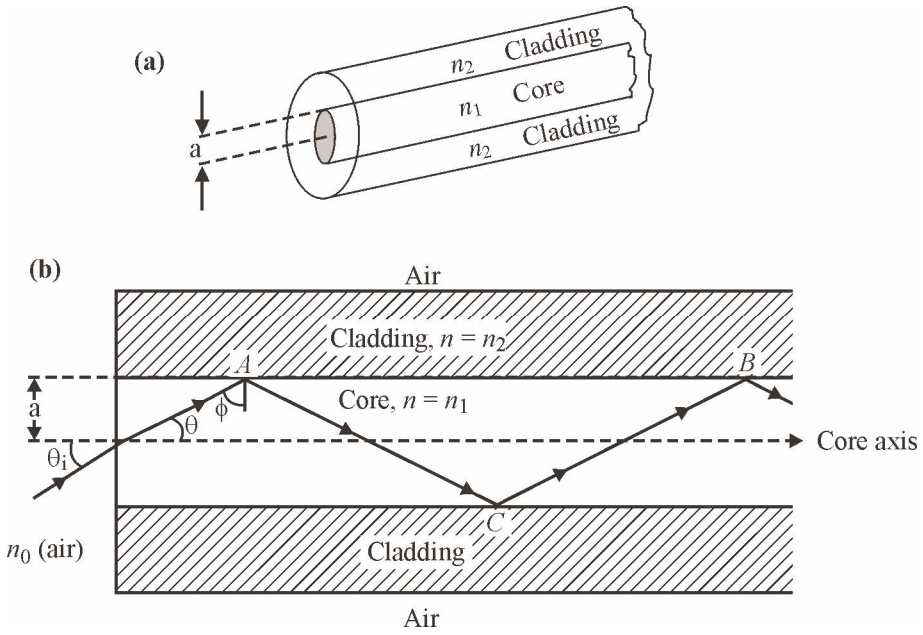

Figure 1-4 *Fiber Geometry*

Example 1

An optical fiber has a core index equal to 1.465 and a cladding index equal to 1.45. Calculate the critical angle for total internal reflection at the interface between core and cladding.

Solution: Using Equation 1-1 we obtain $\phi_c = \sin^{-1}(n_{clad}/n_{core}) = \sin^{-1}(1.45/1.465) = 81.8^o$.

In this case, light inside the waveguide must strike the core-cladding interface at angles greater than 81.8 º to remain confined to the waveguide core.

An important parameter for optical waveguides is the numerical aperture (NA). The numerical aperture of a waveguide is a measure of its *light-gathering ability* and is defined by

$$NA = \sin (\theta_a)_{max} \tag{1-3}$$

where $(\theta_a)_{max}$ is the maximum half-acceptance angle of the waveguide, as shown in Figure 1-5.

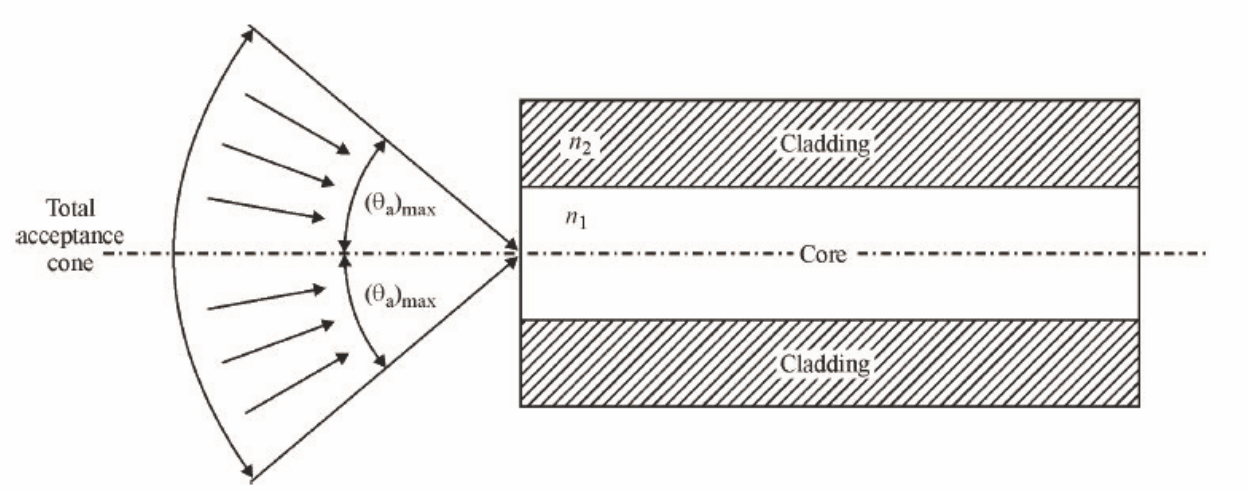

Figure 1-5 *Numerical aperture*

The larger the numerical aperture is, the greater the light-gathering ability of the fiber is. Typical values for NA are 0.1 to 0.2 for single-mode fiber. The numerical aperture is related to the index of refraction of the core and cladding by the following equation:

$$NA = \sin(\theta_a)_{max} = (n_{core}^2 - n_{clad}^2)^{1/2} \quad (1\text{-}4)$$

As can be seen, the larger the difference between the core and cladding indexes, the larger the numerical aperture.

The NA may also be expressed in terms of the *relative refractive index difference* (Δ), where

$$\Delta = (n_{core}^2 - n_{clad}^2)/(2\, n_{core}^2) \quad (1\text{-}5)$$

For the case of n_{core} nearly equal to n_{clad} the equation simplifies to

$$\Delta = (n_{core} - n_{clad})/n_{core} \quad (1\text{-}5a)$$

Combining Equation 1-5 with Equation 1-4, we get Equation 1-6.

$$\Delta = NA^2/(2\, n_{core}^2) \quad (1\text{-}6)$$

Another name for the relative refractive index difference is *refractive index contrast*. Combining Equations 1-4 and 1-6, we obtain a useful relation, Equation 1-7.

$$NA = \sin(\theta_a)_{max} = n_{core}\,(2\Delta)^{1/2} \quad (1\text{-}7)$$

Equation 1-7 shows that a large refractive index difference between core and cladding results in a large acceptance angle and large numerical aperture. Depending on the application for the optical fiber, values for the refractive index contrast are in the range from 0.003 to 0.03 (or 0.3% to 3%).

Example 2

Find the refractive index contrast, numerical aperture, and maximum half-acceptance angle for an optical fiber with core index equal to 1.465 and cladding index equal to 1.45.

Solution: Using Equation 1-5,

$\Delta = (n_{core}^2 - n_{clad}^2)/(2\, n_{core}^2) = (1.465^2 - 1.45^2)/(2 \times 1.465^2) = 0.01 = 1\%$

The numerical aperture is found using Equation 1-7:

$NA = n_{core}\,(2\Delta)^{1/2} = 1.465\,(2 \times 0.01)^{1/2} = 0.21$

The maximum half-acceptance angle can also be calculated from Equation 1-7:

$(\theta_a)_{max} = \sin^{-1}(NA) = 12.1°.$

Optical fibers are made of glass, which is silicon dioxide (also called silica). The cladding is usually pure silica, while the core is silica doped with germanium, which increases the refractive index slightly from n_{clad} to n_{core}.

Optical Waveguide Modes

Total internal reflection requires the angle under which the light beam strikes the core-cladding interface to be greater than the critical angle, ϕ_c. Even with this condition satisfied, not every angle greater than the critical value will result in light propagation in the waveguide. Only certain angles greater than ϕ_c will be able to achieve this.

To understand this, we need to recall the phenomenon of *interference* between light waves. When two light waves are superimposed at a location in space, depending on the phase relationship between them, the result of the superposition can vary between a minimum and a maximum value. If the waves are completely out of phase with each other, we have *destructive interference*. In this case, the result of the superposition is zero, and the waves cancel each other. If, on the other hand, the waves are in phase, the result of the superposition is maximum amplitude. This is the phenomenon of *constructive interference*.

When light propagates inside a waveguide, multiple beams of light may arrive at the same point at the interface between core and cladding at any time. This results in wave interference. If the angle of incidence is such that the waves interfere destructively, the waves cancel one another and do not travel further. If the angle corresponds to constructive interference, the result is maximum amplitude, and light can sustain itself as it continues down the waveguide. Angles in between these two extremes will not allow for the sustained propagation of the light. These light waves will eventually disappear. *Only light with angles that produce constructive interference will eventually remain.*

The condition for *constructive interference*, also called the *phase-matching condition*, is described by the following equation:

$$\Delta\phi = 2\pi m,\ m = 0, \pm 1, \pm 2, \ldots \qquad (1\text{-}8)$$

Here, $\Delta\phi$ is the phase difference between the two interfering waves, and m is an integer. The equation states that constructive interference takes place when the phase difference is an integer multiple of 2π.

When Equation 1-8 is applied to the use of waveguides to determine the specific angles of incidence that allow for the propagation of light, complicated mathematical equations result. Without going into details, the solutions of those equations give us the specific angles of incidence that work for light propagation. The light waves corresponding to these angles are called the *modes* of the waveguide.

The modes are labeled by integer values, denoted by the letter m, starting with 0 for the first mode and continuing with 1, 2, and so on. Negative values of m are not used in waveguides.

The mode with m = 0 is called the *fundamental mode* of the waveguide. It corresponds to the greatest angle of incidence for light traveling in the waveguide. The modes labeled 1, 2, etc. are called *higher-order* modes. The angle of incidence gets progressively smaller as m gets larger, but remains higher than the critical value, ϕ_c. (If the angle drops below ϕ_c the mode will not be guided any longer and will leak out of the core.)

Figure 1-6 shows the direction of the light beams for modes 0 to 3. The fundamental mode travels almost along the axis of the waveguide, while the higher-order modes often strike the core-cladding interface.

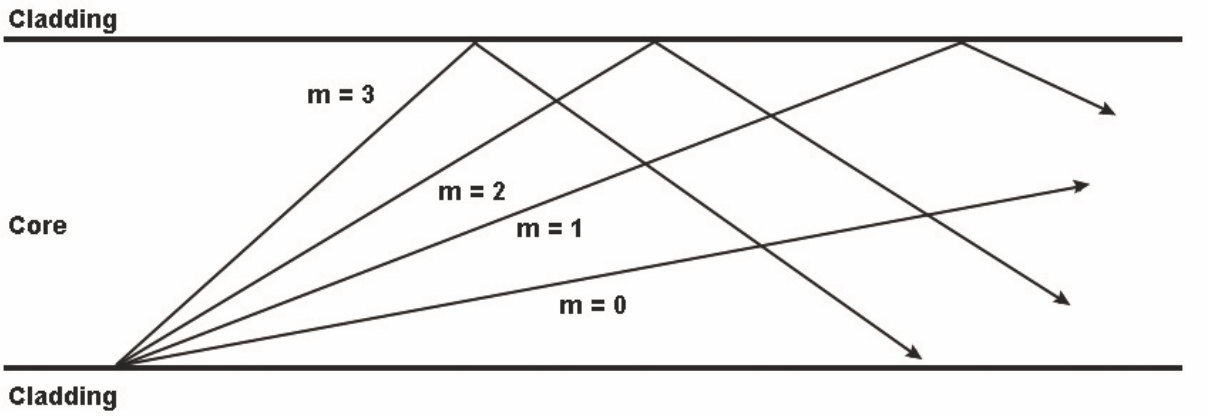

Figure 1-6 *Illustration of the light direction of propagation for fundamental and higher-order modes of a waveguide*

The number of allowable modes to propagate in a waveguide depends on the wavelength and the polarization of the light, the indexes of refraction of the core and cladding materials, and the dimensions of the core. Generally, a large refractive index difference between core and cladding and/or a large core allow for many modes to propagate. For a given wavelength, once the core and cladding indexes have been chosen, the size of the core determines the number of allowable modes. In some applications, only one mode is allowed to propagate. An example is in long-haul optical fiber transmission systems, where light travels for hundreds and even thousands of miles in the optical fiber. Because the different modes travel with slightly different speeds, they do not arrive at a destination together, which introduces distortions in the signal or transmitted data. Using only one mode for light propagation avoids this issue.

A waveguide that only allows the fundamental mode (m = 0) to propagate is called a *single-mode* (SM) waveguide. If more modes propagate in a waveguide, the waveguide is called *multimode*. For a given wavelength and indexes of refraction of the core and cladding, there will be a maximum radius for the core of the fiber that allows the optical fiber waveguide to be single mode. A typical single-mode optical fiber has a refractive index contrast of 0.3% to 0.8% and a core diameter of 8–10 μm.

The *wavenumber* of the light is expressed by the following equation:

$$k = 2\pi/\lambda \tag{1-9}$$

The so-called *V parameter* of the fiber allows us to determine whether a fiber is single or multimode. The V parameter can be calculated with the following equation, where a is the fiber core radius:

$$V = k\, a\, (n_{core}^2 - n_{clad}^2)^{1/2} \tag{1-10}$$

If V is less than 2.405, the fiber is single mode.

Example 3

Determine whether an optical fiber with core radius equal to 9 μm, a cladding index of 1.445, and a core index of 1.455, operating at a wavelength of 1550 nm, is single mode.

Solution: To obtain the correct answer, use Equation 1-10 to calculate the V parameter of the fiber, being careful to express the wavelength and the core radius in the *same units*. Convert the wavelength to microns (λ = 1550 nm = 1.55 μm). Obtain the fiber radius, a = diameter/2 = 9/2 μm = 4.5 μm.

We are now ready to calculate the V parameter.

$$V = (2\pi/1.55\ \mu m)\ (4.5\ \mu m)\ (1.455^2 - 1.445^2)^{1/2} = 3.11.$$

Because V > 2.405, the fiber is multimode. The fiber can become single mode if the core index or the core diameter are reduced.

Polarization of Light Waves Propagating in Optical Waveguides

Light is an electromagnetic wave consisting of an electric field and a magnetic field, coupled to each other and traveling together in the direction of propagation of the wave. Light traveling in free space is a *transverse electromagnetic wave*. For such waves, the electric field and the magnetic field are perpendicular to each other and to the direction of propagation of the wave. Figure 1-7 illustrates a transverse electromagnetic wave. Such waves are labeled “transverse electric and magnetic” or TEM.

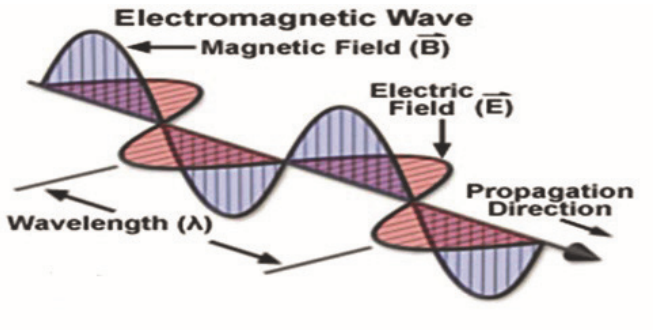

Figure 1-7 *A transverse electromagnetic wave*

Other polarizations for electromagnetic waves are Transverse Electric (TE) and Transverse Magnetic (TM). Let's assume the direction of propagation is along the z axis in a Cartesian system of coordinates. In the case of TE waves, the electric field is perpendicular to the direction of propagation, so the vector is aligned to a direction in the x-y plane, for example the x-axis. For TM waves, the magnetic field is perpendicular to the direction of propagation.

In the case of waveguides, the waves can be TE waves or TM waves, or they can have more complicated types of polarizations. In optical fibers, because of their cylindrical symmetry, the polarization of the fundamental mode propagating in the fiber can be randomly oriented in the x-y plane.

Mode Field Distributions in the Waveguide Cross Section

In addition to having a vector orientation as described above, the electromagnetic field propagating in a waveguide varies in intensity in the waveguide cross section. This variation follows specific patterns for each waveguide mode.

The pattern for the fundamental mode has an intensity maximum in the center of the waveguide core, and the intensity gradually decreases with distance from the center. The field extends for a small distance outside the core, but the intensity of the field in that region is very small. The field decreasing in intensity outside the waveguide core is called the *evanescent field*. The majority of the wave's optical power is contained inside the core of the waveguide. Figure 1-8 shows a representative intensity distribution for the fundamental mode in a single-mode optical fiber. Figure 1-8a shows the intensity pattern in the fiber cross section. Note that the field extending outside the core has very small intensity. Figure 1-8b shows a three-dimensional image of the intensity of the electromagnetic field in the fiber. The wire cylinder depicts the fiber core.

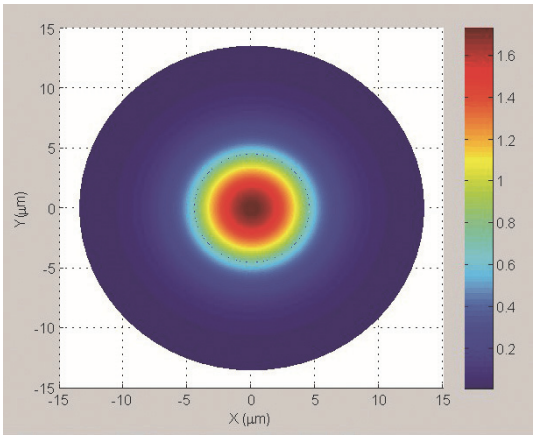

Figure 1-8 a) *Intensity of the electromagnetic field in the waveguide cross section of a single-mode optical fiber for the fundamental mode*

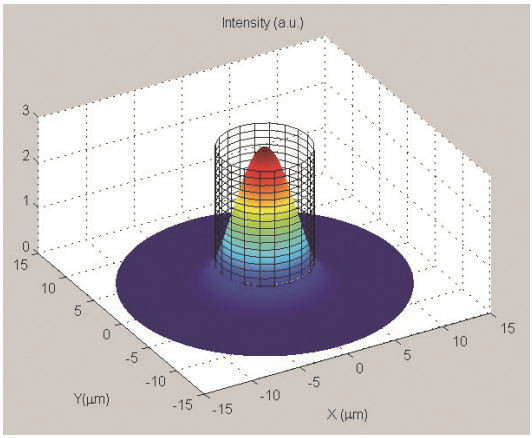

Figure 1-8 b) *Three-dimensional representation of the intensity of the fundamental mode*

Higher order modes have different patterns of variation over the waveguide cross section and in general extend more outside the waveguide core. Figure 1-9 shows the pattern of variation for the fundamental mode and two higher-order modes along one direction, passing through the center of the waveguide core. The waves are TE polarized. Once again the fundamental mode has a maximum in the center and decreases in intensity with distance from the center. The evanescent field extends slightly outside the core. The first higher-order mode has a minimum in the center and two intensity peaks inside the core. It extends a little more outside the core than the fundamental mode. The second higher-order mode has three intensity peaks inside the core.

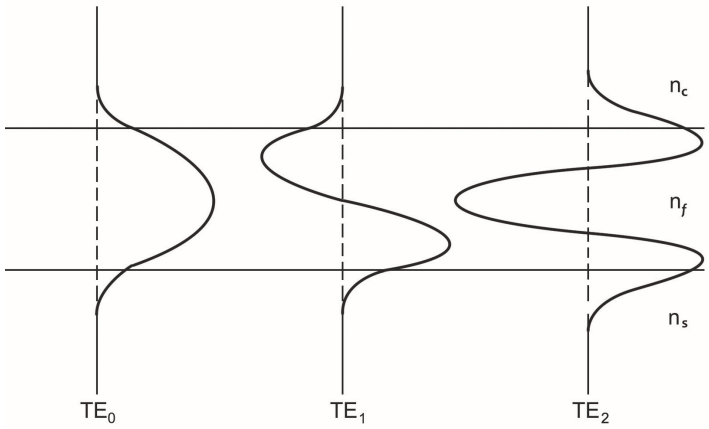

Figure 1-9 *Intensity distribution for fundamental mode and two higher-order modes along a line passing through the center of the waveguide*

It is desirable to have most of the optical power carried by the wave contained in the core of the waveguide. The fundamental mode satisfies this condition best. As mentioned previously, many applications require single-mode waveguides, which only allow for the propagation of the

fundamental mode. Working with a core size close to the maximum allowed by the single-mode condition also helps confine most of the light in the waveguide core.

Planar Optical Waveguides

Photonic integrated circuits are constructed from *planar optical waveguides*. While optical fibers have a cylindrical geometry, planar waveguides are based on a rectangular geometry. The waveguide core in this case has a square or a rectangular shape. The rectangular geometry is associated with the different fabrication process for planar waveguides. As shown later in the module, planar waveguides are realized from thin film layers of materials with different indexes of refraction placed on top of one another. Figure 1-10 illustrates such a waveguide, where the core layer is sandwiched between a substrate layer and a cladding layer.

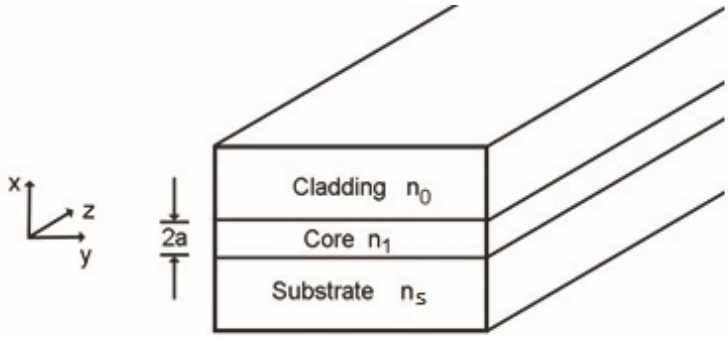

Figure 1-10 *Planar optical waveguide*

Similar to the case of optical fibers, the core of a planar waveguide has a higher index of refraction than the surrounding layers. For the waveguide in Figure 1-10, $n_1 > n_s$, and $n_1 > n_0$. This allows the waveguide to confine and guide the light through total internal reflection the same way it does in optical fibers.

Several names are used for the layers surrounding the core; sometimes these layers are called *lower cladding* and *upper cladding*. The index of refraction of the upper and lower cladding is the same in most cases. The relevant parameters that describe a planar waveguide are the dimensions of the core and the indexes of refraction of the core and cladding materials. As in the case of optical fibers, light propagates in planar waveguides in the form of modes, once again based on the constructive interference condition. The modes are described by the integer m, with values from m = 0 for the fundamental mode to m = 1, 2, . . . for higher-order modes.

There are several types of planar waveguides, each with its associated geometry. A planar waveguide with a very thin core, having a much wider width than height, such as the one illustrated in Figure 1-10, is called a *slab waveguide*. The only dimensional parameter that describe such a waveguide is the thickness, labeled “2a” in the figure. Slab waveguides confine light through total internal reflection only in a vertical direction, labeled “x” in the figure. The electromagnetic fields describing light propagating in the waveguide do not change in the y direction.

The V parameter used to describe single vs. multimode optical fibers can also be used in the case of slab waveguides that have the same upper and lower cladding indexes, n_{clad}. The V

parameter is defined by Equation 1-10, where "a" is only half the core thickness shown in Figure 1-10.

The condition for single-mode slab waveguides is, however, different than for optical fibers. If V is less than $\pi/2$, the slab waveguide is single mode.

Example 4

Determine whether a slab waveguide with thickness equal to 6 μm, upper and lower cladding index of 1.445, and core index of 1.449, operating at a wavelength of 1310 nm, is single mode. Calculate also the refractive index contrast between core and cladding.

Solution: Using Equation 1-10, we calculate the V parameter of the slab waveguide. (Once again, we need to be careful to express the wavelength and the core thickness in the same units to obtain the correct answer.)

Convert the wavelength to microns first: $\lambda = 1310$ nm $= 1.31$ μm

Obtain the half thickness: $a = 6/2$ μm $= 3$ μm

We are now ready to calculate the V parameter.

$V = (2\pi/1.31\ \mu m)\ (3\ \mu m)\ (1.449^2 - 1.445^2)^{1/2} = 1.55.$

Because $V < \pi/2 = 1.57$, the *slab waveguide is single mode.*

The refractive index contrast is calculated using Equation 1-5:

$\Delta = (n_{core}^2 - n_{clad}^2)/(2\ n_{core}^2) = (1.449^2 - 1.445^2)/(2 \times 1.449^2) = 0.003 = 0.3\%$

Slab waveguides are a useful model to understand how light propagates in planar optical waveguides and are relatively easy to solve mathematically.

The most common geometry for planar optical waveguides used in PIC is the *rectangular* or *channel waveguide.* The core of these waveguides has comparable width and height, as shown in Figure 1-11a, illustrating the waveguide cross section. To describe these waveguides, we need both the width, W, and the height, H, in addition to the refractive indexes of the core and cladding. Another possible geometry is *rib* or *ridge waveguides*, illustrated in Figure 1-11b. Ridge waveguides are described by width W and height H, as well as thickness of the ridge layer (r.H), in Figure 1-11.

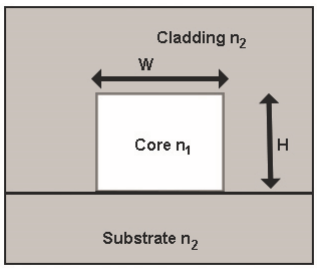

Figure 1-11 a) *Channel waveguide*

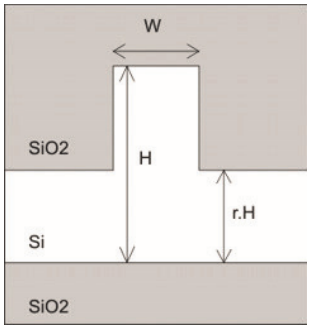

Figure 1-11 b) *Ridge waveguide*

Channel and ridge waveguides are also described by modes and can be single-mode or multimode. The mathematical equations describing these waveguides are more complicated than the slab waveguide equations and depend on all three spatial (x, y, and z) variables. The equations can be solved either using various approximations or numerically, using specialty software programs. It is not possible to determine whether the waveguide is single mode using Equation 1-10 for these waveguides. However, the behavior is similar, and waveguides with a large refractive index difference between core and cladding and/or a large core allow propagation of more modes.

The materials composing the channel and ridge waveguides, together with the wavelength, determine the indexes of refraction of the core and cladding. The thickness chosen for the core layer is the same across the entire PIC. This comes from the fabrication process, which will be explained later in the module. The only parameter that can and does vary throughout the PIC is the waveguide width. With all other parameters fixed, the waveguide width must not exceed a maximum value to keep the waveguide single mode, if required by the application. The maximum width for SM waveguides can be determined using software programs.

Characteristics of Planar Optical Waveguides

Dimensions

Compared with the cores of optical fibers, the cores of planar waveguides have smaller dimensions. For optical fibers, it is advantageous to have large cores. This helps when directing light into the fiber and also makes it easier to handle the fibers. Single-mode fibers typically have a core diameter of 9 μm and a cladding diameter of 125 μm. A coating with a diameter of 250 μm and an external buffer of diameter 900 μm protect the cladding. Multimode fibers have core diameters of 50 μm or 62.5 μm and can have the same cladding, coating, and buffer as SM fibers.

By contrast, in the case of PIC devices, small waveguides are beneficial for creating highly dense circuits that occupy a small footprint. As we discussed previously, waveguides tend to be multimode when the refractive index difference between core and cladding is large and/or the dimensions of the core are large. If single-mode waveguides are required, the higher the refractive index difference is, the smaller the dimensions of the core will be.

Channel waveguides fabricated from silica and doped silica, the same materials optical fibers are made of, typically have square cores with sides of 6 μm. For silica and doped silica, the refractive index contrast is small. It generally varies from 0.8% to 2% for planar waveguides. For other combinations of materials, such as silica and silicon, the refractive index contrast is much higher. Silicon has an index of refraction equal to 3.5, which is much higher than silica's index of 1.45. Because of the higher index difference, single-mode waveguides based on these materials are much smaller. Typical *silicon-on-insulator* channel waveguides have dimensions of 0.5 μm x 0.2 μm. These tiny waveguides hold the promise of a very high level of integration, which will be needed as PIC devices become more complex.

Example 5

Calculate the refractive index contrast of silicon (index of refraction 3.5) and silica (index of refraction 1.45). Compare this with the typical contrast of silica and doped silica, typically 1%.

Solution: Using Equation 1-5 for the index contrast, we obtain:

$$\Delta = (3.5^2 - 1.45^2)/(2 \times 3.5^2) = 0.41 \text{ or } 41\%.$$

This is much higher than the contrast between silica and doped silica.

Bend Radius

Another advantage of strong light confinement in a small waveguide core is the ability to have bends with small radii of curvature in the waveguide. *Bends are necessary to route and connect different portions of the waveguides.* If the bend radius of curvature is too small, the light striking the interface between core and cladding may no longer satisfy the condition of total internal reflection, which would allow light to leak out of the cladding and create losses that affect the performance of the waveguide.

This constraint also holds true for optical fibers, which cannot be bent with a radius of curvature smaller than a known minimum. Figure 1-12 shows how some of the light traveling in a bend waveguide can escape and be lost if the radius of curvature is too small. The red line depicts the light-intensity distribution inside the waveguide, which extends a bit into the cladding, as we have seen before. The angle of incidence at the interface between core and cladding is labeled "θ". In the straight waveguide, the angle is higher than the critical angle, which satisfies the condition for total internal reflection and allows light to propagate inside the waveguide. In the bend waveguide shown on the right, the geometry of the waveguide is such that after two reflections, the angle of incidence becomes smaller than the critical angle. This violates the total internal reflection condition and results in some of the light entering the cladding. The cladding light then escapes the waveguide and is lost. This is also seen in the distribution of the field, which extends more into the cladding and reaches out of the waveguide completely. To avoid such losses, the radius of curvature cannot be less than a minimum value that is specific to each type of waveguide. The larger this minimum bend radius is, the more space the bends will take up, increasing the footprint of the device.

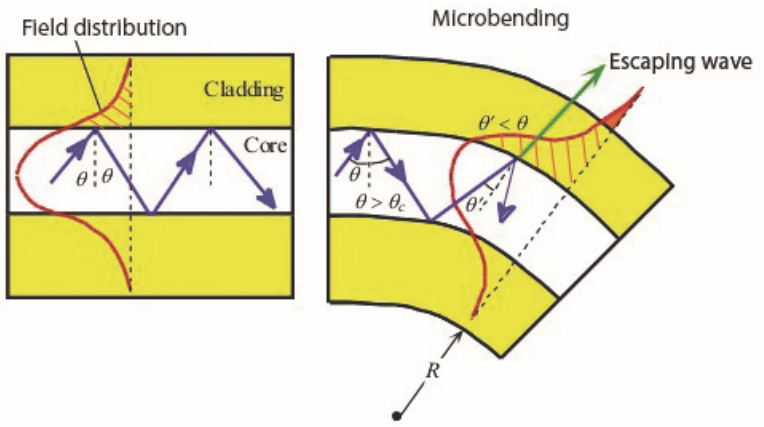

Figure 1-12 *Light-intensity distribution for straight and bend waveguides. A small amount of light is lost in the bend waveguide due to the violation of the total internal reflection condition.*

For comparison, the minimum bend radius for silica and doped silica channel waveguides is 4–5 mm, while the corresponding radius for silicon-on-insulator channel waveguides is about 10 µm. This shows the advantage of using waveguides with a high refractive index contrast. The disadvantage is the difficulty of coupling light into these waveguides.

Propagation Loss

Several other important characteristics of planar optical waveguides depend on the material used to fabricate the waveguides and the technology of fabrication. One of these is the *propagation loss* that light experiences as it travels through the waveguide, with typical units of dB/cm. For long waveguides, it is important to have very little propagation loss, because the loss accumulates with distance traveled. For example, optical fibers used for long-haul transmission (>100 meters) have a loss of only 0.2 dB/km. Planar waveguides have not reached such a high level of performance, due to a different fabrication process, but they are much shorter. An important loss mechanism in planar optical waveguides is *scattering* loss, which can occur due to volume scattering, surface scattering, and sidewall loss. Volume scattering is caused by imperfections in the waveguide material, such as impurities, defects, and voids, among others. Surface scattering takes place at the core-cladding interfaces and is primarily due to surface roughness (the same as sidewall loss.) These losses depend on the process used to fabricate the waveguides. In addition to scattering, *absorption* losses play an important role. These losses depend on the wavelength and are minimized by operating at specific wavelengths. In telecommunications, where light is transmitted for long distances in optical fibers, several windows of operation have been defined that correspond to wavelengths for which glass absorption is minimal. These are shown in Table 1.

Table 1-1. Telecommunications Transmission Windows

Band	Description	Wavelength Range
O band	Original	1260 to 1360 nm
E band	Extended	1360 to 1460 nm
S band	Short wavelengths	1460 to 1530 nm
C band	Conventional	1530 to 1565 nm
L band	Long wavelengths	1565 to 1625 nm
U band	Ultralong wavelengths	1625 to 1675 nm

Thermo-Optic Effect

Another material characteristic is the strength of the *thermo-optic effect*, expressed by the variation of the index of refraction, n, with temperature, through the coefficient of variation dn/dt in units of 1/°C or 1/K. The index at a temperature, T, can be calculated with the following equation, where $n(T_0)$ is the index at a reference temperature:

$$n(T) = n(T_0) + dn/dt\ (T - T_0) \qquad (1\text{-}11)$$

Example 6

Silica's index of refraction has a coefficient of variation with temperature equal to 1.0×10^{-5} /K. If the index of refraction at room temperature (21 ºC) is 1.45, what is the index of refraction at a temperature of 75 ºC?

Solution: Using Equation 1-11, we obtain:

$n(75) = n(21) + 1.0 \times 10^{-5} \times (75 - 21) = 1.45 + 1.0 \times 10^{-5} \times (75 - 21) = 1.4505.$

The index of refraction of silica changes very little as the temperature goes up to 75 ºC from the room temperature of 21 ºC. This is because the coefficient of variation dn/dt for silica has a very low value.

The thermo-optic effect is used in devices, such as switches and modulators, where the behavior of the device is controlled by changing the temperature of the waveguide. For these devices, a large coefficient of variation dn/dt is advantageous. On the other hand, the same effect can negatively affect the performance of certain devices. In resonant devices that need to be precisely tuned to certain wavelengths, small changes in the refractive index with temperature will result in the devices becoming detuned. Such devices require temperature stabilization to operate properly.

Materials Used to Fabricate PICs

PICs are fabricated from many materials, in contrast to EICs, which are primarily based on silicon (Si). The materials used to fabricate PICs will depend mainly on the function of the device. Optical sources such as semiconductor lasers are made from *III-V semiconductor materials*—for example, gallium arsenide, indium phosphide, and other combinations of

compounds. These materials are also used to fabricate semiconductor optical amplifiers (SOA). Optical signal processing devices used in telecommunications can be fabricated from several material platforms, including *silicon-on-insulator (SOI)*, *silicon dioxide* (glass), *lithium niobate ($LiNbO_3$)*, and various *polymers*. Of these materials, the SOI platform has emerged in recent years as the material of choice because it offers the potential to fabricate highly integrated and highly performing PIC devices capable of satisfying the ever increasing bandwidth and capacity requirements of data storage, data transmission, and cloud computing, to name just a few applications. Silicon is also a material of choice for many photodetectors, devices that detect light and convert it to electrical signals.

To date, no single platform or technology is capable of producing the entire array of photonic devices needed in various applications and fields and integrating them in the same circuit. For example, using silicon to build lasers is not feasible, because silicon is an *indirect gap material.* This makes silicon-based lasers inefficient sources of light. One option to integrate an optical source with processing devices based on silicon is to grow gallium arsenide lasers on a silicon substrate. However, this is difficult, due to large lattice mismatch and large difference between the thermal expansion coefficients of the two materials. (The lattice refers to the periodic structure that characterizes crystalline materials.) However, the interest in having such lasers available is huge, because they would allow for monolithic integration of optical sources, processing, and detection devices in the same chip. Research groups around the world are working on creating efficient silicon-based lasers, and there has been progress toward obtaining such a device. Silicon also allows for integration between photonic and electronic integrated circuits (the ultimate goal of the technology), with all the economic and performance advantages that this integration would bring.

Table 2 summarizes the characteristics of waveguides and PICs based on the material platforms and technologies described above. As you can see, each of the platforms has advantages and disadvantages. The III-V semiconductors dominate laser, optical amplifier, and detector applications. *Silicon* refers to waveguides having a silicon core. The most used platform for such waveguides is silicon-on-insulator or SOI. In this platform, the silicon core sits on a silicon dioxide layer, which is an insulator. The upper cladding can be either silicon dioxide or air. “Silica on silicon” refers to devices fabricated from silica and doped silica, created on a silicon wafer. This platform has been successfully used to fabricate many telecommunications devices, such as filters, modulators, switches, and splitters. It allows for very reliable devices with very low propagation loss. However, due to the low index contrast, the devices are relatively large and so occupy a big footprint. Polymers have been used for some applications, but these materials do not allow operation at high temperatures and are less reliable.

The amount of integration between devices on the same platform has not yet been very large. Most devices are made separately and assembled together in modules using fiber connections. As stated previously, silicon has emerged as holding the biggest promise for monolithic integration of PIC and, ultimately, integration of PIC and EIC together for best cost and performance.

Table 1-2. Comparison of material and waveguide characteristics for main material platforms used for Photonic Integrated Circuits Wavelengths

Material	Devices	Refractive index contrast	Propagation loss	Thermo-optic coefficient	Compatibility with CMOS technology	Reliability
III-V Semicon-ductors	Lasers, optical amplifiers, modulators, detectors	Low	Relatively high	High	No	High
Silicon	Filters, modulators, switches	High	Relatively high	High	Yes	High
Silica on silicon	Filters, modulators, switches, splitters	Low	Very low	Low	Yes	High
Polymer	Modulators, attenuators	Low	Low	High	Yes	Low

Photonic Integrated Circuit Fabrication

Several methods have been used historically to fabricate PICs. For high-performance, high-volume production of PICs, the methods of fabrication are the same as the ones used in the electronic integrated circuit industry. The principal steps used in the fabrication process are common to all methods and are focused on creating the essential components in all PICs: the *planar optical waveguides*.

PICs are planar devices in the sense that they are formed on a planar substrate on which layers of materials are grown or deposited. The resulting PICs extend in two dimensions, which limits the devices to 2D configurations. In high-volume manufacturing, the base component is a silicon wafer of various sizes. The most advanced facilities today use 300 mm diameter silicon wafers on which hundreds and even thousands of PICs can fit. The thickness of the silicon substrate is between 0.5 mm and 1 mm.

The main steps in the fabrication of a PIC are the following:

Deposition

Deposition is the process through which layers of materials are added to a silicon wafer. Initially, a substrate layer and a core layer with an index of refraction higher than the substrate are formed on the wafer. The core layer is where the optical waveguide will be formed, while the lower-index layer will serve as the lower cladding. The layers can be formed through a variety of methods: (a) *oxidation* or *thermal growth*, by which a layer of silicon dioxide (silica) forms on top of silicon, (b) *implantation*, (c) *physical vapor deposition* (PVD), (d) *chemical vapor deposition* (CVD), and (e) *spin-on*. The thickness of the layers varies from several hundred nanometers to a few microns. PVD is used for materials such as gold, aluminum, and titanium nitride. CVD is the most common method of deposition and is used for layers of silicon dioxide, silicon nitride, and tungsten. Spin-on is used to deposit photoresist and polymers.

Photolithography and Etching

A process called *photolithography* is used to define the waveguide core geometry. In this step, a material sensitive to light, known as *photoresist,* is deposited on top of the core layer. After deposition of the resist, the wafer is exposed to light through a photomask containing the waveguide patterns we wish to form. The photomask is an opaque plate with areas of transparency that allow light to shine through in accordance to the specified waveguide patterns. The optical design engineer is responsible for designing the waveguide devices and laying out the corresponding patterns in a computer-aided design (CAD) file. The file is then sent to photomask manufacturers, which provide the masks used in photolithography. The next operation is *developing*, during which the resist that has been exposed to light is removed from the wafer, thus creating on the wafer a pattern similar to the one from the mask.

Etching is next used to remove the portions of the core layer outside the waveguide patterns. Etching today is performed through a process named *dry etch* to distinguish it from the older *wet etch* process. A wet etch was performed by immersing the wafer in a tank containing the etch agent. This process did not result in a highly accurate feature geometry and consequently has been replaced by the dry etch process. *Reactive-ion etching* (RIE) is the preferred method of dry etching. It consists of a combination of chemical etching and physical etching. Chemical etching uses a chemical reaction between the wafer material and a chemical etchant. Physical etching is accomplished by bombarding the surface of the wafer with ions from a gas introduced in the chamber. The resist remaining on top of the waveguides after etching is then removed, exposing the waveguides.

Figure 1-13 illustrates the photolithography and etching steps described above, when used to fabricate two oxide waveguides on a substrate.

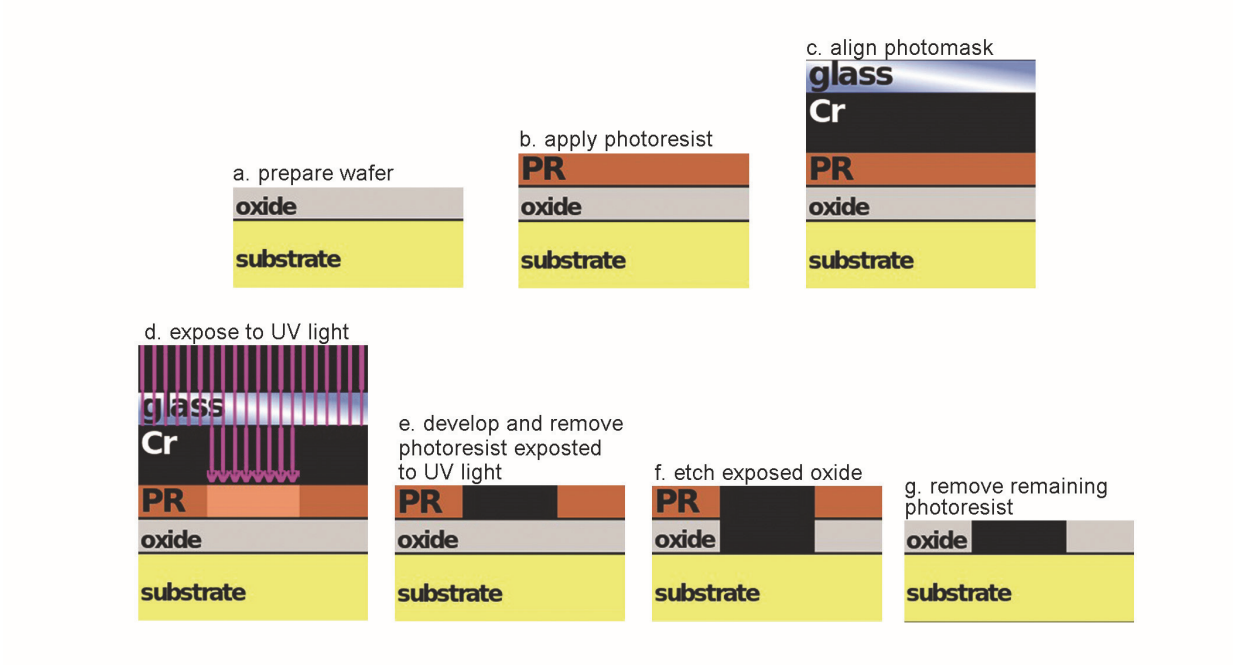

Figure 1-13 *Photolithography and etching*

Photolithography and etching in the case of silicon waveguides with a silica lower cladding.

PMMA A4 is the photoresist material used in this case.

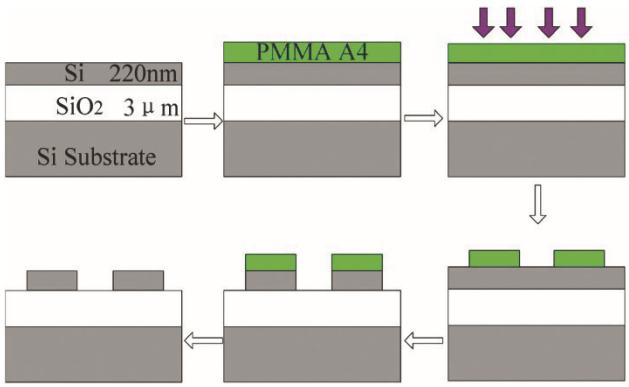

Figure 1-14 *Photolithography and etching of silicon waveguides with silica lower cladding*

Second Deposition

A new *deposition* step is used to cover the patterned core layer with an upper cladding if necessary. In some cases, the upper cladding for the waveguide can simply be air.

Passivation

Depositing a protective layer over the surface of the wafer (if necessary), a process called *passivation*, comes next. Silicon nitride (Si_3N_4) is a material commonly used for this purpose.

Metallization

Some PICs make use of the thermo-optic effect to modulate the amount of light at the output. All materials used to fabricate PICs have an index of refraction dependent on temperature, but the index change with temperature is more pronounced in certain materials than in others. For example, silica (silicon dioxide) has an index coefficient of variation with temperature of 10^{-5}/degree, while silicon has a higher coefficient of about 10^{-4}/degree. To take advantage of this effect, thin film heaters can be formed above certain regions of the optical waveguides. When electric current runs through the thin film heaters, the heat generated over the waveguides changes their index of refraction. The heaters are formed after completing the steps described above and require another round of deposition and photolithography using an additional photomask that contains the heater patterns.

The process described above corresponds to the process used to fabricate electronic integrated circuits in the semiconductor industry. There are other methods used to fabricate PICs, and these methods are specific to certain materials. In the case of lithium niobate, the $LiNbO_3$ crystal is first grown using a method called the Czochralski technique. A waveguide can then be formed in this material by diffusing certain ions into it. One possibility is to diffuse titanium ions, resulting in an area with higher refractive index that will act as the core of the waveguide. The most popular method, however, is the *proton exchange* method, in which lithium ions and protons (hydrogen ions) exchange places in a superficial layer on the surface of the lithium-

niobate substrate. Waveguides can subsequently be patterned in the core layer by photolithography and etching.

Direct Laser Writing

A more recent method of fabrication, which is used for low-volume parts in the laboratory, is direct laser writing. In this method, a femtosecond laser focused to a location inside a piece of glass or other material produces a permanent, local increase in the refractive index. By translating the laser and the glass relative to each other, a waveguide can be created, as shown in Figure 1-15. These waveguides have a low index contrast and high propagation loss, but an advantage is that 3D patterns can be easily created inside the host material, in contrast to the strictly 2D planar devices obtained with traditional methods. This is also an inexpensive method of fabrication that does not require photolithography, etching, and a clean-room environment. Specialty PICs in low volumes are created by direct laser writing.

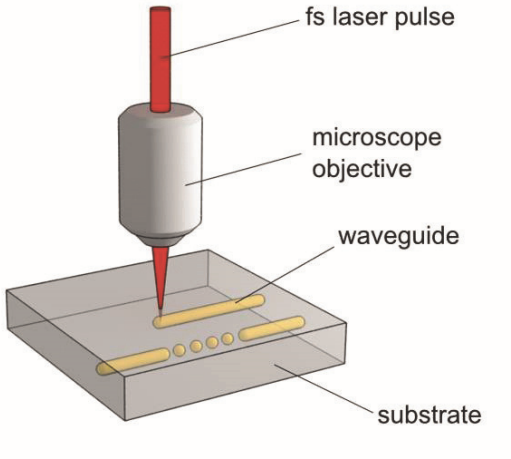

Figure 1-15 *Direct laser writing of waveguides inside a substrate using a femtosecond (fs) laser*

Equipment used in Fabrication of PICs

Deposition Equipment

The most common process used for deposition of thin films is *chemical vapor deposition* (CVD). In this process, reactant gases are introduced in a reaction chamber. The gas molecules move to the wafer's surface and adhere to it in a process called *adsorption*. A chemical reaction takes place on the surface of the wafer in the presence of heat; this reaction forms the thin film layer. The gaseous by-products are then removed from the wafer's surface and vented out of the reaction chamber.

Several parameters influence the CVD process. The pressure in the reaction chamber must be less than the atmospheric pressure but greater than 1 millitorr (medium vacuum range) for *low-pressure chemical vapor deposition* (LPCVD). This requires vacuum pumps to maintain the desired pressure. *Atmospheric pressure chemical vapor deposition* (APCVD) systems do not

require vacuum pumps but need complex exhaust systems to contain the toxic gases in the deposition zone and prevent their release into the environment. LPCVD is used for high-purity, thin films, while APCVD results in a high deposition rate. The second important parameter is the temperature in the reaction chamber. In hot-wall systems, the wafer and chamber are at similar high temperatures, and deposition takes place not only on the heated wafer but also on the chamber walls, which must often be cleaned. In cold-wall systems, the wafer is the hottest element in the system, and deposition takes place primarily on it. Finally, energy must be provided to the reactant gases in the chamber. This can be done through resistive heating, infrared lamp heating, or RF induction heating. *Plasma enhanced CVD* (PECVD) is also used; in this method, the reactant gases are ionized to increase their reactivity and reduce the need for very high temperatures in the chamber.

CVD systems can process wafers in batch, one at a time (single-wafer), or continuous wafer motion. Systems that can process 100 or more wafers at a time have very high throughput but are becoming less practical as the size of the wafers increases. Single-wafer systems have much better film thickness uniformity than batch systems. Continuous-motion systems process wafers in a continuous mode and have good throughput with good uniformity. Examples of CVD equipment include Novellus's Continuous Motion LPVCD, Genus's Cold Wall PECVD, Applied Materials' Radiantly Heated Barrel Reactor, and Pacific Western Systems' Horizontal Flow PECVD Reactor.

Photolithography Equipment

There are two important steps in the photolithography process; each requires specific equipment.

- First, a layer of photoresist must be applied to the wafer using a coater. The goal in this step is to obtain a uniform layer of resist on the entire wafer. The resist is first dispensed in the center of the wafer in a static or dynamic process and then distributed to the entire spinning wafer. The wafer is mounted onto a vacuum chuck and spun at high velocities to uniformly spread the resist on its surface. An exhaust system extracts and eliminates fumes from the photoresist. Fully automated coaters allow for programmed recipes to control the selection and dispensing of photoresist, spin speeds, and event duration times; they also allow the wafers to move through the entire process without manual intervention. The operator control panel handles all activities associated with recipe entry and selection, error reporting, and process and equipment monitoring.
- The second step in the photolithography process is exposure of the coated wafer to light through a photomask to allow the transfer of the mask patterns to the wafer. Methods used for this purpose include contact printing, proximity printing, projection printing, reduction stepping, and reduction scanning. In *contact printing*, the mask is placed on top of the photoresist, which allows for very good accuracy of transferring the pattern onto the wafer. However, the integrity of the mask cannot be maintained, and the feature sizes and resolutions are limited. *Proximity printing* keeps the mask at a small distance from the resist, but, once again, small feature sizes are hard to reproduce. In *projection printing*, additional optics are placed between the mask and wafer, bringing the feature size to less than one micron using a projection aligner. The next step, to obtain very high-resolution images, is to use optics with refractive lens elements, but these will limit the size of the exposure area. In *reduction systems*, only a small area is exposed at a time; this area is called the *reticle*. The

exposure is then repeated over the entire surface of the wafer in a process of "step and repeat." This creates many, identical, high-resolution dies across the wafer. The technology in use today is based on the *reduction scanning* method. In this method, the reticle has features 4 to 10 times bigger than the end product, which is then reduced using a reduction lens positioned between the reticle and the wafer. By continuously moving or scanning the reticle vs. the wafer, higher throughput is achieved together with very high feature resolution. Figure 1-16 shows a schematic representation of an exposure system.

The light source used in the exposure process is either a mercury lamp or an excimer laser. The latter is now used for state-of-the-art feature sizes, which are now well below 0.25 micron. Feature sizes of 45 nm have been achieved using excimer lasers operating at the deep UV wavelengths of 248 nm, 193 nm, and 157 nm. The smaller the source wavelength is, the smaller will be the minimum feature size that can be achieved.

Companies that manufacture photolithography systems include Canon, Nikon, ASML, Ultratech, and others.

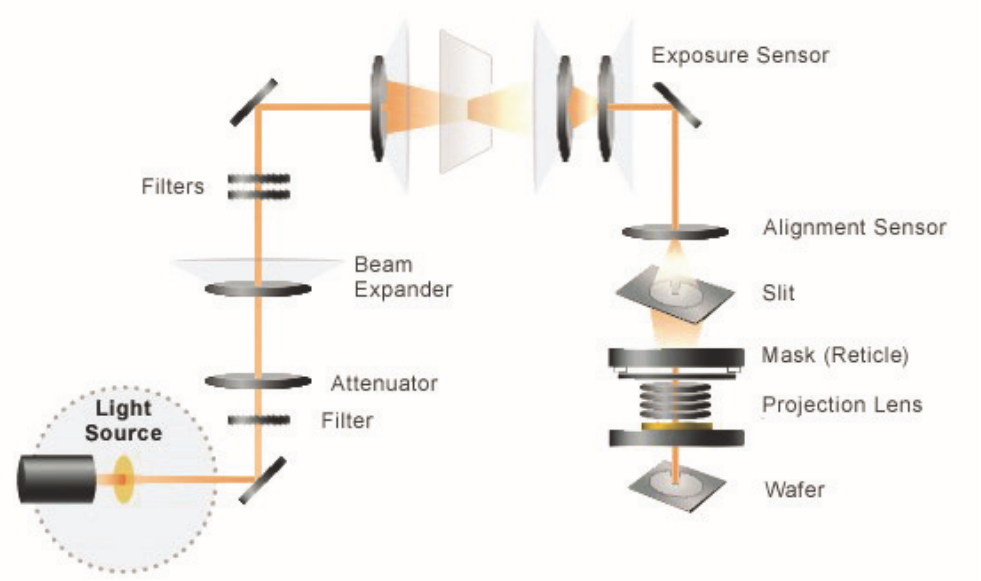

Figure 1-16 *Reduction scanning photolithography system*

Etching Equipment

Reactive-ion etching (RIE) is the current method of choice for the dry etching process used in the fabrication of PICs. The method is based on the use of chemically reactive plasma generated under low pressure by an electromagnetic field to remove material deposited on wafers. The RIE equipment consists of a cylindrical vacuum chamber with a wafer platter at the bottom. Gases are introduced in the chamber at a pressure from a few millitorr to a few hundred millitorr. Plasma is formed when a strong radio frequency (RF) electromagnetic field is applied to the wafer platter. The electromagnetic field ionizes the gas molecules by stripping them of electrons, thus creating the plasma. The electrons hitting the wafer platter build up a negative charge on it, and this charge attracts the positive ions. The ions collide with the material to be etched, and a chemical reaction takes place together with a physical etch, in which material is removed when the ions transfer their kinetic energy to the wafer. The process is controlled

through the RF power, pressure, time, and gas selection. Figure 1-17 shows commercial RIE equipment. Manufacturers of such systems include Hitachi, Canon, Lam Research, Oxford Instruments, Applied Materials, and others.

Figure 1-17 *Commercial RIE equipment used for dry etching*

SUMMARY

This module presented an introduction to photonic integrated circuits, their applications, and their role as a key contributor to the sustained growth of fields such as communications and computing. The module discussed planar optical waveguides, materials for PIC, and PIC fabrication steps and equipment. Subsequent modules will present PIC devices based on various materials and their configurations, functions, and applications. Systems of PIC devices and basic design of PICs will also be presented.

PROBLEM EXERCISES AND QUESTIONS

1. Define and compare photonic integrated circuits and electronic integrated circuits.
2. Give examples of photonic integrated circuits and applications in which they are used.
3. Explain monolithic integration, and describe its advantages.
4. Describe the principle governing the propagation of light in an optical waveguide.
5. Find the critical angle for total internal reflection at the interface between a core of index 1.48 and a cladding of index 1.45.
6. For the indexes of refraction in problem 5, find the refractive index contrast, the numerical aperture, and the maximum half-acceptance angle.
7. Explain waveguide modes, and compare the fundamental mode and higher-order modes of a waveguide.
8. An optical fiber has core and cladding indexes equal to 1.449 and 1.445, respectively. The fiber diameter is 8 μm. Is the fiber single mode for a wavelength equal to 1310 nm?
9. Describe the patterns for the electromagnetic field intensity in an optical waveguide for modes 0, 1, and 2.
10. Define slab, channel, and ridge planar optical waveguides.
11. A slab waveguide with the same core and cladding indexes as in problem 5 has a thickness of 4 μm. The wavelength of the light propagating in the waveguide is 1.55 μm. Determine whether the waveguide is single mode or multimode.
12. Describe two advantages of planar optical waveguides with high refractive index contrasts.
13. Describe loss mechanisms in planar optical waveguides.
14. Calculate the index of refraction of silica at a temperature of 95 ºC.
15. List the main groups of materials used to fabricate PICs, and give examples of devices for each group. Which material has the best characteristics for future developments in integrated photonics, and why?
16. Describe the deposition process used in the fabrication of PICs.
17. Describe photolithography and the materials and equipment used in this process.
18. What is reactive ion etching?
19. What is direct laser writing, and what are its advantages and disadvantages?
20. What kind of equipment is used to deposit thin film layers on a silicon wafer?
21. What is PECVD, and where is it used?
22. What is reduction scanning, and where is it used?
23. What is the minimum-sized feature that can be achieved today in an integrated circuit, and what makes that possible?
24. Research photonic interconnects, and write a short paper describing them.

REFERENCES

Bergman, K., L. P. Carloni, A. Biberman, J. Chan, and G. Hendry. 2014. *Photonic Network-on-Chip Design*. New York: Springer-Verlag.

Deen, M. J., and P. K. Basu. 2012. *Silicon Photonics, Fundamentals and Devices*. Chichester, UK: Wiley.

Lifante, G. 2003. *Integrated Photonics: Fundamentals*. Chichester, UK: Wiley.

Maricopa Advanced Technology Education Center. 2013. *MATEC Module Library* Tempe: Maricopa Advanced Technology Education Center. http://matec.org/ps/library3/

The National Center for Optics and Photonics Education. 2013. *Fundamentals of Light and Lasers.* 2nd ed. Waco, TX: OP-TEC.

Okamoto, K. 2006. *Fundamentals of Optical Waveguides*. Burlington, MA: Academic Press.

Chen, C.L. 2007. *Foundations for Guided Wave Optics*. Hoboken, NJ. John Wiley & Sons.

Silicon Photonic Integrated Circuits and Devices

Module 2

of

Integrated Photonics

OPTICS AND PHOTONICS SERIES

This material was created under Grant # 1303732 from the Advanced Technological Education division of the National Science Foundation. Any opinions, findings, and conclusions or recommendations expressed in this material are those of the author(s) and do not necessarily reflect the views of the National Science Foundation.

For more information about the text or OP-TEC, contact:

Dan Hull
PI, Executive Director, OP-TEC
316 Kelly Drive
Waco, TX 76710
(254) 751-9000
hull@op-tec.org

Taylor Jeffrey
Curriculum Development Engineer
316 Kelly Drive
Waco, TX 76710
(254) 751-9000
tjeffrey@op-tec.org

Published and distributed by
OP-TEC
316 Kelly Drive
Waco, TX 76710
254-751-9000
http://www.op-tec.org/

ISBN 978-0-9903125-6-7

CONTENTS OF MODULE 2

Module 2
Silicon Photonic Integrated Circuits and Devices

INTRODUCTION

Photonic Integrated Circuit (PIC) devices are fabricated from a variety of materials, including silicon, indium phosphide, silicon dioxide, lithium niobate, polymers, and others. Out of all of these, silicon has emerged as the material of choice for integrating multiple components in a single chip. Monolithic integration describes integrating light sources, signal processing devices, and photodetectors in a single chip. Monolithic integration reduces the footprint, the bill of materials, and the cost, and it also improves the system's performance. Moreover, PIC devices based on silicon can be integrated with electronic integrated circuit (EIC) devices in the same chip, further enhancing the functionality of the products. Silicon PICs are fabricated following the same steps used to fabricate EICs by CMOS technology, thus leveraging the advanced technology and equipment of the microelectronics industry.

While silicon is the only material that holds the promise of ultimate integration of both photonic and electronic devices, it is currently not possible to fabricate all photonic devices in silicon with the required level of performance. Today, devices are fabricated separately using the optimal material for performance. They are then assembled together in modules and connected using optical fibers. The assembly operations required to build the modules are complex and expensive, and the modules take up valuable space. This module will describe silicon PIC devices, their current characteristics, and directions leading to future enhanced integration and performance.

PREREQUISITES

OP-TEC's *Fundamentals of Light and Lasers Course 1*

OP-TEC's *Integrated Photonics: Module 1*

OBJECTIVES

Upon completion of this module, the student should be able to:

- Explain the material properties of silicon that are important for silicon PICs

- Classify passive and active photonic devices and calculate insertion loss in dB
- Describe the components of a basic optical fiber transmission system
- Explain attenuation and dispersion in optical fibers and how to mitigate their effects
- Describe characteristics of the following passive silicon PIC devices:
    - SOI waveguide
    - Bend waveguide
    - Coupling between optical fiber and SOI waveguide
    - Directional coupler
    - Y-branch
    - Mach-Zehnder Interferometer
    - Ring resonator
    - Bragg grating
- Describe characteristics of active PIC devices, including laser, modulator, and photodetector
- Describe challenges of integrating active devices in a silicon platform
- Discuss back-end fabrication processes such as testing, assembly, and packaging
- Describe system-in-package technologies and compare wire bond and flip-chip approaches
- Explain advantages and implementation of silicon optical interconnects

SCENARIO

Tiffany works as a photonics test technician for a company that manufactures silicon photonic devices. She works in the testing department, where she wears a lab coat, a hair net, and gloves. At the beginning of the day, she receives a new batch of devices to test. She tests bare devices that do not have optical fibers permanently attached to them.

Tiffany logs into her workstation and records the devices she will test. She cleans the edges of the devices and places them on translation stages to align them with the optical fibers connected to the test equipment. The alignment process is complete when the power transmitted through the device under test is at a maximum. Once the device is aligned, she starts the testing process, which is often run by a computer program in conjunction with the test equipment. She uses a variety of kinds of test equipment, including broadband, fixed wavelength, and tunable light sources; power meters; and optical spectrum analyzers. When necessary, Tiffany splices fibers using fusion-splicing equipment and other techniques.

When the tests end, Tiffany records the test data in the computer and flags devices that fail the test. She runs tests both for production devices and for research and development devices. The latter sometimes require her to come up with new ways of performing the testing. She also assists scientists and engineers in conducting various experiments. Tiffany must maintain a clean and organized work environment and maintain the test equipment in good working condition. She runs periodic calibration for the test equipment and documents the process and results. As the company creates new products, Tiffany continues to learn more about the devices' functions and performance. Her work is an important part of the work that her company is doing.

BASIC CONCEPTS

Material Properties of Silicon

Electronic Integrated Circuits rely on the semiconductor properties of silicon. Silicon is a chemical element that belongs to group IV in the periodic table because it has four electrons in its outer shell. Silicon is a semiconductor; it has low electrical conductivity in pure state, but its conductivity increases as its temperature increases. Conductivity can also be increased by adding small amounts of other chemical elements into the structure, a process called doping.

Doping changes silicon from an intrinsic to an extrinsic semiconductor. Silicon can be doped with elements from group III of the periodic table, which have three electrons in their outer shell, or with elements from group V of the periodic table, which have five electrons in their outer shell. In the first case, doped silicon becomes a p-type semiconductor, a material that has an excess of "hole" charge carriers. Holes are a different type of free charge carrier: they have an electric charge of the same magnitude as the electron's charge but with positive sign. The element used in doping in this case is called an acceptor; examples of these elements include boron, aluminum, and gallium. In the second case, we will have an n-type semiconductor, which has an excess of electron charge carriers. The element used in doping this time is called a donor, and such elements include phosphorus, arsenic, and antimony. The n-type and p-type semiconductors are further combined in p-n junctions, which are the basic building blocks for diodes and transistors. Billions of transistors and diodes are now integrated in electronic integrated circuits or chips, producing devices that are ubiquitously used in computers, cell phones, cameras, and much more.

In the case of PICs, we are interested in the optical properties of silicon in addition to its electronic properties. In particular, we are interested in how silicon absorbs and transmits various wavelengths of interest, from visible to near infrared. Figure 2-1 shows the absorption coefficient of several materials for the wavelength region between 200 and 2200 nm (0.2–2.2 μm). Crystalline silicon (called crystalline due to the regularity of its molecular structure) absorbs light up to a wavelength of about 1100 nm (1.1 μm). Due to this property, silicon is used in the fabrication of photodetectors operating in the visible to near-infrared range.

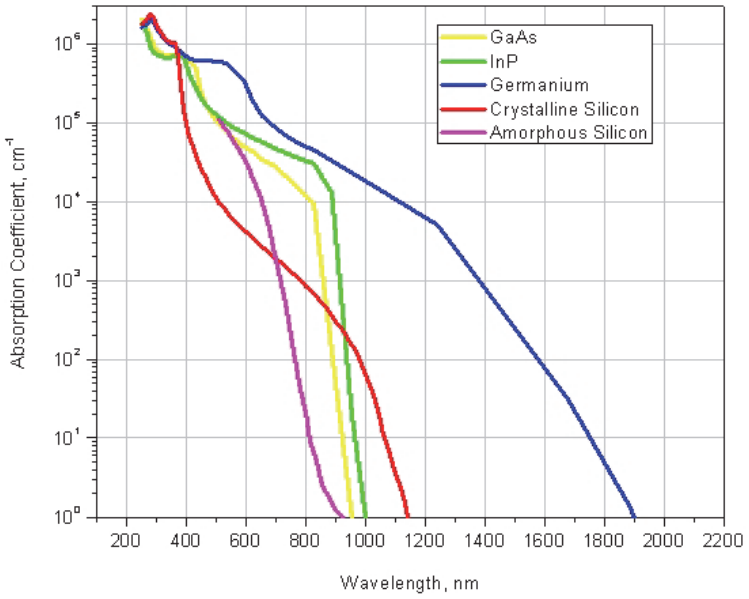

Figure 2-1 *Absorption coefficient of different materials vs. wavelength*

The absorption properties of a material are important for the application of photodetectors. Photodetectors are devices that convert a light input into an electrical output. They are essential elements in any optical power measurement system. They are also used in optical fiber communication systems as part of the receiver modules. Important parameters that characterize photodetectors are responsivity, sensitivity to wavelength, temporal response, and noise level. Silicon PIN photodiodes are fabricated from a p-n junction with an intrinsic, i, layer inserted between the p- and n- regions; these photodiodes have excellent characteristics.

For wavelengths higher than 1.1 μm, silicon becomes transparent, which is a useful property for PIC devices that transmit rather than absorb light. Numerous such devices are used in optical fiber telecommunication systems, which operate in the wavelength range between 1200 nm and 1700 nm, as described in Module 1. The most used transmission band is the C (Conventional) band, centered at 1550 nm. For transmission based devices, the index of refraction is an important parameter. Figure 2-2 shows the index of refraction of silicon for the wavelength range 1100–1700 nm. Compared with silicon dioxide (glass), which is the material used to fabricate optical fibers, silicon has a much higher index of refraction. The index of silicon is about 3.5, as the figure below shows, while silicon dioxide has an index about 1.45. This large index difference allows for compact devices and a high degree of integration, making silicon an attractive PIC platform.

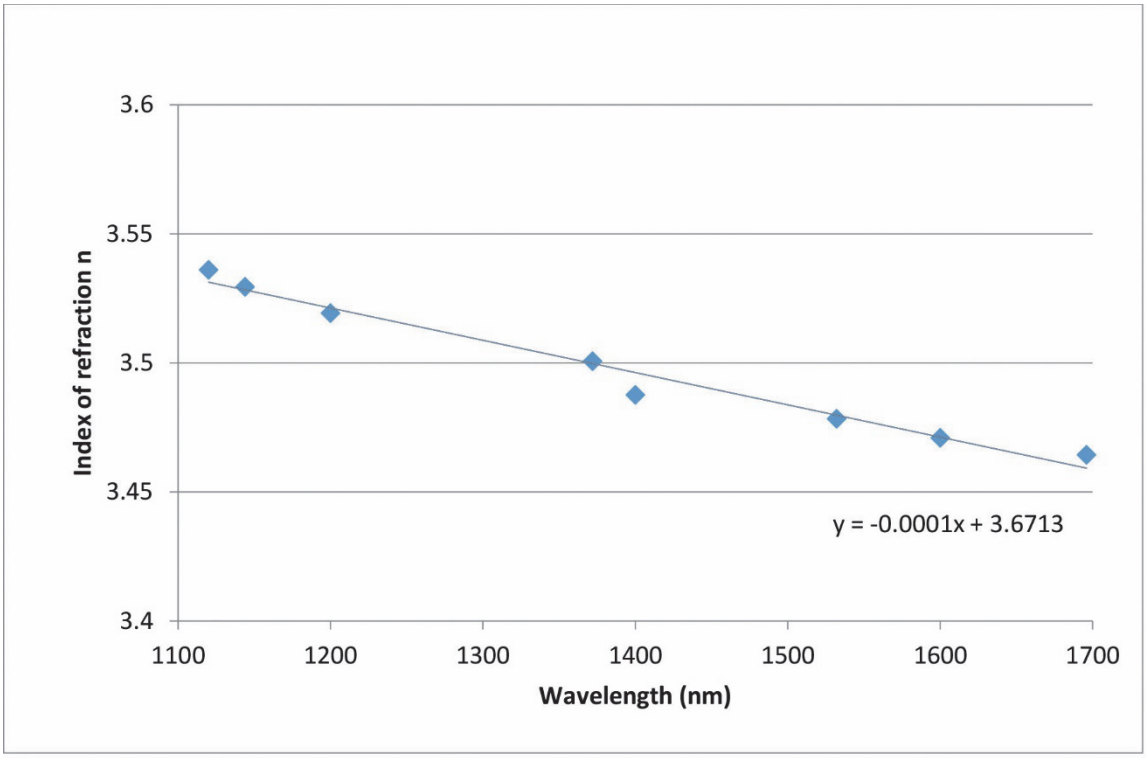

Figure 2-2 *Index of refraction of silicon vs. wavelength*

Figure 2-2 also shows that the index of refraction for silicon decreases with increasing wavelength. The phenomenon of index variation with wavelength is called *dispersion*. For wavelengths between 1100 nm and 1700 nm, the silicon index's dependence on λ can be approximated by a straight line with a decreasing slope equal to -1 x 10^{-4} nm^{-1}.

Silicon's index of refraction also varies with temperature, which is beneficial in certain devices but undesirable in others. Devices such as modulators exploit the index's change with temperature to effect changes in the device's output of optical power. On the other hand, filters and other resonant devices are based on a constant index of refraction and would become detuned if the index were to change as the ambient temperature changed. These latter devices require temperature stabilization to operate properly.

The change in index of refraction with temperature is expressed by the coefficient of variation with temperature, dn/dt. It is equal to the change in index corresponding to a one-degree change in temperature. Here the temperature change is expressed in units of Kelvin (absolute temperature). In the case of silicon, the coefficient of variation = dn/dt = 1.87 x 10^{-4} K^{-1}. As with the index of refraction, this parameter is higher for silicon than for silicon dioxide, whose coefficient is about 1.1 x 10^{-5} K^{-1}.

Active vs. Passive Devices

Photonic devices can be broadly classified as either *active* or *passive* devices. Active devices generate, amplify, or control light. They include lasers as optical sources, optical amplifiers, modulators, and others. Lasers produce light, while amplifiers take in an optical signal and

amplify its power. Active devices require an energy source to operate. The law of conservation of energy states that energy can be neither created nor destroyed; rather, it transforms from one form to another.

Amplification can be described by the *gain* parameter, which equals the ratio of output power to input power. The gain has values greater than 1, expressing the fact that amplification increases output power.

$$\text{Gain} = P_{out}/P_{in} \tag{2-1}$$

A characteristic parameter for lasers is their *efficiency*, which equals the ratio of the total optical output power to the pump power. This parameter describes how efficient these devices are in converting the energy of a pump source into output light energy. In the case of semiconductor lasers, the efficiency is the ratio of the output power to the electrical power used as a pump. Semiconductor-based lasers fabricated from III-V combinations of materials have a high efficiency of 60% and above.

$$\eta = P_{out}/P_{pump} \tag{2-2}$$

Passive devices perform operations on an incoming optical signal. Examples of passive devices include splitters, couplers, and filters. They are not intended to increase the optical power level and so do not require an energy source to operate. Ideally, the optical power at the output of a passive device should equal the input power. In reality, a small amount of power will be lost as the device operates on the light signal. The parameter that characterizes this is the insertion loss (IL), defined as the ratio of the total power at the output of the device to the input power.

$$IL = 10 \times \log_{10}(P_{out}/P_{in}) \tag{2-3}$$

The unit used for IL is the decibel, dB. The advantage of using dB as unit is that the total loss in the optical signal after it travels through a series of devices can be obtained simply by adding the ILs of all the devices.

Example 1

Calculating the insertion loss in dB. A light beam with 1 mW of optical power is incident on a passive PIC device. A power meter indicates that the output optical power is 0.95 mW. Find the insertion loss of the PIC device in dB.

Solution: $IL = 10 \times \log_{10}(P_{out}/P_{in}) = 10 \times \log_{10}(0.95/1.0) = -0.22$ dB

The negative sign in the IL above signifies that the output power is less than the input power. This correctly describes a loss of power. If Equation 2-3 were used to express the amplifier gain of an optical amplifier in dB, it would result in a positive value. Manufacturers of passive devices most often provide the IL values without the negative sign. Even so, remember that IL

expresses a loss of power equivalent to the reduction in power at the output compared with the input of the device.

Example 2

Insertion loss of an optical power coupler/splitter. An optical power coupler/splitter is a passive device that divides an input light beam into two output beams. Assume that the input light beam has a power of 1 mW and the two output beams have powers of 0.43 mW each. Calculate the insertion loss of the coupler.

Solution: The total output power is given by the sum of the powers of each of the two outputs.

P_{out} = 0.43 mW + 0.43 mW = 0.86 mW.

IL = 10 x $\log_{10}(P_{out}/P_{in})$ = 10 x $\log_{10}(0.86/1.0)$ = -0.66 dB

As previously mentioned, total loss from cascaded devices can easily be obtained by summing the losses from each device in the series.

Example 3

Calculate the total loss of an optical signal after it has propagated through two cascaded PIC devices with IL of -0.4 dB and -0.55 dB respectively.

Solution: IL_1 = -0.4 dB, IL_2 = -0.55 dB.

Total loss IL = $IL_1 + IL_2$ = -0.4 + (-0.55) = -0.95 dB.

Important applications of PIC devices at this time are in optical fiber communication systems and fiber optics networks. The following section summarizes the main characteristics of these systems and provides a background about the role that PIC devices play in them.

Optical Fiber Communication Systems

In optical fiber communication systems, the signals or data are transmitted in the form of pulses of light traveling through optical fibers. There are several important advantages of using light signals instead of electrical signals with copper wires. These include high transmission speed, very large capacity or bandwidth, less energy required to transmit the data, and insensitivity to electromagnetic interference.

Recall that the speed of light in vacuum is the highest speed in the universe, c = 3 x 10^8 m/s, and that it remains at the same order of magnitude when light travels inside a material such as glass. The large bandwidth comes from the very high frequency of the light that acts as signal carrier in fiber optics transmission systems. Infrared light with wavelength of 1.55μm has a frequency of 193.5 THz, which greatly exceeds the carrier frequency for electrical signals, which is at most on

the order of GHz. Another advantage of optical fibers related to data capacity is the ability to simultaneously carry light of different wavelengths without any interference between them. *Wavelength division multiplexing* (WDM) is a method that exploits this property to increase the capacity of transmission. It involves combining multiple signals of slightly different wavelengths and launching them in the same optical fiber. At the end of transmission, a process called *demultiplexing* separates the signals. Optical fibers carry light signals with powers on the order of milliwatts, resulting in less energy used in transmission. Finally, light signals traveling through optical fibers are immune to electromagnetic interference.

The basic components of a communication system are a *transmitter*, a *transmission medium*, and a *receiver*. In the case of an optical fiber transmission system, the transmitter impresses the data in the form of an electrical signal onto a light source, resulting in pulses of light that are sent over the optical fiber serving as the transmission medium. At the receiving end, a detector converts the light back into an electrical signal, which the receiver then processes. Recently, manufacturers have introduced devices called *transceivers,* which combine the transmitting and receiving circuits into one device. Figure 2-3 shows the components of a basic optical fiber transmission system.

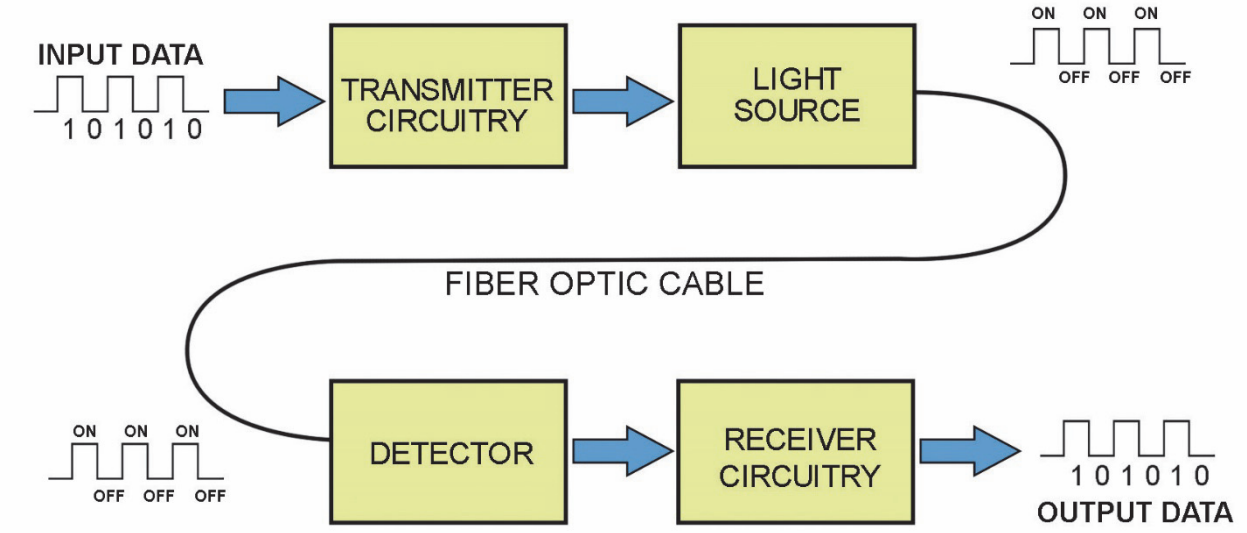

Figure 2-3 *Components of a basic optical fiber transmission system*

Optical fiber transmission systems can be classified as long haul, regional, or metropolitan, depending on the distance covered. Long haul systems extend over thousands of miles to connect states, countries, and continents. Regional and metropolitan systems cover shorter distances and do not require the very high level of performance that long haul systems do. Figure 2-4 illustrates the different types of systems and their interconnections.

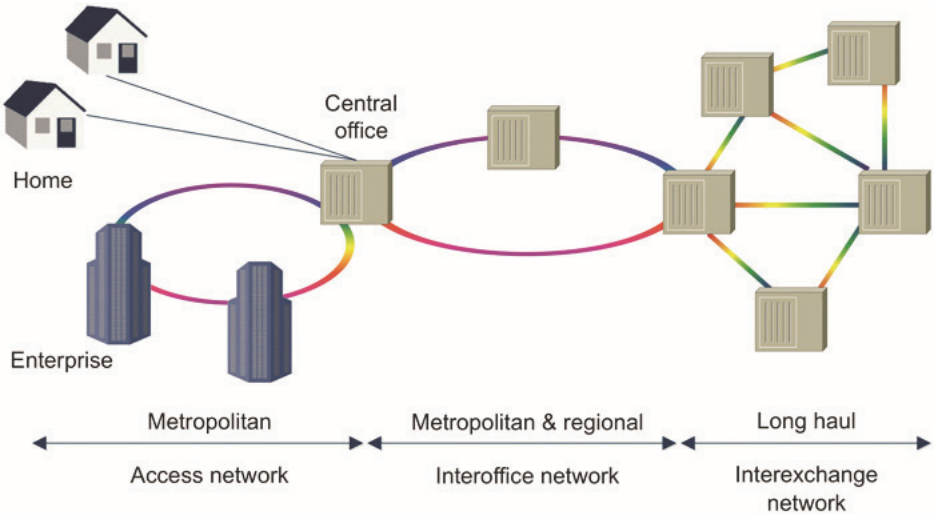

Figure 2-4 *Long haul, regional, and metropolitan networks*

Optical fiber transmission systems, and long haul systems in particular, need to address two issues associated with optical fibers: attenuation and dispersion. *Attenuation* is the gradual loss of optical power due to absorption and scattering of the light in the fiber material. Attenuation can be described by an attenuation coefficient expressed in units of inverse centimeters, similar to the absorption coefficient. (For example, from Figure 2-1 we can find that the absorption coefficient of crystalline silicon at a wavelength of 800 nm is about 10^3 cm^{-1}.) Alternately, we can look at the loss of power per unit length of optical fiber expressed in units of dB/km. Figure 2-5 shows fiber loss in relation to wavelength. The figure indicates the attenuation maxima due to light absorption by water molecules, as well as the regions with minimum attenuation. As illustrated, the minimum loss occurs at the wavelengths of 1310 nm and 1550 nm (1.31 μm and 1.55 μm). For this reason, the wavelengths around these values have been chosen as transmission bands for the light signals in fiber optic communication systems.

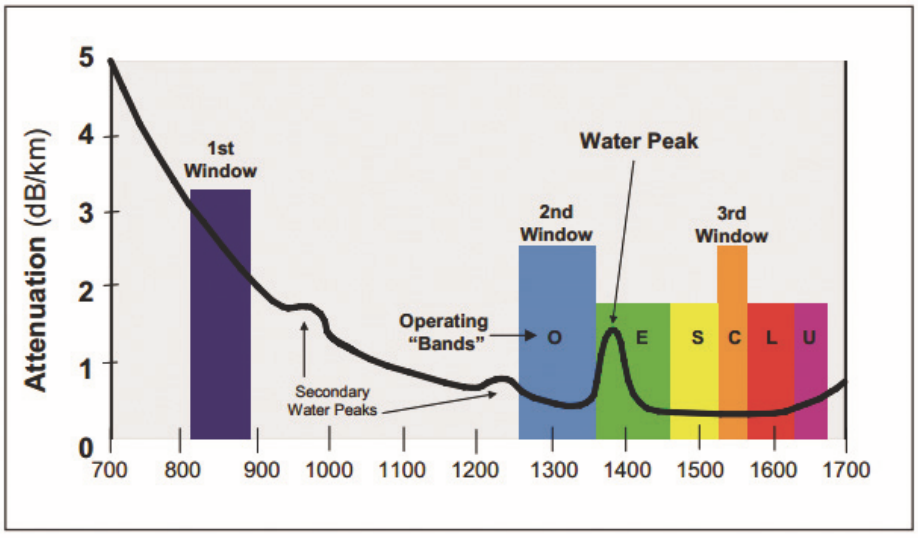

Figure 2-5 *Loss of power in optical fibers vs. wavelength*

Dispersion is the second characteristic that affects how optical fibers transmit light over long distances. Dispersion is caused by the variation of the index of refraction of glass with wavelength. Recall that the speed of light in a material is given by v = c/n. Because n depends on wavelength, different wavelengths travel with different speeds inside the fiber. A pulse of light transmitted through a fiber contains a range of wavelengths, which tend to separate from one another during travel due to dispersion. The net effect is pulse spreading, as shown in Figure 2-6. Two neighboring pulses that have spread out due to dispersion can overlap to the point that the receiving circuits will not be able to interpret them correctly, creating an error in the received signal. To avoid such errors, pulses need to be kept well separated, which means a slower transmission rate or bit rate.

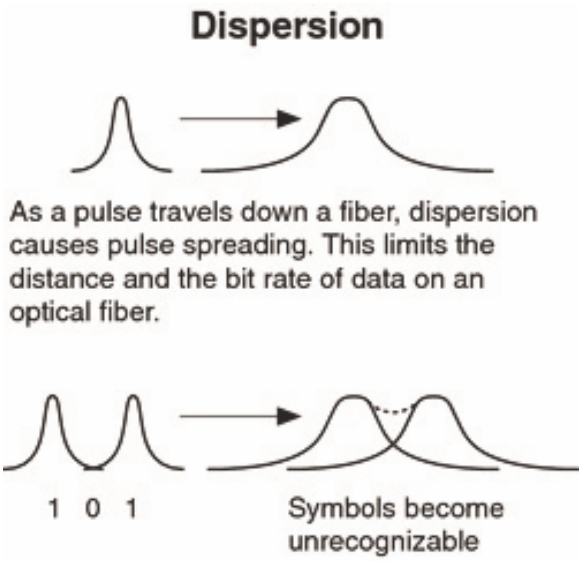

Figure 2-6 *Effect of dispersion on light pulses transmitted through optical fibers*

Single-mode fibers used in long haul transmission have a very small loss coefficient, lower than 0.2 dB/km. Due to the very large distances covered, even this small coefficient of loss results in a reduction of the optical power to levels that detectors cannot sense.

Example 4

Light is transmitted through a 500 km-long fiber with a loss coefficient of 0.2 dB/km. Find the loss of optical power at the end of the fiber.

Solution: Total loss of power = 0.2 dB/km x 500 km = 100 dB

In addition to the power loss caused by attenuation, light pulses are spread out due to dispersion as previously discussed. One solution to both problems is to regenerate the signal every hundred kilometers or so. This is achieved by converting the optical signal to an electrical signal, recreating it according to the original using electronic circuits, converting it back into an optical

signal, and reintroducing it in the fiber. Figure 2-7 shows a system that uses this approach. This system uses a *regenerator* (also called a *repeater*) for this purpose.

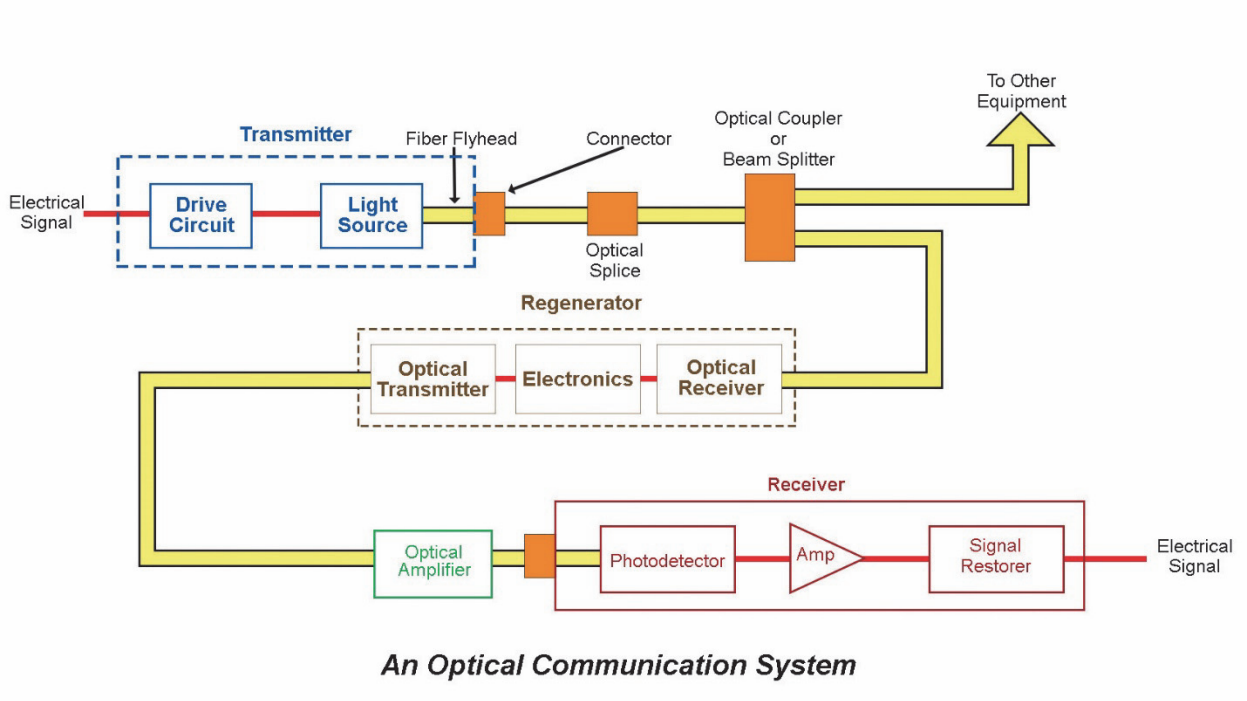

Figure 2-7 *An optical communication system that regenerates the light signal along the transmission path*

Another solution—one based on optical amplifiers—has been introduced in an effort to bring the signal power back up. Using optical amplifiers is advantageous because they operate directly on the optical signal, thus avoiding the expensive conversions between electrical and optical domains. Figure 2-8 shows such a system. The optical receiver here includes a transimpedance amplifier (TIA), which amplifies the current created by the photodiode.

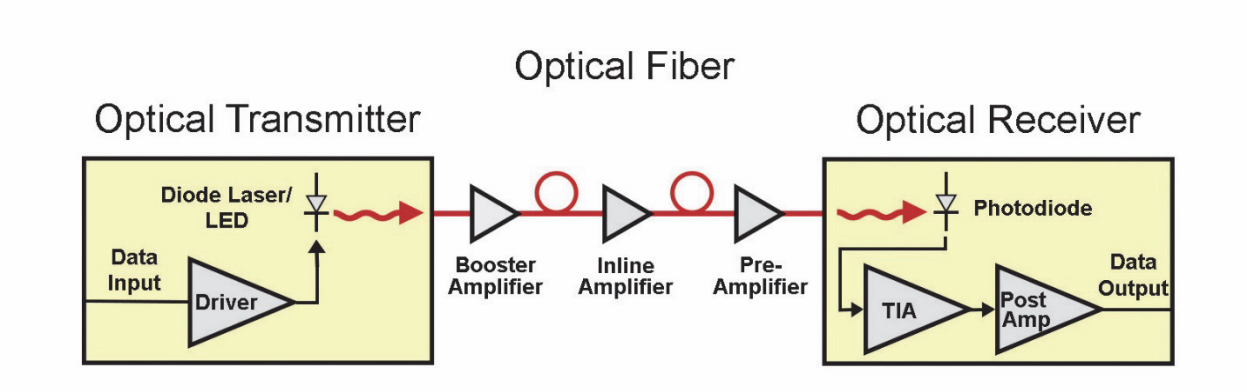

Figure 2-8 *An optical communication system that amplifies the light signal along the transmission path*

Optical amplifiers can boost the signal's power level, but they cannot correct for the effect of dispersion. Figure 2-9 illustrates the effect of an amplifier and the effect of a repeater on a hypothetical pulse that has experienced loss of power and distortion due to attenuation and dispersion. Transmission systems today incorporate repeaters and amplifiers. The advantage of introducing amplifiers is that they have increased the distance between repeaters to several hundred or even a few thousand kilometers. Specialty optical fibers with lower dispersion have also been created and are in use in systems today.

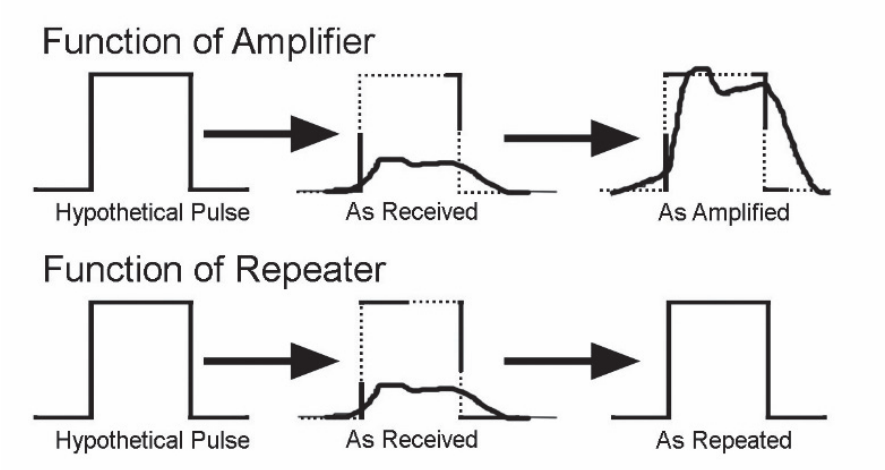

Figure 2-9 *Effect of an amplifier vs. a repeater on a degraded optical signal*

Silicon Photonic Integrated Circuits

Photonic integrated circuit devices play important roles in optical fiber transmission systems as well as in other applications such as sensors and optical interconnects. In transmission systems, PICs are part of all the system components except for the optical fiber itself. PICs can be active devices or passive devices. It is important to note that while there are many PICs deployed in current optical communications networks, very few of these are silicon PICs.

A *light source*, a *modulator*, and a *photodetector* are examples of active devices. In the transmission systems shown in Figures 2-7 and 2-8, the transmitter circuit incorporates a light source, typically a laser diode or LED. The output of the laser diode or LED must be switched between an "on" state and an "off" state according to the digital data signal, a series of square pulses with values of 1 ("on") or 0 ("off"). One way to do this is to control the electric current running through the diode. Another option is to operate the laser diode in continuous wave mode and use an external modulator after the laser. Modulators are devices that can control the amount of output light. The receiver circuit incorporates a photodetector.

A wide range of passive devices are also used in optical fiber transmission systems and other applications. These include couplers, splitters, Mach-Zehnder interferometers, ring resonators, Bragg gratings, arrayed waveguide gratings, and others. These devices can be thought of as building blocks that we use to create systems that perform complex functions. Fundamental passive and active silicon PIC devices are described below; systems are described in a later module.

Passive Silicon PIC Devices

Silicon-on-Insulator Optical Waveguide

As described in Module 1, the basic component of a PIC device is the *optical waveguide*, which most commonly has a geometry described by a channel or a ridge. The material structure that is used most often to fabricate silicon PIC devices is *silicon-on-insulator (SOI)*. The SOI structure is created on a silicon wafer with a typical thickness of 725 μm. The diameter of the wafer is usually 8" (200 mm), but larger wafers with 300 mm diameters are increasingly being used also.

Figure 2-10 a) shows the layer structure of SOI. The typical layer thicknesses are 2 μm for the buried oxide (BOX) layer deposited on the Si substrate and 220 nm for the crystalline Si layer supporting the propagation of light. The upper cladding can be air or another layer of silicon dioxide. Using an oxide upper cladding, rather than air, protects the silicon waveguides and allows for thin film heaters to be deposited for thermo-optic applications in which heat is applied to the waveguides to change their index of refraction. An oxide upper cladding also makes the waveguide more symmetric, which improves its polarization properties. Figure 2-10 b) shows a cross section of a channel waveguide (also called a strip waveguide). Light travels in the z direction perpendicular to the page. The length of the waveguide in the z direction is typically less than 1 mm.

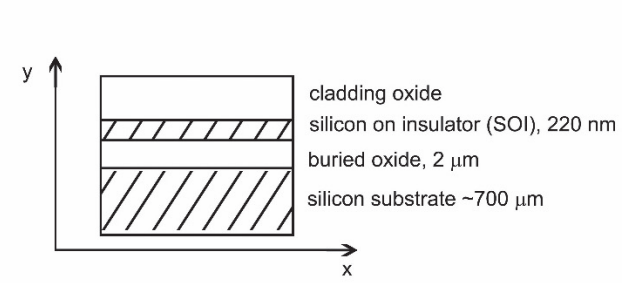

Figure 2-10 a) *SOI material structure*

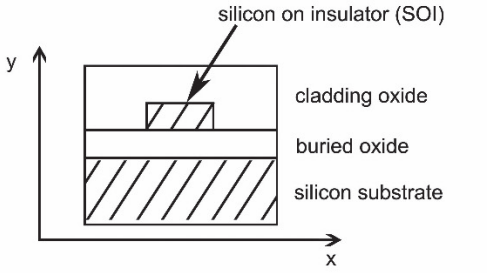

Figure 2-10 b) *Channel (or strip) SOI waveguide*

SOI waveguides have a higher propagation loss than waveguides realized in other material platforms. One component of the loss, due to sidewall roughness, is 2-3 dB/cm. However, SOI waveguides are more compact, and the short length of the devices compensates for some of the higher loss per unit of length.

Example 5

An SOI waveguide 500 μm long has a propagation loss of 2.5 dB/cm. A silicon dioxide (silica) waveguide has a 0.1 dB/cm propagation loss and a length of 2 mm. Find the loss at the end of each waveguide.

Solution: Total loss of power for SOI waveguide = 2.5 dB/cm x 0.05 cm = 0.125 dB

Total loss of power for silica waveguide = 0.1 dB/cm x 0.2 cm = 0.02 dB

Parameters Describing SOI Optical Waveguides

An optical waveguide is described by the indices of refraction of the core and cladding layers and the physical dimensions of the core. The indices of refraction are specific to the materials used for core and cladding. Once these materials are chosen, the indices become known and can be used to calculate quantities of interest when designing waveguides and PIC devices. For an SOI waveguide, the indices of refraction of the SOI layer and the oxide layers at a wavelength of 1550 nm are 3.473 and 1.444 respectively. The index contrast between these two materials is very high and allows for light confinement in very small waveguides, resulting in very compact devices.

Both indices increase linearly with temperature, but the increase is smaller for oxide than for silicon. For silicon, the coefficient of variation = $dn/dt = 1.87 \times 10^{-4}\ K^{-1}$, while for oxide (silica), $dn/dt = 1.1 \times 10^{-5}\ K^{-1}$.

Equation 2-4 gives the index variation with temperature:

$$n(T_2) = n(T_1) + dn/dt * (T_2 - T_1) \tag{2-4}$$

The temperature difference of $T_2 - T_1$ should be expressed in Kelvin or Celsius. If temperatures are provided in Fahrenheit, a conversion will be necessary before Equation 2-4 can be used.

Example 6

Finding the index of refraction of silicon and silica at a temperature of 75 °C. Assume that the indices of refraction at room temperature (21°C) are the ones provided above. Calculate the indices of refraction at 75 °C.

Solution:

For silicon $n(T_2) = n(T_1) + dn/dt * (T_2 - T_1) = 3.473 + 1.87 \times 10^{-4} * (75 - 21) = 3.483$

For silica $n(T_2) = n(T_1) + dn/dt * (T_2 - T_1) = 1.444 + 1.1 \times 10^{-5} * (75 - 21) = 1.445$

Using the solution from Example 6, we can see that with this temperature change, the change in index of refraction for silicon is 0.01, while the change for silica is only 0.001. Because silica's index of refraction changed so little compared with silicon's, when we design devices based on the thermo-optic effect, we can ignore the change in the oxide index with temperature and take into account only the change in index of silicon.

Effects of Geometry on a Channel Waveguide

The width of the channel waveguide depends on specific requirements. In high performance optical transmission systems, devices are based on single-mode (SM) waveguides, which only allow propagation of the fundamental mode. This imposes an upper limit on the waveguide width. For the parameters given above, the upper limit for the SM waveguide width is about 440 nm. This upper limit value is obtained through numerical computation because the equations

governing the propagation of light in such waveguides cannot be solved analytically. There are several modeling software packages available to determine all parameters relevant to planar waveguides. A later module provides a basic introduction to one of these packages.

There are advantages to having waveguides that are slightly wider than the maximum value dictated by the SM condition. Wider waveguides have lower propagation losses (below the 2-3 dB/cm previously described) and also allow for tighter bends in a bend optical waveguide. SOI waveguides with widths of 500 nm are used in practice. Even though they are not technically single mode, they can behave that way if care is taken not to excite higher order modes during light propagation in the waveguides.

Once the waveguide width is chosen, the entire waveguide is defined, including indices of refraction and waveguide dimensions. The next step is to determine the waveguide's *effective index*, n_{eff}. This is done, once again, using computer software programs. The effective index can be used in the design of any number of devices that use a waveguide. Recall that the phase of an electromagnetic wave of wavelength λ traveling a distance L inside a medium with index of refraction n is given by:

$$\Phi = (2\pi/\lambda)\, n\, L \tag{2-5}$$

In the case of a wave confined inside a waveguide with effective index of refraction n_{eff}, the phase is again calculated using the formula above, in this case with the effective index replacing the general index n.

$$\Phi = (2\pi/\lambda)\, n_{eff}\, L \tag{2-6}$$

When determining the effective index of a waveguide, there will generally be two solutions, even in the case of SM waveguides. The two solutions will correspond to two possible polarizations for light traveling inside the waveguide, TE and TM. Recall that TE and TM stand for *transverse electric* and *transverse magnetic* and reflect the light's property as a transverse wave. In the case of TE, the electric field vector is perpendicular to the direction of propagation of the wave, while in the TM case, the magnetic field vector is perpendicular to the direction of propagation of the wave.

Because the two effective indices for TE and TM polarizations are different, the device can experience some performance degradations due to the different speeds of travel of TE and TM components inside the waveguides. The difference between the two effective indices is called waveguide *birefringence*, Δn_{eff}.

$$\Delta n_{eff} = n_{eff}^{TM} - n_{eff}^{TE} \tag{2-7}$$

SOI waveguides have high birefringence, a consequence of the high index contrast between core and cladding. Various methods can be applied to counteract the negative effects of waveguide birefringence: operating with polarized light (either TE or TM), using a special waveguide design to bring the n_{eff}^{TE} and n_{eff}^{TM} close to each other, inserting components that compensate for the effects of birefringence, or separating the two polarizations and balancing their pathways through the waveguides (polarization diversity). Each of these methods has specific advantages and disadvantages that we discuss in a later module.

Table 2-1. Complete Waveguide Parameters for a Typical SOI Waveguide

Single-mode channel SOI waveguide	
Parameter	**Value**
SOI thickness, h	220 nm
SOI width, w	500 nm
Index of refraction of silicon at 1550 nm and room temperature, n_{SOI}	3.473
Index of refraction of silica at 1550 nm, and room temperature, n_{oxide}	1.444
Effective index TE mode, n_{eff}^{TE}	2.35
Effective index TM mode, n_{eff}^{TM}	1.70
Waveguide birefringence	-0.65

Bend Optical Waveguide

PIC devices are almost never constructed exclusively from straight waveguides. Often it is necessary to have light emerge from a different location than directly across from the input to the device. In other devices, waveguides must be brought close to each other for a certain distance and then separated again, such as in the case of the *directional coupler* shown below. This requires using *bend waveguides* to connect straight portions of the waveguides. Bend waveguides are generally circular arcs. The bends in the figure below are S-bends, created by smoothly attaching two arcs, one bending one way and one the other way. S-bends do not change the light's direction of propagation. Other bend waveguides can be 90° arcs that change the initial direction of propagation of the light to a perpendicular one.

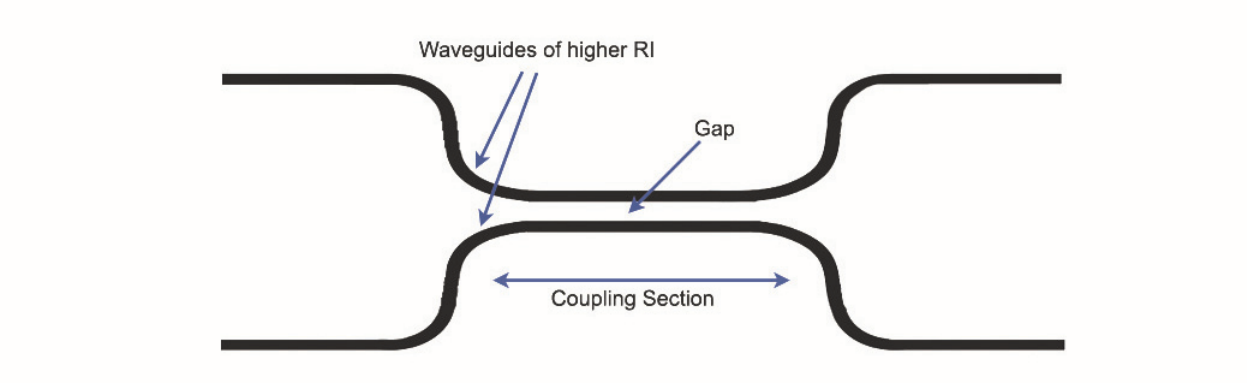

Figure 2-11 *Directional coupler device containing four S-bend waveguides to bring waveguides close to each other and then separate them*

The parameter that characterizes bend waveguides is the radius of curvature, R. As discussed in Module 1, if the radius of curvature is too small, light leaks out of the waveguide as the total internal reflection condition is violated. This results in loss of optical power through radiation. To keep the bend losses negligible, the radius of curvature must be kept above a minimum value, which introduces a trade-off between device loss and footprint. The designer of the device will use the minimum value for bend radius while creating a layout that minimizes the device's footprint.

Light in an SOI waveguide is tightly confined inside its 500 nm width due to the large index contrast between the waveguide's silicon core and its oxide cladding. This allows for very small values for the minimum radius of curvature of the bend portions. Minimum radii of curvature for SOI waveguides are 10 µm or below, and bends with very low losses have been obtained. For example, loss has been measured to be 0.01 dB for a 90° bend with a 5 µm radius of curvature. Bends with such a small radius of curvature occupy a small footprint and help keep a device's overall dimensions compact.

Input/Output Coupling to Silicon PIC Devices

As described in the introduction to the module, optical fibers connect various PIC devices to one another. Optical fibers also form the transmission medium in optical transmission systems. The optical signal transfers from an optical fiber to a PIC device and back multiple times in transmission systems and other applications. It is desirable to efficiently couple light from an optical fiber to a PIC device.

A single-mode (SM) optical fiber has a low index contrast between core and cladding, about 0.35%, so the diameter of the fiber is much larger than the width of the SOI waveguide. A typical SM optical fiber has an 8-10 µm diameter, while an SOI waveguide has a cross section of 500 nm x 220 nm. Due to the very different refractive index contrasts, sizes, and shapes in cross section, a mismatch exists between the distribution of light in the cross section of an optical fiber and the distribution of light in the SOI waveguide. This makes efficient coupling of light from an optical fiber to an SOI waveguide and vice versa very challenging. Figure 2-12 illustrates the TEM_{00} mode (the lowest order transverse electromagnetic mode) of a single-mode fiber and the fundamental mode of an SOI waveguide; the horizontal and vertical units are microns in both figures.

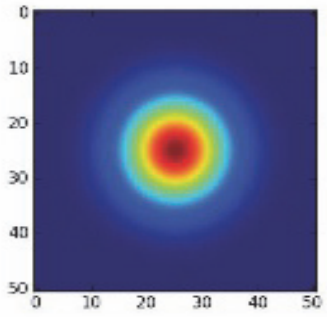

Figure 2-12 a) *Light distribution in optical fiber (TEM_{00})*

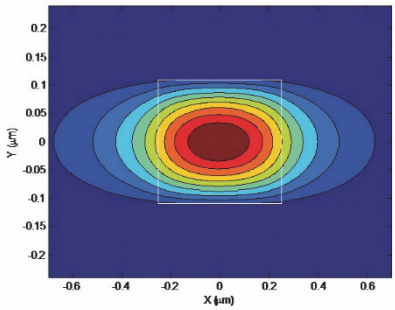

Figure 2-12 b) *SOI waveguide*

Due to the mode mismatch, an optical power loss in excess of 10 dB takes place when the SM fiber is directly attached to the SOI waveguide (a method called *butt coupling*). To avoid this large loss, alternate coupling methods have been found. They are briefly described below and illustrated in Figure 2-13.

End-fire coupling

In this method, a lens is used to focus the light from the optical fiber onto the waveguide facet. Due to the very small, submicron dimensions of the SOI waveguides, this method is difficult to implement and is not used with this type of waveguide.

Grating coupling

A grating is a periodic structure that can diffract light and change its direction of propagation. An SOI waveguide grating coupler can be created by introducing a periodic corrugation at the top of the SOI layer. Light from the optical fiber is incident at an oblique angle onto the SOI waveguide. When the *phase-matching condition* (constructive interference) is met, the SOI waveguide captures a large fraction of the light carried by the optical fiber. The period of the grating (the distance between two successive corrugations) is the most important parameter that determines the coupling efficiency from fiber to waveguide. Efficiencies of 50–60% have been achieved with grating periods between 600 nm and 700 nm. The primary limitation of this method is that for a given grating period only a relatively narrow band of input wavelengths can be efficiently coupled.

Coupling using a spot-size converter

A spot-size converter is a device that gradually converts the fundamental mode of the SOI waveguide to a mode close to the TEM_{00} mode of the optical fiber. To achieve this, the width of the SOI waveguide is gradually tapered down from 500 nm to 180 nm, as shown in Figure 2-13 d). The length of the taper is around 100 µm. Such a spot-size converter is capable of reducing the coupling loss from 10 dB or more, with butt coupling, to a much lower value of around 0.5 dB. The nonzero loss is due to the fact that the expanded mode at the end of the taper does not exactly match the fiber TEM_{00} mode.

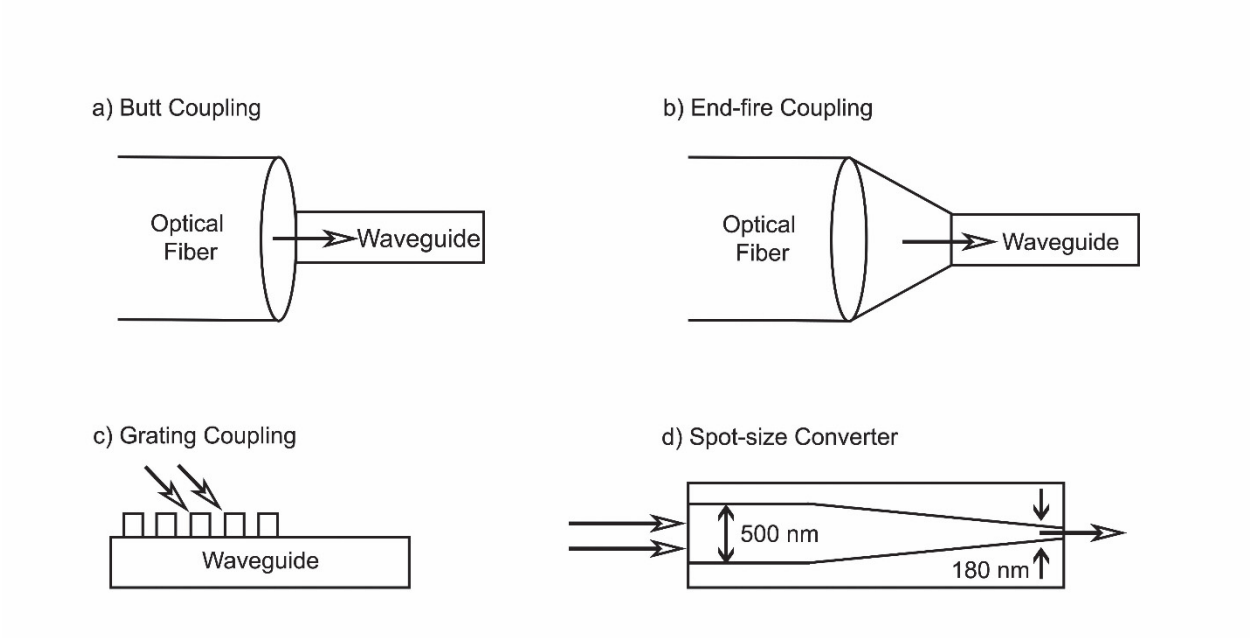

Figure 2-13 a) *Butt coupling*; **b)** *End-fire coupling;* **c)** *Grating coupling;* **d)** *Spot-size converter*

Loss at the interface between the optical fiber and the SOI waveguide is compounded by other factors. The waveguide facet must be very well polished before the fiber attachment is created. Another factor is the alignment between the fiber and SOI waveguide. The fiber must be actively aligned to the waveguide to minimize the misalignment loss. This is done by monitoring the optical power in the waveguide while the fiber moves in the x, y, and z directions. The fiber is permanently attached to the waveguide when the maximum power is obtained. Active alignment is a complex and expensive process.

Another source of loss is reflection at the interface between media with different indices of refraction. The Fresnel coefficients allow us to calculate the amount of reflected light in this case. For normal incidence, the fraction of optical power reflected is given by Equation 2-8, where n_1 is the index of medium 1 and n_2 is the index of medium 2. The reflected power fraction is the same when traveling from medium 1 to 2 as from medium 2 to 1.

$$R = [(n_1-n_2)/(n_1+n_2)]^2 \tag{2-8}$$

For example, the percentage of optical power reflected and thus lost at the interface between glass and air at normal incidence is about 4%. In many cases, SOI waveguides use antireflection coatings to reduce losses due to reflection, since the index difference between optical fiber and silicon is close to 2.

Directional Coupler

A directional coupler is another fundamental building block of PIC devices. It is used both as a stand-alone device and as part of other components. The function of a directional coupler is to split or combine light. It consists of two parallel waveguides that are initially well separated, then brought close together in the coupling region, and then separated again, as shown in Figure 2-14. In the coupling region, due to the close proximity, the waveguides interact with one another, in the sense that light starts to transfer from one waveguide to the other. The distribution of light in the fundamental mode of an SOI waveguide was illustrated on the right side of Figure 2-12, together with the waveguide core edges in white. As that figure shows, the electromagnetic field extends outside the waveguide core and decreases in intensity as it moves away from the core. The field outside the core is called the *evanescent field*. When two parallel waveguides are brought close together, the evanescent field of the waveguide carrying the light extends over the second waveguide, and this is enough to excite or initiate a guided mode in the second waveguide.

If the coupling region is long enough, 100% of the light will transfer to waveguide 2, and then it will gradually transfer back to waveguide 1. The directional coupler can be designed to achieve any split of the optical power between the two waveguides by adjusting the length of the coupling region or the gap between the waveguides. A common use of the directional coupler is to split the light equally between the two waveguides, in which case the device is called a 3dB directional coupler. Figure 2-14 shows the main parameters that determine the power split between two waveguides: the gap between the waveguides in the coupling region, labeled S, and the length of the coupling region, L. With SOI waveguides, the gap can be as small as 200 nm. The coupling length, denoted by L_c and defined as the length at which 100% of the light transfers to the second waveguide, is around 40 μm.

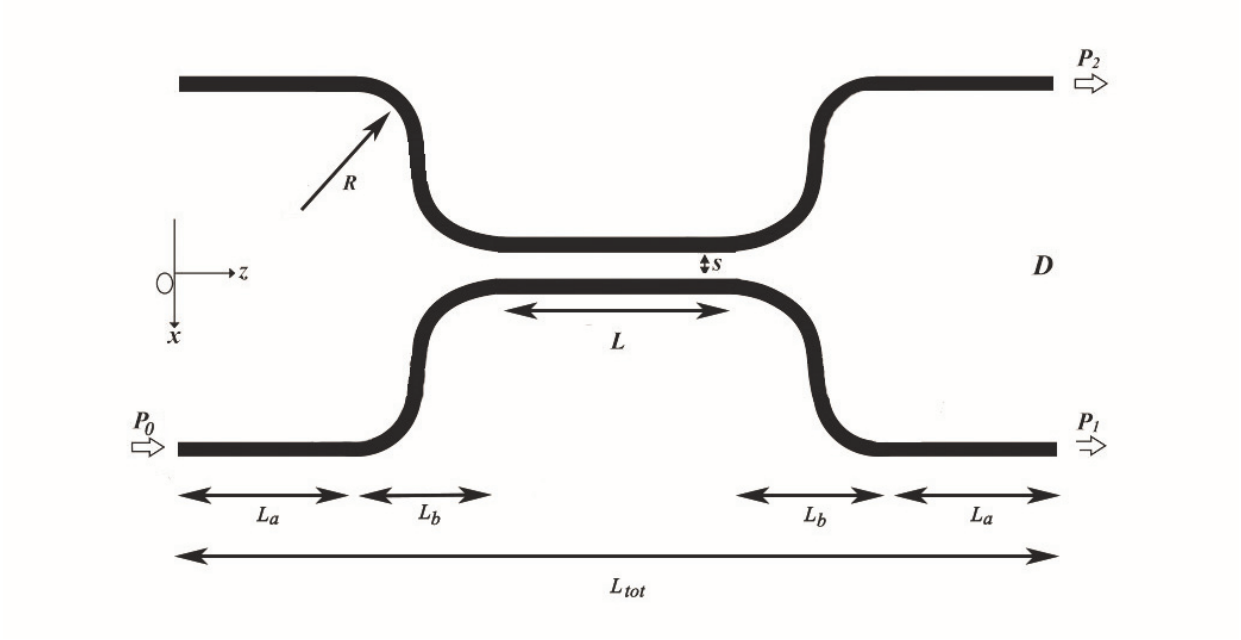

Figure 2-14 *Directional coupler splitting the incident power P_0 into powers P_1 and P_2 in the two output waveguides*

Directional couplers can be described by a coupling coefficient, K. The optical power in each of the two output waveguides is given by the following set of equations, where P_0 is the initial power carried by waveguide 1 and L is the length of the coupling region:

$$P_1(L) = P_0 \cos^2(KL) \quad (2\text{-}9\ a)$$
$$P_2(L) = P_0 \sin^2(KL) \quad (2\text{-}9\ b)$$

To find the coupling length, L_c, that is, the length at which 100% of the light transfers to the second waveguide, we need to set $P_1(L_c) = 0$ and $P_2(L_c) = P_0$. Using Equations 2-9a and b, we find: $\cos^2(K\ L_c) = 0$, and $\sin^2(K\ L_c) = 1$. Solving for L_c, we find:

$$L_c = \pi/(2K) \quad (2\text{-}10)$$

Similarly, for a 3dB coupler, we want an equal split of the power between waveguides 1 and 2. That means $P_1(L) = P_2(L) = P_0/2$. Using Equations 2-9a and b, we find: $\cos^2(KL) = \sin^2(KL)$, or $\tan^2(KL) = 1$. Solving for L, we find:

$$L_{3dB} = \pi/(4K) \quad (2\text{-}11)$$

Directional couplers can also be used as combiners by reversing the direction that light travels. For example, in Figure 2-14, if light enters the device at P_1 and P_2 from the waveguides on the right and is combined into one output, P_0, in the lower waveguide on the left, then the two waves are coherent.

In general, directional couplers are very sensitive to fabrication process variations. One of the challenges of the fabrication process is to maintain a high level of uniformity across the entire silicon wafer. Variations in waveguide width happen, and these also affect the gap between

waveguides. When the width decreases, the gap between waveguides increases, and when the width increases, the gap between waveguides decreases. For this reason, the power split between the two output waveguides will not be the same for all couplers. The power split of the coupler is also slightly dependent on the wavelength of the light.

Directional couplers also illustrate the phenomenon of *crosstalk*, or unwanted transfer of light between parallel waveguides. Power transfer between two waveguides is desirable in the case of the directional coupler, but in other cases we might encounter waveguides running parallel to one another in a device where each waveguide must remain isolated from the others. For such waveguides, there is a minimum separation distance, or gap, that prevents the waveguides from interacting. This distance is around 1.5 to 2 μm in SOI waveguides. With this gap, the resulting crosstalk will be less than -50dB in a 1 cm distance.

Y-Branch

A Y-branch is a device that performs the same function as a directional coupler: power splitting or combining. The device consists of a waveguide that branches into two identical waveguides, as shown at the top of Figure 2-15. When used as a splitter, the Y-branch divides the power evenly between the two outputs. In this sense, it is a simpler device than a directional coupler. As is the case with all devices, the Y-branch has a nonzero insertion loss (IL), meaning that the sum of the two output powers is slightly less than the input power. Design optimized Y-branches have IL < 0.5 dB. When used as a combiner, if the waves traveling in the two waveguides are in phase, the optical powers combine to double the power in the output waveguide (minus the IL). However, if the waves are out of phase, destructive interference will occur and result in zero power at the output.

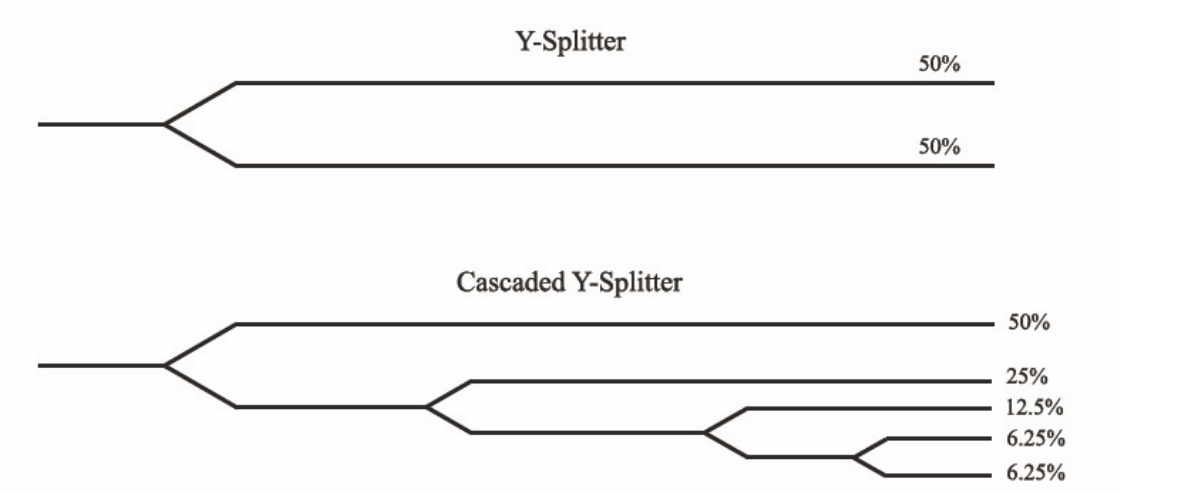

Figure 2-15 *Top: Single Y-branch splitting the incident power into equal powers in the two output waveguides. Bottom: Cascaded Y-branches.*

Y-branches can be used by themselves or as part of more complex devices. They can be cascaded to obtain various power fractions in the output waveguides. The bottom image in Figure 2-15 illustrates a device with five outputs with decreasing amounts of power in

waveguides one through four. Figure 2-16 illustrates the layout of a Y-branch in more detail, including the S-bends used to separate the two output waveguides.

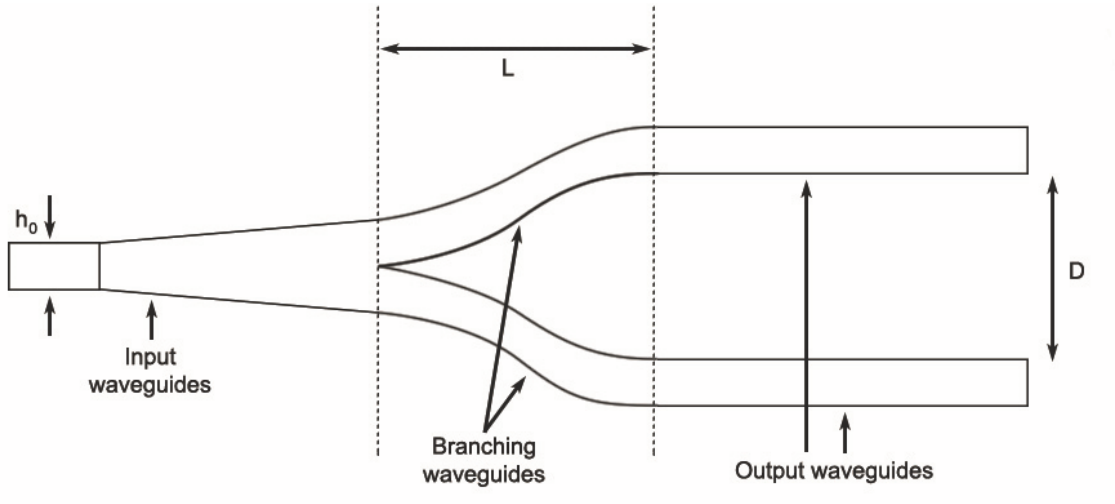

Figure 2-16 *Detailed layout of Y-branch device*

Mach-Zehnder Interferometer

Interferometers are devices based on the phenomenon of wave interference. Interferometers are configured in several ways and are used in a large number of optics and photonics applications. The Mach-Zehnder interferometer (MZI) uses one source of light split into two waves that travel through different pathways before being brought back together and allowed to interfere. Depending on the accumulated path difference between the two waves, the resulting optical power can vary from zero (destructive interference) to a maximum power (constructive interference).

In PIC devices, MZIs are constructed from two power splitting/combining elements connected by two interferometer arms, as shown in Figure 2-17. For power splitting and combining, either 3dB directional couplers or Y-branches can be used.

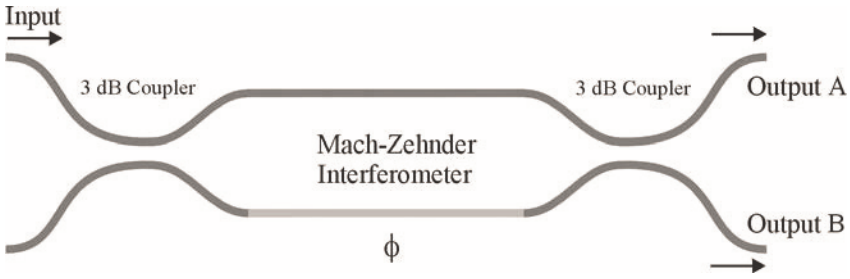

Figure 2-17 *Mach-Zehnder interferometer based on 3dB directional couplers*

The two interferometer arms have different optical path lengths; in the figure the top arm is the reference arm. Consequently, the waves traveling in the two arms accumulate a phase difference of Φ. The two waves interfere in the combiner and, depending on how large Φ is, produce various power outputs in the output waveguides A and B.

The different optical path length in the bottom arm can be produced in several ways. One option is to design the device such that this arm is geometrically longer. Assume the reference arm has a length L_1, and the bottom arm has a length $L_2 > L_1$. In this case, the device will act as a passive device, and the arms will have a fixed phase difference. Because power output is dependent on Φ (see Equations 2-14a and b, below), the power in the output waveguides A and B will also be fixed. The phase difference for a passive MZI is given by Equation 2-12, where λ is the wavelength and n_{eff} is the effective index of the two waveguide arms.

$$\Phi = (2\pi/\lambda)\, n_{eff}\, (L_2 - L_1) \tag{2-12}$$

PIC MZI devices are much more useful as active devices, which allow the amount of power in waveguides A and B to be controlled by changing the phase Φ. One way to achieve this is by changing the effective index (n_{eff}) of the bottom waveguide. It is possible to use the thermo-optic effect by depositing a thin film heater directly above the bottom waveguide. The thin film heater is a resistor that radiates heat when electric current runs through it. In this case, even though the geometrical length can be kept the same, the effective indices of the top and bottom waveguides will not be the same due to the increased heat experienced by the bottom waveguide (recall Equation 2-4 and the variation of index with temperature). The phase difference is now obtained using this equation:

$$\Phi = (2\pi/\lambda)\, (n_{eff}^{\ bottom} - n_{eff}^{\ top})\, L \tag{2-13}$$

By varying the electric current through the thin film heater, it is possible to change the effective index $n_{eff}^{\ bottom}$ and thus change the phase difference Φ, while $n_{eff}^{\ top}$ stays constant.

The dependence of the output powers A and B on the phase difference is given by Equations 2-14a and b. P_0 denotes the input power. To simplify the calculations, the two equations assume zero insertion loss.

$$P_A = P_0 \sin^2(\Phi/2) \tag{2-14 a}$$
$$P_B = P_0 \cos^2(\Phi/2) \tag{2-14 b}$$

Figure 2-18 shows a graph of the two output powers as a function of Φ. Part a shows the ratio of output powers to input power, while part b shows these ratios expressed in dB, the customary unit for PIC devices' power output.

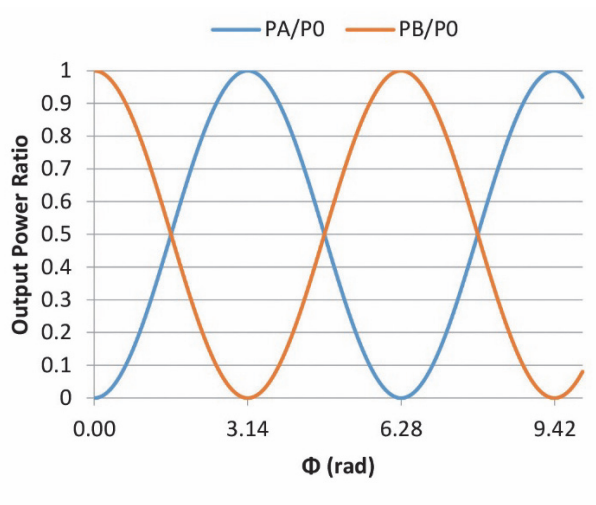

Figure 2-18 a) *Output powers A and B, normalized to input power as a ratio vs. the phase difference between the interferometer arms*

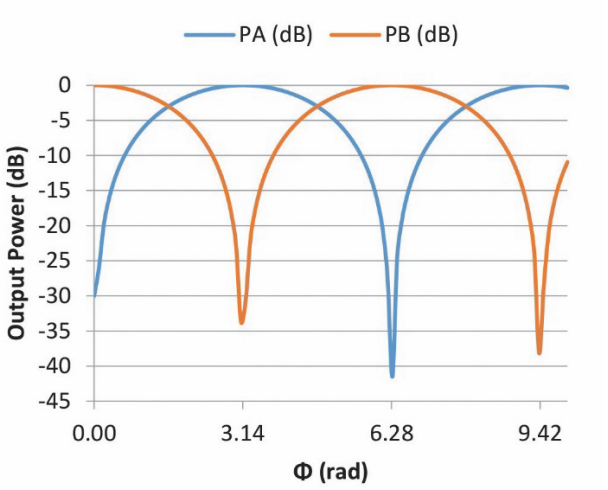

Figure 2-18 b) *Output powers A and B, expressed in dB vs. the phase difference between the interferometer arms*

From the two equations and the graph, we can see that for a phase difference equal to zero, the input power emerges completely from output B (the lower arm), and power in output A is zero. The situation changes completely when the phase difference equals π, or 3.14. In this case, output power B becomes zero, and the entire input power exits from output A. This behavior is exploited in devices called *switches*; these devices are capable of switching light between outputs A and B under user control.

To switch the output from B to A, the phase difference Φ needs to be changed from 0 to π. Assuming a typical length of 50 μm for the arms and a wavelength of 1.55 μm, we can use formula 2-13 to get the necessary index change between the bottom and top waveguides of a switch device, as well as the temperature change necessary to create this index change.

Example 7

Find the effective index change between the two interferometer arms equivalent to a phase difference equal to π.

Solution: Use formula 2-13 to solve for $(n_{eff}^{bottom} - n_{eff}^{top})$ as follows:

$(n_{eff}^{bottom} - n_{eff}^{top}) = (\Phi\ \lambda)/(2\ \pi\ L)$

$(n_{eff}^{bottom} - n_{eff}^{top}) = (\pi \times 1.55\mu m)/(2 \times \pi \times 50\mu m) = 0.0155$

Recall that the silicon index of refraction varies with temperature by $dn/dt = 1.87 \times 10^{-4}\ K^{-1}$.

Rewriting Equation 2-4:

$dn/dt = (n_{eff}^{bottom} - n_{eff}^{top})/(T_2 - T_1)$

$(1.87 \times 10^{-4}\ K^{-1}) = 0.0155/(T_2 - T_1)$

Temperature change $= (T_2 - T_1) = 0.0155/(1.87 \times 10^{-4}\ K^{-1}) = 83$ K or 83 ºC

This change in temperature is difficult to achieve with a thin film heater placed 1-2 μm above the waveguide. A more typical temperature change in the waveguide is about 20 ºC. For this reason, we need to extend the length of the interferometers arms to about 4 x 50 μm = 200 μm.

Example 7 illustrates another trade-off, this time between the size of the device and the heat that can be produced using thin film heaters deposited above the waveguides.

Another important application of PIC MZI devices is in *modulators*. In the case of modulators, we are interested in controlling an output optical power through the entire range of values between minimum and maximum. This range of values can be described as an analog output, while a switch device output can be thought of as a digital value that returns either a 0 or a 1. For example, we can choose output B of the previous MZI. Figure 2-18 a) shows that any value for P_B/P_0 can be obtained by choosing the corresponding value of the phase Φ between 0 and π. This can be achieved by controlling the current running through the thin film heater. An MZI modulator can use Y-branches in the place of 3dB directional couplers. In this case, there is only one output, which is all that is needed for a modulator. A *variable optical attenuator* (VOA) is another application of MZIs. These devices are used to control the overall power levels in PICs.

An entirely different class of applications for PIC MZI devices exists outside fiber optics transmission systems. These are *sensor* applications where the MZI is used to detect certain substances and their properties. The principle of operation of such sensors is illustrated in the figure below, which shows a Y-branch-based MZI. In this configuration, the reference arm is on the bottom and the arm under test is at the top. A trench is created in the top waveguide, where the biochemical substance under test will be placed. The substance has a different refractive index than the waveguide, which will create a phase difference between the two arms. By working backward from the detected output power to the phase difference that produced it, it is possible to determine the substance under test.

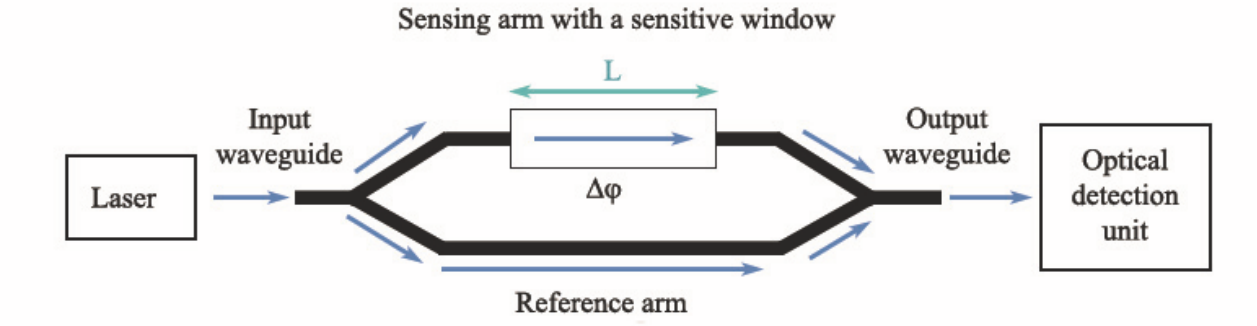

Figure 2-19 *MZI device used in biochemical sensing*

Ring Resonator

A ring resonator is a *filter* type of device that performs operations based on the wavelength of the input light wave. Resonators, in general, oscillate with high amplitude at certain frequencies

called *resonant frequencies*. To describe the behavior of PIC filter devices, we use wavelength as the independent variable, rather than frequency. Recall that electromagnetic waves' frequency and wavelength are related to each other as described by Equation 2-15, where v is the speed of propagation of the wave.

$$\lambda = v/f \tag{2-15}$$

In the simplest case, a PIC ring resonator is formed by bringing a straight waveguide, sometimes called the *bus*, and a ring waveguide close together, as shown in Figure 2-20.

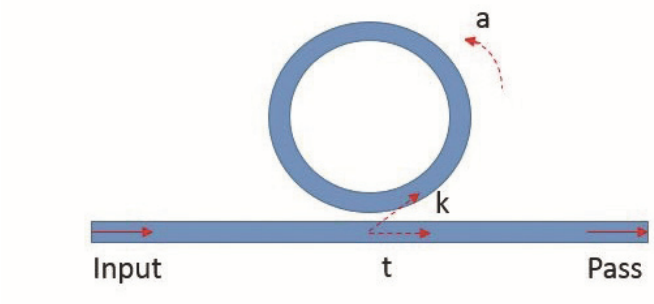

Figure 2-20 *Ring resonator PIC device*

An input light wave traveling from the left in the straight waveguide will transfer to the ring through the evanescent field of the bus waveguide. Recall that light behaves the same way in directional couplers that bring two parallel waveguides close to each other in the coupling region. After completing a round trip around the ring, the light wave will interfere with other waves at the same location. Depending on the phase difference accumulated around the ring, the interference can be constructive or destructive. This phenomenon is analogous to light moving back and forth in a laser cavity. The ring has a different geometrical structure, but the basic behavior is similar. The phase difference accumulated in one round trip around a ring of radius r is given by:

$$\Phi = (2\pi/\lambda)\, n_{eff}\, (2\pi r) \tag{2-16}$$

The resonance condition takes place when the phase difference equals an integer multiple of 2π.

$$(2\pi/\lambda)\, n_{eff}\, (2\pi r) = 2\pi m,\ m = 1, 2, \ldots \tag{2-17}$$

From this we can determine the resonant wavelengths:

$$\lambda_m = 2\pi\, n_{eff}\, r/m \tag{2-18}$$

The resonant wavelengths are almost equally spaced at an interval called the free spectral range or FSR, given by the equation below:

$$FSR = \lambda^2/(2\pi\, n_{eff}\, r) \tag{2-19}$$

The wavelengths that satisfy the resonant condition are amplified by the ring and build up, while other wavelengths are attenuated as they travel around the ring. The nonresonant wavelengths predominantly continue along the straight waveguide. They can be said to *pass through* the filter, as shown in Figure 2-20. A filter of this kind is called a *notch filter*.

Figure 2-21 shows the transmission of the optical signal in the bus waveguide in relation to the light's wavelength. Transmission is defined as the ratio of the output power to the input power. The figure shows that transmission is equal to 1 (or 100%) for nonresonant wavelengths and drops to low values at resonant wavelengths.

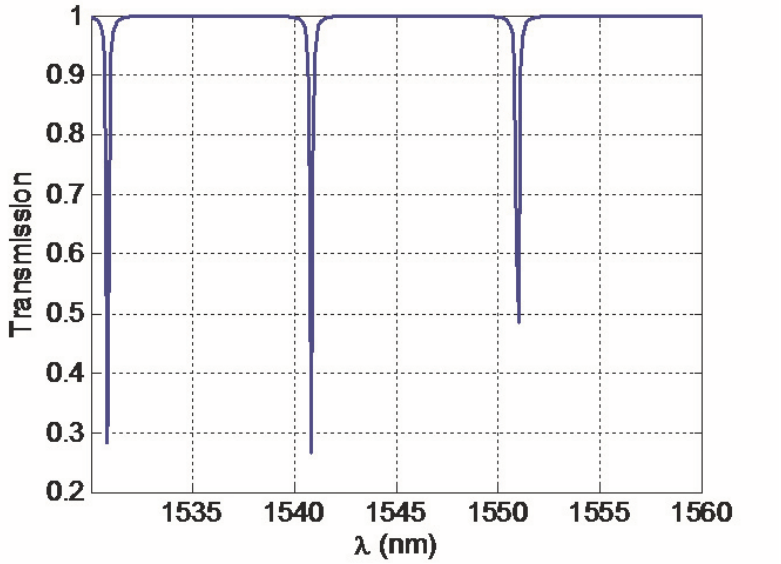

Figure 2-21 *Notch filter transmission vs. wavelength. Resonant wavelengths appear at approximately 1531, 1541, and 1551 nm, with an FSR of about 10 nm.*

Another type of filter is an *add-drop filter*, which can be constructed from a ring resonator placed between two straight waveguides. A device like this has four ports, labeled Input, Through, Add, and Drop, as shown in Figure 2-22. As in the case of the all-pass ring resonator filter described above, light at a resonant wavelength will couple into the ring. This time, however, these wavelengths will exit through the Drop port at the top left in the figure. By symmetry, light at a resonant wavelength sent in through the Add port will be coupled into the ring and exit at the Through port. A device of this type is used in nodes of optical fiber networks where some signals need to be routed to certain locations and other signals need to be introduced in the optical fiber.

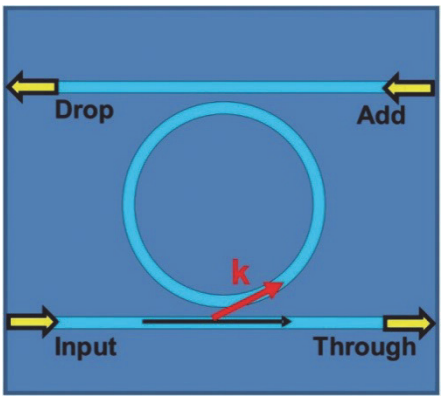

Figure 2-22 *Add-drop filter based on four-port ring resonator device*

Figure 2-23 shows the transmissions in the Through and Drop ports of the add-drop filter, with transmission in units of dB.

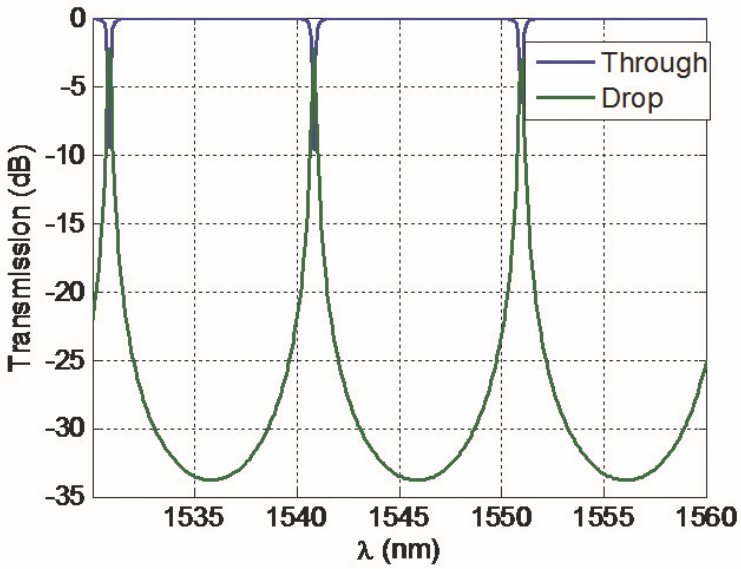

Figure 2-23 *Add-drop filter transmission for the Through and Drop ports vs. wavelength. Resonant wavelengths once again appear at approximately 1531, 1541, and 1551 nm.*

An alternate configuration for the add-drop ring resonator filter is the *racetrack* configuration. Here the ring is divided in two 180 degree sections, and straight waveguides are inserted in between. The figure below shows a microscope image of such a configuration. The racetrack configuration is easier to realize in practice because it allows for a larger gap between the two bus waveguides and the ring. Because the larger gap reduces coupling between the bus and ring waveguides, the straight portions of waveguide have been added to increase the length of the coupling region.

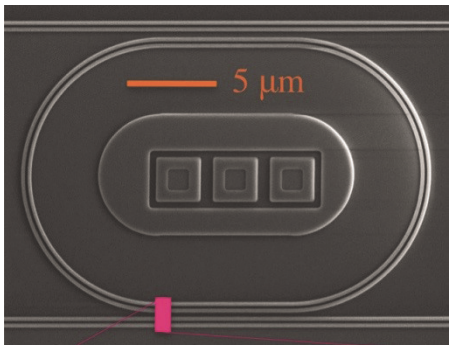

Figure 2-24 *Add-drop filter in racetrack configuration*

Silicon-on-insulator (SOI) waveguides are very well suited for creating ring resonator filters. The strong confinement of the electromagnetic field in the waveguides allows for small bend radii, as low as 5 μm. This makes the entire ring resonator device very compact. A small ring radius will also result in a large FSR (as you can tell from Equation 2-19, where the radius appears in the denominator), and a large FSR is a desirable filter characteristic.

Figures 2-21 and 2-23 correspond to ring resonators of radius 10 μm created from SOI rib waveguides with widths of 500 nm, SOI thicknesses of 220 nm, and rib thicknesses of 90 nm. The SOI waveguides are covered with oxide. Silicon ring resonators can also be used as *biosensors*, in which case the upper cladding material is air. The substance under test can be placed directly on top of the ring silicon waveguide. The unknown substance will change the effective refractive index of the waveguide, and this will change the resonant wavelengths of the ring. The shift in one of the resonant wavelengths is measured and used to determine the index of refraction of the substance under test, allowing for its identification.

Bragg Grating

A waveguide Bragg grating is a structure consisting of a periodic variation of the effective refractive index along the waveguide in the direction of propagation of the light. The structure can be created several different ways, depending on the type of waveguide. In an optical fiber, the structure is called fiber Bragg grating (FBG) and is created by periodically modulating the index of refraction inside the core. This is done by “writing” the grating using an intense ultraviolet (UV) source of light. Because the germanium-doped fiber core is photosensitive, exposing the core to UV light through a mask induces a permanent index change in the exposed regions. In the case of planar waveguides, the fabrication process allows for changing the physical dimensions of the core to create the grating. Either the height or width of the core can be changed, as in cases a and b in Figure 2-25. The period of the grating is denoted by Λ.

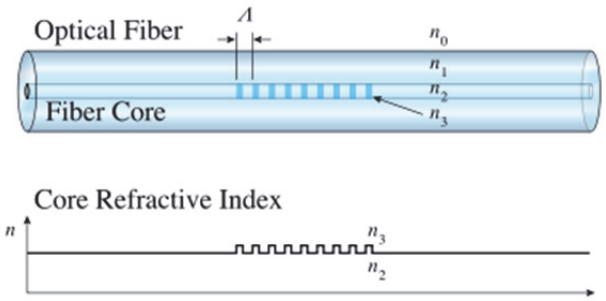

Figure 2-25 a) *Optical fiber Bragg grating and core refractive index along fiber*

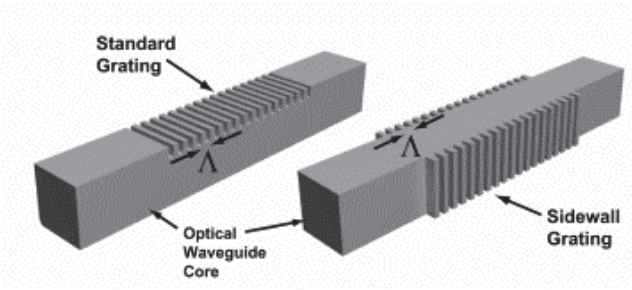

Figure 2-25 b) *Planar waveguide Bragg grating. In one, the grating sits at the top of the waveguide. In the other, the grating is created on the waveguide sidewalls.*

Bragg gratings are resonant structures with a filter response. Recall that when light is incident on an interface between two media with different indices of refraction, some of the light is reflected back to the first medium, and the rest is transmitted in the second medium. In a Bragg grating, successive reflections take place at each location where the index changes. The reflected waves interfere with one another. When the wavelength of the light is such that the interference between all reflected waves is constructive, the reflected wave builds up. This happens in a wavelength region centered on the so-called Bragg wavelength, λ_B.

A typical Bragg grating totally reflects light at wavelengths within a bandwidth centered around the Bragg wavelength. Light outside this bandwidth is transmitted instead of reflected. The Bragg wavelength is given by the following equation, where Λ is the period of the grating and n_{eff} is the effective refractive index of the waveguide:

$$\lambda_B = 2\Lambda\, n_{eff} \tag{2-20}$$

In SOI waveguides, typical Bragg gratings have 200–300 periods, and the period is around 300 nm. The change in waveguide width for a sidewall grating can be tens of nm up to 200 nm.

Example 8

Find the grating period corresponding to a desired reflected wavelength. We want to design a Bragg grating to reflect light around the wavelength of 1535 nm. The grating is created in an SOI waveguide with an effective refractive index equal to 2.35. Find the grating period.

Solution: Use Equation 2-20 to solve for Λ.

$\Lambda = \lambda_B/(2\, n_{eff}) = 1535\text{ nm}/(2 \times 2.35) = 327\text{ nm} = 0.327\ \mu\text{m}$

The example illustrates why SOI waveguides are very appropriate for Bragg gratings. The grating periods corresponding to wavelengths in the communications windows, 1.31 μm and 1.55 μm, have values around 300 nm, a dimension well less than a micron. It is difficult to obtain such small features in some other platforms.

Figure 2-26 shows the spectrum of the reflected light. The spectrum is centered at the Bragg wavelength, λ_B. The bandwidth, labeled $\Delta\lambda$ in the figure, decreases as the number of periods in the grating increases. The bandwidth is typically tens of nm.

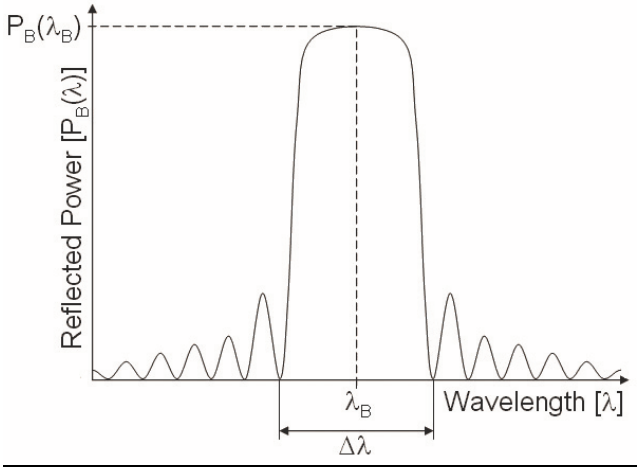

Figure 2-26 *Optical power reflected from a Bragg grating vs. wavelength*

Waveguide Bragg gratings are used as integrated mirrors at the ends of the active medium in diode lasers. They are also used to fabricate narrow-band optical filters and evanescent field sensors. In more complicated configurations, they can also be used to construct add-drop multiplexer devices.

Active Silicon PIC Devices

Lasers

As previously mentioned, a big barrier to achieving monolithic integration on a silicon platform is the lack of a silicon diode laser. Silicon is an *indirect band gap* material. In *direct band gap* materials, an electron can transition between the conduction band and the valence band, emitting a photon in the process. By contrast, in an indirect band gap material, an electron must pass through an intermediate state and emit a particle called *phonon* before a photon can be emitted. This makes the emission process inefficient for these materials, which include silicon and germanium.

Commercial diode lasers are instead fabricated from direct band gap materials, using combinations of elements from groups III and V in the periodic table, such as gallium (Ga), aluminum (Al), arsenic (As), indium (In), and phosphorus (P). These diode lasers have high efficiencies and are capable of high power outputs. GaAs laser diodes emit light with a wavelength of 870 nm. Communications applications use InGaAsP laser diodes emitting in the range 1150-1650 nm.

Diode lasers such as these are used as the light sources in optical fiber transmission systems. The lasers are used as external components and optical fibers typically connect them to the PIC devices. First, light emitted by the diode laser has to be coupled into the optical fiber. The modes of the laser and optical fiber are not well matched because they are made of different materials

and have different dimensions and mode shapes. The laser light has an elliptical distribution, while the optical fiber mode is circular. A lens is used in between the diode and fiber to reshape the mode and increase the coupling efficiency. A component called an *optical isolator* is also inserted in between the diode and the fiber to prevent light reflected from the fiber from returning to the laser. The optical isolator allows one of the light's directions of propagation and blocks the others.

Next, light carried by the optical fiber is coupled to the silicon PIC device. The section above titled "Input/output Coupling to Silicon PIC Devices" described several ways to obtain efficient coupling of light between a single-mode optical fiber and the much smaller SOI waveguide. These include using grating couplers and spot-size converters. Grating couplers can also be used to couple the light emitted by the laser and focused by the lens directly into the PIC device without using an optical fiber. The diode laser is placed on top of the PIC device, and a corner reflector is used to change the direction of the laser light emitted horizontally down into the grating coupler.

Another consideration to take into account when coupling light from a diode laser into a PIC device is polarization dependence. SOI waveguides have large birefringence, which comes from the large refractive index difference between the silicon core (3.47) and the oxide cladding (1.44) or air cladding (1.0), as well as the shape of the waveguide. Earlier, this module described a typical SOI waveguide with a large birefringence $\Delta n_{eff} = n_{eff}^{TM} - n_{eff}^{TE} = -0.65$. To avoid unwanted effects when both polarizations propagate in the PIC device, a diode laser that emits polarized light can be used. In this case, light from the laser is coupled to the PIC device using a special type of fiber called a *polarization maintaining fiber*. Regular optical fibers do not maintain the polarization of the light. They allow for both TE and TM polarization to propagate, and because these are indistinguishable in the circularly symmetric fiber, the polarization of the light at the end of the fiber might be different from that of the input light. However, in the specially designed polarization maintaining fibers, only one polarization can propagate. This ensures that light coupled in the silicon PIC device has only one polarization (either TE or TM).

Wavelength division multiplexing was previously mentioned as a method to increase the capacity of the signals in optical fiber transmissions. For example, 40 light waves with slightly different wavelengths and frequencies can travel simultaneously through the same optical fiber without interfering with one another, thus multiplying by 40 the amount of information sent. To achieve this, multiple diode lasers emitting at different wavelengths have their outputs combined before the signals are being sent through the fiber.

While the use of external lasers allows for good performance, several methods are being pursued to bring monolithic integration closer to commercial devices. One of these involves incorporating the III-V combinations of materials that make up the diode laser in an etched pit in the SOI structure. A space is etched through the SOI structure where the III-V material combination (for example indium phosphide, InP) is placed and bonded to the silicon wafer. This can be accomplished through metal bonding. Another type of bonding between III-V materials and SOI waveguides is *molecular bonding*, also called *adhesive bonding*. In this case, the III-V structure is placed on top of the SOI layer such that the light emitted by the diode travels parallel to the SOI and couples into it through the evanescent field. These devices are called hybrid silicon lasers.

Finally, monolithic integration is possible where the III-V layers are grown in the SOI layer through a process called *molecular beam epitaxy*. In general, growing the III-V layers of materials on the silicon substrate creates stresses due to the mismatch between the lattice constants of the silicon structure and the III-V structure. (The lattice constant is the distance between successive atoms in the periodic structure of the material.) There is also a mismatch between the coefficients of thermal expansion of the two types of materials, which introduces additional stress when temperature changes. To overcome these difficulties, it is helpful to have very small laser devices to minimize stress. Progress has been made in this direction by using quantum wells and quantum dots, which have shrunk the device to a very small size and require only small, milliampere currents to run. Another challenge that remains with III-V materials is their incompatibility with the CMOS process. A material that can be used to alleviate this is germanium. Germanium lasers on silicon substrates have been demonstrated.

Modulators

Modulators are devices capable of adjusting the power level of an optical signal to any value between a minimum value and a maximum value. A controlling signal, usually an electric current, is used to achieve the desired output optical power. The physical effects modulators are based on are *electroabsorption* and *electrorefraction*. In electroabsorption, the controlling signal produces a change in the absorption coefficient, while in electrorefraction, the controlling signal changes the material's index of refraction. Electrorefraction can be achieved by either thermo-optic or electro-optic effects. As the name indicates, a *thermo-optic effect* is a change in the refractive index when heat is applied to the material. The strength of the thermo-optic effect in silicon is described by the index coefficient of variation with temperature, $dn/dt = 1.87 \times 10^{-4}\ K^{-1}$. The *electro-optic effect* is a change in the refractive index when an electric field is applied. The thermo-optic effect is typically slower than the electro-optic effect, because heat transfer through the material is slower than applying an electric field.

In the case of silicon, changes in both the refractive index and the absorption coefficient can be achieved by changing the concentration of charge carriers in the material. This effect is called the *plasma dispersion effect*. Carriers can be either injected into the device or removed from it, using either a PIN junction or a p-n junction.

Modulators based on SOI devices can be created in a Mach-Zehnder interferometer (MZI) configuration or a ring resonator configuration. In the case of MZI devices, heat can be applied by thin film heaters deposited over one of the interferometer arms to achieve the thermo-optic effect. We can pick either one of the two outputs to give the desired level of output power. For example, referring to Figure 2-18, by controlling the phase difference between the values of 0 and π, any level of output power can be achieved in output B, from maximum transmission equal to 1 to minimum transmission equal to 0. In practice the device will have some insertion loss, which means that the maximum power in output B will be slightly less than the input power. Also the minimum transmission in B cannot be exactly zero, but it can be a very small value. The plasma dispersion effect can also be used with an MZI configuration. In this case, a PIN junction is inserted in one of the MZI arms to allow for charge carrier injection through the application of voltage.

A ring resonator, in either the all-pass or add-drop configuration, can also be used to create a modulator. Referring to Figure 2-21, by working in a wavelength range near a resonant

frequency, it is possible to move between a high value and a low value of transmission by changing the phase accumulated around the ring. Once again, the plasma dispersion effect can be exploited by creating a p-n junction around the ring and applying a voltage to control the charge carriers. This is illustrated in Figure 2-27. Modulators based on SOI ring resonators require wavelength stabilization, because they operate within a narrow range of wavelengths around the resonant wavelength. This can be achieved by using a heater over a portion of the ring (not shown in the figure).

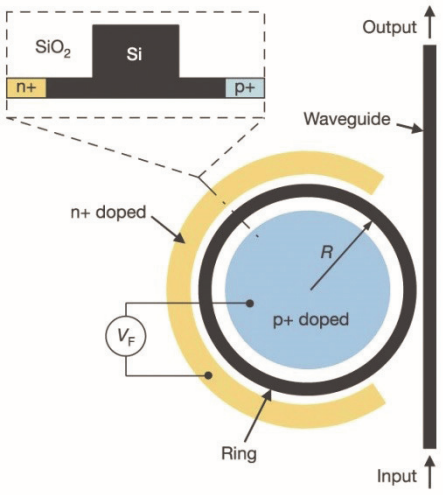

Figure 2-27 *An SOI micro-ring modulator based on the plasma dispersion effect*

Micro-ring modulators are much more compact than MZI devices. The latter need long arms to accumulate the required phase difference, while ring resonators take advantage of the light traveling many times around the same path in the ring. MZI devices are, however, easier to fabricate by not requiring the very tight tolerances ring resonators do.

All modulators are characterized by several important parameters including modulation depth, speed of response or bandwidth, and power consumption. Modulation depth is defined as follows:

$$MD = (P_{out}^{max} - P_{out}^{min})/P_{out}^{max} \quad (2\text{-}21)$$

Here P_{out}^{max} is the maximum output power and P_{out}^{min} is the minimum output power of the modulator. Ideally MD = 1, which requires $P_{out}^{min} = 0$. In practice MD values between 70-90% are common.

With SOI modulators, response times are tens to hundreds of picoseconds (1 ps = 10^{-12} s) and bandwidth values are on the order of GHz. The power consumption is on the order of mW for silicon modulators based on the plasma dispersion effect. These modulators perform excellently and are very compact compared with modulators created in other platforms.

Photodetectors

Photodetectors are devices that convert a light input into an electrical output. They are essential elements in any optical power measurement system. They are also used in optical fiber communication systems as part of the receiver modules. Important parameters that characterize photodetectors are responsivity, sensitivity to wavelength, temporal response, and noise level.

Responsivity, measured in A/W, is the amount of electric current generated by 1 W of power of an incoming optical signal. It can be calculated using Equation 2-22.

$$R = I/P \tag{2-22}$$

Here, I is the electric current generated, and P is the optical power incident on the photodiode.

Example 9

Find the responsivity of a photodiode that generates 800 μA of electric current in response to an input optical power of 1.2 mW.

Solution: Use Equation 2-22 to calculate the responsivity. The units for current and power must be converted to A and W.

$R = 800 \times 10^{-6}\ A/(1.2 \times 10^{-3}\ W) = 0.67\ A/W$

Sensitivity to wavelength is related to absorption's dependence on wavelength, which is illustrated in Figure 2-1 at the beginning of this module, and indicates what material is best suited to detect light for a certain wavelength range. The *temporal response* is the photodetector's ability to produce an electric current when a very short pulse of light falls on it. Finally, the *noise level* reflects the fact that the photodetector will always produce a very small amount of current, even in the absence of any light input. This can be quantified by the dark current, or the current produced when no light is incident on the photodiode. Desired photodetector performance is described by high responsivity, broad wavelength range, short response time, and low noise.

Silicon PIN photodiodes, fabricated from a p-n junction with an intrinsic, i, layer inserted between the p- and n- regions, are a type of photodetector with excellent characteristics in the four categories described above for wavelengths up to 1.1 μm. Figure 2-28 shows the responsivity of these detectors in relation to wavelength and identifies different lasers for which these detectors are appropriate.

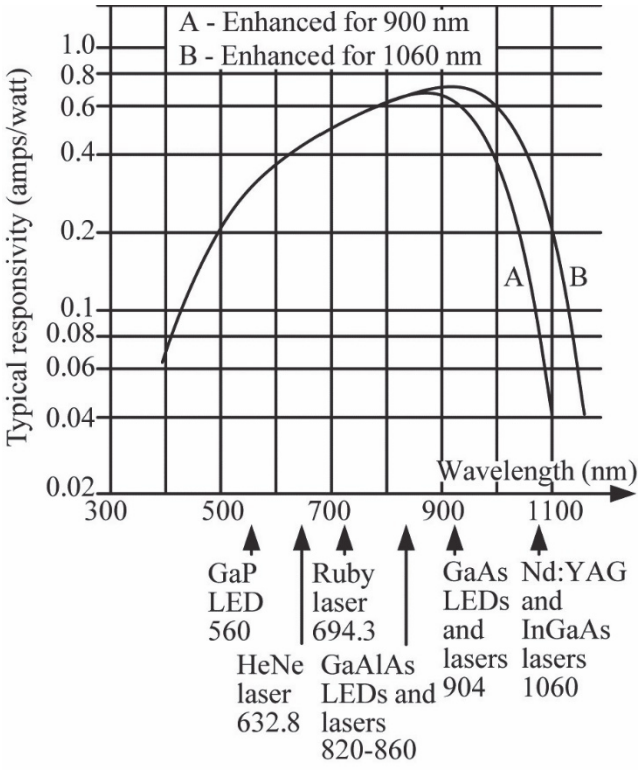

Figure 2-28 *Spectral responsivity of silicon PIN photodiodes*

The wavelengths of light used in optical fiber transmission systems center on 1310 nm and 1550 nm. Silicon is not a good absorber of the light at these wavelengths, and this makes silicon-based photodetectors inefficient in this case. Figure 2-1 at the beginning of the module shows that germanium, also a group IV element, absorbs light more efficiently than silicon at these communications wavelengths. Due to this property, and its compatibility with the CMOS process, germanium grown on silicon has emerged as the material of choice for photodetectors used in optical fiber transmission systems. Some fabrication challenges still exist with such photodetectors due to a 4% mismatch between the lattice constants of silicon and germanium. However, Ge-on-Si detectors with good performance have been obtained.

Similar to the case of silicon photodetectors, the PIN structure is the most used structure for Ge on Si detectors. High responsivity values of 0.9 to 1.0 A/W have been achieved. The bandwidth is typically 20–40 GHz, and higher values up to 120 GHz have been demonstrated. The dark current can be as small as 1–10 μA, with higher values for detectors that have a large area.

Fabrication of Silicon PICs

Module 1 described the fabrication of photonic integrated circuits, starting with a blank wafer and ending with multiple identical devices being formed on the wafer. In the industry, this is referred to as the “front-end” process, and it takes place entirely in a clean room. Figure 2-29 shows examples of completed wafers. In the following section, we discuss additional processes that are necessary to obtain a finished product, together with specifics of the fabrication processes required for silicon PICs.

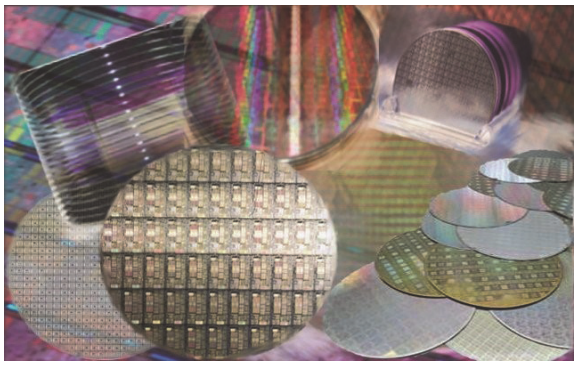

Figure 2-29 *Silicon wafers containing many identical PIC devices created by the fabrication process described in Module 1*

The PIC fabrication process does not end with the creation of the devices on the wafer. Further processing includes inspection, dicing, testing, assembly, and packaging. These usually take place in environments with less stringent requirements than a clean room. These processes are referred to as the "back-end."

The processed wafer is first inspected to find physical abnormalities that indicate if any damage is present. Even though this can be done visually by a human operator, in high-volume production, wafer inspection is performed automatically using specialized equipment. Vendors of patterned wafer inspection equipment include Applied Materials, KLA-Tencor, and Nikon.

Dicing is the process of cutting the wafer to separate the individual devices. A circular dicing blade can be used in this process, as shown in Figure 2-30. An individual device separated from the wafer is known as a die. Dicing allows the individual devices on a wafer to be tested for performance and compliance before being packaged.

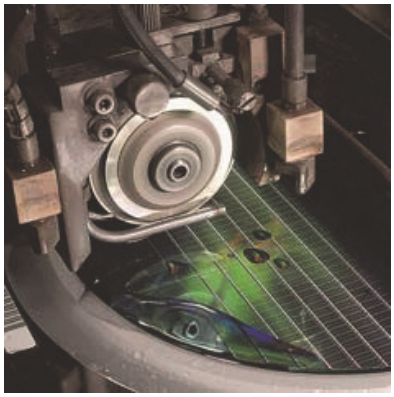

Figure 2-30 *Dicing of wafer into individual devices. Courtesy of Advanced Motion Controls.*

Assembly and packaging are the processes through which a die is bonded to other dies and joined to the package and permanent electrical and optical connections are made to the dies. To have a good yield, the dies need to be tested before they are sent for assembly and packaging. In the electronics industry, this is called using "known good dies."

Testing

Dies are tested on dedicated test stations running specialized test programs. Both optical and electrical measurements can be performed. Optical measurements include output optical power, insertion loss, polarization dependence, and optical spectrum. Electrical measurements can include operation voltage, drive current, bandwidth, bit error rate (BER), and others.

The test station contains test equipment, translation stages and vacuum chucks for mounting the die, a microscope used for precise alignment of the die, and optical fibers and electrical connections to send optical and electrical signals to the die. Equipment used in test stations includes optical sources to provide the optical input signal to the tested die, optical power meters and spectrum analyzers, and photodetectors to convert the optical signals to electrical output. Electrical equipment includes power sources and function generators for providing electrical signals, multimeters, oscilloscopes, network analyzers, and bit error rate testers.

Optical fibers used for input and output to the die can be individual fibers or fiber arrays. Individual fibers are used for PICs with a small number of inputs and outputs. A better approach is to use fiber arrays, which are assemblies of several parallel optical fibers rigidly mounted in a glass or some other substrate package. Fiber arrays typically contain four or eight optical fibers, but fiber arrays of sixty-four or more fibers have also been created for use with PICs that contain a large number of inputs and/or outputs. Fiber arrays are made by placing the fibers in V grooves created in the substrate and then covering them with a lid attached with adhesive. Figure 2-31 illustrates the process of making a fiber array. A fiber array is more rigid, less fragile, and easier to align to a PIC die than an individual fiber.

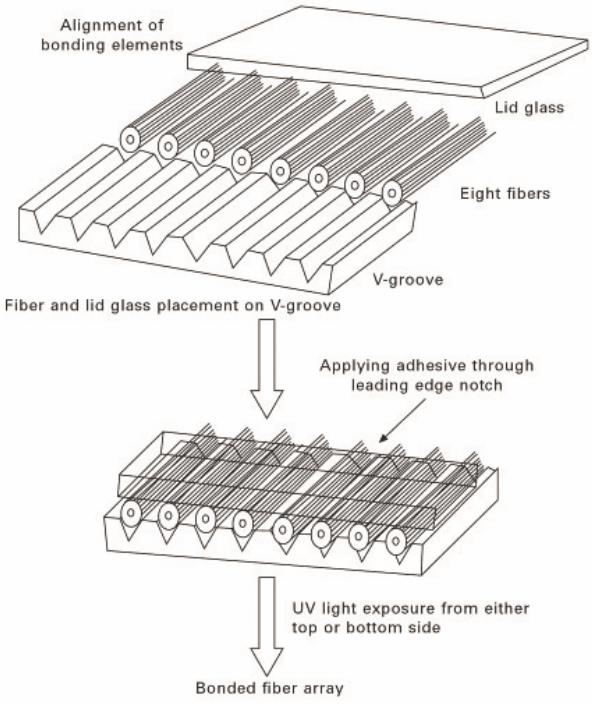

Figure 2-31 *Fiber array fabrication*

Figure 2-32 shows examples of fiber arrays. The end of the fiber array can be polished at an angle, typically 8 degrees, to reduce back reflection of the optical signal up the optical fiber, taking place at the interface between media
with different refractive indices.

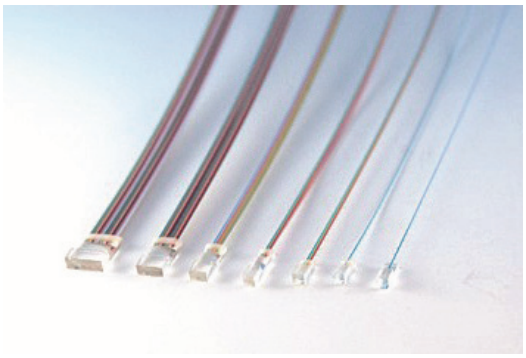

Figure 2-32 a) *Fiber arrays, courtesy of AiDi*

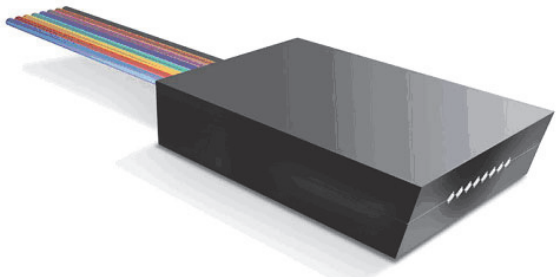

Figure 2-32 b) *Fiber array, courtesy of Hantech. This fiber array is angle polished to avoid back reflections of the optical signal.*

Electrical signals are sent to the die through thin metal wires made of gold, copper, or aluminum. The process of attaching electrical wires to the die is called wire bonding.

Testing individual dies one at a time is a time-consuming process. To speed it up, the wafer might initially be diced into strips rather than individual dies. Each strip is mounted on the test station, and optical fibers are brought into contact with the first die on the input and output sides. In this case, light is coupled into and out of the PIC by edge coupling. Probe conductive needles can be positioned on the surface of the die for electrical signals. The test runs automatically, in conjunction with moving the strip vs. optical fibers and probe needles from die to die until the entire strip has been tested. The strips are then diced to obtain the individual dies, which are dispositioned according to the product specifications and test results.

Currently, state-of-the-art testing of dies is done at the wafer level, without the need to dice the wafer upfront. Both electrical and optical parameters can be tested this way. Light is coupled to and from the die through grating couplers, as described above. Fiber arrays mounted at an angle to the surface of the die are used in many cases. Figure 2-33 shows two automated test stations performing wafer level testing. Fiber arrays are visible in the left picture.

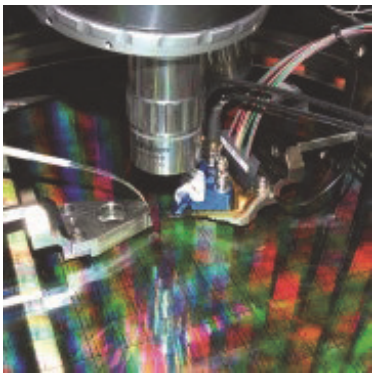

Figure 2-33 a) *Wafer level testing of PICs, courtesy of ACTPHAST*

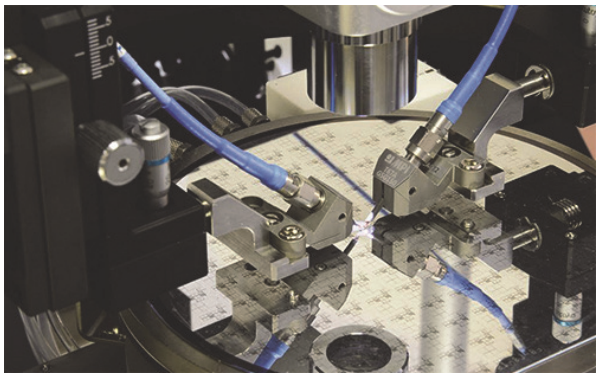

Figure 2-33 b) *Wafer level testing of PICs, courtesy of VI Systems*

Assembly and Packaging

The next process is assembly and packaging of the good dies to create the final product. The role of the package is to protect the device from external influences such as humidity, effects from thermal excursions, contamination, and mechanical forces. Traditionally, a package is created for each individual die. The die is attached to the frame of the package through an operation called *die bonding*. Electrical connections to the die are made by *wire bonding*. Thin metal wires are used for this purpose. Finally, optical fibers are attached through a very precise alignment process called *active alignment*. Alignment occurs in all six degrees of freedom: the X-direction, Y-direction, Z-direction, pitch, roll, and yaw. The metric used in active alignment is usually the optical power emitted or transmitted by the device. Fiber arrays can simplify the alignment process for PICs with multiple inputs and outputs.

A variety of packages exist for PICs, some standardized and others custom made. For example, a diode laser package must contain a heat sink, a port for optical fibers, and leads for mounting the assembly on a circuit board. Figure 2-34 shows the package features and an illustration of the packaged device.

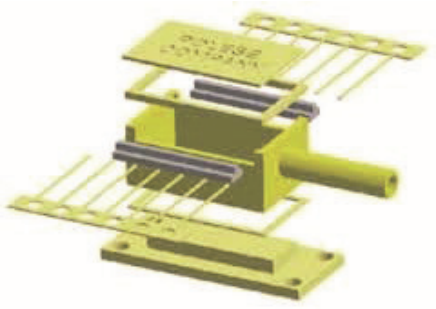

Figure 2-34 a) *Typical diode laser package*

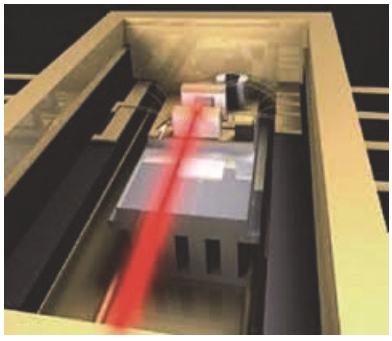

Figure 2-34 b) *Typical packaged device*

In the electronic integrated circuit (EIC) industry, the traditional approach was to separately package each device—processor, memory, and others—and connect them to one another by traces on the circuit board. Figure 2-35 illustrates this approach.

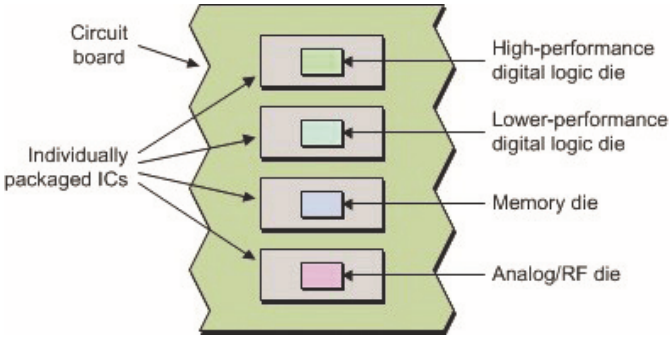

Figure 2-35 *Circuit board with individually packaged chips*

Because of the continued demand for more processing power and higher speed, the electronics industry has recently been evolving to include several chips in a single package, using what is called *system-in-package (SiP) technology*. This approach increases speed and reduces the size of the package. To achieve this, several dies are stacked on top of one another, and wire bonding connects the dies to one another or to the package. This method is known as *3D packaging*.

Often the die at the bottom of the stack is turned upside down and electrically connected to the package through solder material, eliminating the need for wire bonds between the package and chips. This technology is called *flip-chip*. The advantage of the flip-chip technology is that it enables a shorter distance between electrical connections than wire bonds do, and the shorter distance translates to better electrical performance. Figure 2-36 illustrates the wire bond and flip-chip approaches.

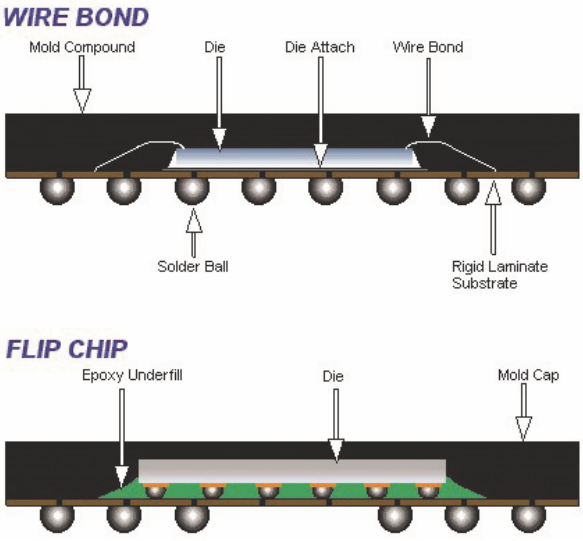

Figure 2-36 *Wire bond vs. flip-chip technologies*

Figure 2-37 shows an example of 3D packaging technology. Two die are stacked vertically and bonded together. The bottom die is flipped and connected to the package through flip-chip bumps, while the top die is connected with wire bonds that run along the edges of the die. The 3D technology has worked well for chips with a relatively small number of wire bonds. With the increasing demand for bandwidth and speed, the density of wire bonds per package is increasing, which requires building larger packages.

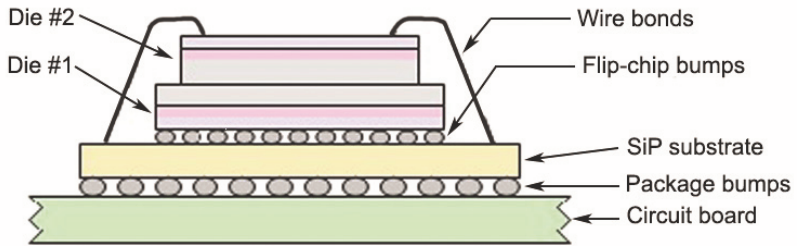

Figure 2-37 *Example of a packaged 3D stacked system*

A solution to the problem of increased wire bond density per package is to use a different method for electrical connections. This method consists of electrically connecting the dies in the stack to one another and the package using *through-silicon vias* or TSVs. These are vertical openings in the silicon substrate that reach all the way down through the die and wafer. The openings are filled with materials such as copper, tungsten, solder material, and conductive adhesive. Many TSVs serve as electrical connections, but some are thermal TSVs (TTSVs) that allow for heat dissipation and thermal management. Compared with wire bonds, TSVs have the advantages of enabling a higher density of electrical connections and allowing for shorter distances, which improve performance.

At this time, the full 3D packaging with TSVs solution is not yet fully implemented due to its very high level of complexity. An intermediate solution denoted as *2.5D packaging technology* is currently used. In this technology, a layer of silicon known as a *silicon interposer* is placed between the dies and the substrate or package. The silicon interposer is where TSVs are formed to connect the dies to one another. Figure 2-38 illustrates the 2.5D technology.

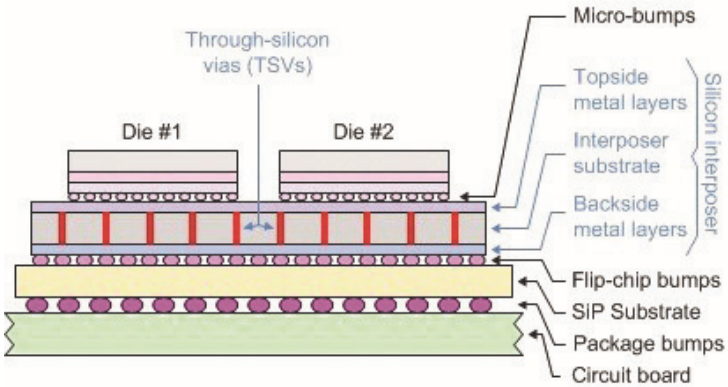

Figure 2-38 *A 2.5D system packaged using a silicon interposer and TSVs*

As the technology matures, the true 3D package with TSVs will be implemented, and the silicon interposer will not be needed anymore. Figure 2-39 shows an example of this technology, with two dies flip-chip stacked vertically.

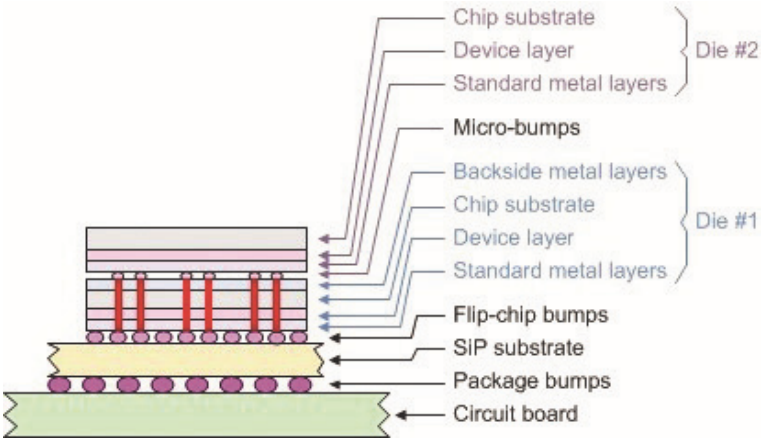

Figure 2-39 *A 3D system packaged using uses TSVs*

As mentioned previously, one important application of silicon PICs is in optical interconnects between electronic integrated circuits (EICs). Using optical rather than electrical interconnects can increase EICs' communication speed and bandwidth and reduce their power consumption. Figure 2-40 shows an example of optical interconnection between two processors. The optical interconnect is placed in a layer that sits underneath the electronic circuits. An optical SOI waveguide (shown in red) carries the laser light modulated by the electronic data from processor 1 to processor 2. A photodetector converts the optical signal back to an electrical signal before feeding it to the second processor chip. Developers are investigating other configurations for the optical layer in an effort to optimize the integration of the optical interconnects with the EIC. Silicon optical interconnects are compatible with the 2.5D and 3D packaging technologies.

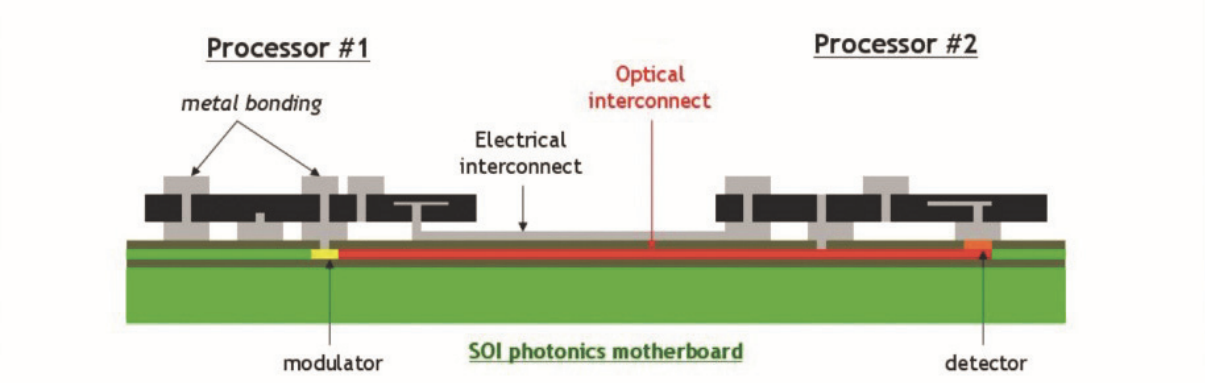

Figure 2-40 *Optical interconnect between two processor chips. Courtesy of APIC Corporation.*

SUMMARY

This module presented an overview of silicon photonic integrated circuits, starting with the material properties of silicon that are foundational for electronic and photonic integrated circuits and ending with advances in packaging of both types of ICs. Because PICs are widely used in optical communication systems, we presented the basic characteristics of optical fibers and optical fiber transmission systems. The module introduced silicon based passive PIC devices such as SOI waveguides, couplers, splitters, Mach-Zehnder interferometers, ring resonators, and Bragg gratings. These constitute building blocks for more complex devices and systems, which future modules will discuss. This module also presented challenges associated with the monolithic integration of optical sources and photodetectors in the silicon platform. We also described the remaining steps in the fabrication process after creation of the PIC devices on the silicon wafer. Finally, the module discussed new technologies used to package integrated circuits that incorporate PICs.

PROBLEM EXERCISES AND QUESTIONS

1. Use Figure 2-1 to find the materials that best absorb light with wavelengths of 600 nm, 800 nm, 900 nm, 1300 nm, and 1500 nm.
2. Does the refractive index of silicon increase or decrease with wavelength in the range 1100–2000 nm? Does it increase or decrease with temperature?
3. Define passive optical devices and active optical devices.
4. Convert the following values to dB: 0.9, 0.5, 0.25, 0.1, 0.01. Convert the following dB values to absolute values: -0.5dB, -1dB, -3dB, -5dB, -10dB, -20dB.
5. Calculate the insertion loss in dB of a device that has an input power of 2.5 mW and an output power of 1.7 mW.
6. Calculate the total loss in a photonic system made of three cascaded devices with insertion losses of -1.2dB, -2.5dB, and -0.6dB.
7. Briefly describe the components of a basic optical fiber communication system.
8. What is attenuation in an optical fiber, and how can the effects of attenuation be mitigated?
9. What is dispersion in an optical fiber, and how can the effects of dispersion be mitigated?
10. Describe silicon-on-insulator (SOI) waveguides. Include material structure, indices of refraction, and geometric parameters.
11. What is waveguide birefringence?
12. The index of refraction of silicon is 3.47 at room temperature (21 ºC). Find the index of refraction at 45 ºC.
13. Explain why butt coupling between single-mode optical fibers and SOI waveguides is a very inefficient way to couple light into the waveguide. Describe methods used to increase the coupling efficiency.
14. Calculate the loss of optical power through reflection at the interface between silica and silicon, and silicon and air. Express the loss as a percentage and in units of dB.
15. Calculate the length of the coupling region, L, for a directional coupler that splits the incoming light in a ratio of 70%-30% between output waveguides 1 and 2. Assume the coupling coefficient k is known.
16. What is crosstalk between two parallel waveguides, and how can it be avoided?
17. A Mach-Zehnder interferometer operating at a wavelength of 1.55 μm has arms that are both 100 μm long. Find the effective index difference between the two arms that results in a phase difference equal to $\pi/2$.
18. Describe how a switch and a variable optical attenuator based on a Mach-Zehnder interferometer work.

19. Find the phase difference Φ needed to produce power $P_B = 0.1\ P_0$ at the B output of a Mach-Zehnder interferometer. Give the phase difference in radians and degrees.
20. Find three consecutive resonant frequencies of a ring resonator with radius equal to 15 μm and a waveguide effective index of 2.35. The resonant wavelengths should be in the range 1530–1560 nm. What is the FSR of the ring in this wavelength range?
21. Describe how an add-drop filter device based on a ring resonator works.
22. What is a racetrack configuration for a ring resonator, and what advantage does it have over a regular configuration?
23. Describe a fiber Bragg grating and a waveguide Bragg grating and how they can be created.
24. Find the grating period, Λ, for a grating formed in a waveguide with an effective index of 1.89 that reflects a wavelength of 1550 nm.
25. Describe the challenges associated with monolithic integration of a light source on a silicon platform. Give examples of how this integration can be achieved.
26. What are the thermo-optic and electro-optic effects, and how are they used in waveguide based modulators?
27. What is the modulation depth of a modulator whose output power varies between 0.3 mW and 1.5 mW?
28. Describe advantages of SOI based modulators.
29. Explain why silicon is not used in photodetectors for optical fiber transmission systems. What other material can be used, and why?
30. Describe the back-end fabrication processes necessary to produce a packaged PIC device.
31. Describe wire bond and flip-chip technologies.
32. Explain and compare the 2.5D and 3D packaging technologies.
33. Describe silicon optical interconnects.

REFERENCES

Chrostowski, L., and M. Hochberg. 2015. *Silicon Photonics Design: From Devices to Systems*. Cambridge, UK: Cambridge University Press.

Deen, M. J., and P. K. Basu. 2012. *Silicon Photonics: Fundamentals and Devices*. Chicheser, UK: Wiley.

Hueners, B.W., and M. K. Formica. 2016. Photonics Component Manufacturing: Moving Toward Automation. *EDU.photonics.com*, March 5. http://www.photonics.com/edu (accessed April 6, 2016).

Lifante, G. 2003. *Integrated Photonics: Fundamentals*. Chichester, UK: Wiley.

Liu D., and S. Park. 2014. Three-Dimensional and 2.5 Dimensional Interconnection Technology: State of the Art. *ASME Journal of Electronic Packaging*.

Maxfield C. 2012. 2D vs. 2.5D vs. 3D ICs 101. *EE Times,* April 8. http://www.eetimes.com/document.asp?doc_id=1279540 (accessed April 6, 2016).

The National Center for Optics and Photonics Education. 2013. *Fundamentals of Light and Lasers*, 2nd Edition.

III-V Semiconductor Devices

Module 3

of

Integrated Photonics

OPTICS AND PHOTONICS SERIES

This material was created under Grant # 1303732 from the Advanced Technological Education division of the National Science Foundation. Any opinions, findings, and conclusions or recommendations expressed in this material are those of the author(s) and do not necessarily reflect the views of the National Science Foundation.

For more information about the text or OP-TEC, contact:

Dan Hull
PI, Executive Director, OP-TEC
316 Kelly Drive
Waco, TX 76710
(254) 751-9000
hull@op-tec.org

Taylor Jeffrey
Curriculum Development Engineer
316 Kelly Drive
Waco, TX 76710
(254) 751-9000
tjeffrey@op-tec.org

Published and distributed by
OP-TEC
316 Kelly Drive
Waco, TX 76710
254-751-9000
http://www.op-tec.org/

ISBN 978-0-9903125-7-4

CONTENTS OF MODULE 3

Module 3
III-V Semiconductor Devices

INTRODUCTION

Previous modules have discussed the importance of semiconductors in photonic integrated circuits and devices. III-V semiconductors are one of the most common types used in PICs. III-V semiconductors are obtained by combining an element from group III in the periodic table with an element from group V. These combinations are also called *binary compound semiconductors*. II-VI and IV-VI binary compound semiconductors are also possible. In addition, ternary (three-element) and quaternary (four-element) alloys from elements in groups III and V have been created.

III-V semiconductors have attractive electrical and optical properties with important applications in both electronic and photonic devices. Electronic transistors based on gallium arsenide (GaAs) and indium phosphide (InP) perform faster than their silicon counterparts and are used in high-power and high-speed electronic integrated circuits. In regard to optical properties, GaAs and InP are good light emitters due to their direct energy bandgap. This property is exploited in the fabrication of highly efficient semiconductor diode lasers. By contrast, silicon and germanium are inefficient light emitters due to their indirect bandgap, as discussed in the previous module. Using ternary and quaternary alloys such as aluminum gallium arsenide, indium gallium arsenide phosphide, and others has expanded the range of wavelengths emitted by diode lasers from 600 nm to 1650 nm.

Numerous photonic devices based on III-V semiconductors, both active and passive, have been developed and are widely used today. Active devices include lasers, modulators, and photodetectors. Passive devices include couplers, gratings, multiplexers/demultiplexers, interferometers, and others. Semiconductor diode lasers are currently the preferred light source for virtually all photonic applications. This includes applications of silicon based photonic integrated circuit (PIC) devices, that lack a practical light source based on silicon. An important advantage of PIC devices based on III-V semiconductors is the possibility of monolithic integration of all devices including light sources, modulators, passives and photodetectors in one chip. Recently a very high degree of integration of 600 optical functions on two indium phosphide chips has been achieved in commercially available devices.

At the same time, there are some disadvantages associated with III-V semiconductor PIC devices. The raw materials from which these are made are not as widely available as silicon, and are consequently more expensive. The processes used to build these devices are not fully compatible with complementary metal-oxide semiconductor (CMOS) technology. The GaAs and InP substrate wafers the devices are built on are more brittle, resulting in smaller wafers. A common diameter for these is wafers is 4 inches, although 6-inch-diameter wafers are now possible. Nevertheless, III-V semiconductor devices dominate in certain applications such as

diode lasers and devices used in long-haul optical fiber transmission systems. This module discusses basic properties of III-V semiconductors and how these are applied in active and passive PIC devices.

PREREQUISITES

OP-TEC's *Fundamentals of Light and Lasers Course 1*

OP-TEC's *Integrated Photonics: Modules 1 and 2*

OBJECTIVES

Upon completion of this module, the student should be able to:

- Explain material properties of III-V semiconductors important for PICs
- Describe characteristics of the following passive III-V semiconductor PIC devices:
    - Straight and bend waveguide
    - Coupling between optical fiber and III-V waveguide
    - Multimode interference coupler
    - Arrayed waveguide grating
- Explain the ITU grid used in wavelength division multiplexing and perform calculations involving ITU frequencies and wavelengths
- Describe characteristics of the following active III-V semiconductor PIC devices:
    - Diode laser
    - Semiconductor optical amplifier (SOA)
    - Modulator
    - Photodetector
- Provide examples of monolithically integrated III-V PIC devices and discuss their advantages over discrete devices
- Describe the MOCVD deposition process used to obtain III-V semiconductor thin films

BASIC CONCEPTS

Material Properties of III-V Semiconductors

Like silicon, III-V compounds such as gallium arsenide (GaAs) and indium phosphide (InP) have semiconductor properties. Elements in group III in the periodic table including boron (B),

aluminum (Al), gallium (Ga) and indium (In) have three electrons in their outer shell, while elements in group V, including nitrogen (N), phosphorus (P), arsenic (As), and antimony (Sb) have five electrons in their outer shell. Combining an element in group III with one in group V results in an average of four electrons per atom in the outer shell, like silicon, which belongs to group IV. The resulting III-V compounds have semiconductor properties, making them suitable for electronic as well as photonic devices. Examples of electronic devices based on gallium arsenide and indium phosphide include electronic integrated circuits and several types of transistors, such as heterojunction bipolar transistors (HBT) and field effect transistors (FET). These are used in high-power, high-speed, and high-frequency applications, for which their properties are superior to those of their silicon based counterparts.

A variety of photonic devices based on III-V semiconductors exist. These materials are especially suitable as light emitters due to their direct energy bandgap, and the availability of many different bandgaps resulting in a wide range of emitted wavelengths, from 600 nm to 1650 nm. Transmission-based waveguide photonic devices, including splitters, couplers, Mach-Zehnder modulators and others are also produced commercially. The III-V semiconductor waveguides have a lower refractive index contrast than silicon-on-insulator (SOI) waveguides, resulting in somewhat larger devices. What makes them very attractive however, is the possibility of monolithic integration of all devices including light sources, modulators, passives and photodetectors on the same chip. Monolithic integration was discussed briefly in Module 1, and offers many benefits, including smaller devices, lower manufacturing cost, and faster processing.

Figure 3-1 shows the absorption coefficients of several semiconductors for the wavelength region between 0.3 to 1.8 μm. Gallium arsenide and indium phosphide absorb light up to a wavelength of about 1.0 μm. Like silicon, these compounds can be used to fabricate photodetectors operating in the visible to near-infrared range. For the telecommunication wavelengths 1.31 μm and 1.55 μm, photodetectors are fabricated from germanium or indium gallium arsenide (InGaAs). The wavelength range for commercial InGaAs based photodiodes has been extended to wavelengths as high as 2.6 μm (not shown in the figure).

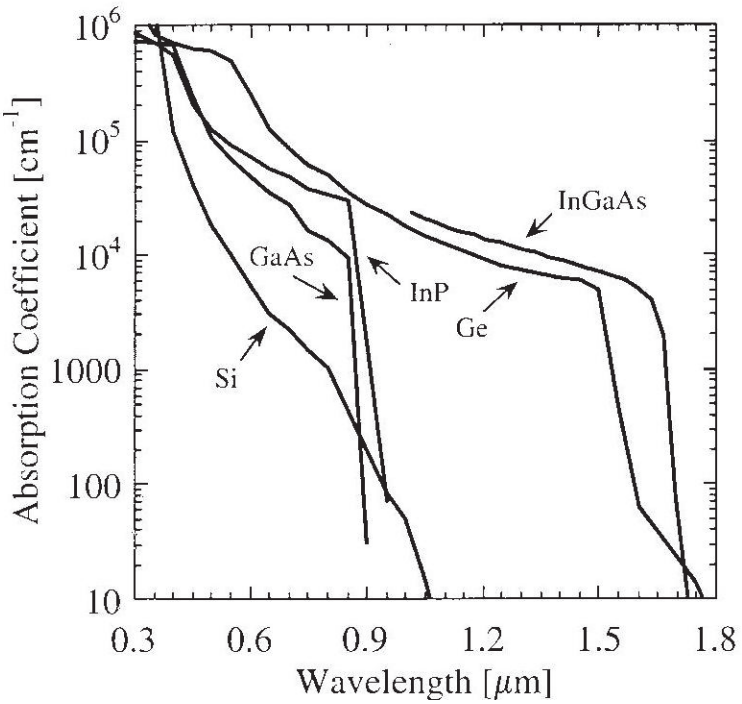

Figure 3-1 *Absorption coefficients of different semiconductor materials vs. wavelength*

Figure 3-2 shows the variation of the index of refraction of gallium arsenide and indium phosphide with wavelength, based on experimental measurements. At the communication wavelength of 1.55 µm, the index of refraction of GaAs is about 3.37, while the index of refraction of InP is about 3.17. Similar to the indices of refraction of glass and silicon, the index of refraction of the two III-V semiconductors decreases with increasing wavelength.

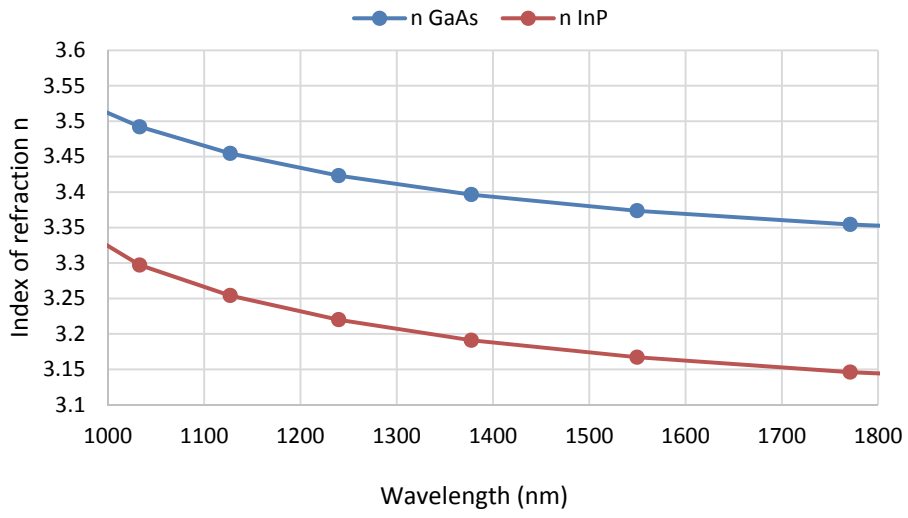

Figure 3-2 *Index of refraction of gallium arsenide and indium phosphide vs. wavelength*

The index of refraction of the two compound semiconductors also varies with temperature. As described in Module 2, the change in index of refraction with temperature is expressed by the coefficient of variation with temperature, dn/dt. At the wavelength of 1.55 μm, the value of dn/dt for gallium arsenide is 2.33×10^{-4} K^{-1}, while for indium phosphide it is 1.90×10^{-4} K^{-1}. These are relatively large values for the coefficient of variation with temperature. Because of this, temperature stabilization is required for many PIC devices built from these materials.

III-V Semiconductor Photonic Integrated Circuits

Module 2 described a wide variety of passive and active PIC devices based on silicon and insulator (silicon dioxide) materials. These types of devices can also be fabricated from III-V semiconductor materials. Two very important classes of III-V semiconductor devices are lasers and photodetectors, for which these materials have excellent properties. Passive waveguide based III-V PICs are also fabricated commercially. The fabrication process for III-V semiconductor PICs has advanced in recent years, resulting in very good device performance and improved yield, and making this platform especially attractive for optical communication devices and systems. The drawback of this platform is its lack of full compatibility with the CMOS fabrication process. However, hybrid devices, in which III-V semiconductor devices have been integrated with silicon devices manufactured in CMOS fabs, appear to be a good solution at this time. This module, presents passive III-V semiconductor devices first, followed by active devices.

Passive III-V Semiconductor PIC Devices

III-V Passive Optical Waveguide

As previous modules discussed, an optical waveguide generally consists of a high-index core and a low-index cladding that in combination allow for total internal reflection of the light to take place repeatedly when light strikes the interface between the core and cladding. Light confined this way travels for long distances in the waveguide core. When referring to semiconductor materials, a combination of two different types of semiconductors is called a *heterostructure*. A single heterostructure waveguide is based on a lower cladding made out of one kind of semiconductor, a core of another semiconductor, and an upper cladding of air. A *double heterostructure* waveguide has an upper cladding that is also a semiconductor, most likely the same as the lower cladding one. Double heterostructure waveguides are the most common combination with III-V semiconductors.

Several configurations for passive waveguides based on III-V semiconductors are used, including buried channel, buried rib, ridge or raised strip, and deep ridge (or deep etched) waveguides. Figure 3-3 presents examples of these configurations, based on InP substrates. In these waveguides the lower and upper cladding are indium phosphide (InP) and the core is a quaternary alloy of indium gallium arsenide phosphide (InGaAsP). The indices of refraction for these cladding and core materials are 3.17 and 3.29 respectively, and by using Equation 1-5 in Module 1, we find that the relative refractive index contrast is 3.58%.

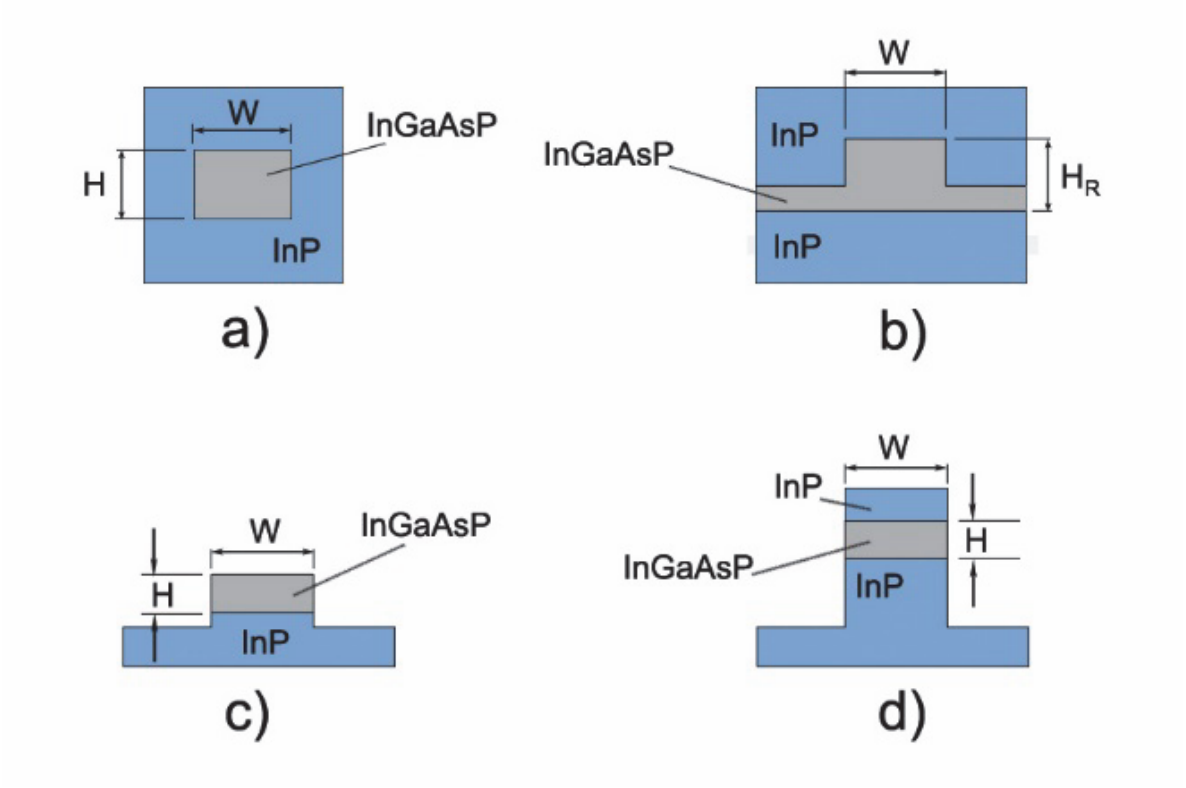

Figure 3-3 a) *Buried channel waveguide;* **b)** *Buried rib waveguide;* **c)** *Ridge or raised strip waveguide;* **d)** *Deep ridge waveguide*

Typical dimensions for the core of the channel waveguide in Figure 3-3 a) are 1 to 5 μm width, and 0.5 to 2 μm thickness or height. The buried channel is surrounded by InP on all sides. For the buried rib waveguide in Figure 3-3 b) the height of the rib, H_R, is typically 1 to 2 μm, and the width is 3 to 7 μm. The buried rib waveguide has the advantage of remaining single-mode even for the wider widths of 6 or 7 μm.

The raised strip and deep ridge waveguides in Figure 3-3 c) and d) have air as cladding on three or two sides. This increases the index contrast in those directions and results in better confinement of the light inside the core. The deep ridge can have a very thin core, 0.3 - 0.5 μm, which makes it easier to fabricate.

Example 1

Lateral refractive index contrast for deep ridge waveguide. Calculate the lateral refractive index contrast of waveguides having InGaAsP cores and air as lateral cladding.

Solution: The refractive index contrast is calculated using Equation 1-5 in Module 1

$\Delta = (n_{core}^2 - n_{clad}^2)/(2\, n_{core}^2) = (3.29^2 - 1^2)/(2 \times 3.29^2) = 0.45 = 45\%$

Historically, the propagation loss of III-V semiconductor waveguides has been high, on the order of 10 dB/cm or more. Advances in the design and fabrication process have brought

the propagation loss down to values as low as 0.6 dB/cm for buried channel waveguides. Similar to SOI waveguides, wider III-V waveguides have lower propagation losses than narrower waveguides. Ridge and rib III-V waveguides have been demonstrated with propagation losses as low as 0.2 dB/cm.

Bend radii of III-V waveguides are on the order of hundreds of microns. Values commonly used vary between 100 µm to 400 µm. These are bigger than the radii used with SOI waveguides, which are below 10 µm. Due to this larger bend radius, the III-V devices have a larger footprint than SOI devices. Using deep ridge waveguides increases the index contrast in lateral direction and allows for tighter bend radius. Devices with a bend radius of 30 µm have been demonstrated.

Recall that birefringence is the difference between two effective indexes of refraction, and is expressed by Equation 2-7 in Module 2. Due to material properties, III-V semiconductor waveguides can have a relatively large amount of birefringence which is undesirable for certain PIC devices. The birefringence can be controlled by careful design of the waveguide. For example, buried channel waveguides with square cross section have almost zero birefringence due to the symmetry of the structure, making the TE and TM modes almost identical.

Deep ridge waveguides with very low birefringence have also been obtained. Figure 3-4 shows the effective index of the TE and TM modes of a deep ridge waveguide as a function of the waveguide width. The two effective indices are equal for a core width of approximately 1.5 µm (indicated by the arrow in the figure). The core thickness for this waveguide is 0.5 µm.

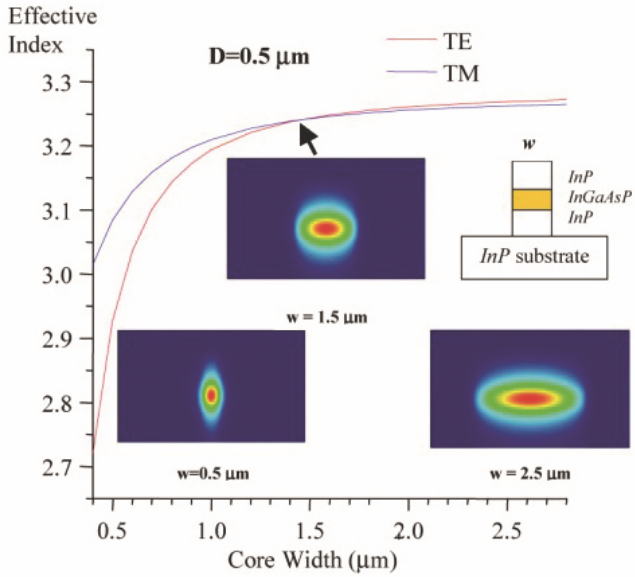

Figure 3-4 *Effective indices of TE and TM modes of a deep ridge waveguide as a function of the waveguide core width*

Table 3-1 shows the complete waveguide parameters for a single-mode buried channel waveguide.

Table 3-1. Single-mode Buried Channel InGaAsP/InP Waveguide

Parameter	Value
Thickness, H	700 nm
Width, W	1100 nm
Index of refraction of InGaAsP at 1550 nm and room temperature, n_{core}	3.294
Index of refraction of InP at 1550 nm, and room temperature, n_{clad}	3.167
Effective index TE mode, n_{eff}^{TE}	3.213
Effective index TM mode, n_{eff}^{TM}	3.212
Waveguide birefringence	-0.001

Input/Output Coupling to III-V Semiconductor PIC Devices

III-V semiconductor waveguides have a slightly larger cross section than SOI waveguides, but they are still considerably smaller in size than single-mode optical fibers. Due to the size and asymmetric shape of the core, the optical mode of the semiconductor waveguide does not match the mode of the optical fiber. This mismatch results in high loss when the waveguides are butt-coupled to optical fibers. To improve the coupling loss, devices known as spot-size converters (SSC) are used at the ends of the PLC chip to convert the waveguide mode to a mode closer to the optical fiber one.

SSCs in III-V semiconductor waveguides can be created in several ways. To enlarge the optical mode of the waveguide, either its width or its thickness can be increased or decreased. This needs to be done gradually resulting in a relatively long taper, of several hundred microns. If the taper is too short, some of the light will radiate out of the taper, introducing loss, which goes against the goal of reducing the coupling loss between waveguide and optical fiber. A taper that satisfies the low loss requirement is called an *adiabatic taper*. A taper that changes the waveguide width is referred to as a *lateral taper*, while a taper that changes the waveguide thickness is known as a *vertical taper*.

A lateral taper will be shorter and thus more efficient when the waveguide width is reduced rather than increased. To substantially reduce the coupling loss, however, the waveguide width needs to be reduced to values less than 0.5 μm. This might be difficult to realize from the fabrication point of view. A more sophisticated lateral taper can be realized by adding a second core layer, of larger width, under the main waveguide core. As the main waveguide core width is reduced, the mode will be forced to move down into the added core layer, which has a mode closer to the fiber mode. From there the mode gets coupled to the optical fiber. Figure 3-5 illustrates the two lateral tapers.

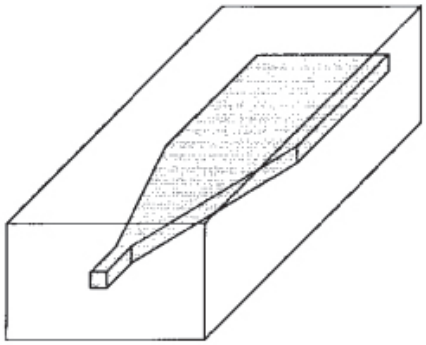

Figure 3-5 a) *Lateral down-tapered buried waveguide*

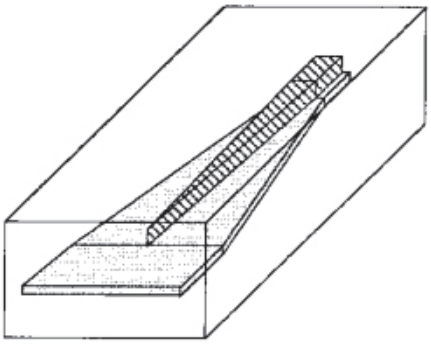

Figure 3-5 b) *Lateral down taper with second core layer under main waveguide*

A vertical taper works similarly to the lateral taper, but this time the thickness of the waveguide is tapered down. Even though the principle of operation is the same, the fabrication process for such a taper is quite different from the one used to change the waveguide width. The waveguide width is determined during the photolithography process. A thickness change is more complicated; one possible solution is to use several etching steps.

Combined lateral and vertical tapers are also possible. SSCs are capable of reducing the coupling loss between III-V semiconductor waveguides and single-mode optical fiber to values less than 1dB, which is considered an acceptable loss.

Other Passive Devices

A wide range of passive PIC devices can be constructed from straight and bend III-V semiconductor waveguides. Module 2 presented devices such as a directional coupler, a Y-splitter, a Mach-Zehnder interferometer (MZI), and a ring resonator, all based on silicon-on-insulator (SOI) waveguides. These types of devices are also fabricated from III-V semiconductor waveguides, with similar performances. The main difference is that III-V devices are slightly larger in size than their silicon counterparts due to the larger bend radius.

The following section introduces additional passive devices that were not described in Module 2. These include a multimode interference (MMI) coupler and an arrayed waveguide grating (AWG).

Multimode Interference (MMI) Coupler

A multi-mode-interference coupler consists mainly of a wide waveguide that allows for the propagation of several modes. This is in contrast to the single-mode waveguides that the vast majority of PIC devices are based on. The multimode section is fitted with input and output access waveguides, which are single-mode. Figure 3-6 shows the configuration of an MMI coupler. The width of the wide section is denoted W and its length L. The MMI illustrated below has two input and two output waveguides. Other numbers of inputs and outputs are also possible.

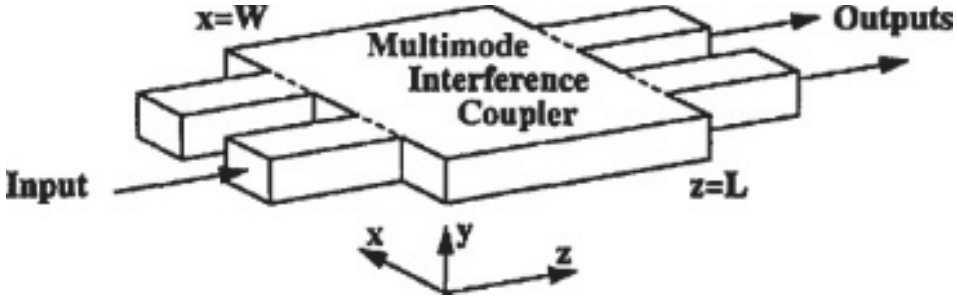

Figure 3-6 *Multimode interference coupler*

The principle of operation of an MMI device is based on interference between the waveguide modes. Light enters the device through one of the single-mode input access waveguides. When it arrives at the entrance to the wide section, it excites the modes available in the wide section and creates a certain distribution of the electric field. The different optical modes each travel with a slightly different speed inside the wide waveguide. Consequently, each mode will accumulate its own phase difference after traveling the distance L. If the phase differences between all modes at the end of the wide waveguide are multiples of 2π, the modes will interfere constructively, and the final distribution of the electric field will reproduce the initial distribution at the start of the wide waveguide. This phenomenon is denoted as *self-imaging*. Specifically, when phase differences are multiples of 2π we obtain a single image that exactly reproduces the input light, that is, the output light exits from the waveguide directly across the input waveguide. This is called a direct single image. MMI devices are often designed to achieve self-imaging.

A mirrored single image is also possible with an MMI coupler; this happens when light exits an output waveguide in a mirror position from the input waveguide. In addition to single images, we can also create multiple images by extending the distribution of the electric field over several output waveguides. In this case, the input power is split between the output waveguides.

The width W of the wide waveguide determines how many modes can propagate through the device. This is a critical parameter for the MMI coupler imposing tight fabrication tolerances. In general, MMI couplers are designed to allow from 3 to 8 modes in the wide region. The length, L, is the parameter that determines what kind of image forms at the exit from the wide region. Of interest are direct single, mirrored single, and certain multiple images.

Recall that each mode has its own effective refractive index, n_{eff}, that determines the phase accumulated by the light traveling in the waveguide. The equation for the phase was given in Module 2 and is repeated below.

$$\Phi = (2\pi/\lambda)\, n_{eff}\, L \qquad (3\text{-}1)$$

The different modes of the waveguide are labeled 0, 1, 2, …, with mode 0 being the fundamental mode. The corresponding effective refractive indices are n_{eff0}, n_{eff1}, n_{eff2}, … We define a length L_π to be equal to:

$$L_\pi = \lambda/[2\,(n_{eff0} - n_{eff1})] \qquad (3\text{-}2)$$

where λ is the wavelength of the light.

The reults of different lengths of L of the wide waveguide are as follows:

1) Direct single images form when L is an even multiple of 3 L_π.
   $L = p\ (3\ L_\pi)$ with p = 0, 2, 4, … (3-3a)
2) Mirrored single images form when L is an odd multiple of 3 L_π.
   $L = p\ (3\ L_\pi)$ with p = 1, 3, 5, … (3-3b)
3) Multiple images form when L is a half integer of 3 L_π.
   $L = p/2\ (3\ L_\pi)$ with p = 1, 3, 5, … (3-3c)

Figure 3-7 illustrates a 4 x 4 MMI coupler where light enters the chip through waveguide 2 and is then split equally between the four output waveguides. The device thus implements a splitter with four outputs. Part b) of the figure shows the simulated distribution of the electric field through the entire length of the device.

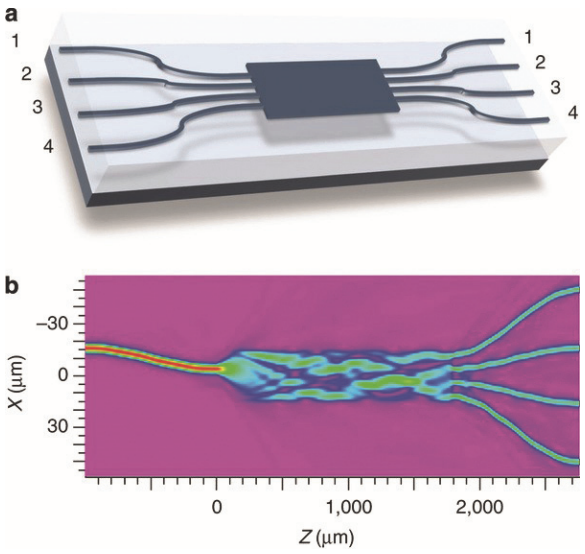

Figure 3-7 a) *Multimode interference coupler in 4 x 4 coupler configuration;* **b)** *Simulation of the electric field of the light wave over the length of the device*

Due to the properties described above, MMI devices are used in coupler and splitter applications. Module 2 described directional couplers and Y-branches that achieve these functions. Recall that a directional coupler has two inputs and two outputs and that we can create any power splitting ratio between the two outputs by controlling the length of the coupling region. The most used application of a directional coupler is equal power splitting between the two outputs, in which case the device is known as a 3dB coupler. 3dB directional couplers are used by themselves or as part of Mach-Zehnder Interferometer devices. A Y-branch has one input and two outputs that carry equal power.

The MMI coupler in Figure 3-6 has the same functionality as a directional coupler. Depending on the length L, power can exit entirely from the output waveguide, which is located directly across the input waveguide; this is called the *bar state* of the coupler. Power can also exit from the output located diagonally across from the input, in which case the coupler is said to be in *cross state*. Power can also be split equally between the two outputs.

MMI couplers have several advantages over directional couplers (DC). Because they do not rely on a precisely controlled narrow gap between two waveguides, they are easier to fabricate than DCs. They are also less dependent on the light's wavelength and polarization. For splitters with 3, 4, or more outputs, these can be achieved with just one MMI coupler. To obtain a 1 x 4 splitter using DC or Y-branches, we need cascaded devices to successively divide the power between the output ports. Because of their advantages, MMI couplers are often used in devices such as Mach-Zehnder interferometers and others.

Example 2

Find the shortest length L of an MMI coupler with two inputs and two outputs that results in a cross state for the coupler, and in a 3dB coupler. Assume that the effective refractive indices of the fundamental and first order modes of the wide waveguide are 3.2380 and 3.2343 respectively. The wavelength is 1.55 μm.

Solution: First calculate length L_π using equation 3-2.

$L_\pi = \lambda/[2\ (n_{eff0} - n_{eff1})] = 1.55\ \mu m/[2\ (3.2380 - 3.2343)] = 209.5\ \mu m$

The cross state for the coupler corresponds to a mirrored image. Using equation 3-3b the first mirrored image is obtained when $L = 3\ L_\pi = 628\ \mu m$.

The 3dB coupler corresponds to a multiple image. Using equation 3-3c the first multiple image is obtained when $L = (1/2)\ (3\ L_\pi) = 314\ \mu m$.

Arrayed Waveguide Grating

An arrayed waveguide grating (AWG) is a device capable of multiplexing and demultiplexing light waves with different wavelengths. It is an important component for wavelength division multiplexing (WDM), a method used to increase the amount of information transmitted in an optical communication system. The method consists of combining, or *multiplexing*, multiple signals of slightly different wavelengths and launching them in the same optical fiber. At the end of transmission, a process called *demultiplexing* separates the signals.

An AWG is a quintessential example of the high level of integration that can be achieved by a PIC and the advantages it can afford. Before AWGs were invented, devices for wavelength division multiplexing included micro-optics elements and cascaded filters. Micro-optics perform very well but occupy more space than integrated optics devices and are not easy to manufacture. Cascaded filters have their own disadvantage: because each filter works with only one wavelength, multiple filters corresponding to the desired wavelengths must be cascaded, which gives the device a high total insertion loss. To limit the insertion loss, these devices operate with 4 to 8 different wavelengths or channels. By contrast, in an AWG the insertion loss does not scale with the number of channels. AWGs with 32 or 40 channels are common, but higher numbers of channels are possible, for example AWGs with 96 channels have been demonstrated.

An AWG is a complex PIC that includes several important elements, illustrated in Figure 3-8. The device in the figure works as a *demultiplexer*, with light entering through one input waveguide on the left and exiting through multiple output waveguides on the right. The input

signal is coming from an optical fiber and consists of a multitude of wavelengths. In the case of the outputs, each output carries a single wavelength.

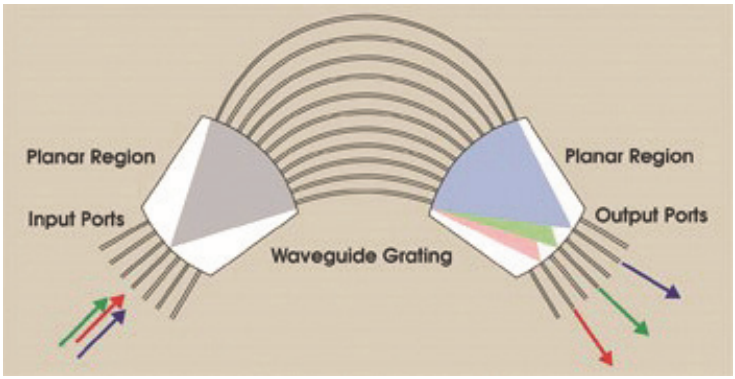

Figure 3-8 *Arrayed waveguide grating*

The following phenomena take place as we follow the light signal along the AWG, resulting in the separation of the wavelengths at the exit. The input light enters the first planar region, also called the input slab. Recall from Module 1 that a slab waveguide confines light in only one direction, the vertical direction in this case. In the horizontal direction, the large width of the slab allows for the broadening shown in the figure. This is needed to allow light to be coupled to all the waveguides in the arrayed region.

When the light reaches the end of the planar region, it enters the arrayed waveguide grating region. This region is made up of waveguides of varying lengths, with shorter waveguides on the bottom and progressively longer waveguides as we move toward the top. The length difference between any two adjacent waveguides is the same and is equal to an integer multiple of the central wavelength of the demultiplexer. We denote the central wavelength by λ_c and the length difference between waveguides by ΔL.

The individual light waves carried by the arrayed waveguides will interfere in the second planar region (or output slab). Light traveling in each of the arrayed waveguides will accumulate a certain phase, whose value depends on the wavelength. For a wavelength equal to λ_c the phases at the end of the arrayed waveguides will differ by multiples of 2π. This will result in constructive interference at the end of the second planar region, which will have the effect of recreating the input field at the output. The green arrow in Figure 3-8 illustrates this effect.

For wavelengths different from λ_c, the phases at the end of the arrayed waveguides differ by quantities other than 2π. Because of this, the input field will now be recreated in a different output location than across from the input. The red arrow, corresponding to a higher wavelength than the green one, illustrates wavelengths larger than λ_c exiting from the bottom half of the chip. Shorter wavelengths (represented by the blue arrow) will exit from the top half of the chip.

If the direction of propagation of the light in Figure 3-8 is reversed, the AWG functions as a *multiplexer*. In this case, multiple beams of light, each with a different wavelength, enter the device from the right. The exit to the left is through one output carrying all the different wavelengths in the same waveguide.

The basic equation describing the relationship between the central wavelength and the length difference between two adjacent arrayed waveguides in an AWG is given by:

$$\Delta L = m\lambda_c/n_{eff} \tag{3-4}$$

Here, m is an integer called the grating order, and n_{eff} is the effective index of the waveguides in the array.

Example 3

Find the ΔL of an AWG with central wavelength equal to 1550 nm, based on arrayed waveguides with effective index equal to 3.21. Assume that the grating order m is equal to 64.

Solution: Using equation 3-4, we obtain $\Delta L = m\lambda_c/n_{eff} = (64)(1.55\mu m)/3.21 = 30.9\ \mu m$.

Figure 3-9 shows more details about the geometry of the AWG's elements. In this figure, the planar regions are called *free propagation regions*, or FPR. As the figure shows, the first FPR ends in a circular arc, centered at the point where light enters the slab. The radius of the arc is denoted by R. The second planar region which is symmetric to the first one, has the same radius of curvature, R. Other parameters that determine the separation between the wavelengths at the output of the AWG are: the effective index of the slab, n_s; the distance between two adjacent arrayed waveguides at the end of the first planar region, also called the pitch of the arrayed waveguide, d; and the distance between two adjacent output waveguides at the exit from the second planar region, D.

The array pitch, d, is a critical element for an AWG: it directly influences the device's insertion loss. It is desirable for the pitch to be very small so that the field exiting from the first slab can be coupled in its entirety to the arrayed waveguides. In practice, there will always be a small amount of coupling loss between slab and waveguides, because the fabrication process cannot reduce gaps between waveguides below certain values. With III-V semiconductors, we can create waveguide gaps of about 0.5 μm, which results in very little coupling loss. We need to keep in mind, though, that this loss is multiplied by two because there are two slabs.

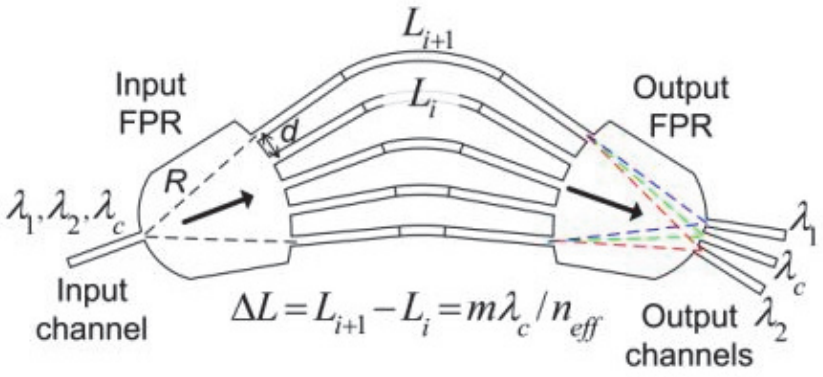

Figure 3-9 *Arrayed waveguide grating*

The response of the AWG is periodic in wavelength. We explained previously that as wavelength increases, light at the exit moves from the top to the bottom output waveguides. However, if we keep increasing the wavelength of the light in the input waveguide, at some point we will see a jump from the bottom output waveguide to the top one. After this jump, the cycle repeats. The quantity that describes the maximum wavelength range we can have before jumping back to the top is called the *free spectral range* or FSR. The FSR of an AWG can be obtained with the following equation:

$$FSR = \lambda_c/m \tag{3-5}$$

Here, λ_c is the central wavelength and m is the grating order.

The FSR of the AWG dictates the maximum number of wavelengths channels, N, that the device can demultiplex. This number can be obtained by dividing the FSR by the wavelength separation between two channels, $\Delta\lambda$. Some typical values for the wavelength separation are 1.6 nm and 0.8 nm.

$$N = FSR/\Delta\lambda \tag{3-6}$$

Example 4

For the AWG in Example 3, find the FSR and the maximum number of channels. Assume a wavelength separation between channels equal to 0.8 nm.

Solution: The AWG in Example 3 has a central wavelength λ_c equal to 1.55 μm and a grating order m = 64. Using Equation 3-5, we obtain FSR = 1550 nm/64 = 24.2 nm.

The maximum number of channels can be obtained using equation 3-6:

N = 24.2 nm/0.8 nm = 30.27. By rounding the result to an integer we obtain N = 30.

International Telecommunications Union (ITU) Grid

The wavelengths used with wavelength division multiplexing have been standardized by the International Telecommunication Union (ITU). These wavelengths and their corresponding frequencies form what is called the *ITU grid*. Recall the relation between wavelength, λ, and frequency, f, of light, which allows us to determine one quantity when the other is known:

$$\lambda = c/f \tag{3-7}$$

On the ITU grid a common spacing of the channel frequencies is 100 GHz. Using Equation 3-6, we can see that this corresponds to an approximate wavelength spacing of 0.8 nm for wavelengths around 1550 nm. In the C-band that spans the wavelength range between 1530 nm and 1565 nm we can fit about 40 channels separated by 100 GHz. By extending the C-band, 72 ITU channels are defined as follows:

Channel #1, f_1 = 190,100 GHz, λ_1 = 1577.03 nm
Channel #2, f_2 = 190,200 GHz, λ_2 = 1576.20 nm
Channel #3, f_3 = 190,300 GHz, λ_3 = 1575.37 nm
Channel #72, f72 = 197,200 GHz, λ_{72} = 1520.25 nm

Example 5

Find the channel number and the frequency on the ITU grid corresponding to a wavelength of 1550 nm.

Solution: For light with wavelength equal to 1550 nm, the frequency can be calculated from equation 3-5.

$f = c/\lambda = 299{,}792{,}458 \text{ m/s}/(1550 \times 10^{-9} \text{ m}) = 1.93414 \times 10^{14} \text{ Hz} = 193{,}414 \times 10^{9} \text{ Hz} = 193{,}414 \text{ GHz}.$

The frequencies on the ITU grid are multiples of 100 GHz. The closest such multiple to the value 193,414 GHz is 193,400 GHz.

Channel #1 has a frequency equal to 190,100 GHz. The difference between the two is

193,400 – 190,100 = 3,300 GHz.

Dividing this by 100 GHz we find 3,300/100 = 33. The channel number is 1 + 33 = 34.

The channel number corresponding to the wavelength 1550 nm is 34, and the ITU frequency is 193,400 GHz. However, the wavelength of this channel is not exactly equal to 1550 nm.

The exact value for the wavelength is given by

$\lambda = c/f = 299{,}792{,}458 \text{m/s}/(1.93414 \times 10^{14} \text{ s}^{-1}) = 1550.12 \text{ nm}.$

Note: To obtain accurate results in this example, we used a more precise value for the speed of light in a vacuum. This value is 299,792,458 m/s (vs. the rounded value 3×10^{8} m/s that is usually considered).

Note that the ITU frequencies are represented by whole numbers, and are equally spaced. By contrast, the corresponding ITU wavelengths are not whole numbers, and are not equally spaced. We can determine the wavelength spacing $\Delta\lambda$ corresponding to a known frequency spacing Δf by using the following equation:

$$\Delta\lambda = \lambda^2 \, \Delta f/c \qquad (3\text{-}8)$$

Example 6

Find the wavelength spacing corresponding to a 100 GHz frequency spacing for a wavelength equal to 1530 nm and a wavelength equal to 1560 nm.

Solution: For light with wavelength equal to 1530 nm, the wavelength spacing can be calculated from equation 3-8.

$\Delta\lambda = \lambda^2 \, \Delta f/c = (1530 \times 10^{-9} \text{ m})^2 \times (100 \times 10^{9} \text{s}^{-1})/(299{,}792{,}458 \text{ m/s}) = 7.81 \times 10^{-10} \text{m} = 0.781 \text{ nm}$

Applying the same equation for the wavelength of 1560 nm, we obtain:

$\Delta\lambda = \lambda^2 \, \Delta f/c = (1560 \times 10^{-9} \text{ m})^2 \times (100 \times 10^{9} \text{ s}^{-1})/(299{,}792{,}458 \text{ m/s}) = 8.12 \times 10^{-10} \text{m} = 0.812 \text{ nm}$

The two wavelengths spacings are approximately equal to 0.8 nm. However, if we need to know the precise ITU wavelengths we cannot obtain them by repeatedly adding 0.8 nm the same way we add 100 GHz to the ITU frequencies.

For wavelength division multiplexing (WDM) the most common values for channel spacing are 200 GHz, 100 GHz, and 50 GHz. The corresponding approximate wavelength spacings are 1.6 nm, 0.8 nm, and 0.4 nm. When a spacing of 200 GHz is used, we can use either the even numbered channels or the odd numbered channels described above. When 50 GHz is used, channels placed at the mid points of the ones described above must be obtained.

AWG Spectral Response

An AWG is a filter type of device. Such devices perform operations based on the wavelength of the input light. Module 2 presented an example of a filter device, the ring resonator. Like the behavior of ring resonator, the behavior of the AWG device can be described by the transmission of the optical signal through the AWG vs. the wavelength. Transmission is defined as the ratio of the output power to the input power, and is most commonly expressed in dB.

Figure 3-10 shows a typical transmission curve for one output of an AWG device. The figure shows the transmission for both light polarizations, TE and TM. Ideally, the transmission for the two cases should be identical. The maximum transmission for the TE polarization is about -4 dB, and the maximum for the TM polarization is about -5 dB. The two maxima both appear at a wavelength approximately equal to 1560 nm.

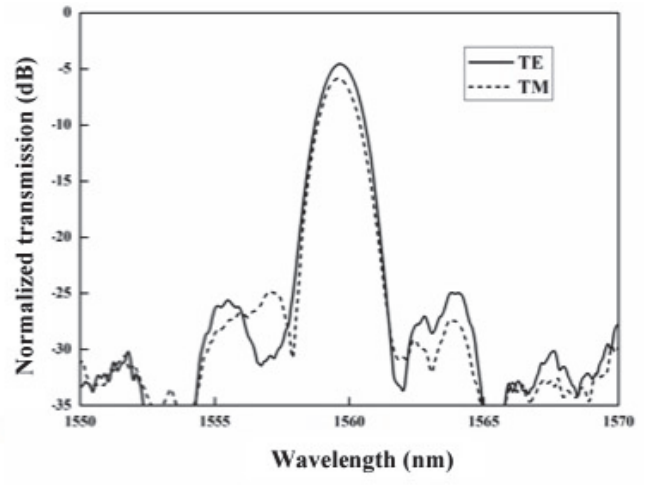

Figure 3-10 *Transmission vs. wavelength for one output of an arrayed waveguide grating, for TE and TM polarizations*

Figure 3-11 shows the superimposed transmission curves for all outputs of an AWG. Each color represents a different output. The device illustrated has 8 outputs, with a channel spacing of 200 GHz, or about 1.6 nm. The periodic response of the AWG is illustrated by the repetition of the eight channels every 30 nm. Three such repetitions are visible in the figure.

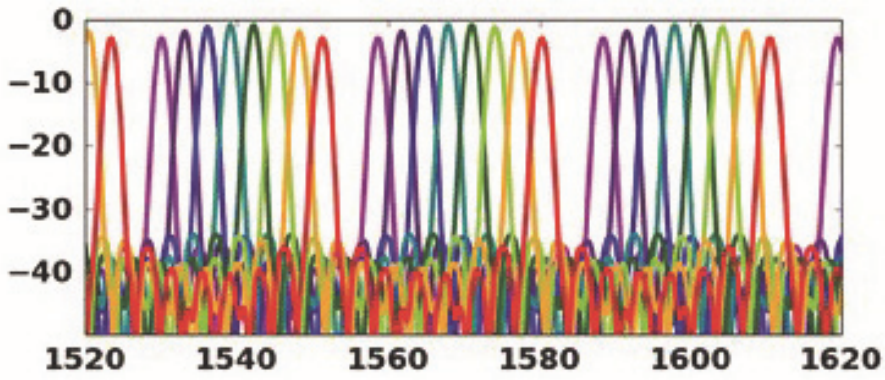

Figure 3-11 *Eight-channel, 200 GHz arrayed waveguide grating transmission vs wavelength. The FSR of the AWG is about 30 nm.*

Characteristic Parameters of AWG

AWG devices have several characteristic parameters, which we define below. Most of these parameters are illustrated in Figure 3-12.

The *number of channels* is given by the number of wavelengths that the device can multiplex or demultiplex. Typical numbers of channels used are 8, 16, 32, and 40.

The *channel spacing* (nm or GHz) is the wavelength or frequency separation between two adjacent channels. Common values for channel spacing are 200 GHz, 100 GHz, and 50 GHz.

The *channel wavelengths* (nm) are the wavelengths corresponding to the peak of the transmission for each AWG output. These wavelengths must be aligned to the ITU grid.

The *wavelength accuracy* (nm) is the maximum difference between the ITU wavelengths and the actual center wavelengths of the AWG across all outputs. This parameter reflects how closely the channel wavelengths are aligned to the ITU grid. Values less than 0.05 nm are desirable for a channel spacing of 0.8 nm.

There is a direct dependence between the channel wavelengths and the effective index, n_{eff}, of the arrayed waveguides. Because the index of refraction of the materials used to fabricate AWGs varies with temperature, the device temperature must be kept constant to maintain the alignment to the ITU grid. This is achieved by using an RTD (resistive temperature-sensing device) or thermistor. The drawback to RTDs is that they increased the device's power consumption.

The *passband* (GHz or nm) is the range of wavelengths of interest around the center wavelength of each channel. This parameter serves to define other parameters as shown below. For channels separated by 100 GHz the passband is 25 GHz. For example, the center frequency of ITU channel #34 is 193,400 GHz. The passband for this channel extends 12.5 GHz to the left and right of the center frequency, from 193,387.5 GHz to 193,412.5 GHz.

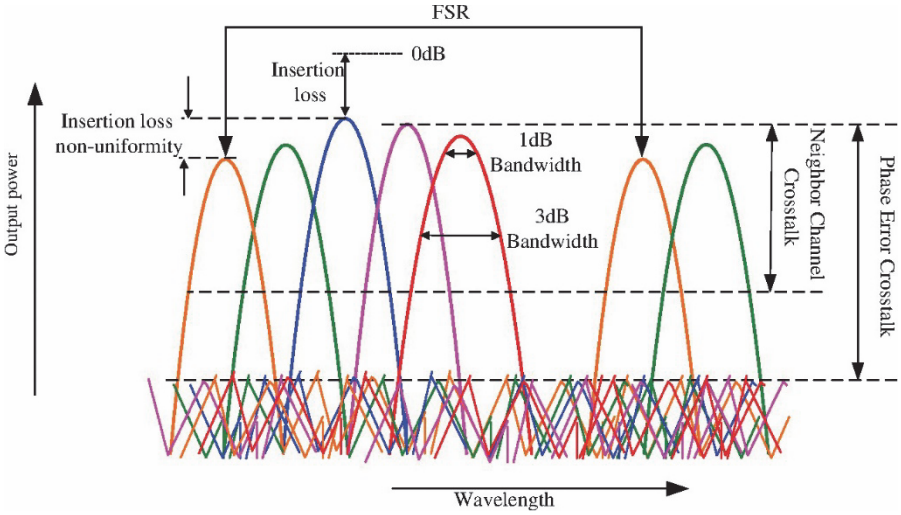

Figure 3-12 *AWG parameters*

The *FSR (nm or GHz)* is the minimum wavelength (or frequency) range corresponding to two input signals that exit from the same AWG output.

The *insertion loss* (dB) can be found using the peak of the transmission curve in each channel; the minimum peak loss across all channels is the device's insertion loss. The insertion loss should be minimized to avoid losing optical power as light travels through the AWG. Values below -3dB are desirable. Recall that insertion loss is typically expressed as a negative number.

Insertion loss non-uniformity (dB) is the maximum spread between the peak losses of all channels. This non-uniformity should be as close to zero as possible, desirable values being less than 1.0 dB. There is a typical insertion loss roll-off as we move from an AWG's center channel to an edge channel (shown in Figure 3-12). This roll-off can be 3dB or even higher. Edge channels tend to have the most loss non-uniformity, while channels closer to the center are closer in insertion loss.

One way to reduce the non-uniformity is to design the AWG with a higher FSR than necessary, and not use the edge channels. For example, we might use only the 16 outputs of an AWG that has been designed with an FSR that allows for 24 channels. In this case, empty slots will appear in the AWG's transmission. For example, the AWG in Figure 3-11 was designed to allow for 10 channels, but only 8 channels are used. Using this method, we can acheive non-uniformity of values less than 1 dB, at the expense of increasing the size of the device (bigger FSR requires bigger radius for the free propagation regions).

Polarization dependent loss (PDL) (dB) is the difference between the insertion loss corresponding to the TE and TM polarizations. This parameter was illustrated in Figure 3-10, where the PDL was about 1 dB. This parameter should be less than 0.5 dB.

3dB Bandwidth (nm or GHz) is the wavelength (or frequency) range for two points on the transmission curve of one output for which the transmission is 3dB down from the peak. The 3dB bandwidth should be as large as possible to accommodate drifts, particularly drifts in the center wavelengths of the lasers used as light sources for the system. 3dB bandwidth values

greater than 50 GHz or more are desirable with 100 GHz spacing. The 3dB bandwidth and the shape of the transmission curve can be improved with special waveguide design.

In *flat-top AWGs*, the shape of the transmission curve is much flatter at the top, which increases the 3dB bandwidth. The AWGs illustrated in Figures 3-10, 3-11, and 3-12 have a Gaussian type of transmission (the name comes from the mathematical equation that describes the transmission).

1dB Bandwidth (nm or GHz) is the wavelength (or frequency) range for two points on the transmission curve of one output for which the transmission is 1dB down from the peak.

Adjacent (neighbor) channel crosstalk (dB) refers to how much light from a neighboring channel appears in the channel of interest. Consider the orange curve on the right-hand side of Figure 3-12. From the center wavelength of the orange curve (assumed to coincide with an ITU wavelength) we need to move to the right 12.5 GHz to find the edge of the passband. At that point, we move down until we intersect with the green curve, which is the neighbor channel. The value of the insertion loss at that intersection point, shown by the dotted line, represents the adjacent channel crosstalk. It is desirable to have a very small amount of adjacent channel crosstalk, less than -25dB.

Non-adjacent channel crosstalk (dB) is defined similarly to adjacent crosstalk, except that we are now looking at channels other than the adjacent ones to see how much they contribute to the output light in the channel of interest. Basically, non-adjacent channel crosstalk is shown by the noise background at the bottom of the figure. In the figure, this is called *phase error crosstalk*, which indicates that this crosstalk is caused by imperfections in the waveguides in the arrayed region. This value should also be very small, less than -30dB.

Power consumption specifies how much electrical power the packaged AWG device uses. Power is primarily consumed by the elements required to maintain the device at a constant temperature. Typical values for the power consumption in such case are about 4 or 5 W. *Athermal AWG* devices do not require external elements to keep the device temperature constant.

Other parameters, such as chromatic dispersion and polarization mode dispersion, complete the description of an AWG device. These parameters are not described in this course.

Performance of III-V Semiconductor AWG Devices

As a stand-alone component, AWGs based on III-V semiconductor materials do not have the best performance compared with AWGs fabricated from other material platforms. This is especially true for the insertion loss and crosstalk parameters. Contributions to the higher insertion loss include propagation loss, reflection loss at the interface between semiconductor and air, and coupling loss to optical fibers. The propagation loss is somewhat mitigated by the small size of the device, which results in shorter waveguides. The reflection loss can be reduced by antireflection coatings. Even with these measures, insertion loss values greater than 5 dB are common with III-V semiconductor AWGs. The higher crosstalk on the other hand is due to errors in the arrayed waveguide dimensions, which translate to non-uniformities in the effective index of the waveguides. Advances in the fabrication process have improved the waveguide uniformity and resulted in crosstalk values around 25-30 dB for III-V semiconductor AWGs.

Several advantages compensate for these drawbacks. AWG devices are very compact. Moreover, various active elements can be easily integrated on the same substrate with AWGs, for example photodetectors and optical amplifiers. AWGs with integrated photodetectors can be used advantageously in monitoring applications to provide information about the power level in each channel. When AWGs are integrated with optical amplifiers, the insertion loss issues can be eliminated by direct amplification of the optical signal in each channel. We will describe these types of applications and their advantages after we take a look at active III-V semiconductor devices.

Active III-V Semiconductor PIC Devices

Diode Lasers

III-V semiconductors have excellent light emitting properties, which are exploited in the fabrication of diode lasers. Diode lasers are described below starting with the first such laser realized in gallium arsenide (GaAs), followed by double heterostructure and other types of diode lasers that are used in photonic integrated circuit devices.

Emission of Light by Semiconductor Diodes

The word laser is an acronym for *light amplification by stimulated emission of radiation.* The basic components of any laser are an *active medium* capable of light emission, a *feedback cavity* containing the active medium with mirrors at both ends, and a *pump source*. The mirrors must have very high reflectivity so that the light emitted by the active medium can bounce back and forth many times inside the cavity and build up.

In the case of semiconductor lasers, the active medium is the semiconductor p-n junction. The pump source is the electric current running through the junction. Figure 3-13 shows the energy-level diagram of a semiconductor diode, which is formed by bringing together an n-type and a p-type material. In semiconductor materials, electrons may have energies within certain bands. In the figure, the lower region is called the valence band and represents the energy states of bound electrons. The upper region is the conduction band and represents the energy states of free or conduction electrons. Electrons may have energies in either of these bands, but not in the gap between the bands.

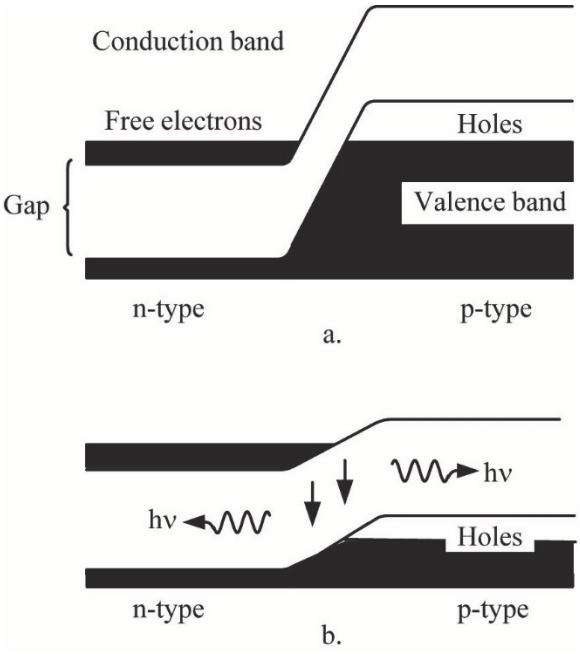

Figure 3-13 *Energy-level diagram of a semiconductor diode*

Figure 3-13a shows the relative populations of the energy bands on both sides of a p-n junction with no external voltage applied to the diode. The conduction band of the n-type material contains electrons that act as current carriers, whereas the valence band in the p-type material has holes that act as current carriers. When a forward voltage is applied to a diode, the energy levels across the junction region of the diode shift, as shown in Figure 3-13b. This shift allows electrons in the n-type material and holes in the p-type material to diffuse more readily into the junction region to establish a current through the diode. While diffusing through the junction, some electrons will combine with holes. Since the electrons in the conduction band have energies greater than those in the valence band, the electrons that combine with holes lose an amount of energy equal to the semiconductor's band gap energy. These electrons' energy loss appears as photons of light with a wavelength λ given by Equation 3-9.

$$\Delta E = hc/\lambda \tag{3-9}$$

Where ΔE is the bandgap energy, *h* is Planck's constant, *c* is the speed of light, and λ is the wavelength of the emitted photon.

As the forward voltage is increased across the diode, the current in the diode increases, and more and more electrons and holes enter the junction region and combine with one another.

Each time a hole and an electron combine, the electron drops from the conduction band to the valence band and generates a photon. At this point, the diode is operating as a light emitting diode (LED). As the forward voltage is further increased, the number of photons generated in the junction region becomes large enough to initiate the process of stimulated emission. This means that photons produced from the combining of electrons and holes stimulate other conduction band electrons in the junction region to drop to the valence band and release photons that are identical to the stimulating photon. The diode current at which stimulated emission begins is called the *threshold current*. At the threshold current, the diode begins operating as a laser.

Crystal Preparation and Internal Structure of GaAs Laser

The first material used to fabricate a semiconductor laser was GaAs, and the first laser was demonstrated in 1962. GaAs lasers may be prepared from ingots of gallium arsenide crystals that are mounted on glass plates with wax and cut into slices about 0.5 mm thick. After the slice is formed, the junction is prepared by diffusing impurities in from the surface. Thus, if the original ingot is n-type, a p-type impurity (for example, zinc) is diffused into it. Zinc vapor diffuses a short distance (a few micrometers) into the surface of the slice and forms a p-n junction. The slice then is cut or cleaved into blocks of suitable size to form the individual lasers. The blocks are small and fragile and are mounted by sandwiching them between two gold-clad metal disks. The block's dimensions are typically about one or two millimeters. The light-emitting region, that is the junction from which the radiation originates, is a thin layer only a few micrometers thick. The completed laser diodes are then attached to a copper heat sink on one side and a small electrical contact on the other.

Figure 3-14 is a diagram of the simplest (and earliest) type of gallium arsenide laser. The laser is a brick-shaped piece of GaAs prepared according to the process described above. GaAs cleaves easily along certain crystal planes, leaving flat parallel surfaces.

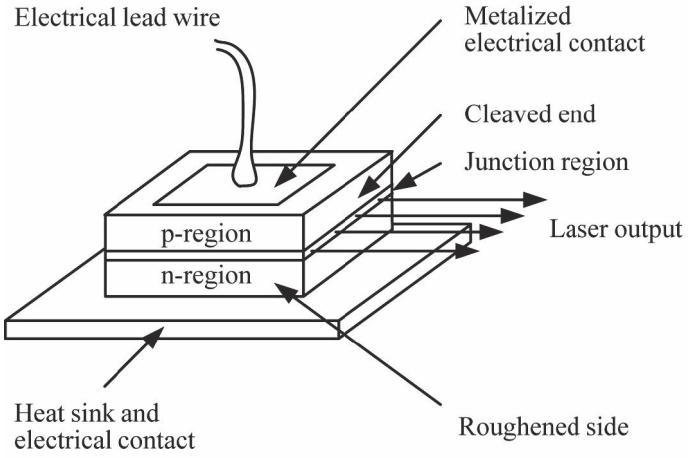

Figure 3-14 *Gallium arsenide laser diode*

Usually, the mirrors at the ends of the laser cavity are formed from the cleaved ends of the laser diode, with no further coating. The reflectivity at the interface between gallium arsenide and air is approximately 36%. If output is desired from only one end of the device, or if mirrors of higher reflectivity are desired to reduce the threshold for laser operation, the reflectivity may be increased by coating the surfaces with metal films. Optical standing waves may exist between any two of the parallel surfaces of the diode. Two sides are purposely roughened to reduce reflection and prevent lasing "across" the diode cavity.

The output power available from this laser is limited by the gain of the active medium, which is dependent on the current density through the junction. Higher currents produce greater power, but higher currents also increase heating effects that can damage the device.

Losses in the laser cavity have two primary causes. The first is diffraction loss. The active region has a width of only about one micrometer. Thus, light quickly diverges out of the active region. This loss may be reduced by making the junction wider and by better confining the light to the

active region. The second loss factor is absorption of the laser light by free carriers in the junction region. This loss may be reduced by lowering the device's temperature, which reduces the number of free carriers.

The bandgap (ΔE in Equation 3-9) of GaAs is 1.43 eV at a temperature of 300º K. This is the energy required to raise an electron from the valence band to the conduction band. Using

Equation 3-9, we find that the wavelength of the GaAs laser is around 870 nm. It is possible to develop laser diodes composed of many different chemical elements, each of which has its own unique band gap. As a result, diodes composed of different combinations of p- and n-type materials can produce laser light with many different wavelengths.

Good heat sinking is essential to remove the heat generated by the electrical current and to cool the laser. The heat sink may simply be a flat piece of metal, such as copper. A copper sheet with dimensions around $0.2 \times 2 \times 3$ cm may dissipate about 200 mW of electrical power. To minimize thermal resistance, the laser must be mounted in very close contact to the heat sink.

It's also necessary to control the temperature of the laser in order to stabilize the wavelength. The wavelength increases with increasing temperature, sometimes in discontinuous hops. If a specific operating wavelength is needed, the laser temperature must be controlled. For many applications that require only low power, it's enough to simply mount the laser on a copper plate to spread the heat. For applications requiring higher power, or those requiring good control of the laser wavelength, active cooling is necessary. This may be accomplished with thermoelectric coolers or with water cooling. Thermoelectric coolers, also called Peltier coolers, rely on the fact that if an electric current passes through a thermocouple made of two different metals joined at two points, heat is absorbed at one junction, called the cold junction, and heat is dissipated at the other junction, called the hot junction.

Characteristics of Light Emitted by Diode Lasers

The spectral width of the radiation from the semiconductor laser is typically around two or three nanometers, much larger than the spectral width of most other lasers. However, these lasers have many advantages, for example they can be easily modulated at high frequencies by modulating the current through the junction. They are efficient, small, and rugged, and are much less expensive than other types of lasers.

The output of semiconductor lasers is very strongly dependent on the temperature of the laser diode. As temperature increases, the threshold current for laser operation rises rapidly. Early GaAs lasers were cryogenic devices and operated only at 77ºK. Now, semiconductor lasers may be operated at room temperature or even somewhat above room temperature. Still, increased temperature decreases output, so the temperature must be limited. Manufacturers frequently state a maximum temperature at which their devices may be operated. Temperature control is also necessary to control the spectrum of the laser output. Figure 3-15 shows how the wavelength of emission of a semiconductor laser may vary with temperature. The figure shows the wavelength of a commercial device operating at a wavelength near 810 nm. There is a gradual shift toward longer wavelength, accompanied by discontinuous jumps. For any application in which the exact wavelength is important, the laser must be in a temperature-stabilized environment and the temperature must be held constant.

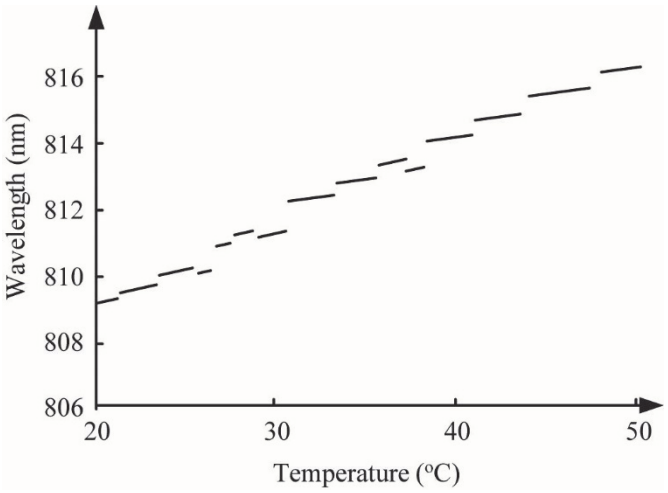

Figure 3-15 *Variation of the wavelength of a commercial semiconductor laser with temperature*

Figure 3-16 illustrates the beam divergence of a typical semiconductor laser. The emission from a semiconductor laser tends to be an elliptical beam with a full angle divergence around 20° in the direction perpendicular to the junction and around 5° in the direction parallel to the junction. These angles may vary considerably between different lasers. The elliptical beam may be rounded by using lenses that have different focal lengths in the two directions perpendicular to the direction of propagation. This will produce a beam with a more circular profile.

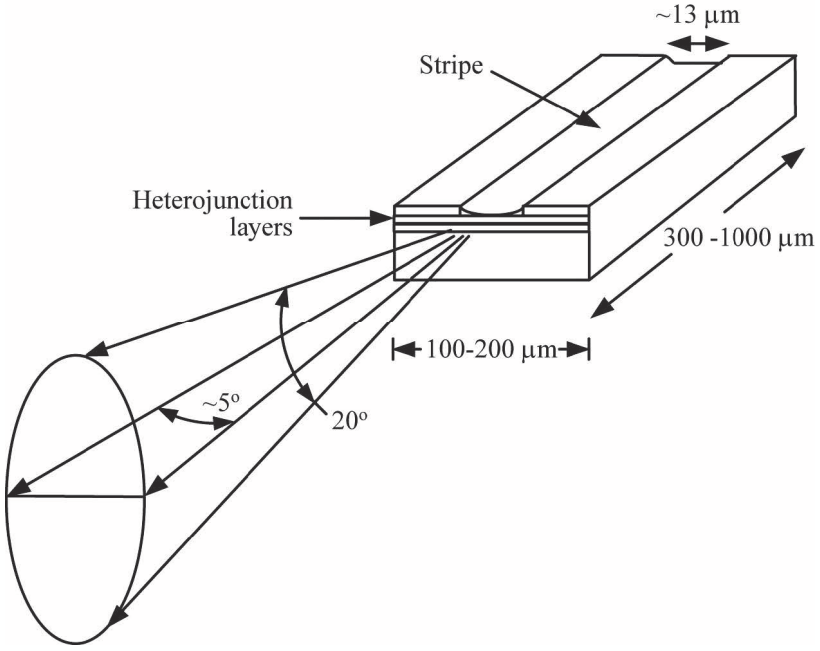

Figure 3-16 *Beam profile from a stripe geometry heterojunction semiconductor laser*

The wavelength of the semiconductor laser emission may be varied over a large range by varying the composition of the material. The most widely used semiconductor materials are the so-called III-V compounds, based on materials from columns III and V of the periodic table. Gallium arsenide is an example. But many more material compositions have been used, including ternary

compounds, which contain three elements, such as Al*x*Ga1-*x*As; or quaternary compounds, which contain four elements, such as In*x*Ga1-*x*As*y*P1-*y*. These two compounds are commonly called aluminum gallium arsenide and indium gallium arsenide phosphide, respectively. Here, both x and y are composition parameters that may each vary from zero to one independently. This allows for a wide range of material compositions with different values of bandgap, index of refraction, etc. These materials are usually grown as thin crystalline films on a crystalline substrate by a process called liquid phase epitaxy. Substrates may be materials such as gallium arsenide or indium phosphide. In this process, a mixture of materials with the desired composition is melted in contact with the substrate. Additional impurity elements may be added to make the material n-type or p-type. The melt is then cooled slowly, and the material in contact with the substrate resolidifies in single crystalline form. The resulting crystalline films are then subjected to a number of processes - including etching, metal deposition, oxide deposition, polishing, and cleaving - to form the laser devices.

Table 3-2 presents some of the III-V compounds that have been used for lasers, along with the range of wavelengths that may be obtained using each compound. The materials in the table are often simply represented by their chemical symbols, not including the composition parameters x and y. Thus, aluminum gallium arsenide may be represented as AlGaAs.

Table 3-2. III-V Semiconductor Laser Materials

Material	Wavelength Range (nm)
Aluminum Gallium Arsenide	780–880
Indium Gallium Arsenide Phosphide	1150–1650
Aluminum Gallium Indium Phosphide	630–680
Indium Gallium Arsenide	around 980
Indium Aluminum Gallium Arsenide	780–1000
Gallium Arsenide Antimonide	1200–1500
Indium Arsenide Phosphide	1000–3100
Gallium Arsenide Phosphide	600–900

Of the materials in the table, the most widely used ones have been indium gallium arsenide **phosphide (for communication applications), aluminum gallium arsenide (for data-storage** applications, such as compact disc players) and aluminum gallium indium phosphide for shorter wavelength applications (such as replacements for helium-neon lasers).
The materials discussed so far emit light in the red and infrared portions of the spectrum. Applications requiring shorter wavelengths, in the blue or near-ultraviolet regions, use materials based on gallium nitride, such as aluminum gallium nitride ($Al_xGa_{1-x}N$) or indium gallium nitride ($In_xGa_{1-x}N$). The wavelengths available from these devices cover the range from 375 nm to 640 nm. They have become important in data-storage devices requiring high packing density.

Advances in Laser Junction Structure

The simplest type of advanced junction structure is called a stripe structure. It is illustrated in

Figure 3-17, in conjunction with a double heterojunction configuration. The configuration is called a double heterojunction because there are two junctions of different materials: one between GaAs (p-type) and AlGaAs (p-type) and another between AlGaAs (p-type) and

AlGaAs (n-type). The active region of the laser is in the latter junction. The index of refraction is higher in the active region than in the materials adjacent to it. This situation increases the amount of laser light that reflects back into the active cavity, which increases the gain and lowers the threshold current needed for laser operation.

The stripe in this structure is the indentation in the top surface of the laser shown in Figure 3-17.

This indentation runs the entire length of the structure, which makes it look like a stripe. An insulating coating, most often silicon dioxide, is evaporated on the surface of the device, and the stripe is formed through techniques like photolithography and etching. A metallic layer is then deposited to form a contact; the metal is in contact with the semiconductor only in the region of the stripe. As a result, the current in the semiconductor is limited to just this region, which leads to higher current densities and larger gains in the active region.

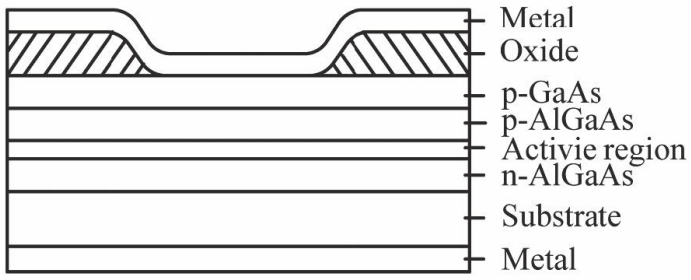

Figure 3-17 *Diagram of GaAs/AlGaAs laser with oxide stripe geometry*

This structure improves the electrical and optical confinement of semiconductor lasers and reduces the threshold currents required to operate them, thus increasing the output laser power.

This is only one example of the many variations in semiconductor laser structures that have been developed, but it shows how changes in laser structure can improve performance.

In many modern lasers, feedback is caused by reflection from a structure of finite length. These structures are said to cause *distributed feedback*. There are a number of types of distributed-feedback structures. Here, we describe two of them: *distributed-feedback lasers* and *distributed Bragg reflectors*. Both rely on a concept called *Bragg reflection*, which uses the periodic variation in some property of a material, such as thickness, to produce reflection. Bragg reflection occurs when the light passes through a structure consisting of multiple layers of alternating materials with different indices of refraction. It can also be caused by a periodic variation of some property, such as height, in a waveguide. At each boundary between successive layers with different properties, there is a partial reflection of the light. If the optical thickness of the layers is close to one-fourth of the wavelength of the light, the partial reflections can interfere constructively. The structure can serve as a high-quality reflector for a specific wavelength. If the laser's output has a broad spectrum, the reflector can select the wavelength that is four times the layer thickness and reflect that wavelength, thus acting like a narrow band filter.

In the distributed-feedback (DFB) semiconductor laser, there is a periodic corrugation in the active medium. This causes reflection and replaces the cleaved end mirrors. A DFB laser is illustrated in Figure 3-18 a).

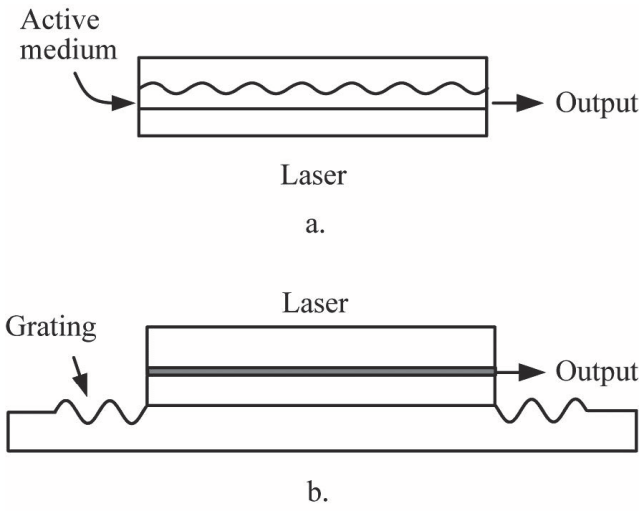

Figure 3-18 *Diagram of the side view of:* **a)** *a distributed-feedback semiconductor laser and* **b)** *a distributed Bragg reflector*

In the DFB laser, the entire laser cavity has a periodic structure that acts as a reflector.

A distributed Bragg reflector (DBR) is similar to the DFB device, both in construction and operation; see Figure 3-18 b). But the periodic structure is a grating that is outside the laser's active medium. This makes the device easier to fabricate. The gratings are at each end of the active medium and act as reflectors.

Both the DFB and DBR devices act as wavelength-selecting elements. The spacing of the periodic variations is chosen to select only a narrow band of wavelengths. Thus, they can reduce the spectral width of the laser output substantially, as compared to what was described earlier.

Additionally, these devices allow the selection of a longitudinal mode from the spectrum. If the temperature of the device changes, thermal expansion will change the spacing of the periodic variations, and the wavelength of the laser will change. Thus, if a stable wavelength is needed, the temperature of the laser must be controlled.

Multiple Quantum Well Lasers

As discussed above, strong confinement of the light inside the active medium of the laser results in a more efficient, higher power laser. An advanced approach to increasing the confinement of the light in the active layer is the use of quantum wells. These are very narrow structures that have the ability to confine electrons inside them through a quantum mechanical effect.

In multiple quantum well (MQW) lasers, the active region of the laser includes several very thin layers of semiconductor materials with alternating bandgaps smaller than the bandgaps of the surrounding material. The thickness of these layers is only several tens of nanometers (up to 50 nm). The realization of such structures was made possible by advances in the fabrication technology of semiconductor thin films. The MQW structure allows for another way to control

the emitted wavelength of the laser. In regular diode lasers the wavelength depends on the energy bandgap as shown in Equation 3-9. In the case of MQW lasers it is possible to change the wavelength of the emitted light by changing the thickness of the quantum wells. An example of an MQW laser is shown in Figure 3-19.

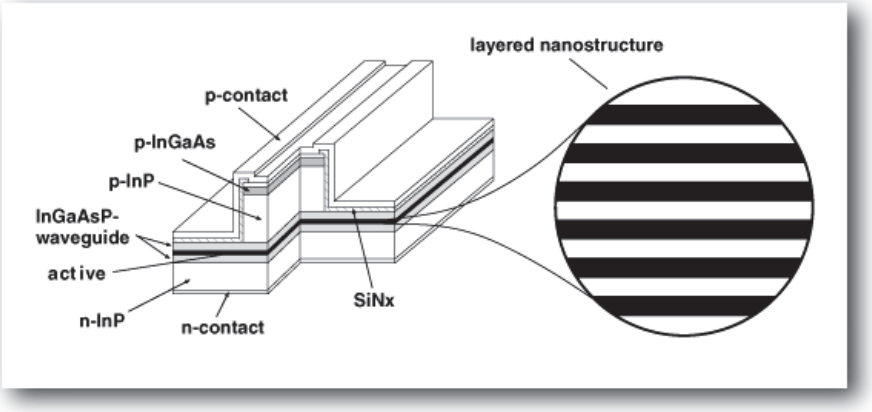

Figure 3-19 *A semiconductor laser using a multiple quantum well structure in the active region*

Semiconductor lasers offer important advantages over other lasers:

- High efficiency, up to near 50% in many cases.
- Compactness, with single diodes in packages of sub-centimeter size.
- Low power consumption – both voltage and current.
- High reliability and long life – up to tens of thousands of hours.
- Relatively low cost.

Because of these factors, semiconductor lasers have widespread usage in a very broad range of applications. Hundreds of millions of semiconductor lasers are manufactured and sold each year, the great majority in the areas of optical data storage and retrieval and optical telecommunications.

Semiconductor Optical Amplifier (SOA)

An optical amplifier is an active device that produces an output power greater than the input power. The amplification is described by the gain parameter, equal to the ratio of the output power to the input power.

$$G = P_{out}/P_{in} \tag{3-10}$$

Example 7

Find the gain in dB of an optical amplifier that takes in 15 μW of power and produces an output power equal to 2.5 mW.

Solution:

Using Equation 3-10 we find that G = (2.5 mW)/(15 x 10^{-3} mW) = 166.67

We can convert this value to dB using the following equation:

G = 10 x $\log_{10}$(166.67) = 22.2 dB

Amplification corresponds to a gain, G, greater than one. To create a gain in the optical power, the amplifier needs a pump or an energy source. In the case of the semiconductor optical amplifier (SOA), the gain is created by the active region of the amplifier under the action of an electric current running through it which acts as the pump. In other words, the SOA is similar to a semiconductor laser except that it does not have feedback, which was provided by the cavity mirrors in lasers. For the amplifier, reflection of the light at the ends of the active region must actually be prevented for the device not to start lasing. This can be achieved by depositing antireflection coatings at the two ends.

Figure 3-20 shows a schematic of an SOA. The pump current runs vertically between the two metal electrodes. The active or gain region is the layer of intrinsic InGaAsP semiconductor. This layer also acts as the core of the optical waveguide that guides the light through the structure.

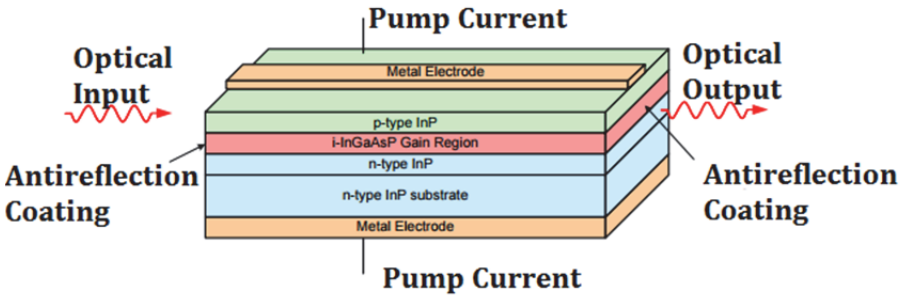

Figure 3-20 *Semiconductor optical amplifier based on InGaAsP/InP materials*

Like other optical amplifiers, the SOA exhibits certain characteristics. One of these is gain nonlinearity or saturation. This happens when the output optical power reaches high levels, at which point the gain starts to level off. For an SOA the maximum output power is about 63 mW.

SOAs also have some amount of noise, meaning that there is a background to the output power that is coming from other sources than the input light. This background is called *amplified spontaneous emission* (ASE) and is made out of photons spontaneously emitted in the active medium. By contrast, it is the stimulated emission photons that are responsible for the amplification of the input light. To reduce the effect of the ASE noise, filters can be used at the exit from the amplifier. Table 3-3 summarizes some of the main properties of SOAs.

Table 3-3. Main properties of SOAs

Gain (dB)	> 30
Wavelength (nm)	1280 – 1650
Polarization sensitivity	Yes
Noise figure (dB)	8
Pump power (mA)	< 400
Size	Small
Cost factor	Low

Important advantages of SOAs include their electrical pumping, small size, low cost, and potential to be integrated with other semiconductor PICs. One example of such monolithic integration resulting in a high performance PIC device is the multiwavelength laser.

Integrated Multiwavelength Laser

An integrated multiwavelength laser device can be created by inserting an array of SOAs together with an AWG multiplexer inside a feedback cavity with high reflectivity mirrors. Figure 3-21 shows a schematic representation of this type of laser. The laser's principle of operation is as follows: because of the feedback provided by the cavity mirrors the SOAs act as lasers, rather than just amplifiers. The multiplexer selects the wavelengths the SOAs will amplify according to the channels the AWG is designed for. The multiplexer also combines the four input channels into a single output.

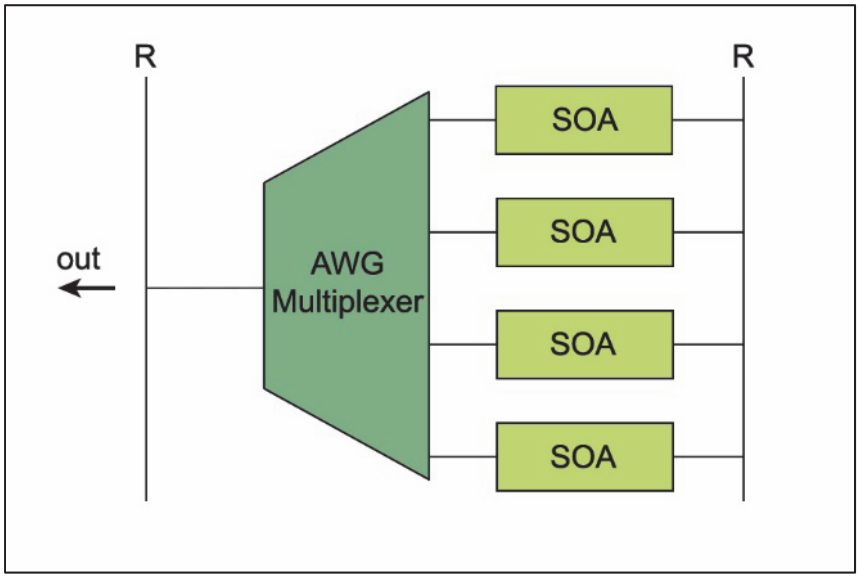

Figure 3-21 *Integrated multiwavelength laser based on SOA array and AWG multiplexer*

A recent advanced device based on this principle was demonstrated in the form of a four-wavelength, short-pulse laser integrated on a single chip. Figure 3-22 illustrates the chip, which is based on InP materials, including multiple quantum well structures in the active devices. The

devices integrated together in the 3 mm x 6 mm chip include: an array of four SOAs as optical sources, an array of four delay lines based on passive waveguides, an AWG acting as a wavelength selector and multiplexer for the four channels, a saturable absorber (SA), a common SOA, and a spot-size converter to convert the waveguide mode to a mode close to the optical fiber's mode. The edges of the chip are cleaved to create the feedback reflective elements. The active devices are shown in yellow in the figure, and the passive waveguide devices are shown in green.

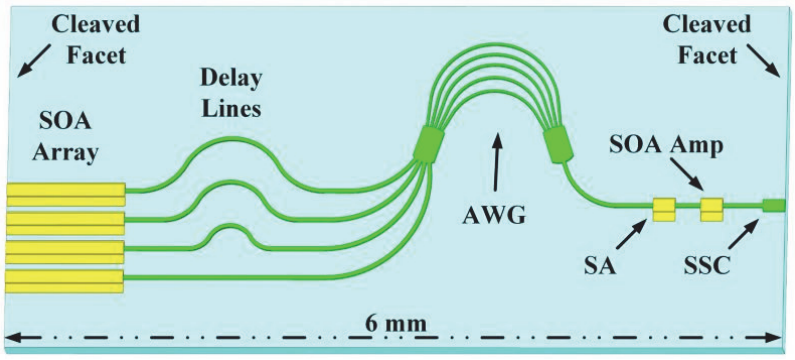

Figure 3-22 *Monolithically integrated short pulse multiwavelength laser*

The integrated multiwavelength laser is emitting 4 channels separated by 400 GHz, each producing short pulses of light with a repetition frequency of 2.53 GHz. This is the first demonstration of a monolithically integrated short pulse multiwavelength laser. Previous such devices were based on discrete (bulk) optical elements, making the device much bigger in size, more expensive, and harder to create in high volume.

Modulators

Modulators are devices capable of adjusting the power level of an optical signal to any value between a minimum value and a maximum value. A controlling signal, usually an electric current, is used to achieve the desired output optical power.

Modulators fabricated from III-V semiconductors are based on the phenomenon of electroabsorption: the absorption of the material changes when an electric field is applied to it. When the amount of light absorbed by the material increases, the optical power transmitted at the output decreases. The increase in absorption is achieved by applying a reverse voltage. These modulators are called *electroabsorption modulators* (EAM).

The voltage applied to the modulator consists of short *radio frequency* (RF) square pulses. Under the action of the applied voltage, the modulator switches the optical power at the output on and off. The *extinction ratio* (ER) of the modulator, expressed in dB, is defined as the ratio between the output power in the ON state and the minimum output power that can be achieved in the OFF state (Equation 3-11). This minimum cannot be made exactly zero, but it can be a small value.

$$ER = P_{out\ ON}/P_{out\ OFF} \tag{3-11}$$

Example 8

Find the extinction ratio of a modulator that takes in 1.5 mW of power and reduces it to an output power of 60 μW in the off state.

Solution:

The extinction ratio can be calculated using equation 3-11:

$ER = 10 \times \log_{10}(P_{out\ ON}/P_{out\ OFF}) = 10 \times \log_{10}(1.5\ mW/0.06\ mW) = 14.0\ dB$

EAMs can be realized in several configurations. The simplest one is based on a single straight waveguide as shown in Figure 3-23a. The applied square voltage pulses together with the output optical power are shown in Figure 3-23b. The waveguide can have a double heterostructure and can also contain quantum well structures. The ER of these modulators can be increased by increasing the length of the waveguide, but that increases the propagation loss. The typical ER for such modulators is 15 dB. The applied voltage has an amplitude of 2-3 volts. The speed of response is high, which is characteristic of semiconductor materials. Rates of 10 Gb/s can be achieved. The chip temperature needs to be kept constant due to the material's sensitivity to temperature changes; this is often done using a thermo-electric cooler.

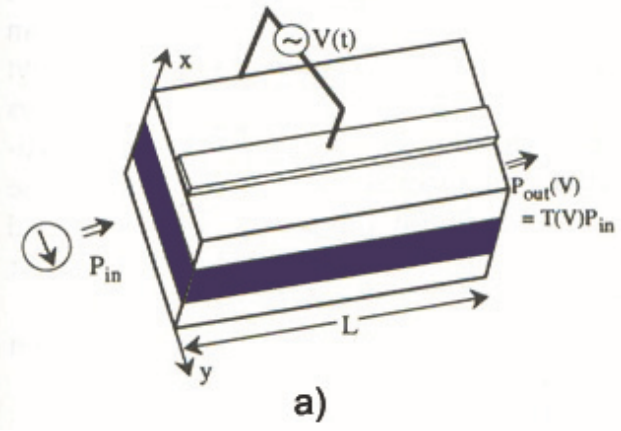

Figure 3-23 a) *Waveguide-based electroabsorption modulator*

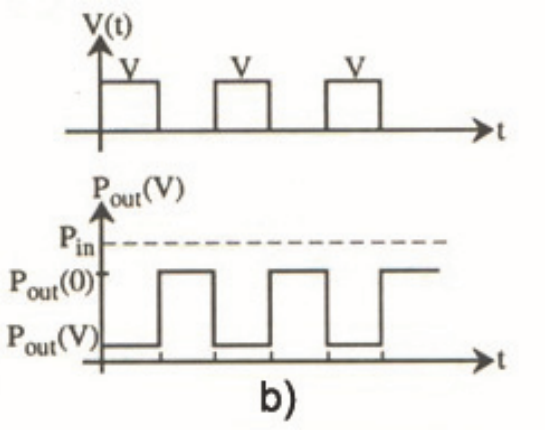

Figure 3-23 b) *Applied voltage and output optical power*

Another configuration for EAMs is based on the Mach-Zehnder interferometer (MZI), described in Module 2. An MZI consists of two 3dB couplers with two parallel waveguide arms running between them. The 3dB couplers can be realized in different ways. In Module 2 these were either based on directional couplers or Y-splitters. Semiconductor modulators based on MZI are called Mach-Zehnder modulators or MZM. Many times the 3dB couplers in MZM are implemented as multimode interference couplers (MMI), which were introduced earlier in this module. The two arms of the MZM can be equal in length or can have a length difference to bias the modulator. To modulate the output power a reverse voltage is applied to one of the arms.

Figure 3-24 illustrates the configuration of an MZM. The blue color shows the waveguide paths. As the bottom figure shows, the waveguide includes a multiple quantum well (MQW) structure. The 3dB couplers are based on MMI devices. The gold color shows the configuration of the electrodes used to apply the electric field to the modulator. This configuration, called a traveling wave configuration, allows for the electrical signal to be synchronized with the optical light signal moving through the device.

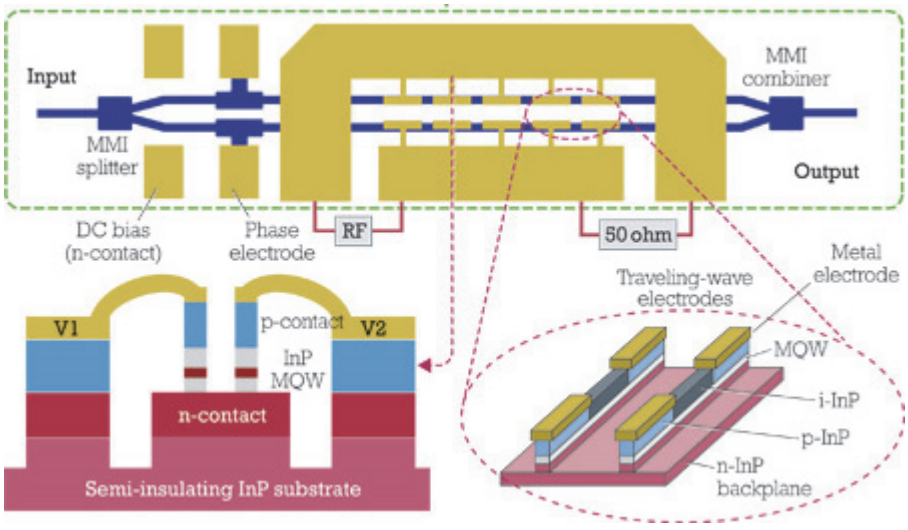

Figure 3-24 *Semiconductor Mach-Zehnder modulator configuration. The bottom half of the figure shows the waveguide structure and the traveling-wave electrode structure.*

Semiconductor MZMs have better performances than waveguide based EAM. They require smaller voltages to operate, typically 1.5 V. They have better ERs, around 25 dB, and are also faster being capable of operating at rates of 30 Gb/s and even 40 Gb/s.

Like SOAs, semiconductor modulators have the big advantage of being able to be integrated with other PIC devices in the same chip. Modulators are commonly integrated with semiconductor lasers for example.

Integrated Laser – Electroabsorption Modulator

Figure 3-25 presents an example of a semiconductor laser integrated with a waveguide-based electroabsorption modulator in the same chip. An isolation barrier electrically insulates the laser section from the modulator section using an isolation barrier. The facet of the chip that emits the laser light is coated with antireflection materials to prevent light from getting back into the chip. The laser emits continuously, and modulation is achieved in the absorption region. Semiconductor lasers integrated with MZMs are also used.

A semiconductor laser with an integrated modulator is more cost effective, because it eliminates the connection between different chips that is necessary with the combination of a laser and external modulator. The output optical power is higher with the integrated device. If the integrated device is carefully designed, it can also be faster than its discrete counterpart.

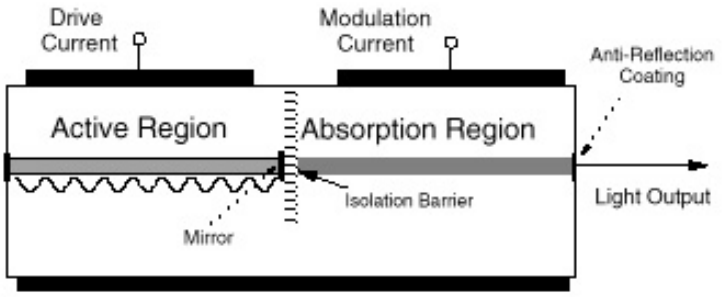

Figure 3-25 *Semiconductor DFB laser integrated with an electroabsorption modulator*

Photodetectors

Module 2 presented photodetectors (PD) and their characteristic parameters. For silicon-based PICs, germanium-based photodetectors are preferable, since germanium can be grown on silicon substrates. With III-V semiconductors, indium gallium arsenide (InGaAs) is a material combination that works for a wide range of wavelengths, including the telecommunications wavelengths of 1.31μm and 1.55 μm, as shown in Figure 3-1 at the beginning of this module.

The general principle of operation for semiconductor photodetectors is the creation of charge carriers (electron-hole pairs) under the action of light. When a semiconductor material is illuminated by photons of an energy greater than or equal to its bandgap, the absorbed photons promote electrons from the valence band into the conduction band. Electrons in the conduction band behave like free electrons able to travel long distances across the crystal structure under the influence of the applied electric field. In addition, the positively-charged holes left in the valence band contribute to electrical conduction by moving from one atomic site to another under the effect of the electric field. In this way the separation of electron-hole pairs generated by the absorption of light gives rise to a photocurrent.

The most common structure of a semiconductor photodetector is either the p-n junction or the p-i-n junction. P-i-n photodetectors are faster than p-n ones. The p-i-n structure is also used to build avalanche photodetectors which have larger responsivity than regular photodetectors.

InGaAs photodetectors are used in a variety of applications including optical power meter, optical communications, laser monitors, and others. The InGaAs photodetectors used in the wavelength range 1.0 to 1.7 μm have excellent characteristics. These include high responsivities around 1A/W, low dark current on the order of nA, and high cutoff frequencies of hundreds of MHz to a few GHz.

Like the other active III-V semiconductor devices, the photodetectors can be integrated on the same chip with other PIC devices, leading to space and cost savings, and improved performance. For example, an AWG demultiplexer device can be integrated with photodetectors for each channel. The applications for this combined device are in receiver circuits at the end of the transmission, as well as in power monitoring devices in wavelength division multiplexing optical communication systems.

Integrated Demultiplexer – Photodetectors

Figure 3-26 presents an example of integration between a 16 channel AWG demultiplexer and 16 photodetectors. The size of the chip is 3.2 mm x 4.3 mm. When integrating an AWG with photodetectors, it's necessary to take into account the different materials that make up the two devices. The AWG is based on passive waveguides with an InGaAsP core and InP cladding. The photodetectors on the other hand are based on a p-i-n structure where the absorbing layer of intrinsic (undoped) layer of InGaAs is sandwiched between n- and p-doped InP layers. To integrate these the following layers are grown on top of each other in succession: a 0.5 μm thick n-InGaAsP layer is grown first, followed by a 0.1 μm thick undoped-InP spacer layer, a 0.3 μm thick undoped InGaAs absorption layer, a 1.0 μm thick p-InP cladding layer, and a 0.3 μm thick p-InGaAs contact layer. Light is coupled vertically from the output waveguides of the AWG into the photodetectors. This is possible due to the *evanescent field* of the waveguide modes (the field extending into the cladding of the waveguide). Using the evanescent field, coupling of the light between the waveguides and photodetectors can be achieved with coupling efficiencies close to 99%.

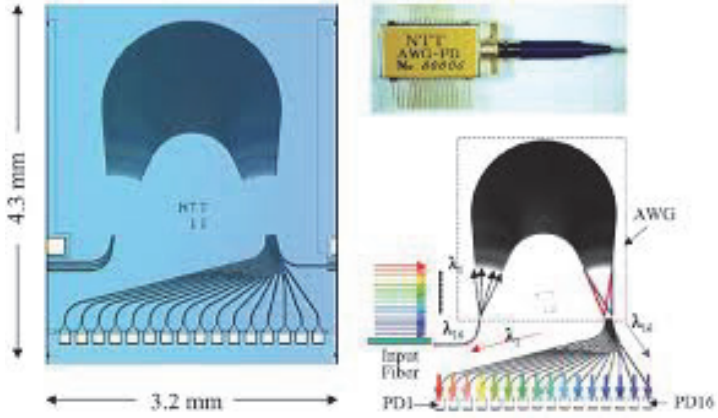

Figure 3-26 *Semiconductor AWG demultiplexer monolithically integrated with photodetectors*

Fabrication of III-V Semiconductor PICs

The fabrication process for III-V semiconductor PICs generally follows the steps described in Module 1. Some aspects of the process, however, are specific to these materials. The deposition process used to obtain the layers of materials that make up the structure of the waveguides and devices is the *metalorganic chemical vapor deposition* (MOCVD) method, also called *metalorganic vapor phase epitaxy* (MOVPE). The deposition starts with wafers of GaAs or InP. In this method, ultrapure gases are injected into a reactor. The various compounds containing the required chemical elements introduced in the reactor undergo a chemical reaction that results in the deposition of very thin layers of atoms onto the semiconductor wafer. The concentration of the source material in the reactor and the deposition rate are controlled through the vapor pressure of the metal organic compounds. This method allows for the deposition of binary semiconductor layers, as well as layers of ternary, quaternary, and higher-order alloys in a very precise fashion. Because of this, it is now the most used method for the fabrication of all the PIC devices described in this module.

This first deposition step is followed by photolithography and etching, second deposition (also called regrowth), passivation, and metallization.

SUMMARY

This module presented an overview of III-V semiconductor photonic integrated circuits. The material properties of III-V semiconductor were presented first, followed by descriptions of passive and active building-block devices. New passive devices introduced in this module included multimode interference (MMI) couplers and arrayed waveguide gratings (AWG). Active devices presented included diode lasers, semiconductor optical amplifiers (SOA), modulators, and photodetectors. Monolithically integrated devices combining passive and active PICs were discussed together with their advantages over discrete devices.

PROBLEM EXERCISES AND QUESTIONS

1. What materials can be used to fabricate photodetectors working at the wavelengths 1.31 μm and 1.55 μm, and why?
2. Calculate the refractive index contrast between GaAs and InP at the wavelength 1550nm.
3. Describe a buried channel waveguide. Include material structure, indices of refraction, and geometric parameters.
4. Describe a deep ridge waveguide and give an example of a deep ridge waveguide that has zero birefringence.
5. Explain what an adiabatic taper is and where it is used.
6. Describe multimode interference couplers, their parameters, and their advantages.
7. Find the shortest length L of an MMI coupler with two inputs and two outputs that results in a bar state for the coupler, and in a 3dB coupler. Assume that the effective refractive indices of the fundamental and first order modes of the wide waveguide are 3.225 and 3.216 respectively. The wavelength is 1.31 μm.
8. Describe the principle of operation of an AWG.
9. Calculate the central wavelength and FSR of an AWG that has $\Delta L = 41$ μm and grating order 85. The effective index of the arrayed waveguides is 3.25.
10. How many channels separated by 100 GHz can the AWG in problem 9 have?
11. Research the ITU channels for the S-band and L-band. Indicate the frequency and wavelength corresponding to the first and last channel in each band. (If needed, use c = 299,792,458 m/s for the speed of light in vacuum.)
12. Find the frequency of a channel on the 50 GHz ITU grid, between the wavelengths of 1544.5 nm and 1545.3 nm. (If needed, use c = 299,792,458 m/s for the speed of light in vacuum.)
13. What is the wavelength difference between channels 45 and 46 on the 100 GHz ITU grid?
14. Research manufacturers of arrayed waveguide grating devices and provide one set of specifications for a Gaussian and a flat-top 100 GHz AWGs.
15. Indium gallium arsenide has a bandgap of 0.75 eV (1 eV = 1.6×10^{-19} J). Find the wavelength of the light emitted by an InGaAs diode laser.
16. Calculate the loss of optical power through reflection at the interface between InGaAsP and air. Express the loss as a percentage and in units of dB.
17. A semiconductor optical amplifier has a gain of 15 dB. If the input power to the SOA is 12 μW find the output power.
18. Explain how a multiwavelength integrated laser based on an array of SOA and a multiplexer works.
19. Describe semiconductor modulators, including waveguide and MZM.

20. Summarize the most important differences between PIC devices based on SOI waveguides and III-V semiconductor waveguides.
21. Research three companies that manufacture III-V semiconductor PIC devices and give examples of the devices they commercialize. Include both passive and active PICs.

REFERENCES

Bachmann, M., P. A. Besse, and H. Melchior. 1994, General self-imaging properties in N x N multimode interference couplers including phase relations. *Applied Optics* Vol. 33(18): **3905-3911.**

Bernasconi, P., J. Simsarian, J. Gripp, M. Dülk, and D. Neilson. 2006. Toward optical packet switchin. *Photonics Spectra*, March, http://www.photonics.com/Article.aspx?AID=24582 (accessed May 7, 2016).

Chin, M.K., 2003, Polarization dependence in waveguide-coupled microresonators. *Optics Express* Vol. 11(15): 1724-1730.

Ismail, N., F. Sun, G. Sengo, K. Wörhoff, A. Driessen, R. M. DeRidder, and M. Polinau. 2011. Improved arrayed-waveguide-grating layout avoiding systematic phase errors. *Optics Express* Vol. 19(9): 8781-8794.

Liu, S., H. Wang, M. Sun, L. Zhang, W. Chen, D. Lu, L. Zhao, R. Broeke, W. Wang, and C. Ji. 2016. AWG-Based Monolithic 4 × 12 GHz Multichannel Harmonically Mode-Locked Laser. *IEEE Photonics Technology Letters* Vol. 28(3): 241-244.

The National Center for Optics and Photonics Education. 2013. *Fundamentals of Light and Lasers*, 2nd Edition.

Optical Amplifier. *Tutorials of Fiber Optic Products*. http://www.fiberoptictutorial.com/category/networksolutions/opticalamplifier (accessed May 7, 2016).

Peruzzo, A., A. Laing, A. Politi, T. Rudolph, and J. L. O'Brien. 2011. Multimode quantum interference of photons in multiport integrated devices. *Nature Communications*, March 1, doi: 10.1038/ncomms1228, http://www.nature.com/ncomms/journal/v2/n3/full/ncomms1228.html.

Toward Optical Packet Switching. *Photonics Spectra*. March 2006, http://www.photonics.com/Article.aspx?AID=24582 (accessed May 7, 2016).

Wada, O., Hasegawa, H. 1999. *InP-Based Materials and Devices: Physics and Technology*. Chichester, UK: Wiley.

Wang, G. 2015. *Optical IQ modulators for coherent 100G and beyond. Lightwave*, March 19. http://www.lightwaveonline.com (accessed May 27, 2016).

Dielectric and Polymer Waveguides and Waveguide Devices

Module 4

of

Integrated Photonics

OPTICS AND PHOTONICS SERIES

This material was created under Grant # 1303732 from the Advanced Technological Education division of the National Science Foundation. Any opinions, findings, and conclusions or recommendations expressed in this material are those of the author(s) and do not necessarily reflect the views of the National Science Foundation.

For more information about the text or OP-TEC, contact:

Dan Hull
PI, Executive Director, OP-TEC
316 Kelly Drive
Waco, TX 76710
(254) 751-9000
hull@op-tec.org

Taylor Jeffrey
Curriculum Development Engineer
316 Kelly Drive
Waco, TX 76710
(254) 751-9000
tjeffrey@op-tec.org

Published and distributed by
OP-TEC
316 Kelly Drive
Waco, TX 76710
254-751-9000
http://www.op-tec.org/

ISBN 978-0-9903125-8-1

CONTENTS OF MODULE 4

Module 4
Dielectric and Polymer Waveguides and Waveguide Devices

INTRODUCTION

The term “integrated optics” was proposed by S. E. Miller in 1969. It encompasses devices based on optical waveguides, particularly planar optical waveguides. The motivation for developing waveguide devices was provided by the emerging field of optical communications. Diode lasers and optical fibers demonstrated in the sixties were envisioned as acting as optical sources and as transmission media for optical sources. However, optical communication systems also needed optical components such as transmitters, receivers, modulators and others. Several categories of material are used to create both waveguides and some optical devices; silicon-based PICs and III-V semiconductor PICs were introduced and discussed in depth in previous modules.

Silica, also called silicone dioxide, is a natural choice of material for planar waveguide devices, because it was also the material that optical fibers were (and continue to be) made of. Efficient coupling of light between optical fibers and silica-based planar waveguides was initially expected, and strategies used to minimize insertion loss with silica waveguides are discussed later in the module. Silica does not have light-emitting properties. Consequently, it is used for passive PICs. Its advantages are low cost, excellent transparency, high threshold of optical damage, high reliability, and mechanical rigidity. Silica PIC devices can be fabricated in high volume using the same advanced technology used to fabricate electronic integrated circuits. Many high-performance, passive PIC devices based on silica have been fabricated commercially and deployed in optical transmission systems since they were envisioned five decades ago.

Another material that was adopted for early use in integrated optics devices is lithium niobate ($LiNbO_3$). Lithium niobate is a crystalline material with electro-optic properties; that is, its index of refraction can be changed by applying an electric field. This material shares many of the properties of silica: it is highly transparent in the near-infrared region used in optical communications; it is thermally, chemically, and mechanically stable; and it is compatible with integrated circuit fabrication technology. Because of its electro-optic properties, lithium niobate has been used extensively to fabricate optical modulators. These devices are often used as external modulators in combination with diode lasers.

A different class of materials used to fabricate a variety of PICs is polymers. Polymers have several advantages, including low cost, simpler fabrication processes, and compatibility with various substrates. Specific properties that make them attractive for PICs are their large thermo-optic and electro-optic coefficients, photosensitivity, and tunability of the refractive index. A

new class of PICs, one that takes advantage of the flexibility of some polymer materials, has been proposed. The new class is called *flexible integrated optic devices*. Polymer materials also have disadvantages, the most important of which are their low thermal and chemical stability.

Many polymers cannot withstand very high temperatures, for example. This imposes more stringent environmental requirements for polymer-based devices than for devices made of materials like lithium niobate or silica.

For the different reasons just listed, silica, lithium niobate, and polymers are all attractive materials for the fabrication of PICs. Their general disadvantage is that none can be a platform for monolithic integration, as opposed to silicon and III-V semiconductors. The devices must be used in conjunction with optical sources and photodetectors made of different materials. Connections between them are made using optical fibers, which adds cost and complexity to the system. This module presents properties of silica, lithium niobate, and polymer materials and discusses several PIC devices based on them.

PREREQUISITES

OP-TEC's Fundamentals of Light and Lasers Course 1

OP-TEC's Integrated Photonics: Modules 1-3

OBJECTIVES

Upon completion of this module, the student should be able to:

- Explain material properties of the following materials that are relevant to the fabrication of PICs:
    - silica
    - lithium niobate
    - polymers
- Describe characteristics of the following passive silica PIC devices:
    - straight and bend waveguide
    - coupling between optical fiber and silica waveguide
    - arrayed waveguide grating including athermal AWG
    - AWG integrated with other PICs
- Describe characteristics of lithium niobate waveguides and Mach-Zehnder Interferometer electro-optic modulators
- Describe characteristics of the following polymer PIC devices
    - straight waveguide
    - waveguide interconnects
    - Variable optical attenuator
    - digital optical switch
    - tunable Bragg grating
    - tunable wavelength laser
    - strain sensor based on Bragg grating

- Compare optical waveguides based on the silicon-on-insulator, III-V semiconductors, silica on silicon, and polymer platforms

BASIC CONCEPTS

Material Properties of Silica, Lithium Niobate, and Polymers

Silica

Silica, SiO_2, is abundant in the natural world. About 10% of the earth's crust is made out of quartz, which is silica. The material is also produced synthetically. Silica is the main component of silicate glass, the most common type of glass. While quartz is a crystalline material, glass is amorphous, lacking the ordered atomic or molecular structure that crystals possess. Optical fibers and planar optical waveguides are based on glass.

A very thin layer of silica, about 1 nm thick, forms naturally on top of silicon wafers through thermal oxidation of the silicon. The oxide formed this way is called *native oxide*. PIC devices require much thicker layers of silica; these are obtained through controlled oxidation of silicon at high temperature, between 600ºC and 1200ºC.

Silica is an electrical insulator—a material that does not conduct electricity. One of its applications is to electrically isolate various parts of electronic and photonic integrated circuit devices. On the other hand, glass has excellent optical properties. It is transparent for a wide range of wavelengths in the visible and infrared portions of the spectrum. Figure 4-1 shows a representative percent transmission vs. wavelength variation for fused silica. Transmission above 90% is observed for the visible range as well as the optical communications windows around the wavelengths of 1.31 µm (1310 nm) and 1.55 µm (1550 nm).

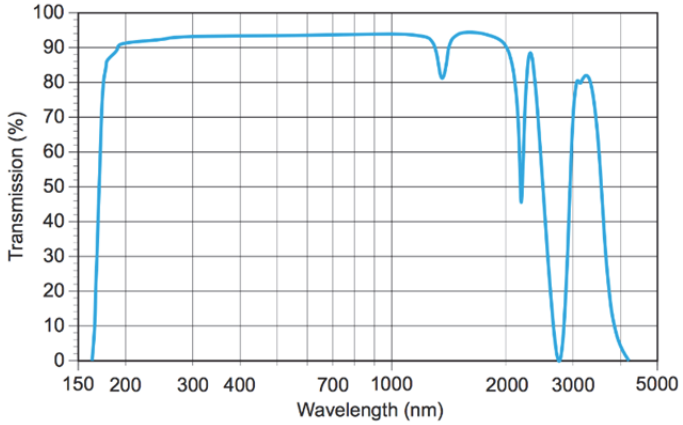

Figure 4-1 *Fused silica glass percent transmission vs. wavelength*

Figure 4-2 shows the variation of the index of refraction of silica with wavelength, based on experimental measurements. At the communication wavelength of 1.55 µm, the index of

refraction of silica is about 1.444. Like the materials discussed in previous modules, glass has an index of refraction that decreases with increasing wavelengths.

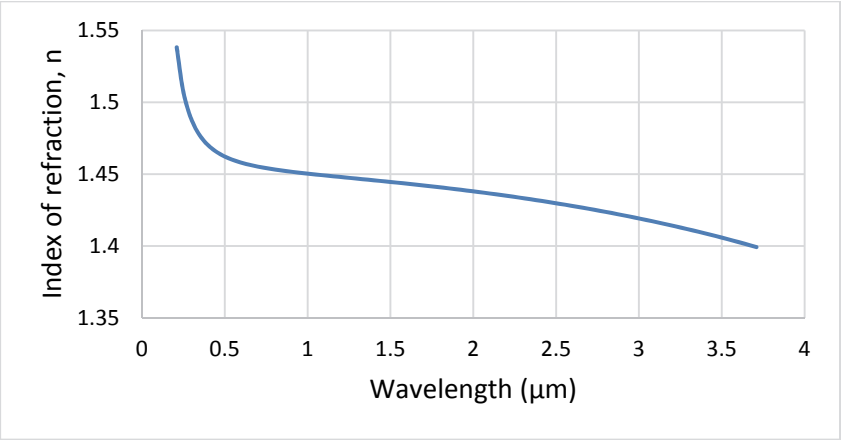

Figure 4-2 *Index of refraction of glass vs. wavelength*

Silica optical waveguides use pure silica for the cladding and doped silica for the core. The core needs a higher refractive index than the cladding (recall the conditions necessary for total internal reflection, discussed in Module 1). This can be obtained by introducing small amounts of certain materials (dopants) in the silica in a process called *doping*. Materials that can be used as dopants to increase the refractive index of silica are germanium dioxide (GeO_2), titanium dioxide (TiO_2) and phosphorus pentoxide (P_2O_5). It is also possible to decrease the index of silica by adding boron oxide (B_2O_3) or fluorine (F). Figure 4-3 shows representative variations of the index of refraction vs. wavelength for silica and doped silica materials. The concentrations of the dopants are shown in the legend. For each material, the remainder to 100% is SiO_2. By varying the concentration of the dopants, the refractive index can be adjusted throughout a range of values.

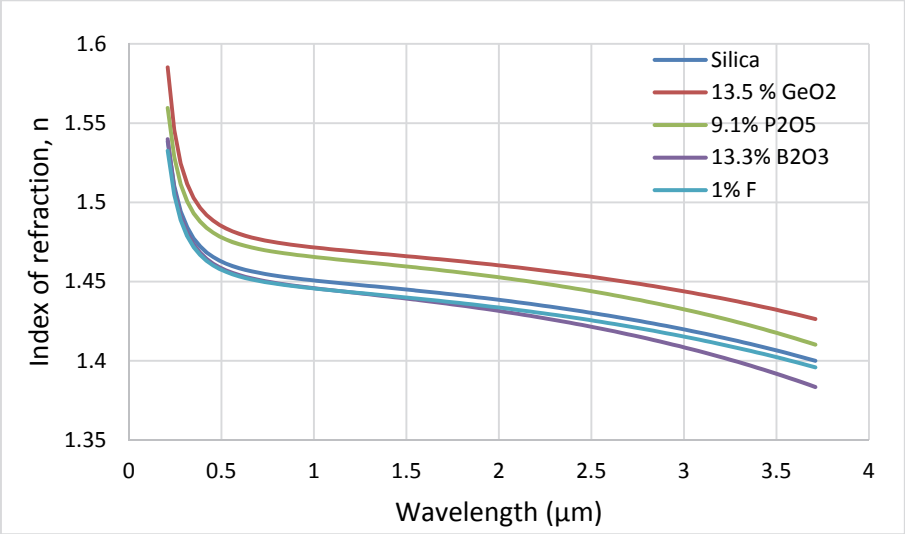

Figure 4-3 *Index of refraction of silica and doped silica vs. wavelength*

For the concentrations in the figure, the refractive indices at wavelength 1.55 μm are 1.466 for GeO_2 doped, 1.459 for P_2O_5 doped, and 1.439 for both B_2O_3 and F doped silica.

The indices of refraction of silica and doped silica also vary with temperature. Silica's index coefficient of variation with temperature, dn/dt, is approximately 1.1×10^{-5} K^{-1}. This is a smaller value than the corresponding coefficients for silicon and III-V semiconductors. Even in this case, devices that need precise wavelength alignment, such as arrayed waveguide gratings, require temperature stabilization.

Lithium Niobate

Lithium niobate is a synthetic material with applications in a wide range of fields including radar, microwave communications, optical communications, and others. Its chemical formula is $LiNbO_3$. The material is transparent for a wide range of wavelengths, from 350 nm to 5200 nm. Figure 4-4 shows the percent of external transmission vs. wavelength of $LiNbO_3$.

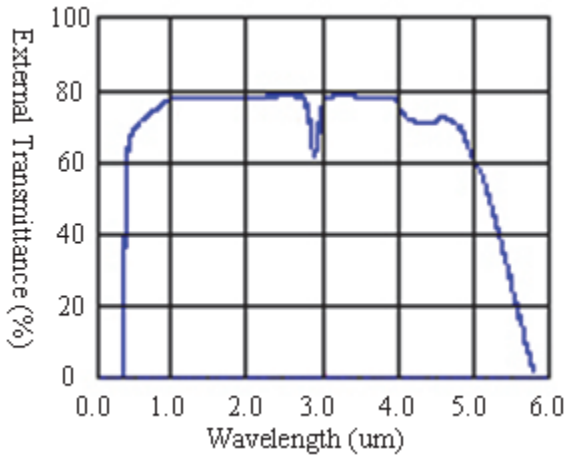

Figure 4-4 *Percent transmission vs. wavelength for lithium niobate*

Lithium niobate is a crystal; its constituent atoms are arranged in an ordered, periodic structure. The crystal structure, shown in Figure 4-5, is not symmetric. Like other crystals lacking symmetry, lithium niobate is birefringent. This means that two different indices of refraction are associated with it. The two indices are called the ordinary index, n_o, and the extraordinary index, n_e.

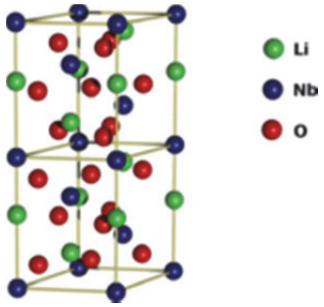

Figure 4-5 *Crystal structure of lithium niobate*

The lithium niobate crystal is characterized by an optic axis, which is usually chosen as the z axis in a Cartesian coordinate system. In Figure 4-5, this is the vertical direction. The index of refraction for light polarized perpendicular to the optic axis is equal to the ordinary index, while the index of refraction for light polarized along the optic axis is equal to the extraordinary index.

When the direction of propagation of the light is such that light wave travels along the optic axis, the index of refraction of the material is the ordinary index, n_o. For other directions of travel, the situation is more complicated, resulting in an index of refraction with a value between n_o and n_e.

Figure 4-6 shows the variation of the ordinary and extraordinary indices of refraction with respect to wavelength. The indices decrease as the wavelength increases. At the communication wavelength of 1.55 µm, the ordinary index of refraction is 2.211 and the extraordinary index of refraction is 2.138. Because n_e is smaller than n_o, lithium niobate is called a *negative uniaxial crystal*.

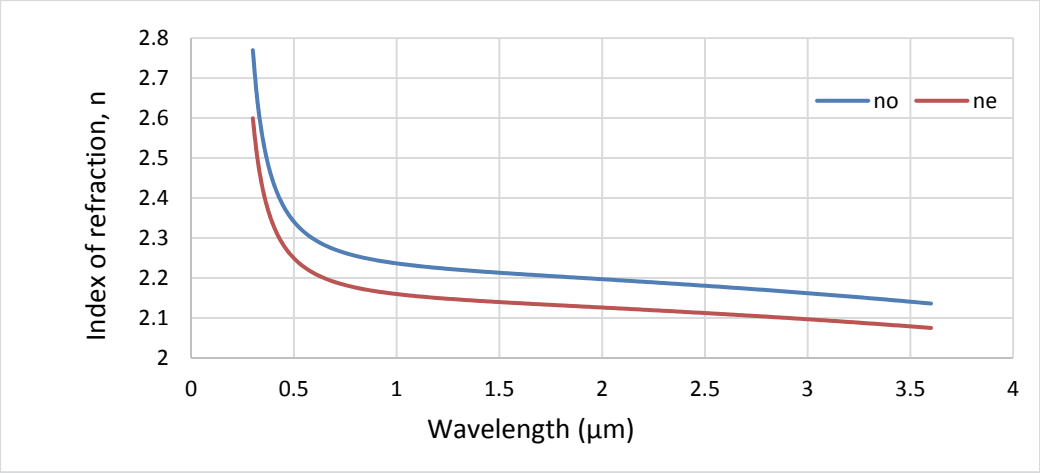

Figure 4-6 *Ordinary and extraordinary indices of refraction of lithium niobate vs. wavelength*

Two main methods are used to create an optical waveguide using lithium niobate. In the first method, a stripe of titanium is deposited on the lithium niobate substrate. The materials are heated at high temperature (900ºC), which facilitates the diffusion of titanium ions into the lithium niobate. The addition of titanium raises the index of refraction in the area with diffused ions. This area will act as the core of the waveguide, and the undoped lithium niobate will act as the cladding. Using this method, both the ordinary and the extraordinary indices of refraction increase by the addition of the titanium ions.

The second method is called the *annealed proton exchange* (APE) process. This process can take place at lower temperatures than titanium diffusion, typically 120ºC–250ºC. The material is immersed in an acid bath in which protons from the bath exchange places with lithium ions from the $LiNbO_3$. The exchange is followed by annealing at 250ºC–400ºC to stabilize the index of refraction. In this method, only the extraordinary index of refraction increases in the area where the exchange has taken place. The ordinary index of refraction remains the same. The waveguides obtained this way only work with one polarization of the light, TM. Both methods produce moderate refractive index increases in the core region, typically less than 0.1 at optical communication wavelengths.

Polymers

Polymers are materials with a specific structure of very long chains of repeated basic units, known as monomers. This structure gives polymers some unique properties, such as flexibility and large temperature dependence. Polymers are good thermal and electrical insulators. In regard to optical properties, amorphous polymers are usually transparent. The amorphous structure is the result of the long chains becoming tangled.

A very large variety of polymers exists. Polymers with applications in optical waveguide devices are polyacrylates, polyimides, polymethyl methacrylate (PMMA), photoresist, and others. These can be formed on any substrate and can also be a substrate for other materials. The process of creating a polymer waveguide is very cost effective. The polymer layers are created by spin coating the substrate. Layers with thicknesses from 0.1 to 100 μm can be obtained in a short time. Dopants can be added to polymers to change their refractive index. Another method to obtain a desired index of refraction is to blend together two polymers with different refractive indices. A wide range of indices can be obtained this way, exceeding the range that can be obtained with doped silica. In addition to the wide range, the method allows for fine control of the index of refraction to the fourth decimal place, or 0.0001. One application that takes advantage of this precise control of the refractive index is the creation of a waveguide with very low refractive index contrast. Such a waveguide can have a large size and still be single-mode. The large core size makes coupling to an optical fiber easier and more efficient.

Refractive indices of polymers used in PICs range from 1.3 to 1.6 depending on the type of polymer. Figure 4-7 shows the percent transmission and refractive index vs. wavelength for SU-8, which is an epoxy used as photoresist.

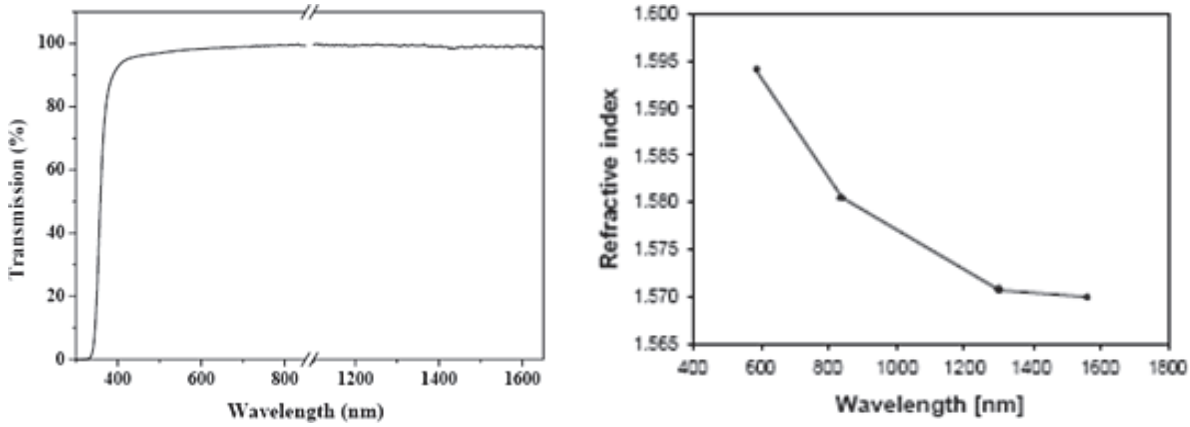

Figure 4-7 *Percent transmission and index of refraction of SU-8 vs. wavelength*

Polymers have an interesting behavior relative to temperature variation. The index of refraction of polymers depends primarily on packing density. When temperature increases, the density goes down, and this results in a decrease in the polymer's index of refraction. The coefficient of variation, dn/dt, will thus be negative. Typical values of dn/dt for polymers range between -1×10^{-4} K-1 to -3×10^{-4} K^{-1}. The materials described previously, including silicon, silica, and III-V semiconductors, all had positive dn/dt values. In addition to being negative, the dn/dt of polymers is also large in absolute value. This allows for the construction of specific PICs that cannot easily be realized in the other materials.

Silica-Based Photonic Integrated Circuits

Silica-based PICs are constructed from silica-on-silicon waveguides. These waveguides are obtained by depositing thin films of silica and doped silica on a silicon wafer. Six- or eight-inch silicon wafers, 500–700 μm thick, are commonly used. An advantage of silica waveguides is their very low propagation loss of less than 0.05 dB/cm. This comes from the low absorption and scattering in pure silica, as well as advances in the fabrication process of the waveguides. The very low propagation loss and the reliability of the materials are important factors that resulted in the successful commercialization of numerous silica PIC devices for optical communication systems.

The vast majority of silica PIC devices are passive, including couplers, splitters, Mach-Zehnder interferometers, switches, variable optical attenuators, and arrayed waveguide gratings. Devices such as these can be used independently or can be connected together to form complex systems with multiple functions, some of which will be described in the next module. Active devices based on silica waveguides are also possible but are not commonly used. One example is an active optical amplifier device based on silica waveguides. The amplifier's active region consists of silica doped with erbium ions capable of emitting light. This is the same method that optical fiber amplifiers are based on. For efficient amplification, the active region needs to be very long, which can be easily accomplished with fibers but not with planar waveguides.

Silica-on-Silicon Straight and Bend Waveguides

Silica-on-silicon waveguides are buried channel waveguides constructed from thin films of silica and doped silica on a silicon wafer. Figure 4-8 illustrates the configuration of such a waveguide. The lower and upper cladding are pure silica, with the core usually GeO_2 doped silica. The lower cladding has a thickness of 12–15 μm and the upper cladding is 10–12 μm thick.

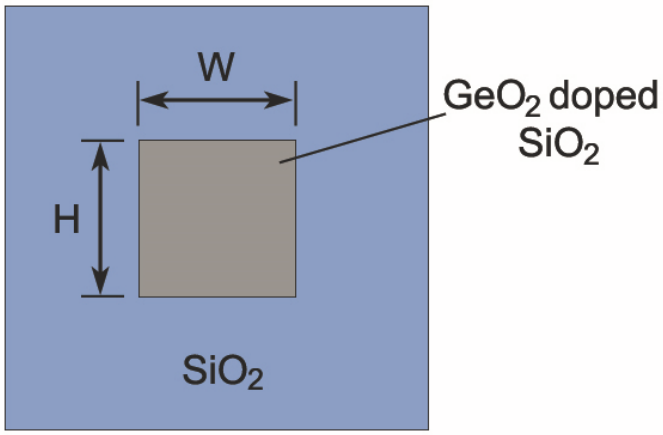

Figure 4-8 *Silica-on-silicon buried channel waveguide*

The waveguides can be characterized by the refractive index contrast (Δ) between core and cladding, given by equations 4-1 and 4-2. Initially, waveguides were constructed with small delta (Δ), similar to the delta of optical fibers. Those waveguides had very large cross sections

and very large bend radii. The index contrast was then increased, and high and super-high delta waveguides are defined as follows:

- high delta waveguides, $\Delta = 0.75\%$

- super-high delta waveguides, $\Delta = 1.5\%$

Recall the equation introduced in Module 1 for the refractive index contrast (Δ) between core and cladding:

$$\Delta = (n_{core}^2 - n_{clad}^2)/(2\, n_{core}^2) \quad (4\text{-}1)$$

When Δ is small, about 1% or less, an approximate equation for delta can be used instead, shown below:

$$\Delta = (n_{core} - n_{clad})/n_{core} \quad (4\text{-}2)$$

Example 1

Calculate the core refractive index of a high delta silica waveguide. Assume the wavelength is 1.55 μm and the cladding index is 1.444.

Solution: High delta silica waveguides have $\Delta = 0.75\%$. Use equation 4-2 to solve for n_{core}.

$\Delta = (n_{core} - n_{clad})/n_{core}$

$n_{core} = n_{clad}/(1 - \Delta) = 1.444/(1 - 0.0075) = 1.455$

In Example 1, we arrived at a useful equation for solving for the core index when the cladding index and refractive index contrast are known. This equation can only be used when Δ has small values, about 1% or less.

$$n_{core} = n_{clad}/(1 - \Delta) \quad (4\text{-}3)$$

The high delta waveguides have a 6 μm x 6 μm cross section. This is much larger than the cross section of both silicon-on-insulator (SOI) waveguides and III-V semiconductor waveguides. A large cross section is advantageous for butt-coupling planar waveguides to single-mode optical fibers. However, the drawback of $\Delta = 0.75\%$ silica waveguides is that they require a minimum bend radius of 5 mm. This is about three orders of magnitude larger than the bend radius of SOI waveguides (10 μm) and one order of magnitude larger than the bend radius of III-V semiconductor waveguides (300 μm). The consequence of the larger bend radius of silica waveguides is larger PIC devices.

Super-high delta waveguides ($\Delta = 1.5\%$) were introduced as a way to decrease the size of PICs using silica-on-silicon waveguides. The refractive index contrast of a super-high delta waveguide is double that of a high delta waveguide. The super-high delta waveguides have smaller cross sections, about 4.5 μm x 4.5 μm, and the bend radius is reduced to 2 mm. This is still very large compared with SOI and III-V waveguides, but it does allow for a good reduction in the size of PIC devices compared to PIC devices with high-delta waveguides ($\Delta = 0.75\%$).

Silica-on-silicon waveguides have a small amount of birefringence, $\Delta n_{eff} = n_{eff}^{TM} - n_{eff}^{TE}$, between -1×10^{-4} and -1×10^{-3}. This is mostly due to mechanical, compressive stress acting on the waveguide core. Silicon, the substrate material, has a higher coefficient of thermal expansion than silica. The deposition of the thin film layers includes high temperature processes. During the cool down, silicon contracts more than silica, resulting in a bowed (bent) wafer. One effect of this bowing is stress applied to the waveguide, resulting in increased birefringence.

Several methods can be used to reduce the waveguide birefringence in silica waveguides. Using a quartz substrate instead of the silicon substrate would eliminate the stress, but quartz wafers are more expensive, smaller, and more brittle, which makes this method impractical for high-volume production. Another method uses an upper cladding with a thermal expansion coefficient closer to that of silicon. This is achieved using specific dopants for the upper cladding. With this method, waveguide birefringence can be reduced to small and negligible values.

Table 4-1 shows the complete waveguide parameters for a single-mode, buried channel silica waveguide with $\Delta = 0.75\%$.

Table 4-1. Waveguide Parameters for a Single-mode, Buried Channel Silica Waveguide

Parameter	Value
Thickness, H	6 μm
Width, W	6 μm
Index of refraction of GeO_2 doped silica at 1550 nm and room temperature, n_{core}	1.455
Index of refraction of silica at 1550 nm, and room temperature, n_{clad}	1.444
Effective index TE mode, n_{eff}^{TE}	1.450
Effective index TM mode, n_{eff}^{TM}	1.450
Waveguide birefringence	negligible

Input/Output Coupling to Silica PIC Devices

When silica waveguides are butt-coupled to an optical fiber, they result in less coupling loss than when SOI and III-V waveguides are used. This is due to silica waveguides' large core size and indices of refraction that are closer to those of the optical fiber. For high delta silica waveguides, the coupling loss is about 0.5 dB. The loss increases to about 2 dB for super-high delta waveguides, which have smaller cores.

Insertion loss is an important parameter for PIC devices used in optical communication systems, where the entire system has a maximum allowable total loss. PIC devices with very small losses are highly desirable, but they require optimizing every contribution to the insertion loss of the device. Therefore, input/output coupling loss should be reduced as much as possible.

A common approach for this is to use a spot-size converter, a method described in previous modules. The simplest spot-size converter used with silica waveguides is a one-dimensional

taper that gradually widens the waveguide width up to the maximum at the edges of the chip. This method does not add processing steps, since the waveguide width is defined in photolithography for the entire chip at the same time. The taper must be an adiabatic taper to gradually change the mode from the original one to one closer to the mode of the optical fiber. For example, a typical one-dimensional taper that increases the waveguide width from 6 μm to 10 μm has a length of 1000 μm, or 1 mm. With such a taper, the coupling loss can be reduced from 0.5 dB to 0.25 dB.

A bigger reduction in coupling loss can be obtained with a structure called *periodically segmented waveguides* (PSW). This structure resembles a taper in that the overall effect is to increase the waveguide width at the edges of the chip. However, what is different here is that portions of core material alternate with portions of cladding material along the taper in a periodic fashion, hence the name. When light encounters a cladding region with a lower refractive index, it is not guided anymore and the mode broadens slightly. Light is then guided again in the region with core material. The alternating of core and cladding regions is more efficient in broadening the mode than a simple one-dimensional taper. With this method the coupling loss can be reduced to very low values, less than 0.1 dB. Figure 4-9 shows an illustration of a periodically segmented waveguide taper. The period of repetition of the segments is denoted by Λ, and the length of the segments is denoted by l(z). While Λ stays constant, the width and the length of the segments change along the taper. Careful design of the structure is needed to achieve the low loss previously mentioned for both the TE and TM polarizations of the light.

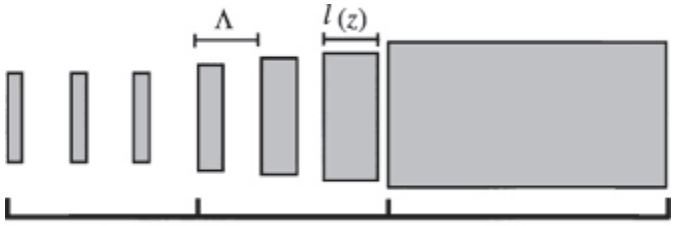

Figure 4-9 *Periodically segmented waveguide taper*

Silica Passive Devices

Numerous passive PIC devices are constructed from silica-on-silicon waveguides. The very low propagation loss of silica waveguides is the foundation on which high-performance devices are obtained. Moreover, the excellent mechanical and chemical stability of the material result in highly reliable PICs.

Directional couplers, multimode interference couplers, Y-splitters, Mach-Zehnder interferometers, and arrayed waveguide gratings are commonly realized in the silica-on-silicon platform. In the following section, we discuss the performance of some of these devices and present some combinations of devices offering increased functionality.

Arrayed Waveguide Grating

Arrayed waveguide gratings (AWGs) and their characteristic parameters were introduced in Module 3, where parameters specific to III-V semiconductor based AWGs were discussed. The

highest-performance AWG devices to date use a silica-on-silicon platform. AWGs with a large number of channels, 40 or more, and densely spaced channels at 100 GHz, 50 GHz, and even 25 GHz, are available commercially. Silica AWGs have low insertion loss, low polarization dependent loss, very low crosstalk, large 3dB bandwidth, and high uniformity across channels.

Specifications for two typical 40 channel, 100 GHz AWGs are presented in Table 4-2, together with the transmission spectra for all channels. The first AWG (Figure 4-10a) has a Gaussian type of passband with a rounded shape at the top. The second AWG (Figure 4-10b) has a flat-top passband, which increases the 1 dB and 3 dB bandwidth but comes with a small penalty in the insertion loss. The advantage of the flat-top AWG is that it is more tolerant of drifts in the wavelength emitted by diode lasers.

Table 4-2 shows typical performance of 40 channel, 100GHz Gaussian and flat-top AWGs.

Table 4-2. Performance features of Gaussian and flat-top AWGs

Parameter	Performance/value	
	Gaussian AWG	Flat-top AWG
Channel spacing	100 GHz	100 GHz
Number of channels	40	40
Wavelength accuracy	±0.02 nm	±0.02 nm
Passband	±12.5 GHz centered at each ITU frequency	±12.5 GHz centered at each ITU frequency
Insertion loss	3.0 dB	5.0 dB
Insertion loss uniformity	1.0 dB	1.0 dB
1 dB passband	0.25 nm	0.44 nm
3 dB passband	0.42 nm	0.62 nm
Polarization dependent loss	0.2 dB	0.2 dB
Adjacent channel crosstalk	-30 dB	-30 dB
Non-adjacent channel crosstalk	-40 dB	-40 dB

The transmission vs. wavelength of all 40 channels for the two AWGs is shown in Figure 4-10. Each channel is represented by a different color. Both figures illustrate the excellent uniformity across channels and the low level of background noise characteristic of a well-controlled fabrication process.

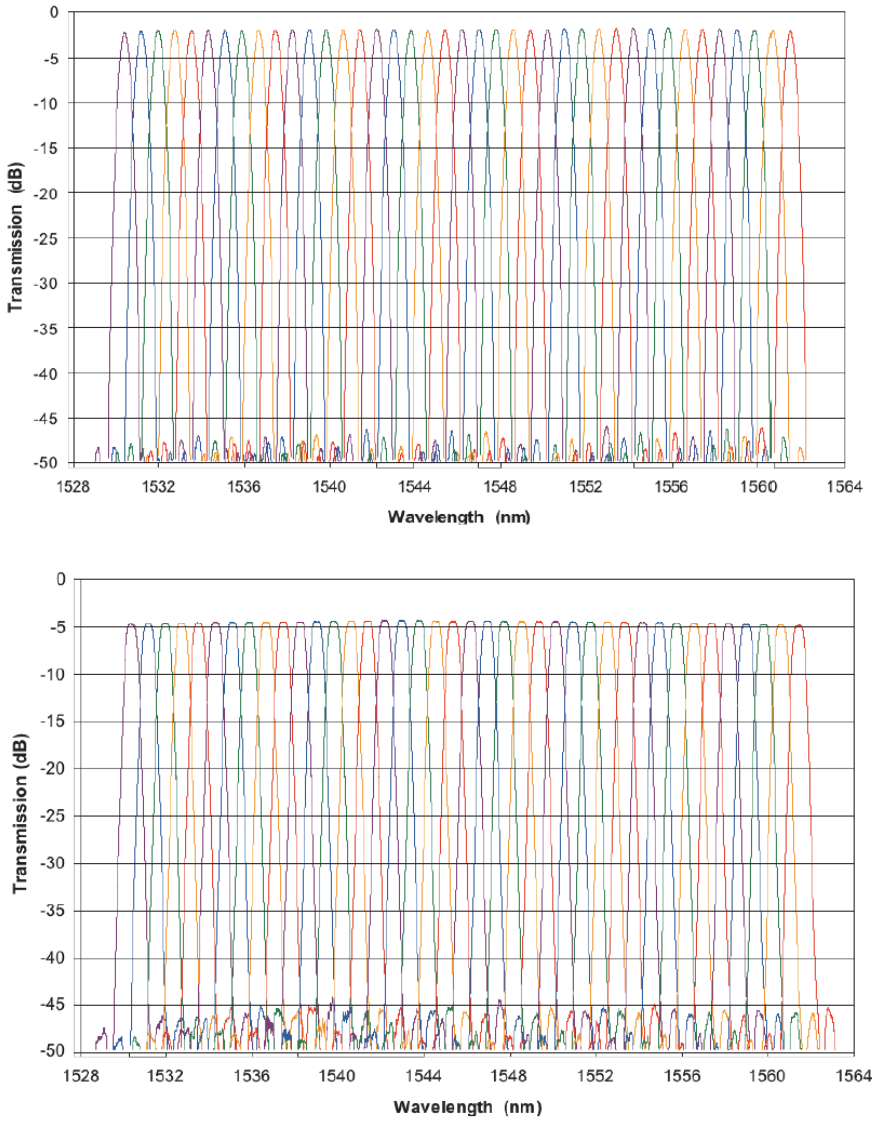

Figure 4-10 *Top: Spectrum of Gaussian AWGs; Bottom: Spectrum of flat-top AWGs*

Wavelength accuracy vs. temperature

The wavelength accuracy is an important AWG parameter. It describes how well the wavelengths corresponding to each channel match the ITU grid. The wavelength accuracy is adversely affected by the waveguide effective index variation with temperature. The central wavelength of the AWG, λ_c, is related to the length difference between two adjacent arrayed waveguides, ΔL, as follows:

$$\lambda_c = n_{eff}\, \Delta L/m \qquad (4\text{-}4)$$

Here, m is an integer called the *grating order*, and n_{eff} is the effective index of the waveguides in the array.

The refractive indices of silica and doped silica increase with temperature according to the coefficient of variation $dn/dt = 1.1 \times 10^{-4}\ K^{-1}$. The coefficient of variation for the waveguide effective index, n_{eff}, can be taken to have the same value.

Example 2

Calculate the change in the central wavelength of an AWG when the temperature rises from room temperature, 21˚C, to 55˚C. Is this change acceptable in light of the required wavelength accuracy given in Table 4-2? The effective index of the silica waveguides at room temperature is 1.45, the grating order of the AWG is 45, and the length difference ΔL is 48.1 μm.

Solution: Using Equation 4-4, calculate the central wavelength at room temperature.

$\lambda_c\ (21^\circ C) = n_{eff}\ \Delta L/m = 1.45 \times 48.1\ \mu m/45 = 1.55\ \mu m$

At higher temperature, the effective index increases according to equation 2-4 in Module 2.

$n(T_2) = n(T_1) + dn/dt\ *(T_2 - T_1) = 1.45 + 1.1 \times 10^{-4} \times (55 - 21) = 1.454$

Using equation 4-4 one more time, calculate the central wavelength at the high temperature.

$\lambda_c\ (55^\circ C) = n_{eff}\ \Delta L/m = 1.454 \times 48.1\ \mu m/45 = 1.554\ \mu m$

The change in wavelength is given by $1.554 - 1.55 = 0.004\ \mu m = 4$ nm.

This change is much higher than the required accuracy of ±0.02 nm.

Example 4-2 shows the effect of temperature variation on the waveguide effective index, which results in a change in the central wavelength of the AWG. Other thermal effects include the expansion of the substrate and silica layers with increasing temperature. This changes the waveguide dimensions, resulting in a change in ΔL. It also changes the stress state of the waveguide, due to the different coefficients of thermal expansion of silicon and silica, as explained previously. Due to the influence of these effects on the central wavelength, the temperature of the AWG must be kept constant using an external device, an RTD (resistive temperature-sensing device) or a thermistor. The drawback of these elements is that they increase the device's power consumption. An elegant solution that does not require additional components to keep the temperature constant is the *athermal AWG*, described below.

Athermal AWG

An athermal AWG is a device capable of maintaining an almost constant central wavelength (within some very tight limits) when the ambient temperature changes without the use of external elements. Such AWGs are commercially available and use one of two primary approaches to maintain wavelength. One approach is through mechanical control, and the other is through control of the refractive index. The mechanical control method, illustrated in Figure 4-11, relies on inserting a thin copper plate in the first free propagation region (FPR). When the copper plate heats, it expands and produces a movement of the output waveguides coming out of the second FPR. When correctly designed, the center output waveguide will move to the

correct position corresponding to the desired central wavelength. The parameter that determines the correct match between center output waveguide and the desired λ_c is the thickness of the copper plate.

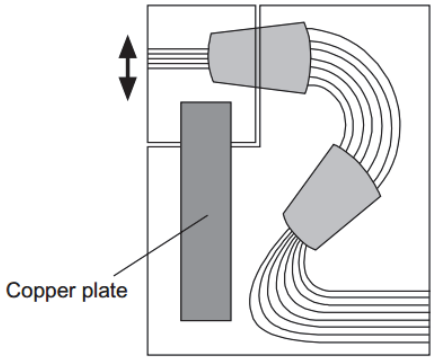

Figure 4-11 *Athermal AWG based on mechanical control*

In the second approach, trenches are formed in the first FPR that will be filled with a resin. Alternatively, trenches or grooves filled with resin are placed in the arrayed waveguide region. The two options are shown in Figure 4-12. The resin (a polymer) has a refractive index that decreases as temperature increases. Thus the effect of the polymer is to compensate for the increase in effective index in the doped silica portion of the waveguides. Moreover, the coefficient of variation with temperature of the polymer index of refraction is much higher than the silica coefficient. So only a short length of resin will be needed to compensate for the variation of the index of silica with temperature.

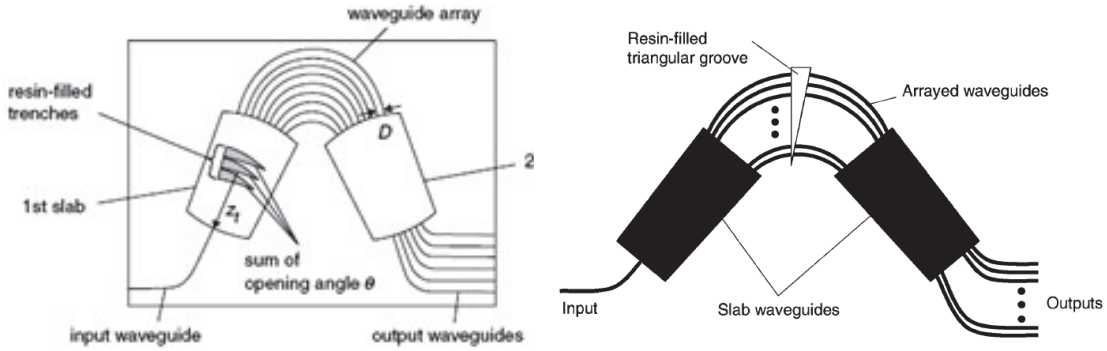

Figure 4-12 *Athermal AWG based on refractive index control*

The methods presented above to athermalize the AWG require additional fabrication steps. However, these methods result in very good stability of the central wavelength, ±0.04 nm or better, for a wide temperature range from –5 ˚C to 65 ˚C.

AWGs can be further integrated with other PICs to form devices with increased functionality. Ideally, all PICs are integrated in the same chip, which eliminates the need to use optical fibers

to connect them together. When fibers are eliminated, using fewer parts results in cost savings and eliminates some of the complex fiber-to-chip alignment operations. In practice, the process yield will dictate if integration in one chip will be used or not. With same-chip integration, if there is a defect in one of the PICs, the entire chip needs to be discarded. By contrast, if the PICs are fabricated as separate chips, all the good chips can be used to assemble the end device. Two examples of AWGs integrated with other PICs are presented below.

VOA/Multiplexer

When AWGs are used as multiplexers (MUXs), they combine multiple wavelengths and send them into an optical fiber. It is often desirable to control the power level of each channel to make it possible to equalize all powers or for other purposes. This can be achieved by inserting a variable optical attenuator (VOA) in each channel. For a 40 channel AWG, an array of 40 VOAs is used either as a separate chip or in the same chip with the AWG.

The VOA's function is to adjust the power of the light wave going through it. Power modulation can be obtained with a Mach-Zehnder interferometer device, as discussed in Module 2. The device is based on the thermo-optic effect, which is the only one available in silica, since the electro-optic effect is absent. One arm of the interferometer will have a thin film heater deposited on top of it to heat the waveguide below. This will change the index of refraction and create a phase difference compared with the reference arm. The thermo-optic effect works well for VOA function, but it has the drawback of being slow. It takes a couple of milliseconds for the heat to propagate to the waveguide and achieve the desired phase difference. By contrast, the electro-optic effect in semiconductors is very fast, on the order of nanoseconds and below. The latter effect allows for the construction of electro-optic modulators used for the modulation of high data rate signals.
The main parameters of VOA are insertion loss, dynamic range (or maximum attenuation), and polarization dependent loss (PDL). Silica VOAs have insertion loss around 2 dB, dynamic range of 20 dB, and PDL around 0.5 dB.

The VOA/MUX combination, called a VMUX, can be further enhanced with the option of *power monitoring* in each channel. To measure the optical power in a channel, a small fraction of the light wave is deviated into a secondary waveguide and then coupled to a photodetector. This is achieved using a *tap*, which is usually a directional coupler with a 95%–5% splitting ratio. A tap and photodetector are placed after the VOA in each channel. In this case, 5% of the power is tapped and measured by the photodetector, while the rest continues to the multiplexer. Another tap and photodetector can be placed at the output of the AWG multiplexer to monitor the total power. In this case, the amount of power used for the tap can be even lower, for example 2%.

Example 3

Calculate the length of the coupling region, L, for a directional coupler that splits the incoming light in a ratio of 95%–5% between output waveguides 1 and 2. Assume the coupling coefficient k is known.

Solution: The equations for the powers in outputs 1 and 2 of a direction coupler are:

$P_1(L) = P_0 \cos^2(kL)$ and $P_2(L) = P_0 \sin^2(kL)$.

We can use the first equation to find the length L. In our case, $P_1(L)/ P_0 = \cos^2(kL) = 0.95$.

Solving for kL, we find $kL = \cos^{-1}(\text{sqrt}(0.95)) = 0.226$ (in radians).

We find the length $L = 0.226/k$.

This directional coupler will have a shorter length than the 3dB coupler, which splits the power equally between output waveguides 1 and 2. The length for the 3dB coupler was found in Module 2 to equal $\pi/(4k) = 0.785/k$.

The VMUX with optical power monitoring allows for very precise control of the power in each channel. The measurement of the actual power in each channel provides a feedback mechanism and transforms the system into a *closed-loop control system*. By contrast, the VMUX without power monitoring is an *open-loop system*, where the desired power level is set by the VOA but there is no mechanism to check if the actual power is equal to the desired one.

Figure 4-13 shows a schematic representation of the open-loop and closed-loop VMUX devices.

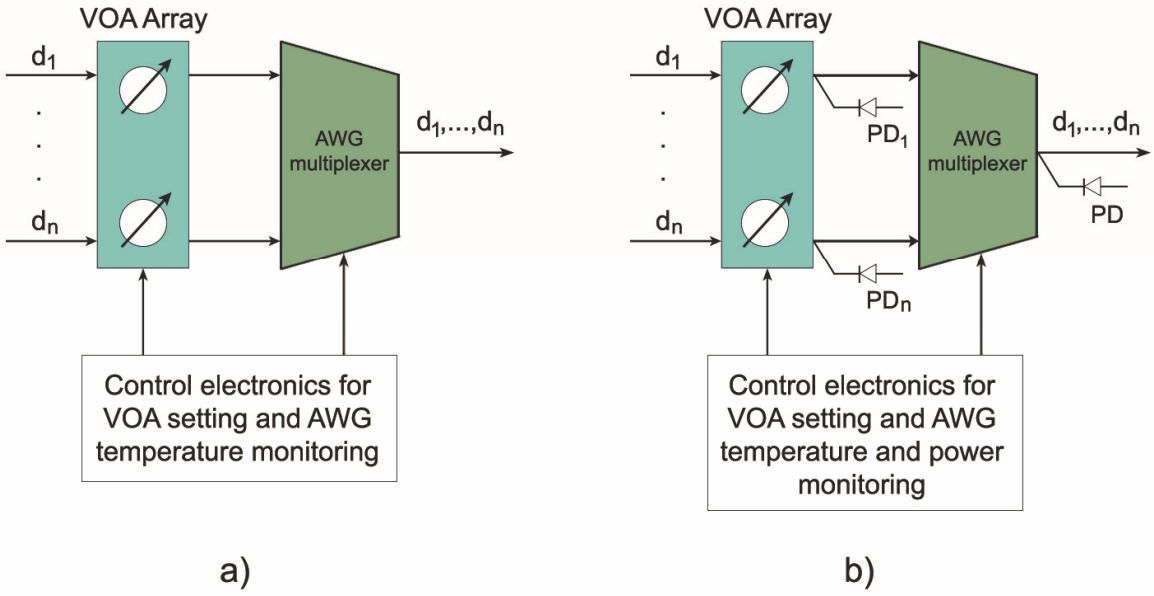

Figure 4-13 a) *VMUX device*

Figure 4-13 b) *VMUX with optical power monitoring*

Optical Channel Monitor

A related application of an AWG is the optical channel monitor. This device combines an AWG demultiplexer with an array of photodiodes to simultaneously measure the optical power of multiple wavelengths. An athermal AWG can be used for such an application, as shown in Figure 4-14. The device in the figure can monitor 48 channels.

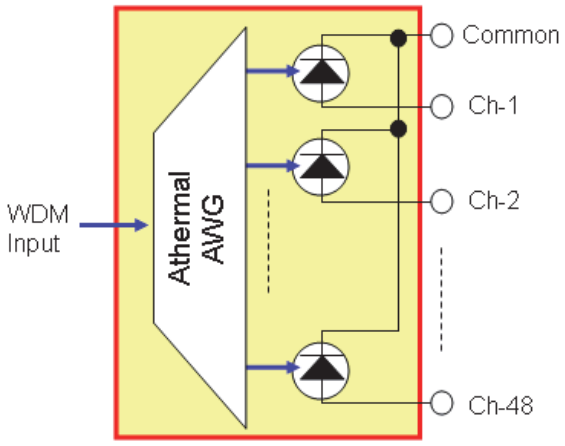

Figure 4-14 *Optical channel monitoring of 48 channels using an athermal AWG*

Lithium Niobate Photonic Integrated Circuits

Lithium niobate is used in several optical devices, the most common being the electro-optical modulator. These devices are based on optical waveguides fabricated through the methods described previously.

Lithium Niobate Waveguides

The titanium diffusion or annealed proton exchange (APE) methods are used to create a region with increased refractive index in a lithium niobate substrate. This region will act as the waveguide core. The increase in refractive index when titanium diffusion is used is very small, typically about 0.01. In this case, the core has a rounded shape, because titanium ions diffuse in a circular pattern. Single-mode waveguides with large width and large bend radii can be obtained this way. Figure 4-15 illustrates the titanium diffusion fabrication method and the resulting waveguide.

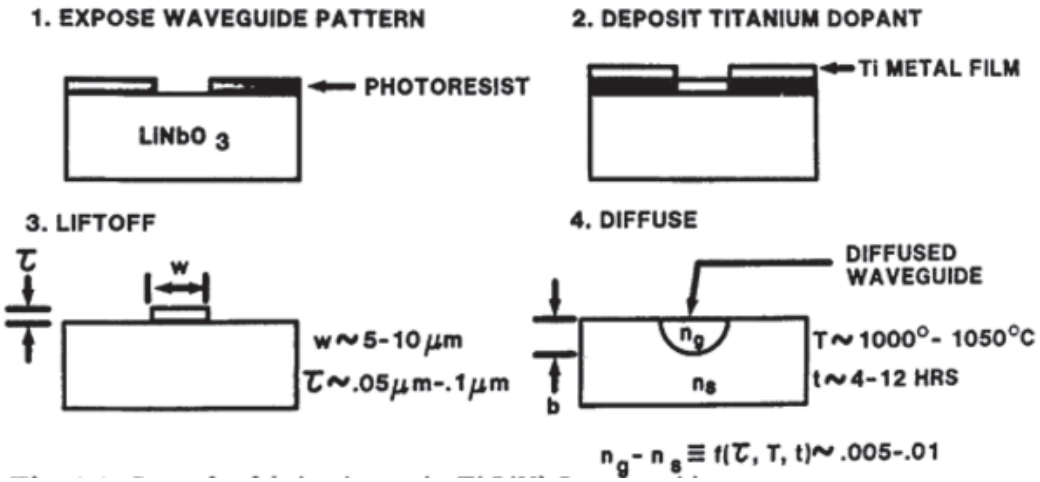

Figure 4-15 *Titanium diffused lithium niobate waveguide*

With the APE method, larger increases can be obtained in the extraordinary refractive index. Values around 0.1 can be obtained. The APE method also produces smoother boundaries between core and cladding, which result in smaller propagation loss. The waveguides have cross sections around 1 μm^2.

To increase the refractive index contrast and shrink the size of devices, waveguides with lithium niobate as the waveguide core and glass or polymer as cladding are being researched. The refractive index difference between lithium niobate and glass is considerable, 2.211 vs. 1.444 at a wavelength of 1.55 μm, so lithium niobate allows for much smaller dimensions and bend radii. Such waveguides are called *lithium niobate on insulator* or LNOI, similar to silicon-on-insulator or SOI waveguides. These waveguides are not yet used commercially because their propagation loss is quite high. More progress is needed in this area of research.

Lithium Niobate Modulators and Switches

Lithium niobate is an electro-optic material; that is, its index of refraction can be changed by the application of an electric field. This property is exploited in the fabrication of modulator and switch PIC devices. Compared with the thermo-optic effect, the electro-optic effect is much faster, allowing for high-speed devices operating on the order of Gb/s (10^9 bit/s) rates.

Lithium niobate modulators are commonly based on a Mach-Zehnder interferometer (MZI) configuration. MZI devices have been described previously. In this application, electrodes are placed on top of the device to create the electric field that changes the refractive index of one arm with respect to the other. The electrodes can be configured in several ways, depending on the lithium niobate crystal orientation. Figure 4-6 illustrates one of these configurations. The electric field set-up by the electrodes is shown by the curved lines, with arrows indicating the direction of the electric field. A buffer layer is placed between the electrodes and the waveguides to prevent interference between the metal material of the electrodes and the electromagnetic field of the light wave.

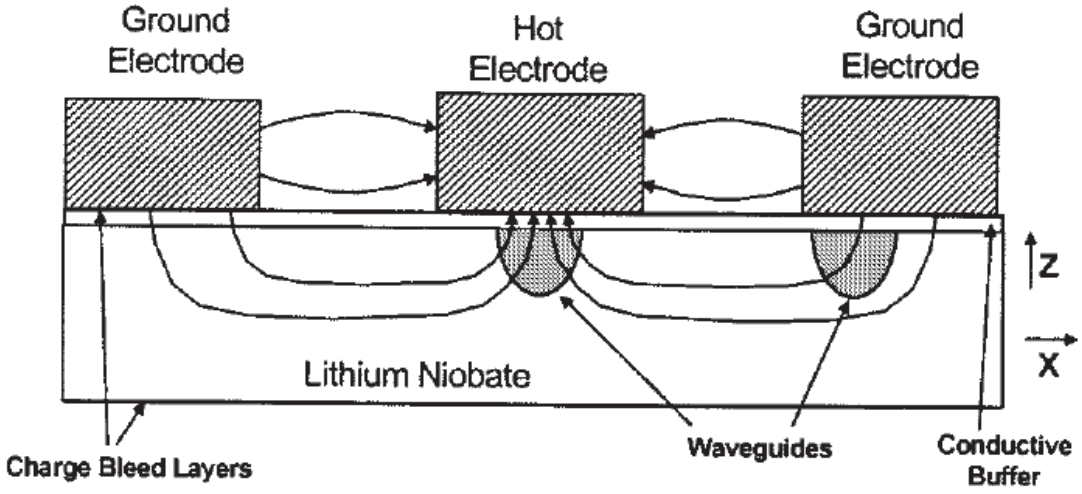

Figure 4-16 *Electrode configuration for MZI lithium niobate modulator*

Lithium niobate modulators require voltages of 5–10 V. The applied voltage can be reduced by increasing the length of the MZI arms. Most modulators require careful control of the polarization of light. Polarization-maintaining fibers are used at the input to the device to ensure that light with the desired polarization is used. By careful design, broadband modulators have been obtained that maintain the same switching voltage over the wavelength range 1530–1610 nm. More than 100,000 lithium niobate modulators have been deployed in optical transmission systems in the past decades.

Multiple lithium niobate MZIs can be integrated together in the same chip to increase the functionality of the device. Arrays of parallel MZIs integrated in one chip can be used in wavelength division multiplexing applications, with one modulator for each channel. In another application, the data modulation and variable attenuation functions can be implemented using cascaded MZIs in the same chip.

Polymer-Based Photonic Integrated Circuits

Polymers are attractive materials for integrated optics applications due to their low fabrication cost, ability to work on a variety of substrates, versatility in adjusting their refractive index, and large thermo-optic and electro-optic effects. Polymers used in optical applications include polyacrylates, polyimides, polymethyl methacrylate (PMMA), photoresist, and others. One of these, fluorinated UV-curable acrylates, has been demonstrated to have low absorption losses and remain stable at temperatures above 350ºC. The special properties of polymers allow for the realization of some simple but useful devices which do not work efficiently in other material platforms. Some of these devices are presented below, starting with general characteristics of polymer waveguides.

Polymer Waveguides

The process of creating a polymer waveguide is very cost effective. A layer of polymer that will act as the waveguide lower cladding is spin coated on the substrate, followed by baking and UV curing. The core layer is then spin coated, baked, and UV cured. Patterning through photolithography will define the circuit paths. Direct laser writing can also be used for this purpose. The upper cladding layer is then added through the same process as the lower cladding.

Polymer waveguides can be obtained on various substrates, including glass, quartz, silicon, and others. A typical polymer waveguide on silicon substrate is a buried channel waveguide with polymer cladding and a polymer core with higher refractive index than the cladding, as shown in Figure 4-17. To obtain the higher index for the core, polymers with different indices can be blended together. This versatile method can produce a wide range of well controlled values of the refractive index.

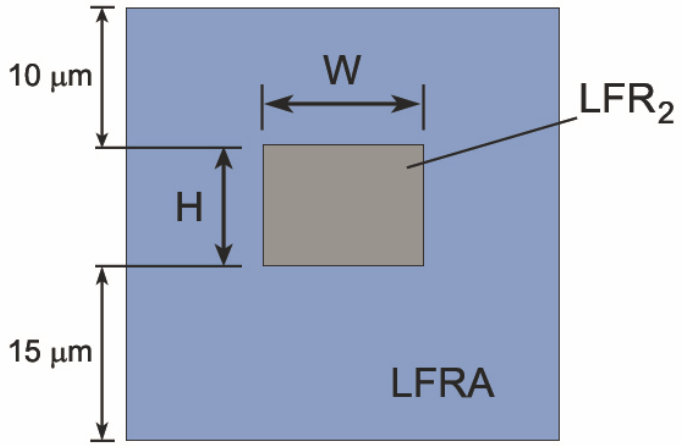

Figure 4-17 *Polymer buried channel waveguide*

Similar to silica-on-silicon waveguides, polymer waveguides can be obtained with the typical values of 0.75% and 1.5% for the refractive index contrast. For these values, the waveguide cores have cross sections of 6 μm x 6 μm and 4.5 μm x 4.5 μm. The birefringence of the waveguides is very low, and the propagation loss can be as low as 0.1 dB/cm. Bend radii are between 2 mm and 5 mm. The advantage of some polymer devices is that they can be constructed with very few bends, thus occupying less space than devices with the same functions made of other materials.

Waveguide Interconnects

Polymer waveguides are an efficient and cost-effective solution for high bit rate interconnections of electronic and optical components and modules. High-speed interconnections based on copper suffer from high losses and electromagnetic interference. Optical interconnections using fibers require complex assembly operations and occupy large volumes due to the fiber requirements for minimum bend radius. Polymer waveguides can eliminate these issues and are less expensive than other types of waveguides. Using a polymer for interconnection allows for close integration of electrical and optical functions. An example of polymer waveguide interconnections is shown in Figure 4-18.

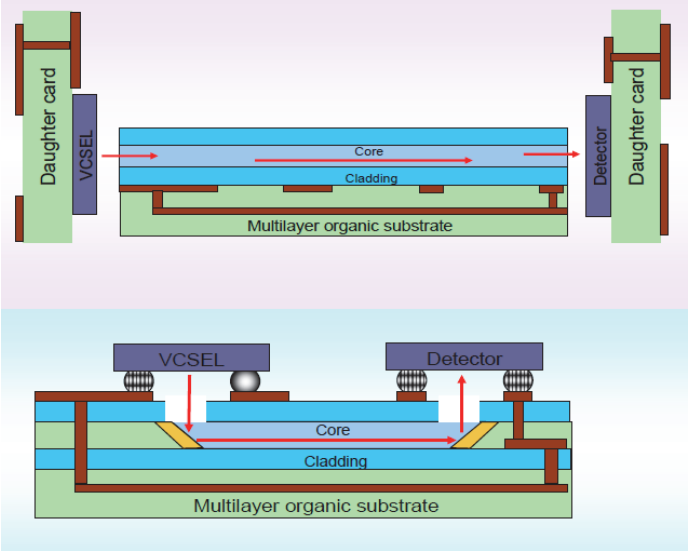

Figure 4-18 *Polymer waveguide connecting a VCSEL laser and a photodetector. Top: in-plane interconnection. Bottom: out-of-plane connection using 45° mirrors.*

A polymer used in waveguide interconnections is silicone, a cross between glasses and organic polymers. Silicone (not to be confused with the chemical element silicon) shares the thermal stability and transparency of glass, the ease of fabrication and tailoring of polymers, and the optical properties of organic polymers. This makes it attractive for optical waveguide applications. Silicone can be deposited on a flexible substrate, as shown in Figure 4-19, and waveguide sheets can be stacked on top of one another. The structure shown consists of eight stacked sheets.

Figure 4-19 *Silicone waveguides for optical interconnects. Courtesy of Dow Corning.*

Variable Optical Attenuator

A variable optical attenuator (VOA) is a passive device that can control output power, modifying it to be anywhere between a value equal to the input power to a value 100 times smaller than the input power or less. VOAs can be realized in an MZI configuration, as described in Module 2. The MZI is constructed from two 3dB couplers with two waveguide arms running between them. Polymer waveguides enable a much simpler VOA configuration that takes advantage of the large thermo-optic coefficient of these materials.

Figure 4-20 a) shows a polymer-based VOA. The VOA consists of a straight, multimode waveguide with tapers to connect the wide waveguide to the narrower, single-mode input and

output waveguides. Note that this device does not use any bend waveguides. A heater is placed at an angle over the multimode waveguide. Remember that the index of refraction of polymers decreases with increasing temperature. Thus, when the heater is activated, the refractive index contrast for the waveguide underneath the heater will decrease. Different waveguide modes are excited in this structure, and not all modes will be able to travel efficiently through the output taper and single-mode waveguide, eliminating some of them. In addition, some of the light is reflected by the angled interface and radiated out of the waveguide. In this way, by increasing the heat applied to the multimode waveguide, it is possible to decrease the output optical power to very low values.

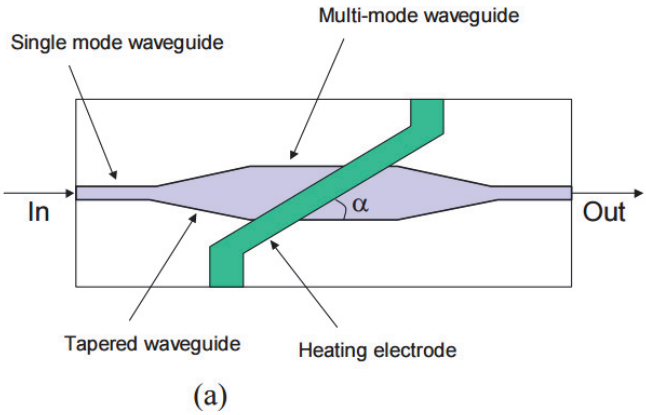

Figure 4-20 a) *Polymer multimode waveguide-based VOA*

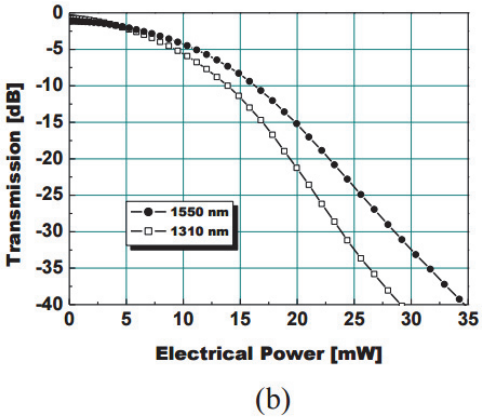

Figure 4-20 b) *VOA transmission vs. applied electrical power for the wavelengths of 1.31 μm and 1.55 μm*

Figure 4-20b shows the VOA transmission vs. the electrical power applied to the heater at the two optical communications wavelengths 1.31 μm and 1.55 μm. Very high values of attenuation, up to 40 dB, can be achieved. The electrical power used by such a VOA is considerably smaller than the power needed by silica-on-silicon MZI-based VOAs. The latter devices require about 250 mW of electrical power to switch off the optical power. The excellent performance of the simpler polymer VOA is made possible by the large index change with temperature of these materials. For example, a large change of 0.01 in the refractive index is possible with a polymer having $dn/dt = -2 \times 10^{-4}\ K^{-1}$ by a change in temperature of 50ºC.

Digital Optical Switch

Another simple device exploiting the large thermo-optic coefficient of polymer waveguides is the *digital optical switch* (DOS). The device is based on a Y-branch structure with heaters placed over the two branches. Figure 4-21 shows the switch's configuration. The principle of operation of the switch is based on adiabatic evolution of the optical mode of the waveguide. When one branch of the Y-splitter (for example, the top branch) is heated, the index of refraction decreases in that branch. The optical mode will be guided in the branch not heated, thus light will switch to the bottom branch. In addition to the Y-branch, the device includes an attenuator portion. The role of the attenuator is to eliminate any remaining light in the arm that is off, in this case the top arm. This improves the crosstalk of the device. The attenuator works on the same principle as VOA devices.

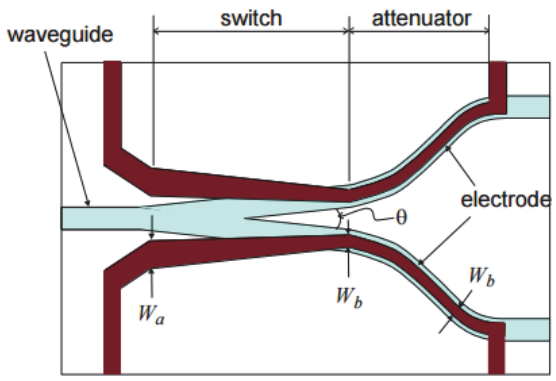

Figure 4-21 *Digital optical switch*

A drawback of the DOS is that electrical power has to be applied at all times, on one branch of the Y-splitter or the other, to have light exit through one of the outputs. Different configurations have been designed to allow one path to be achieved with zero electric power applied to the heaters, with the other path requiring the application of electric power. Such a configuration is presented in Figure 4-22. In this configuration, the bar states, I-1 to O-1 and I-2 to O-2, do not require electric power to the heaters. Electric power is applied only when the paths I-1 to O-2 or I-2 to O-1 are desired.

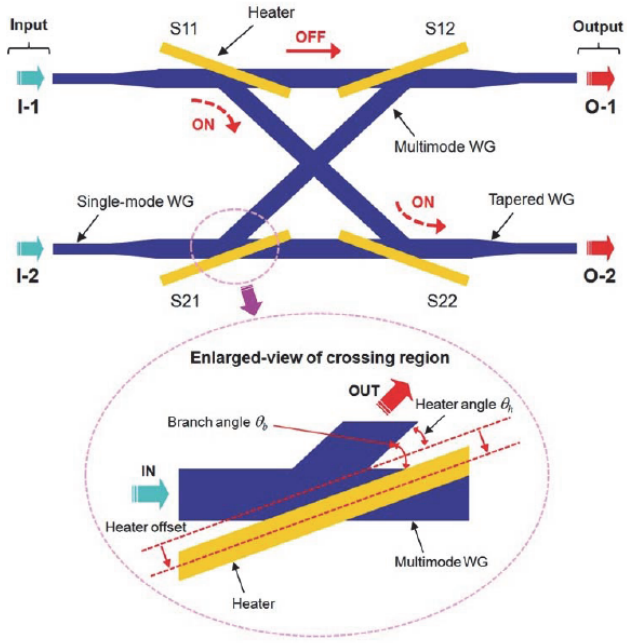

Figure 4.22 *2 x 2 polymer digital optical switch*

Tunable Bragg Grating

Introduced in Module 2, a waveguide Bragg grating is a structure consisting of a periodic variation of the effective refractive index along the waveguide in the direction of propagation of

the light. Bragg gratings are resonant structures with a filter response. A typical Bragg grating totally reflects light at wavelengths within a bandwidth centered around the Bragg wavelength. Light outside this bandwidth is transmitted instead of reflected. The Bragg wavelength is given by the following equation, where Λ is the period of the grating and n_{eff} is the effective refractive index of the waveguide:

$$\lambda_B = 2\Lambda\, n_{eff} \qquad (4\text{-}5)$$

A tunable Bragg grating is a device for which the Bragg wavelength can be controlled over a desired range of values. Such gratings can be used in conjunction with a laser to tune the wavelength emitted by the laser. As equation 4-5 indicates, the Bragg wavelength λ_B depends linearly on the effective index of the waveguide. The Bragg wavelength can be controlled by changing n_{eff}. The effective index of polymer waveguides can be adjusted over a wide range using the thermo-optic effect. Using a heater over a polymer waveguide Bragg grating, a tuning range of 30 nm has been demonstrated. The polymer used for this device was a high-index material, Resole, which allowed for a high refractive index contrast waveguide.

Tunable Wavelength Laser

The tunable polymer waveguide Bragg grating described above was used as a component of a tunable laser, as shown in Figure 4-23a. The tunable laser includes a superluminescent diode (SLD) with a broad gain spectrum, a lens coupling the light emitted by the diode laser to the polymer waveguide, and the Bragg grating. Figure 4-23b shows the spectrum emitted by the tunable laser. The wavelength was tuned over 32 channels with a separation of 100GHz by applying a maximum electric power of 150 mW to the heater. The tuning was done in steps of 0.1 nm.

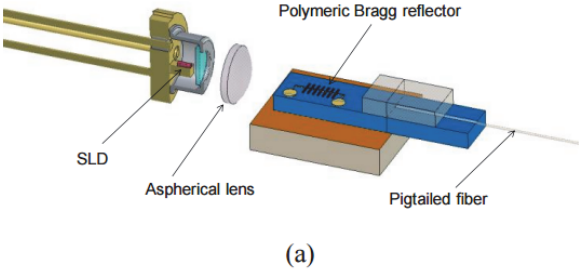

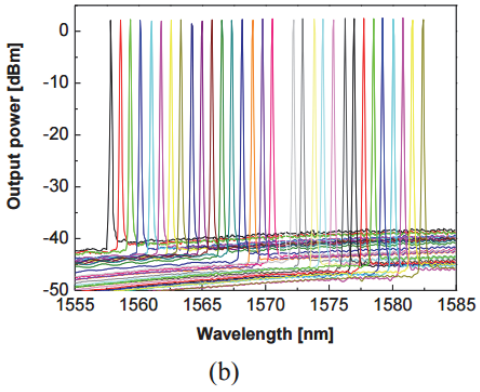

Figure 4-23 a) *Laser configuration of a tunable wavelength laser with a polymer Bragg grating*

Figure 4-23 b) *Output power emitted by the tunable wavelength laser with a polymer Bragg grating*

Tunable lasers such as the one described above are very attractive for optical communication systems using wavelength division multiplexing. A system with 40 channels that uses diode lasers emitting at fixed wavelengths requires 40 different lasers. If tunable lasers are used, the same laser can be used throughout the system and the wavelength can be easily adjusted by applying power to the Bragg grating.

Example 4

Calculate the temperature change needed to tune the wavelength of a tunable laser across a range of 32 nm using a polymer Bragg grating with $dn/dt = -2.5 \times 10^{-4}\ K^{-1}$. The grating has a period of 1 μm.

Solution: Using equation 4-5, we can find the range of tuning for the effective index corresponding to a 32 nm wavelength range

$\Delta n_{eff} = \Delta\lambda_B/(2\Lambda) = 32\ nm/(2 \times 1000\ nm) = 0.016$.

The temperature change needed can be calculated from the equation $\Delta n_{eff}/\Delta T =$

$2.5 \times 10^{-4}\ K^{-1}$ (in absolute values).

$\Delta T = \Delta n_{eff}/2.5 \times 10^{-4}\ K^{-1} = 0.016/2.5 \times 10^{-4}\ K^{-1} = 64°C$.

Strain Sensor with Tunable Bragg Grating

A proposed application of polymer waveguide Bragg gratings is in strain sensors. In this case, the device exploits the great flexibility of polymers. The Bragg grating is built on a flexible substrate, which requires modifications in the fabrication process. The new process is shown in Figure 4-24. A gold layer is deposited on the silicon wafer, and a layer of the SU-8 photoresist is placed over the gold. The SU-8 can easily be peeled off the substrate after the waveguide has been obtained, but it adheres well to gold. The packaged device is shown in Figure 4-25. When strain is applied to the device, the period of the Bragg grating changes and the Bragg wavelength shifts. By measuring the changes in Bragg wavelength, the strain can be determined. The device performs better than optical-fiber-based strain sensors because of the smaller Young's modulus of the polymer material vs. silica. A smaller Young's modulus means that the polymer remains elastic up to higher values of strain.

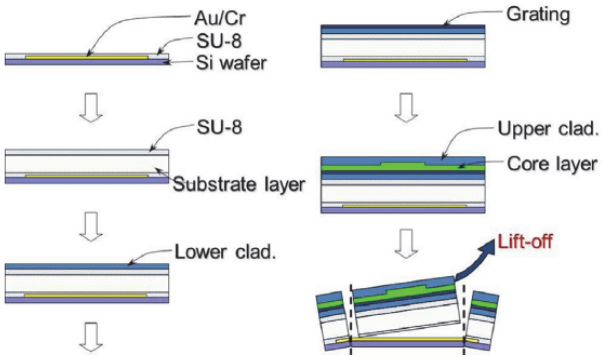

Figure 4-24 *Fabrication process for polymer strain sensor*

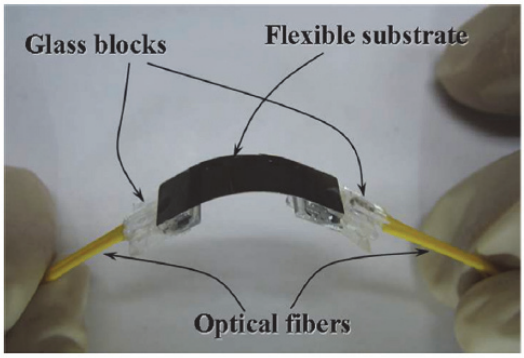

Figure 4-25 *Strain sensor based on polymer waveguide grating*

Comparison of Waveguide Parameters across Materials Platforms

Table 4-3 shows the main waveguide parameters for representative waveguides based on the materials presented in Modules 2, 3, and 4. Advantages and disadvantages of each material are apparent when considering each parameter and its impact on PIC devices.

Table 4-3. Waveguide parameters for representative waveguides

Material platform	Waveguide dimensions (μm^2)	Refractive index range	Refractive index contrast	Propagation loss (dB/cm)	Bend radius (μm)	Coupling loss to optical fiber with SSC (dB)	Index variation with temperature (K^{-1})
Silicon on insulator (SOI)	0.2 x 0.5	3.4 – 3.6	40%	2	10	0.5	2×10^{-4}
III-V semiconductors	0.5 x 2	3 – 3.6	Few %	0.6	100 - 300	1	2×10^{-4}
Silica on silicon	5 x 5	1.44 - 1.47	0.8% to 1.5%	0.05	2000 - 5000	0.1	1.1×10^{-5}
Polymer	5 x 5	1.3 – 1.6	0.8% to 1.5%	0.1	2000 - 5000	0.1	-2×10^{-4}

SUMMARY

This module presented an overview of several insulator materials used in PIC fabrication. The material properties of silica, lithium niobate, and polymers used in integrated optics devices were presented first, followed by descriptions of PIC devices based on these materials. Combinations of silica-based devices with expanded functionality were introduced. Electro-optic modulators based on lithium niobate were briefly described. A variety of polymer devices were presented, including devices that are not easy to realize in other material platforms. Finally, parameters for representative waveguides based on the materials in Modules 2, 3, and 4 were summarized.

PROBLEM EXERCISES AND QUESTIONS

1. Calculate the refractive index contrast of waveguides with silica cladding and silica doped with 13.5% GeO_2 core, at the wavelength of 1.55 μm. Repeat for waveguides with cladding of silica doped with 1% F and core of silica doped with 9.1% P_2O_5.
2. Describe the ordinary and extraordinary indices of refraction of lithium niobate.
3. For a polymer with $dn/dt = -3 \times 10^{-4}\ K^{-1}$, how much should the temperature increase from room temperature (21ºC) to result in a decrease of 0.015 in the polymer's index of refraction?
4. Calculate the refractive index of the core layer in a super-high delta silica-on-silicon waveguide. Assume a wavelength of 1.55 μm.
5. Describe two types of tapers used to reduce the coupling loss between a silica-on-silicon optical waveguide and a single-mode optical fiber.
6. Calculate the maximum temperature variation allowed with an AWG so that the wavelength accuracy remains within ±0.02 nm. The effective index of the silica waveguides at room temperature is 1.45, the grating order of the AWG is 45, and the length difference ΔL is 48.1μm.
7. Research specifications for a 50 GHz flat-top arrayed waveguide grating device. How do these compare with a 100 GHz flat-top AWG from the same manufacturer?
8. Research specifications for a 100 GHz athermal arrayed waveguide grating device. How do these compare with a 100 GHz regular AWG from the same manufacturer?
9. Calculate the length of the coupling region, L, for a directional coupler that splits the incoming light in a ratio of 98%–2% between output waveguides 1 and 2. Assume the coupling coefficient k is known.
10. Discuss advantages of polymers as materials used in the fabrication of planar optical waveguides.
11. Describe the fabrication process of polymer waveguides.
12. What is a digital optical switch, and how does it compare to a Mach-Zehnder interferometer–based switch?
13. Calculate the temperature change needed to tune the wavelength of a tunable laser across a range of 20 nm using a polymer Bragg grating with $dn/dt = -2 \times 10^{-4}\ K^{-1}$. The grating has a period of 0.8 μm.
14. Discuss advantages and disadvantages of waveguides based on silicon-on-insulator, III-V semiconductors, silica-on-silicon, and polymers.
15. Research three companies that manufacture silica-on-silicon PIC devices, and give examples of the devices they commercialize.

REFERENCES

Bruckner, V. 2014. To the use of Sellmeier formula. Elements of Optical Networking: Basics and Practice of Optical Data Communication. Wiesbaden, Germany: Vieweg+Teubner Verlag, http://www.springer.com (accessed June 29, 2015).

Hunsperger, R.G. 2009. Integrated Optics, Theory and Technology. New York: Springer.

Kamei, S., Y. Inoue, T. Shibita, and A. Kaneko. 2009. Low-loss and compact silica-based athermal arrayed waveguide grating using resin-filled groove. IEEE Journal of Lightwave Technology 27(17): 3790-3799.

Kim, K., J. Seo, and M. Oh. 2008. Strain induced tunable wavelength filters based on flexible polymer waveguide Bragg reflector. Optics Express 16(3): 1423-1430.

The National Center for Optics and Photonics Education. 2013. Fundamentals of Light and Lasers, 2nd ed. Waco, TX: The National Center for Optics and Photonics Education.

Oh, M., K. Kim, W. Chu, J. Kim, J. Seo, Y. Noh, and H. Lee. 2011. Integrated photonic devices incorporating low-loss fluorinated polymer materials. Polymers 3(3): 975-997, doi: 10.3390/polym3030975.

Oh, M., W. Chu, J. Shin, J. Kim, K. Kim, J. Seo, H. Lee, Y. Noh, and H. Lee. 2016. Polymeric optical waveguide devices exploiting special properties of polymer materials. Optics Communications 362: 3-12, doi: 10.1016/j.optcom.2015.07.079.

Okamoto, K. 2006. Fundamentals of Optical Waveguides. Burlington, MA: Academic Press.

Saito, T., K. Nara, K. Tanaka, Y. Nekado, H. Hasegawa, and K. Kashihara. 2003. Temperature insensitive (athermal) AWG modules. Furukawa Review 24: 29-33, https://www.furukawa.co.jp/review/fr024/fr24_06.pdf (accessed June 29, 2016).

Selviah, D., Polymer Wave Guide Optical Interconnect Manufacturing. University College London, http://discovery.ucl.ac.uk/19094/1/19094.pdf (accessed May 22, 2016).

Swatowski, B. W., C. M. Amb, W. K. Weidner, R. S. John, and J. D. Mitchell. Advances in Manufacturing of Optical Silicone Waveguides High Performance Computing. Dow Corning, https://www.dowcorning.com/content/publishedlit/IEEE_AVFOP_Presentation.pdf (accessed June 29, 2016).

Weissman, Z. and A. Hardy. 1993. Modes of periodically segmented waveguides. IEEE Journal of Lightwave Technology 11(11): 1831-1838.

Wooten, E. L., K. M. Kissa, A. Yi-Yan, E. J. Murphy, D. A. Lafaw, P. F. Hallemeier, D. Maack, D. V. Attanasio, D. J. Fritz, G. J. McBrien, and D. E. Bossi. 2000. A review of lithium niobate modulators for fiber-optic communications systems. IEEE Journal of Selected Topics in Quantum Electronics 6(1): 69-82.

Integrated Photonics Circuits and Systems

Module 5

of

Integrated Photonics

OPTICS AND PHOTONICS SERIES

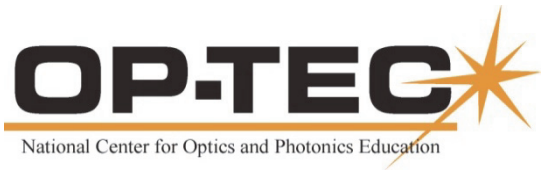

This material was created under Grant # 1303732 from the Advanced Technological Education division of the National Science Foundation. Any opinions, findings, and conclusions or recommendations expressed in this material are those of the author(s) and do not necessarily reflect the views of the National Science Foundation.

For more information about the text or OP-TEC, contact:

Dan Hull
PI, Executive Director, OP-TEC
316 Kelly Drive
Waco, TX 76710
(254) 751-9000
hull@op-tec.org

Taylor Jeffrey
Curriculum Development Engineer
316 Kelly Drive
Waco, TX 76710
(254) 751-9000
tjeffrey@op-tec.org

Published and distributed by
OP-TEC
316 Kelly Drive
Waco, TX 76710
254-751-9000
http://www.op-tec.org/

ISBN 978-0-9903125-9-8

CONTENTS OF MODULE 5

Module 5
Integrated Photonics Circuits and Systems

INTRODUCTION

Previous modules introduced planar optical waveguides and fundamental PIC devices based on the material platforms silicon-on-insulator, III-V semiconductors, silica-on-silicon, lithium niobate, and polymers. This final module presents subsystems obtained by combining several PIC devices. These subsystems have applications in telecommunications, data center processing, sensing and other areas. The level of integration of multiple functions in the same chip in these subsystems varies depending on the material platform used and the number of functions. Some are monolithically integrated, while others are based on separate chips connected by optical fibers or directly attached to each other. PIC systems are expected to continue grow at a very high rate because they offer significant improvements in size, power consumption, reliability, and cost.

PREREQUISITES

OP-TEC's *Fundamentals of Light and Lasers Course*

OP-TEC's *Integrated Photonics: Modules 1–4*

OBJECTIVES

Upon completion of this module, the student should be able to:

- Describe subsystems of integrated PIC devices used in telecommunications and data communications:
    - Wavelength division multiplexing transmitter and receiver
    - Reconfigurable optical add/drop multiplexer (ROADM)
    - Transceiver
- Describe PICs used for sensing applications:
    - Biosensors
    - Lab-on-a-chip applications

- Discuss micro-electro-mechanical systems (MEMS), micro-opto-electro-mechanical systems (MOEMS), and their applications
- Discuss advantages offered by PIC devices and systems

BASIC CONCEPTS

PIC Subsystems Used in Telecommunications

Wavelength Division Multiplexing Transmitter and Receiver Based on III-V Semiconductors

As described previously, the fundamental components of an optical communication system are the transmitter, transmission medium, and receiver. The role of the transmitter is to impress the data in the form of an electrical signal onto a light source, resulting in pulses of light that are sent over the optical fiber serving as the transmission medium. The transmitter thus requires, at a minimum, a driver circuit and an optical source—usually an LED or a laser, as shown in Figure 5-1. For this transmitter, one stream of data modulates the light wave from the LED/diode laser centered around a single wavelength.

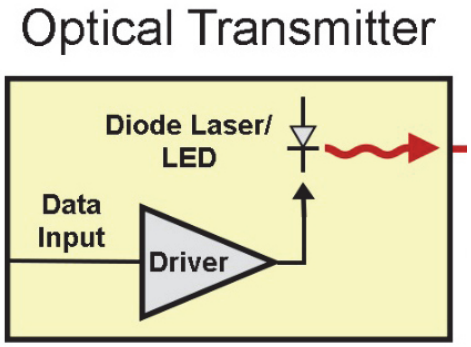

Figure 5-1 *Optical transmitter device*

Current optical transmission systems send multiple data streams, each modulating a different wavelength of light, through the same optical fiber. This method is called *wavelength division multiplexing* (WDM), with a subset called *dense wavelength division multiplexing* (DWDM) in which the frequency separation between channels is on the order of 100 GHz. With this approach, a much larger amount of information can be transmitted simultaneously. For such a system, the transmitter contains multiple light sources, each controlled by its own driver, as well as a multiplexing device that combines the different channels together before launching them in the optical fiber.

While the multiplexer and the light sources can be separate chips connected to each other by optical fibers, it is more advantageous to integrate all the transmitter functions for DWDM systems onto a single PIC. Monolithic integration of the transmitter functions can only be achieved with III-V semiconductors, because these materials are the only ones that have efficient light emitting properties. One example of an advanced transmitter PIC is the indium phosphide based TX LS-PIC (Transmitter Large-Scale Photonic Integrated Circuit), commercialized by Infinera Corporation. The device aggregates 10 channels, each operating at 10 Gb/s, thus achieving a total transmission rate of 100 Gb/s. A schematic of the chip architecture is shown in Figure 5-2.

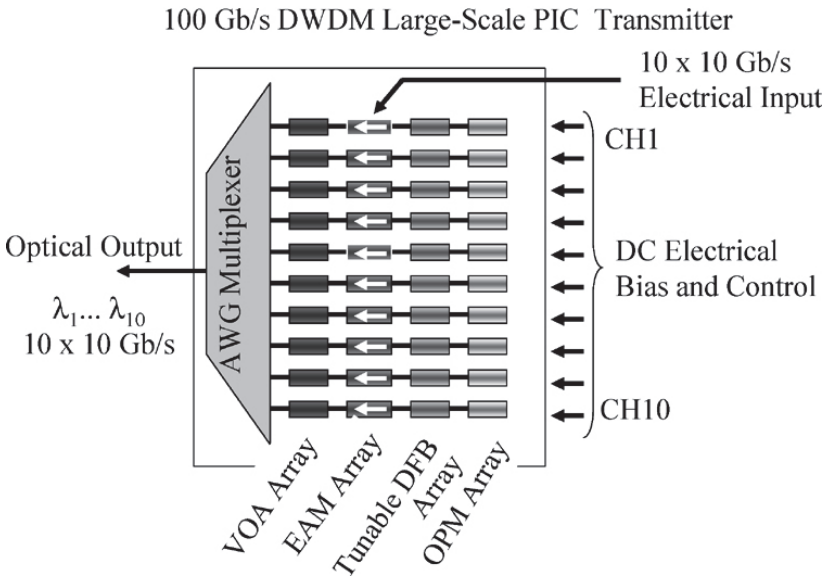

Figure 5-2 *Ten-channel LS-PIC transmitter architecture. Direction of propagation of light is from right to left. Courtesy of Infinera*

Five different types of fundamental devices are used in the TX LS-PIC: tunable distributed feedback (DFB) diode lasers, electro-absorption modulators (EAM), variable optical attenuators (VOA), optical power monitors (OPM), and arrayed waveguide grating (AWG) multiplexer. The principles of operation of these devices were described in previous modules. The TX PIC thus integrates 50 optical functions on the same chip.

The DFBs emit a narrow spectrum of light around a central wavelength that can be tuned over a 300 GHz range. The electro-absorption modulators achieve the high-speed modulation of the light emitted by the diode lasers needed to encode the 10 Gb/s data signals onto the light carriers. The AWG combines the ten signals into one optical output that is sent through the optical fiber. Both the DFBs and the AWG are thermally tuned so that their channels are aligned to each other and to the ITU grid. The channel spacing of the AWG is 200 GHz. Figure 5-3 shows the spectrum of the output light from the transmitter chip.

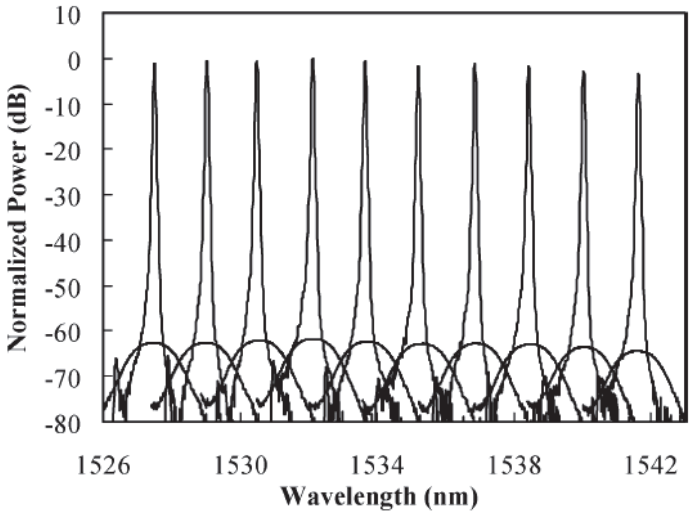

Figure 5-3 *Spectrum of the output light from a transmitter chip, showing the ten channels separated by 200 GHz. Courtesy of Infiner.*

Complementing the essential light emission, modulation, and multiplexing functions of a WDM transmitter, two additional functions enhance its operation. These are power attenuation and power monitoring. The attenuation provided by the VOAs allows control over the output power profile across all channels. It is important for the performance of the entire optical transmission system to have the same optical power in all ten channels. The VOAs can compensate for small power differences between the output powers of the DFB lasers. Figure 5-4 shows the output spectrum of a transmitter PIC in which the VOAs were used to equalize the power level in the ten channels. The output power of the lasers is monitored using the OPMs, which are implemented by monolithically integrating photodiodes into the back of each channel. The OPMs perform optical power monitoring of the diode lasers over the lifetime of the chip.

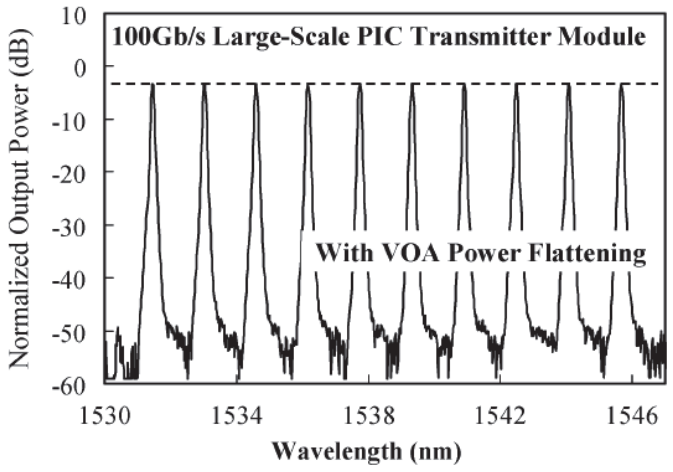

Figure 5-4 *Spectrum of the output light from transmitter chip with equal power in the ten channels. Courtesy of Infinera*

Example 1

In a WDM transmitter with four channels, the diode lasers emit light with the following power levels: P1 = 1.0 mW, P2 = 0.89 mW, P3 = 0.94 mW, and P4 = 0.76 mW. What attenuation settings must be used with the VOAs to flatten the optical power across the four channels?

Solution: The channel with the lowest amount of power will dictate the overall power level. In this case, this is channel 4, for which the VOA setting will be 0.0 dB. For the other channels, the attenuation level can be calculated using equation 2-3 from Module 2, where the Pout and Pin were reversed to obtain a positive attenuation:

Attenuation = 10 x log10(Pin/Pout)

VOA #1: Attenuation = 10 x log10(1.0 mW/0.76 mW) = 1.19 dB

VOA #2: Attenuation = 10 x log10(0.89 mW/0.76 mW) = 0.69 dB

VOA #3: Attenuation = 10 x log10(0.94 mW/0.76 mW) = 0.92 dB

VOA #4: Attenuation = 0.0 dB

The TX LS-PIC is capable of transmitting data at the rate of 100 Gb/s with excellent performance over a total 375 km of optical fiber. This distance was covered in five spans of 75 km each, with an erbium doped fiber amplifier (EDFA) inserted after each span. The performance described above requires a tightly controlled PIC manufacturing capable of producing waveguides with precise dimensions (thickness, width and waveguide spacing) and low propagation loss. Such manufacturing processes are available today for indium phosphide PICs.

At the other end of the transmission system, a receiver converts the optical signal into an electrical signal that is further processed to recover the transmitted information. A basic receiver configuration for a receiver working with one optical wavelength is shown in Figure 5-5. The electric current at the output of the photodiode passes through the transimpedance amplifier (TIA) and the post amplifier for noise filtering and amplification.

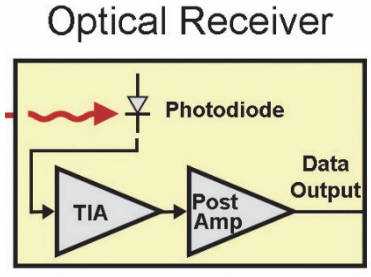

Figure 5-5 *Optical receiver device*

In WDM systems, the multiple light waves of different wavelengths traveling simultaneously through the optical fiber are first separated using a demultiplexer and then converted by

photodiodes into electrical signals. The receiver in this case contains a demultiplexer and arrays of photodiodes, TIAs, and post amplifiers. III-V semiconductors allow for monolithic integration of the demultiplexing and optical detection functions. As an example, we present Infinera's indium phosphide based receiver chip, which is paired with the TX LS-PIC. The monolithically integrated receiver PIC contains a ten-channel AWG with channel spacing of 200 GHz and an array of ten PIN high speed photodiodes. The output spectrum of the receiver is shown in Figure 5-6.

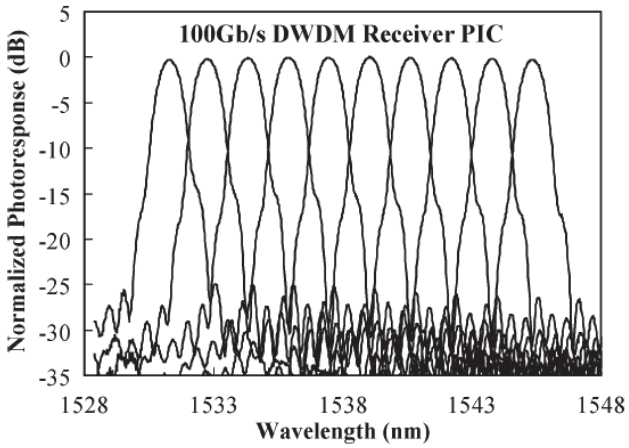

Figure 5-6 *Spectrum of the receiver chip output showing the ten channels separated by 200 GHz. Courtesy of Infinera*

When light reaches the end of transmission, its state of polarization is unknown. For this reason, the AWG demultiplexer in the receiver must be polarization independent. The polarization dependence of an AWG is described by the polarization dependent loss (PDL) parameter described in Module 3. The AWG used in the receiver chip of our example device has a PDL less than 0.4 dB in all ten channels. The adjacent channel crosstalk is better than -25 dB for all channels. The high-speed PIN photodiodes have low dark current values, below 10 nA. As in the case of the transmitter chip, this level of performance for the receiver is possible due to the excellent control of the manufacturing process of active and passive indium phosphide waveguides.

Since the transmitter and receiver subsystems described above became available commercially several years ago, Infinera has continued to integrate more functions on a single indium phosphide chip, recently reaching 600 total functions.

Reconfigurable Optical Add/Drop Multiplexer (ROADM) Based on Silica-on-Silicon and Polymer Waveguides

A point-to-point optical transmission system directly connects an origin to a destination. Such a system can be constructed from the basic components of transmitter, optical fiber, and receiver, as illustrated in Figure 2-3 in Module 2. Today's optical networks have more complicated configurations, some of which were presented in Figure 2-4. These networks feature multiple origins and destinations, requiring traffic to be routed between various parts of the network, with routing taking place at various points called nodes. The routing can be accomplished in several ways. The first approach was to perform the routing in the electrical domain, which

required multiple signal conversions optical-to-electrical (OE) and electrical-to-optical (EO) in the network nodes. These conversions are expensive and should be avoided whenever possible. A better solution in use now consists of routing the optical signals directly, without the need to convert back and forth between electrical and optical domains.

One of the subsystems used for routing optical signals between various paths in an optical network is the *reconfigurable optical add/drop multiplexer* (ROADM). ROADMs are used in DWDM systems with 32 or 40 channels separated by 100 GHz or 50 GHz. ROADMs can be constructed from different types of components, including liquid crystal, micro-electro-mechanical system (MEMS), and planar lightwave circuit (PLC). PLC is the traditional name given to silica-on-silicon and polymer waveguide devices. In this course, we have referred to these components as PICs, but we will use the traditional PLC name in this module. PLCs are an efficient and low-cost technology for ROADMs. Here we describe the basic characteristics and performance of PLC ROADMs.

Several pathways for the optical signals are associated with a network node. One pathway is called *Express*, meaning that the wavelengths taking this path pass through the node and move forward. Other wavelengths can be removed from the forward path by following a *Drop* pathway. These wavelengths get routed to different destinations than the wavelengths traveling in the Express path. At the same time, some or all of the dropped wavelengths can be replaced by corresponding wavelengths coming from other origins. These wavelengths come in through *Add* paths.

The Express, Add and Drop operations can be achieved as follows: an AWG demultiplexer first separates the N channels coming into the node. Typically, N is 32 or 40. In each channel, a 1 x 2 switch determines whether the signal follows the Express pathway or the Add pathway. Continuing on to the Express pathway, a second 2 x 1 switch is used to send forward the signal coming in from either the Express or the Add path. Alternatively, the operations of the two 1 x 2 switches can be performed by a single 2 x 2 switch. Finally, the N channels are multiplexed by another AWG and inserted back into the fiber. The minimum number of components that can be used to construct the ROADM is thus two AWGs and an array of N 2 x 2 switches (or two arrays of N 1 x 2 switches). As was the case with the transmitter chip described previously, the functionality of the subsystem can be enhanced by adding a variable optical attenuator (VOA) and a monitoring photodiode in each channel.

The ROADM described above is called a 2 degree, type I ROADM, and its configuration is illustrated in Figure 5-7. The “2 degree” name refers to the fact that one wavelength is associated with either the Express path or the Add/Drop path. Such ROADMs are used in networks with a ring configuration, where signal traffic circles around a ring. With such a configuration, where traffic passes successively through each node, if equipment in one node stops working, the entire network can be brought down. This can be avoided by adding a second ring with traffic moving in the opposite direction from the first ring. With this addition, if one node fails, traffic can be rerouted through the counter-propagating ring. The two directions are denoted by “East” and “West” in the figure below. Even though the figure shows only one ROADM, there is a second one in each node with the east and west directions reversed.

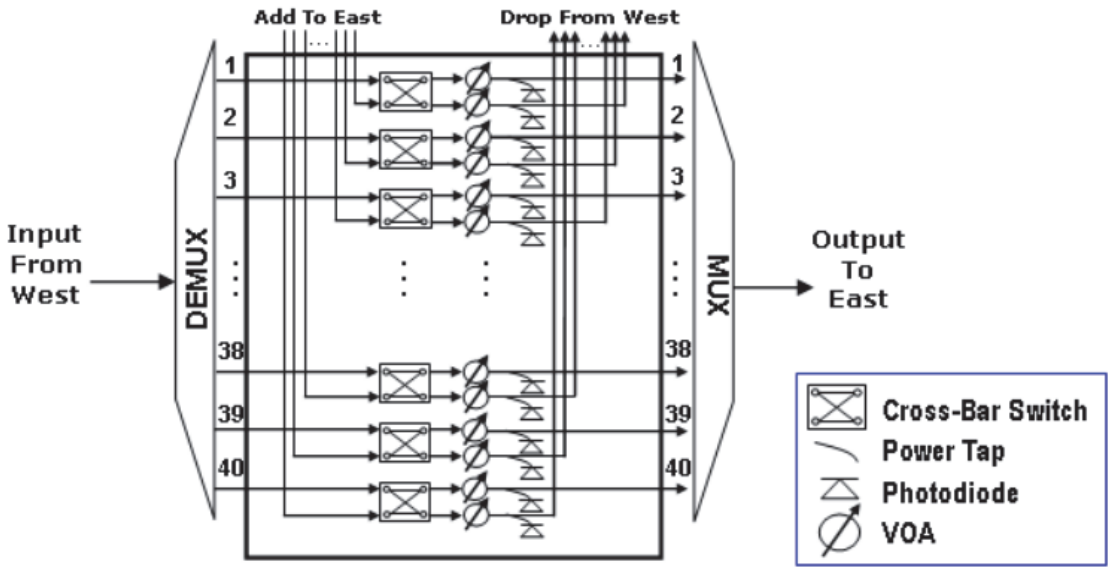

Figure 5-7 *Type I ROADM based on planar lightwave circuit (PLC) components*

The advantages of such a ROADM are the capability to drop or add all N channels, its simplicity, and its low cost. However, there are also some disadvantages associated with such a configuration. Primarily, each Add and Drop port corresponds to a fixed wavelength, dictated by its position relative to the AWG. Manual operations are required to connect a certain wavelength to its specific position.

A low-power-consumption, compact, type I PLC 40 channel ROADM is produced commercially by the company Enablence. To optimize the power consumption, the subsystem uses silica-on-silicon, athermal AWGs that do not require temperature stabilization devices and polymer-based thermo-optic switches and VOAs. The athermal AWGs are flat-top, wide-bandwidth devices for which the center wavelength is maintained within a range of ±0.3pm/°C when temperature varies from -30°C to 70°C. The 1 dB bandwidth of the AWGs is 0.48 nm, and the 3dB bandwidth is 0.65 nm. Figure 5-8 shows the transmission for one of the AWG channels for three different temperatures. No changes are seen in the center wavelength or the filter shape as the temperature changes from the minimum to the maximum value.

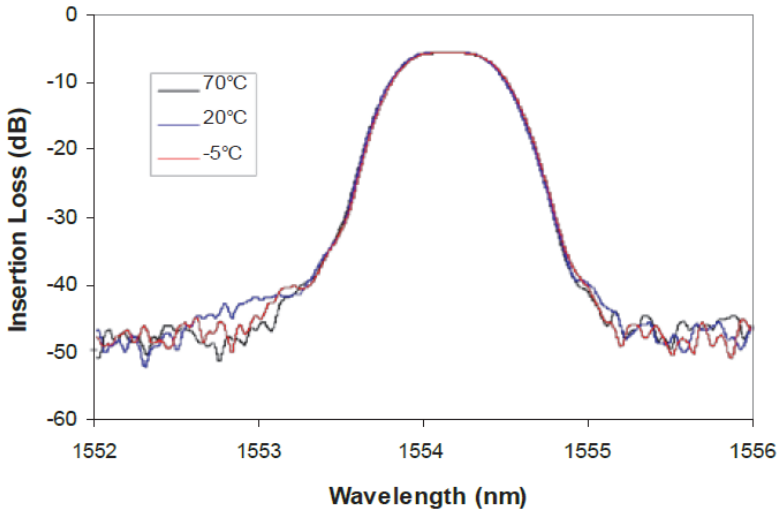

Figure 5-8 *Transmission for one of the athermal AWG channels at three different temperatures. Courtesy of Enablence*

The second low-power technology used to construct the ROADM is based on the use of polymer materials for the thermo-optic switches and VOAs. A basic device configuration used for thermo-optic switches and VOAs is the Mach-Zehnder interferometer (MZI). MZIs can be constructed from all materials used for PICs, including silicon, III-V semiconductors, silica, polymers, and lithium niobate. Due to the high thermo-optic coefficient of polymer materials, it is possible to obtain a very low-power MZI VOA using these materials. The Enablence VOAs use only 1.4 mW to achieve an attenuation of 30 dB and have excellent polarization dependent loss (PDL) performance of less than 0.2 dB for the entire attenuation range. For switches, Enablence is using a different configuration than MZI. Digital optical 1 x 2 switches were described in Module 4; these devices have a power consumption of about 3 mW, with an isolation in the off state of -40 dB. Using these technologies, the Enablence ROADM achieves a worst-case low power consumption of 5W for both the optical and electronic components.

The arrays of polymer switches and VOAs are integrated together in one small chip. Because the polymers have a high thermo-optic coefficient as well as low thermal conductivity, it is possible to have dense arrays of switches and VOAs. The components can be placed close to each other, resulting in a very compact chip. Photodiodes are attached to this chip through flip-chip bonding, avoiding the used of optical fibers in between. For the light to be redirected at 90° toward the photodiodes mounted on top of the chip, 45° mirrors are created in the polymer material by excimer laser ablation followed by metallization of the mirror surface.

The different polymer and silica AWG chips are attached to each other directly through chip-to-chip bonding. This method is similar to the one used to attach a fiber array to a silica-on-silicon chip. The advantages of chip-to-chip bonding are cost reduction, achieved by eliminating the fiber arrays to connect different chips; space reduction, since the fibers require a large minimum bend radius; reduced optical power loss at the interface between fibers and planar waveguides; elimination of the time and expense associated with active alignment of fibers to chip; and increased reliability.

Figure 5-9 shows a subassembly of the Type I ROADM consisting of the chip-to-chip assembly of a silica AWG chip and polymer switch/VOA array.

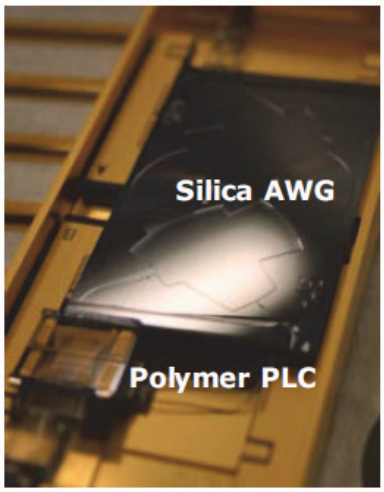

Figure 5-9 *Chip-to-chip bonded silica AWG and polymer switch/VOA array subassembly for type I ROADM. Courtesy of Enablence.*

The ROADM described above has very good performance, with 7 dB total loss for the Express path, VOA dynamic range of 20 dB, channel-to-channel crosstalk of 50 dB, and switch extinction of 50 dB. Another important specification for ROADMs is related to the cascadability of these devices. With each pass through an optical filter such as an AWG, the bandwidth becomes a little bit smaller. If the bandwidth gets reduced too much, then the signal will be distorted at the end of the transmission. The ROADM described above allows for cascading 16 subsystems in a ring network before performance degradation is observed.

Type I ROADMs are successfully used in *ring networks*. However other network configurations, such as *mesh networks*, which have multiple connections between nodes, require higher functionality for ROADMs. Multi-degree ROADMs are needed to provide the capability to switch between multiple Express paths as well as Add/Drop. In addition, the add/drop function should be *colorless*, *directionless*, and *contentionless*. *Colorless* means that the ROADM should be capable of adding or dropping any wavelength to any port, not just the fixed ones that are possible with the Type I sub-system. *Directionless* means that the wavelength could come from any direction, while *contentionless* means that the same wavelength, coming from multiple directions, can be dropped at one port.

These requirements can be described by an M x N ROADM that has M inputs and N outputs or, in other words, M directions and N drop (or add) ports. A much more complex configuration is needed to realize such a ROADM. While different architectures exist to implement it, we again present a solution offered by Enablence based on silica-on-silicon AWGs and polymer switches, VOAs, and tap arrays. The configuration of an M x N ROADM operating with X wavelengths is illustrated in Figure 5-10. The number of components is much higher for this configuration, and some new components are included. The configuration requires M demultiplexer AWGs at the input and N multiplexer AWGs at the output. An M x N switch is required for each of the X wavelengths. The X switches are represented by the block of rectangles in the middle of the figure. Finally, two waveguide shuffling components are inserted between the AWGs and switches. The first waveguide shuffling component reorders the M x X signals such that wavelength λ_1 from all the M demultiplexers go to switch number 1, wavelength λ_2 from all the M demultiplexers go to switch number 2, and so on. On the output side, the second waveguide

shuffling component rearranges the signals such that the correct wavelengths λ_1 to λ_X go to multiplexer number 1 to multiplexer number X, respectively.

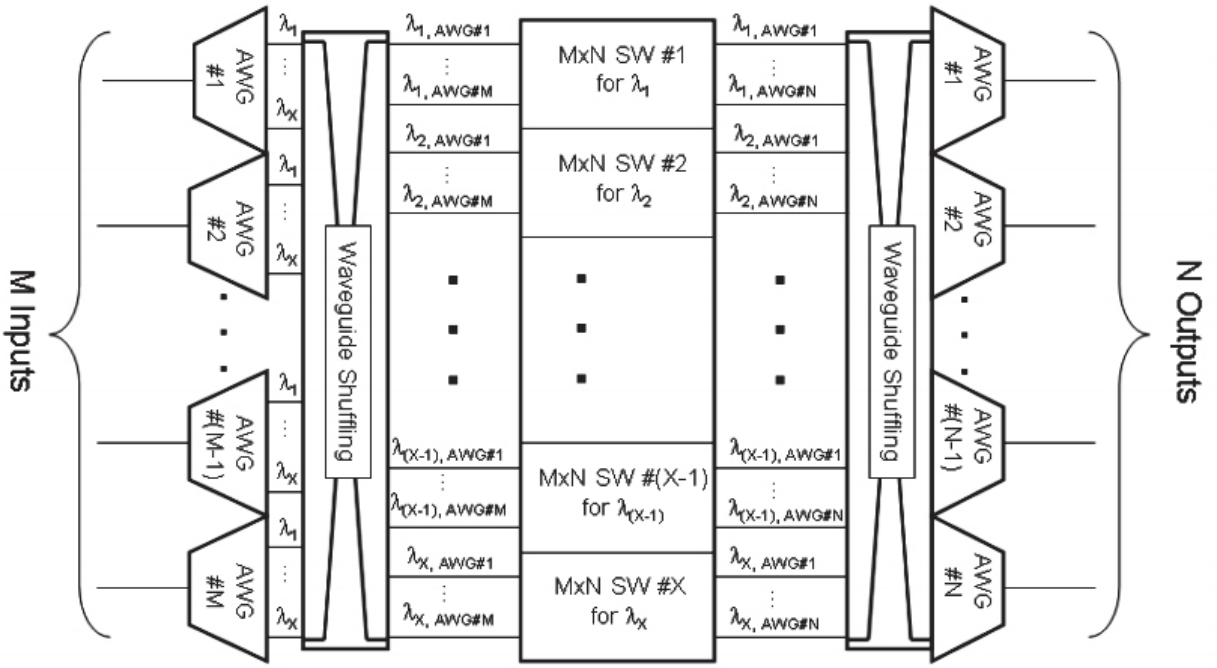

Figure 5-10 *M x N ROADM based on PLC components*

An illustrative example is an 8 x 8, 40 channel ROADM with M = 8 inputs and N = 8 outputs and operating with X = 40 wavelengths. Three types of chips are used to realize this subsystem. The first chip contains eight 40-channel athermal AWGs based on super-high delta waveguides with refractive index contrast of 1.5%. The higher index contrast allows for smaller AWGs and a more compact chip. The AWG chip is shown in Figure 5-11. Its size is 9.0 cm x 3.0 cm.

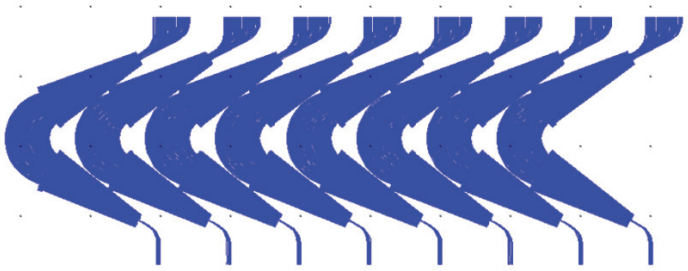

Figure 5-11 *Super high delta silica-on-silicon chip integrating eight AWGs*

The forty 8 x 8 switches are implemented using polymer waveguides, as described in our discussion of the Type I ROADM subsystem. The chip containing the switches also has VOAs for power balancing and taps and photodetectors for power monitoring for each output. The 8 x 8 switches are realized by combining 112 1 x 2 switches. Each 1 x 2 switch is a Y-branch digital optical switch with heaters on both arms that uses only 7.5 mW of electrical power. The polymer waveguides also have a refractive index contrast of 1.5%, making the chip compact and the interfacing with the silica-on-silicon waveguides efficient. The area occupied by the

forty 8 x 8 switches is 9.0 cm x 1.8 cm. Figure 5.12 illustrates the configuration of the switch/VOA/tap and photodetector chip. Once again, 45° mirrors are created at the 8 outputs for directing light to the array of 8 photodetectors flip-chip mounted to the chip.

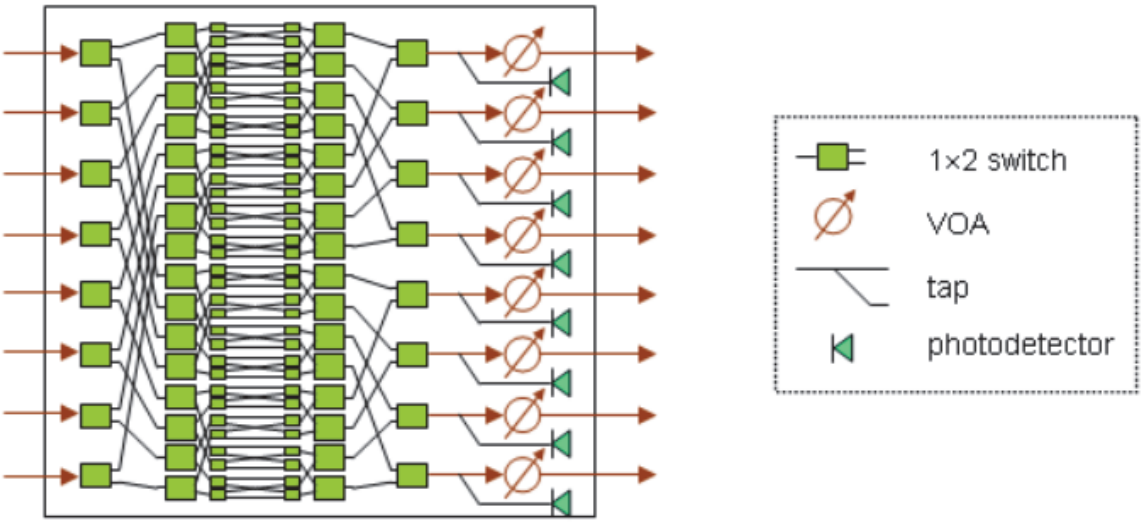

Figure 5-12 *Super-high delta polymer chip integrating switches, VOAs, and taps for photodetectors*

The third component is the waveguide shuffling chip. This chip consists of polymer waveguides that connect a specific input to a specific output. The simplest solution is to use bends to route the waveguides in the desired fashion. This solution, however, results in a large number of waveguide crossings. When two optical waveguides cross each other at a large angle (close to 90°), there is very little crosstalk, meaning that a negligible amount of light gets transferred from one waveguide to the other. The crosstalk is equivalent to a small loss of light in each waveguide. This small loss can be considered negligible when there are only a few crossings in the path of a waveguide. However, in the case of the 8 x 8, 40 channel ROADM, there are 320 waveguides that need to be shuffled (8 inputs x 40 channels). The number of crossings in this case is very large and creates a non-negligible loss of optical power. An alternate solution is to use an interposer polymer chip, which sits on top of and is flip-chip bonded to the main shuffling chip. Light is directed to the interposer and back to the main chip using 45° mirrors. The interposer allows all the waveguides to be shuffled without any waveguide crossing. The length of the interposer is less than 1 cm.

Once again, the silica and polymer chips are chip-to-chip bonded together. Together, the chips occupy a space of only 9.8 cm x 9.0 cm. The overall power consumption is 14.7 W, and the total insertion loss is 18.6 dB, both of which are comparable to those of ROADMs based on other technologies. The small size, low power consumption, very good optical performance, and high reliability of PLC components result in a ROADM subsystem that competes very well with those fabricated using other technologies.

PIC Sub-Systems Used in Data Communications

Optical Transceiver Based on Silicon Photonics (SiP)

A versatile component widely used in data communication and telecommunication systems is the optical transceiver. A *transceiver* combines into one subsystem the transmitter and receiver components described at the beginning of this module. Compact, low-power-consumption transceivers are used in systems ranging from very short reach, such as those used in data centers, to medium and long haul. They operate at data rates up to 100 Gb/s, with higher-rate subsystems currently in development.

The devices incorporated in a transceiver perform both optical and electronic functions. They are as follows: transmitter devices, including drivers and other electronic circuits, diode lasers, modulators, and a multiplexer; receiver devices, including a demultiplexer, photodiodes, and electronic circuits, such as transimpedance amplifiers, post amplifiers, filters, and others.

Several technologies are used to construct optical transceivers, with various levels of integration of the devices into one or more chips. Using silicon photonics/CMOS technology allows for the integration of all optical and electronic devices except the lasers into one single chip. In this module we present an example of a silicon photonics transceiver used for short and medium interconnect applications. The transceiver, produced by the company Luxtera, operates at 40 Gb/s by aggregating four DWDM signals separated by 200 GHz, each transmitted at a rate of 10 Gb/s.

The diode lasers are the only component that is not monolithically integrated in the silicon chip. The four diode lasers used are hermetic, micro-packaged DFB lasers attached to the chip using epoxy. Grating couplers similar to the ones described in Module 2 are used to couple the light from the lasers into the chip.

Light emitted by the diode lasers is modulated using high-speed, free-carrier-effect, on-chip modulators. The modulators are based on Mach-Zehnder interferometers that have p-n junctions in each arm. The modulated signals are combined into one output using a multiplexer. When a small number of channels needs to be multiplexed, in this case four channels, using an AWG is not the most efficient solution. A different device that achieves the same function as the AWG but works well with a small number of channels is the *interleaver*. An interleaver is based on cascading together several unbalanced Mach-Zehnder interferometers, as shown in Figure 5-13. The interleaver is a passive device that is similar in function to an AWG. This is different from the MZI used as a modulator described above, which is an active device. The MZIs used in the interleaver do not have p-n junctions in the arms, but can have a resistor in one of the arms. The resistors are heating elements used to tune the device, as explained below. They are depicted as phase tuners in the figure.

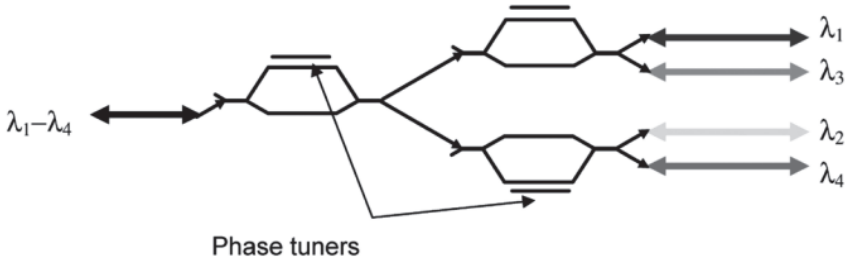

Figure 5-13 *Four channel interleaver with phase tuners in the interferometer arms*

The optical path difference between the arms of each MZI is critical in achieving a low level of crosstalk between channels, as in the case of AWGs. Variations in the manufacturing process can result in effective index differences between the arms that affects the path difference of the interferometers. Temperature variations also influence the path length difference, due to silicon's large thermo-optic coefficient (about 2 x 10^{-4} K^{-1}). These unwanted effects are compensated by introducing a resistor in one arm of each interferometer. Such resistors are implanted in the waveguides. When heated, the effective index of the waveguide is controlled to achieve the necessary path length difference between the arms.

The measured transmission of a tuned interleaver is shown in Figure 5-14. Crosstalk values better than 20 dB are obtained for each of the four channels.

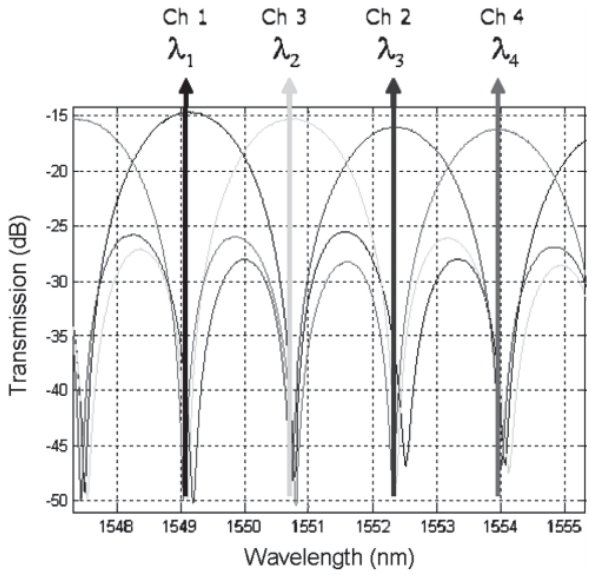

Figure 5-14 *Transmission of the four channel tuned interleaver*

The transmission path ends with the output of the multiplexer being coupled out of the chip using another grating coupler. The receiver portion of the chip starts with light with the four multiplexed wavelengths being coupled from the receiving fiber to the chip by a grating coupler. Light is guided to an interleaver similar to the one above but working as a demultiplexer in this case. The four channels are detected by high-speed germanium photodiodes that are

monolithically integrated in the chip. The electrical signals generated are processed by the transimpedance amplifiers (TIA) and other electronic circuitry.

A microscope image of the monolithically integrated transceiver chip is presented in Figure 5-15. There is space on the chip to add more channels, since the area occupied by the optical and electronic devices is relatively small. Luxtera has used a similarly configured chip to achieve transmission at 100 Gb/s by increasing the data rate in each channel to 25 Gb/s while maintaining the same level of performance. Data rates higher than 100 Gb/s are achievable with this technology.

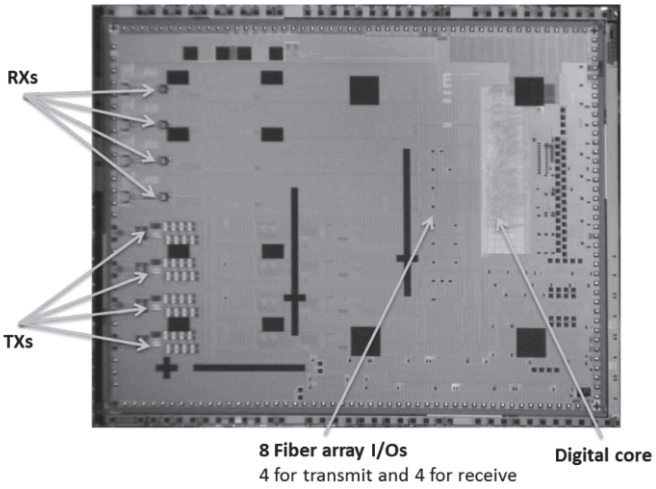

Figure 5-15 *Microscope view of monolithically integrated transceiver chip.* TX *indicates transmitters;* RX *indicates receivers. Courtesy of Luxtera.*

PICs Used in Sensors

Waveguide-Based Photonic Biosensors and Lab-on-a-Chip Devices

Optical sensors based on a variety of platforms, including optical fibers, planar waveguide structures, microresonators, micro-opto-electro-mechanical systems, and others, are in use today. Optical fiber sensors, for example, are commonly used to measure strain, temperature, and pressure and are appropriate to use in harsh environmental conditions. Fiber optic sensors are also used in seismic, sonar, and navigation applications. Integrated optics sensors based on planar waveguides provide the same advantages over their discrete counterparts as those discussed in Module 1: low cost through high volume production, compact size, low power consumption, robustness, reliability, and the potential to integrate all necessary components (sources, detectors, waveguides, and electronics) in one chip.

Biosensors, which detect biological substances, are one of the most important types of sensors. Their application areas extend from medicine and clinical diagnostics to environmental monitoring, chemical and biological warfare surveillance, and food industry, veterinary, and industrial process control. Photonic biosensors based on planar waveguides fabricated on a silicon substrate have been intensively researched in recent decades and have been demonstrated to be capable of detecting biological substances with very high sensitivity in a stable and reliable fashion.

Currently most diagnostic methods are based on specialized techniques performed by trained technicians in a laboratory setting. These are time consuming and expensive because they require other substances to be used during the process. The ideal method would use point-of-care, handheld, portable devices that regular people without specialized training could use right where patients are. Such devices would be extremely helpful all over the world, especially in countries where access to advanced health care is not readily available. Devices such as these are described as *lab-on-a-chip* (LOC).

Most waveguide-based photonic biosensors are evanescent field sensors. They can have several configurations, such as Mach-Zehnder interferometer, ring resonator, or multimode waveguide. In all configurations, a microfluidic channel is created in the cladding of an optical waveguide. A receptor layer is immobilized on the surface of the channel. This is called functionalizing the surface. When the substance under test flows through the microfluidic channel, a chemical reaction takes place between the substance and the receptor layer that changes the refractive index of the waveguide cladding. This change is detected optically and is related to the concentration of the substance under test. A wide variety of patient fluid samples can be tested, including saliva, blood, serum, urine, tears and cerebrospinal fluid.

Silicon-on-insulator (SOI) ring resonators, such as the ones presented in Module 2, can be used as photonic biosensors. SOI channel (strip) waveguides 220 nm thick and 400 nm or 500 nm wide are used with the racetrack configuration shown in Figure 2-24. The ring radius can be as low as 5 μm. Light with wavelength 1550 nm and single polarization (either TE or TM) is input into the ring. Changes in the waveguide effective index due to the presence of the substance under test result in a shift of the resonant frequency of the ring. This shift is measured, and its value is related to the index change and ultimately the concentration of the substance under test. The sensitivity of this sensor is very high, up to several hundred nanometers per refractive index unit (RIU). It is also possible to test for multiple substances in one measurement.

Another platform for photonic biosensors is based on waveguides with silicon nitride (Si_3N_4) cores and silica (SiO_2) cladding built on a silicon wafer. The core and cladding indices of refraction are 2.00 and 1.46 respectively. The waveguides have a rib (ridge) structure with core thickness around 200 nm, rib height of only a few nanometers (2–5 nm) and width around 4 μm. These waveguides have low propagation losses, of 0.1–0.3 dB/cm. The configuration of the waveguides is shown in Figure 5-16. Visible light of wavelength 632.8 nm (HeNe laser) and one polarization (TE or TM) is used with these sensors.

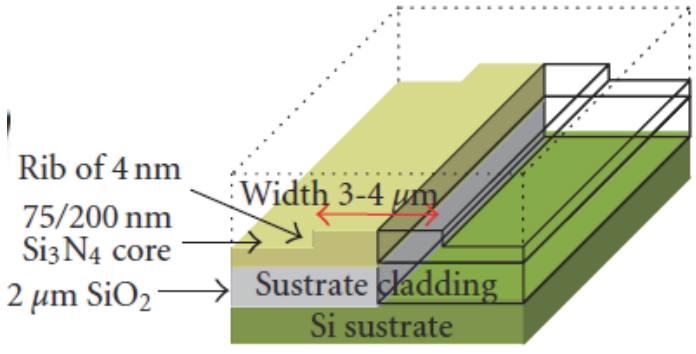

Figure 5-16 *Rib waveguide structure used in photonic biosensor*

A Mach-Zehnder interferometer configuration based on the waveguides above resulted in an extremely sensitive biosensor, capable of detecting refractive index changes on the order of 10^{-7} when TM polarization was used. While the sensitivity of the sensor is exceptional, the devices suffer from variations in the coupling ratio of the couplers that make up the MZI structure, described in Module 2. A very stable coupling ratio is needed to achieve the very high sensitivity of the sensors, but the coupling ratio tends to vary across the silicon wafer.

A second configuration, based on silicon nitride waveguides, is simpler and eliminates the issues with the directional couplers above. This configuration uses a bimodal waveguide, which is a thicker waveguide that supports the propagation of two modes at the 632.8 nm wavelength. Figure 5-17 illustrates the bimodal waveguide and the two sectional photodetector (TSP) used in detection of the output light.

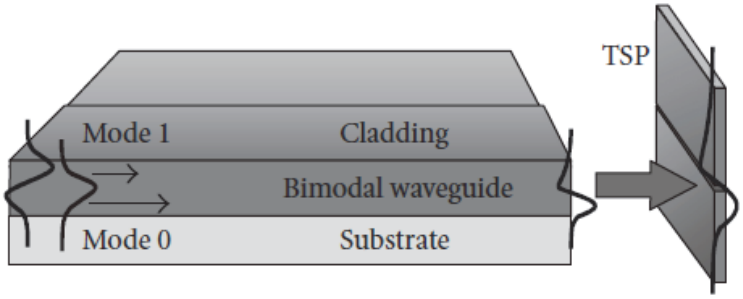

Figure 5-17 *Bimodal waveguide for photonic biosensor*

The propagation of light through the multimode waveguide is based on mode interference. In Module 3, multimode interference (MMI) couplers were described. They split the optical power between two or more output waveguides. In the current application, the interference of the two modes produces a specific pattern for the distribution of the electric field at the end of the bimodal waveguide, as shown in the figure. This pattern is related to the change in the refractive index that takes place when the substance under test flows above the waveguide. A photodiode with two sections is used to detect the pattern. The TSP produces two outputs, V_{up} and V_{down}. From these two voltages, a combined output is calculated using the following equation:

$$S = (V_{up} - V_{down})/ (V_{up} + V_{down}) \qquad (5\text{-}1)$$

The value of the parameter S shows whether there is more power in the top half or bottom half of a photodiode. If there is equal power in both, S will be 0. In experimental measurements with a 1 cm long bimodal waveguide with sensing area 3 mm long, the parameter S varied between 0 and 0.96. The ideal range for S is 0 to 1.

The configuration of the entire sensor is shown on the left side of Figure 5-18. The image on th e right shows a chip with five sensors and grating couplers coupling the light to the chip. The gratings are written directly onto the waveguides. They have a depth of 20–40 nm, periods between 300 nm and 500 nm, and length up to 100 μm.

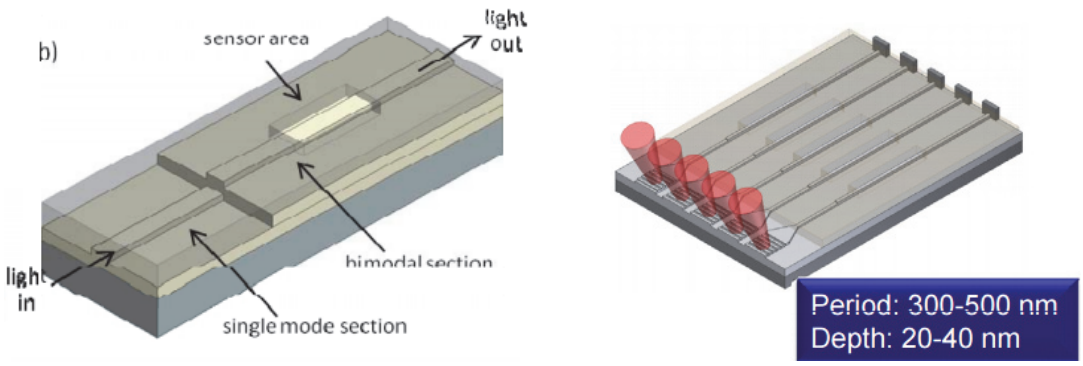

Figure 5-18 *Left: bimodal waveguide based photonic biosensor. Right: five-sensor chip with light coupled to the chip through gratings.*

As mentioned above, the substance under test must flow above the waveguide in order to interact with the evanescent field of the waveguide. Microfluidic channels have to be created in the chip for this purpose, and their method of fabrication must be compatible with the fabrication process of the waveguide sensor. The group that developed the bimodal waveguide sensor created channels with height of 20–100 µm and width of 50–150 µm in a biocompatible polymer (SU-8) layer above the waveguides. The microfluidic channels were perfectly sealed.

The sensor was capable of detecting index changes as low as 3.3×10^{-7} m and is configured much more simply than the MZI based sensor. The group chose this configuration to continue developing a complete lab-on-a-chip device.

A true LOC device needs to integrate the following components into one chip: photonic sensors, flow cells and flow delivery system, light sources and photodetector array or miniaturized CCD camera, processing electronics, and the final package with required firmware and software. This ultimate integration is illustrated in Figure 5-19. While some of these elements have been integrated in the same chip, others, such as sources, photodetectors, and electronics, have not yet been integrated. Silicon photonics has been the key to integration in the past, and it may also be the key to achieving the ultimate integration for a lab-on-a-chip device.

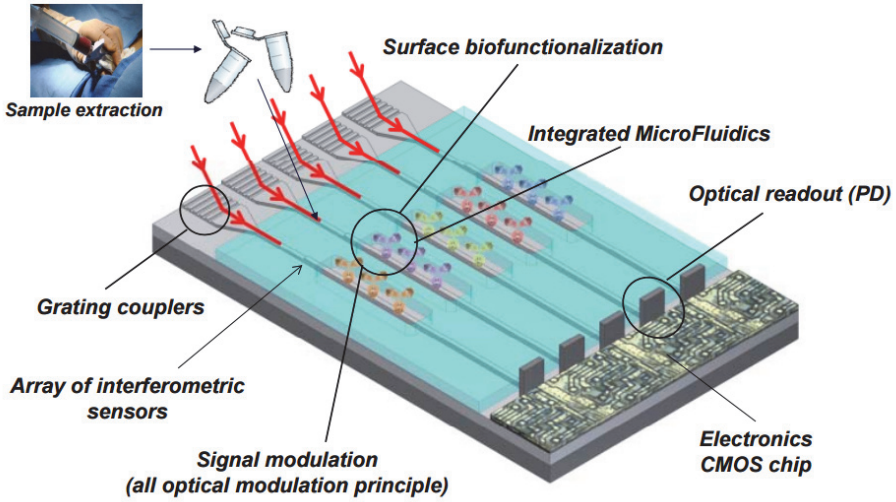

Figure 5-19 *Lab-on-a-Chip biosensor platform*

Micro-Opto-Electro-Mechanical Systems (MOEMS)

MEMS and MOEMS

Micro-electro-mechanical systems (MEMS) are systems that combine mechanical microstructures and electronic devices in the same chip. Micromechanical structures have dimensions less than 1 mm and tolerances less than 1 μm. They are created using micromachining techniques such as bulk micromachining, in which substrate material is removed through selective chemical etching, and surface micromachining, in which material is deposited and patterned using a mask.

MEMS devices generally fall into two categories: sensors and actuators. Sensors are devices that enable the detection or measurement of a certain property, while actuators have moving parts that make it possible to create motion. Examples of MEMS sensors include length, pressure, vibration, voltage, and temperature sensors. Examples of MEMS actuators include micromotors, switches, scanners, interferometers, and voltage generators.

Some very successful commercial MEMS sensors are the integrated pressure sensor and the accelerometer. The pressure sensor is widely used in automobile engines, environmental monitoring, and blood pressure sensing. Accelerometers are now ubiquitous components found in cell phones, personal fitness devices, and other consumer electronics. They are also used to measure acceleration in vehicles and vibration in cars, machines, buildings, and safety installations.

The most common material used in the fabrication of MEMS is silicon, due to its wide availability, low cost, ease of fabrication, and good mechanical properties. Sensor and actuator MEMS are configured based on several elements, such as thin membranes, cantilever beams, and torsion plates.

The thin membrane used in MEMS is a thin layer of semiconductor material supported only at its edges. The membrane will deflect and bend in response to a force or pressure applied to it. By measuring the amount of deflection, it is possible to determine the force or pressure applied. If the force or pressure is applied through electrical or magnetic means, the membrane acts as a transducer converting the electrical or magnetic energy into mechanical motion. The motion can be used to move a surface, in which case the device is an actuator. The membrane can also vibrate and has a characteristic resonant frequency.

A *cantilever beam* is a bar of material that is fixed at one end but is free to deflect at the other end. A force can be applied to the cantilever beam either concentrated in one point or distributed along the beam. The cantilever will respond to the force by deflecting. Figure 5-20 depicts a cantilever beam of length l, thickness t, and width w. A force F is applied at its end.

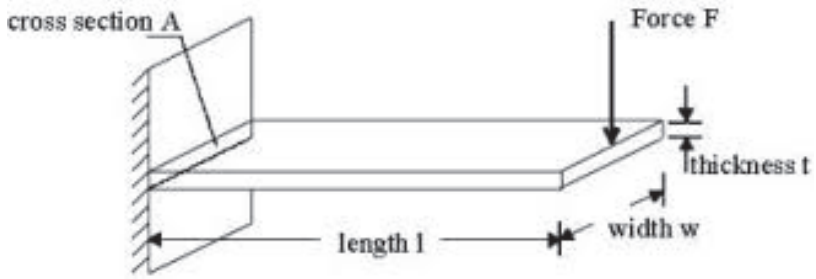

Figure 5-20 *Illustration of cantilever beam*

As with the thin membrane, we can determine the applied force by measuring the beam's deflection. The device acts as a sensor in this case. If the cantilever beam is deliberately moved under the action of the force, the element acts as an actuator.

A torsion plate is a thin plate of semiconductor material supported by small beams at two points. The beams supporting the plate form torsional springs that allow the plate to rotate through an angle without snapping off. The plate can be made to rotate by application of an electric or magnetic field.

Optical elements can be integrated with micromechanical and electronic elements in the same chip through a similar fabrication process as the one used for PICs. In this case, we have MOEMS or *micro-opto-electro-mechanical systems*. The acronym MEMS often includes MOEMS, since MEMS is easier to use. Examples of optical elements constructed this way are microlenses, micromirrors, couplers, filters, and beam splitters. Microlenses with a cylindrical shape have been fabricated directly on the emitting surface of a diode laser. The microlens converts the elliptical shape of the beam emitted by the laser into an almost circular shape that matches the mode of optical fibers much better.

The pressure sensor mentioned above uses a thin circular silicon membrane to sense the force or pressure applied to the sensor. The sensor is fabricated by etching a shallow cavity of depth 53 μm and diameter 600 μm in a glass substrate. A layer of silicon is bonded on top of the cavity. The thin membrane is formed by etching the silicon layer down to a thickness of 26 μm. The deflection of the membrane can be sensed using an interferometer with an optical fiber carrying light of wavelength $\lambda = 850$ nm acting as the light source. The sensor measures pressure in the range 0 to 30 psi, with a maximum deflection of $\lambda/8$.

Silicon membranes can also be used to make deformable mirrors (DM). These are devices capable of correcting aberrations in an optical beam. To achieve this, the shape of the membrane must change from a flat surface to a surface with peaks and valleys in various locations. The peaks and valleys are created by a controllable array of electrostatic parallel-plate actuators placed under the silicon membrane. The device is illustrated in Figure 5-21.

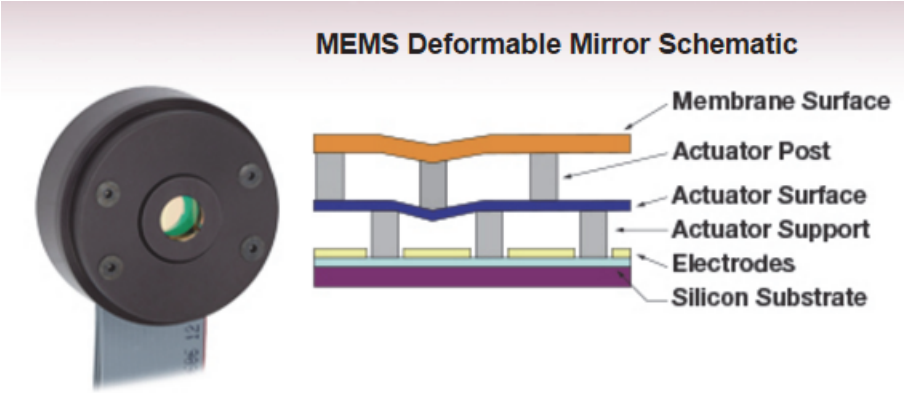

Figure 5-21 *MEMS deformable mirror with a 12 x 12 actuator array. Courtesy of Thorlabs.*

A related application is the steerable micromirror array, with applications in digital display technology and other imaging applications. The number of mirrors in the array can be as high as 2048 x 512, with each mirror independently controlled. An example of a 12-element micromirror array is shown in Figure 5-22.

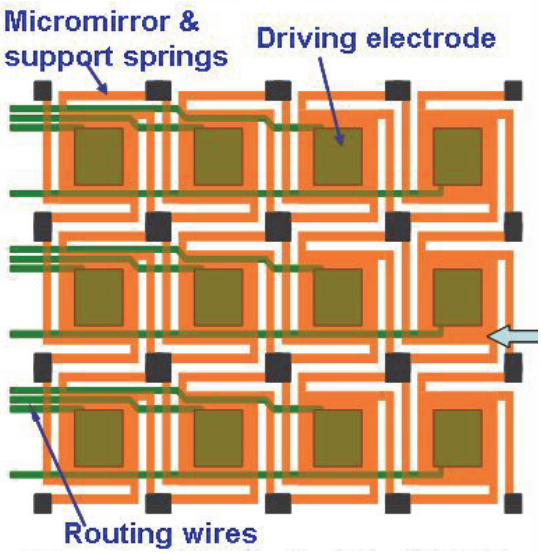

Figure 5-22 St*eerable micromirror array illustration*

Cantilever beam-based MEMS can be used for optical switching applications. Numerous configurations exist for such optical switches. Figure 5-23 illustrates one simple configuration for an on-off switch.

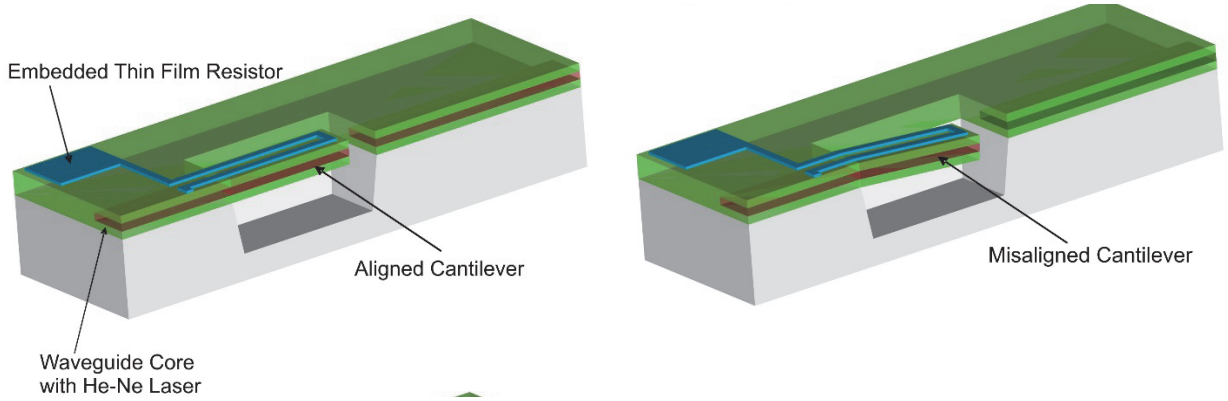

Figure 5-23 *Cantilever beam on-off optical switch*

A light wave of wavelength 633 nm emitted by a helium neon (HeNe) laser propagates in a silicon oxynitride (SiO_xN_y) waveguide formed on a 2.5 cm silicon substrate. The refractive index of SiO_xN_y depends on the relative concentration of oxygen and nitrogen in the chemical formula. This material is used for both the core and cladding layers of the waveguide. The indices of the core and cladding are 1.98 and 1.61 respectively, and the core dimensions are approximately 2 μm x 2 μm. A thin film resistor is deposited on top of the cantilever beam.

When the heater is off, the cantilever is horizontal and the two waveguide segments are aligned, allowing light to pass. The switch is in the ON state. When current is sent through the resistor, the heated cantilever moves down due to the difference in thermal expansion of the materials. In this case, the light path is blocked and the switch is OFF. The free end of the cantilever was displaced a maximum distance of 30 μm when a 25 mA current was applied to the heater.

The cantilever beam is also the structure that accelerometers are based on. Most commonly, the acceleration is measured by the difference between two electrical capacitances induced by the motion of the cantilever arms. The acceleration can also be measured through optical means, where the motion of the cantilever changes the distribution of optical power between two optical waveguides. MEMS and MOEMS are versatile and reliable devices with numerous applications. New devices with higher levels of integration and performance are expected in the future.

SUMMARY

This final module of *Integrated Photonics* built on information about the foundation PIC devices previously introduced to present complex subsystems with applications in telecommunications, data communications, and sensors. This module included almost all material platforms from previous modules, including silicon-on-insulator, III-V semiconductors, silica-on-silicon, and polymers. The high performance, highly integrated subsystems are made possible by the continuous advances in PIC fabrication processes and technologies.

The five modules in this course are intended as an introduction to photonic integrated circuits and their applications. While fundamental devices and systems were presented, the course material is not exhaustive; many other devices and systems exist that could not be included due to size and prerequisite knowledge limitations.

The market for photonic integrated circuits is expected to continue to grow at a phenomenal rate because PICs offer significant improvements in system size, power consumption, reliability, and cost. Silicon photonics technology and monolithically integrated indium phosphide technology are expected to dominate the market, represented by companies such as Infinera Corporation, NeoPhotonics Corporation, Oclaro, Luxtera, Kotura, OneChip Photonics, and others. The major areas of applications are optical fiber communications, optical sensors, the biomedical field, and in the near future, quantum computing. The future will undoubtedly bring much more in this exciting and growing field.

PROBLEM EXERCISES AND QUESTIONS

1. Explain the role of the transmitter in a WDM optical transmission system, and discuss the devices that make up the transmitter.
2. Describe the Infinera TX LS-PIC devices and their functions.
3. In a WDM transmitter with eight channels, the diode lasers emit light with the following power levels: P1 = 0.95 mW, P2 = 1.25 mW, P3 = 0.88 mW, P4 = 0.75 mW, P5 = 1.0 mW, P6 = 0.67 mW, P7 = 0.96 mW, and P8 = 0.82 mW. What attenuation settings must be used with the VOAs to flatten the optical power across the eight channels?
4. Explain the role of the receiver in a WDM optical transmission system, and discuss the devices that make up the receiver.
5. Describe the Infinera receiver devices and their functions.
6. Explain what a ROADM is, where it is used, and its advantages.
7. Describe the PLC components that make up up a 2 degree, type I ROADM.
8. Explain the solution used by Enablence to reduce the power consumption and the size of the type I ROADM. Include details of the ROADM components.
9. What components are needed to construct an M X N ROADM? Exemplify with the case of a 4 x 4, 32 wavelength ROADM.
10. Explain what a transceiver is and where it is used.
11. Describe the devices used by Luxtera to construct their 40 Gb/s silicon photonics transceiver.
12. Explain what an interleaver is and how tuning can improve its performance.
13. List the desired characteristics of a lab-on-a-chip device.
14. Discuss the principle of operation of a waveguide-based evanescent field biosensor. Include details about the interaction of the substance under test with the mode field of the waveguide.
15. Describe silicon nitride waveguides used in photonic biosensors, and discuss two possible configurations for such sensors.
16. Calculate the output of a bimodal waveguide photonic sensor if the two output voltages are Vup = 250 mV and Vdown = 130 mV.
17. Explain what MEMS and MOEMS are, and give examples of these components and their applications.
18. Research MEMS micromotors and summarize their characteristics and areas of applications.
19. Research and summarize MEMS-based optical switches with different configurations than the one presented in the text.
20. Research two applications of PICs that were not presented in the course, and summarize the types of PICs used and their characteristics.

REFERENCES

Chrostowski, L., S. M. Grist, , S. Schmidt, and D. Ratner. 2012. Assessing silicon photonic biosensors for home healthcare. *SPIE Newsroom*, March 1, doi: 10.1117/2.1201202.004131.

Duval, D., A. B. Gonzales-Guerrero, and L. M. Lechuga. 2012. Silicon photonic based biosensors: The future of lab-on-a-chip diagnostic devices. *IEEE Photonics Society News* 26:4, http://photonicssociety.org/newsletters/aug12/26photo04-Web.pdf (accessed July 11, 2016).

Eldada, L., J. Fujita, A. Radojevic, T. Izuhara, R. Gerhardt, J. Shi, D. Pant, F. Wang, and A. Malek. 2006. 40-channel ultra-low-power compact PLC based ROADM subsystem. *Optical Fiber Communication Conference and Exposition and The National Fiber Optic Engineers Conference*. Technical Digest, Optical Society of America, paper NThC4, doi: 10.1109/OFC.2006.215775.

Fujita, J., R. Gerhardt, T. Izuhara, W. Lin, H. Wei, and B. Grek. 2011. The integration of silica and polymer waveguide devices for ROADM applications. *Proceedings of SPIE* 7942, Optoelectronic Integrated Circuits XIII, 79420N, January 17, doi:10.1117/12.877604.

Hunsperger, R. G. 2009. *Integrated Optics: Theory and Technology*. New York: Springer.

Lechuga, L. 2012. Lab-on-a-chip integration of silicon photonic biosensors for advanced point-of-care devices. Centre d'Investigado en Nanoccencia i Nanotecnologia (CIN2) and Consejo Superior de Investigaciones Científicas (CSIC). http://www.imel.demokritos.gr/minasens/presentations/L.Lechuga.pdf (accessed July 2, 2016).

Marketsandmarkets. 2012. Photonic integrated circuit (IC) & quantum computing market (2012–2022): By application (optical fiber communication, optical fiber sensors, biomedical); components (lasers, attenuators); raw materials (silica on silicon, silicon on insulator). Marketsandmarkets, report code SE 1336, December. http://www.marketsandmarkets.com/Market-Reports/photonic-integrated-circuit-ic-optical-computing-chip-market-881.html (accessed July 5, 2016).

Nagarajan, R., C. H. Joyner, R. P. Schneider, J. S. Bostak, T. Butrie, A. G. Dentai, V. G. Dominic, et al.. 2005. Large-scale photonic integrated circuits. *IEEE Journal of Selected Topics in Quantum Electronics* 11(1): 50-65.

Narasimha A., B. Analui, Y. Liang, T. J. Sleboda, S. Abdalla, E. Balmater, S. Gloeckner, et al. 2007. A fully integrated 4 x 10 Gb/s DWDM optoelectronic transceiver implemented in a standard 0.13 µm CMOS SOI technology. *IEEE Journal of Solid-State Circuits* 42(12): 2736-2744, doi: 10.1109/JSSC.2007.908713.

The National Center for Optics and Photonics Education. 2013. *Fundamentals of Light and Lasers*, 2nd ed. Waco, TX: The National Center for Optics and Photonics Education.

Pinguet, T., P. M. De Dobbelaere, D. Foltz, S. Gloeckner, S. Hovey, Y. Liang, M. Mack, et al. 2012. 25 Gb/s silicon photonic transceivers. *The 9th International Conference on Group IV Photonics (GFP)*, IEEE paper ThC1, doi: 10.1109/GROUP4.2012.6324129.

Rehder G., M. I. Alayo, H. B. Medina, and M. N. P. Carreño. 2007. Electro-opto-mechanical cantilever-based logic gates. *Proceedings of SPIE* 6466, MOEMS and Miniaturized Systems VI, 64660C, January 22, doi: 10.1117/12.699341.

Zinoviev K., L. g. Carrascosa, J. S. del Rio, B. Sepúlveda, C. Dominguez, and L. M. Lechuga. 2008. Silicon photonic biosensors for lab-on-a-chip applications. *Advances in Optical Technologies* 2008, Article ID 383927, doi: 10.1155/2008/383927.

Glossary of Terms

2.5D packaging – the current method of using TSV connections in packaging; requires a silicon interposer between dies for the TSVs to connect the dies, rather than making vertical openings through the dies themselves.

3D packaging – when several dies are stacked on top of one another, using wire bonding to make connections between the die and the package.

Absorption coefficient – a parameter that defines how far light of a particular wavelength can penetrate a material before it is absorbed. It has units of cm^{-1}.

Absorption loss – loss that can occur within the waveguide. It is dependent on wavelength and can be minimized by operating at specific frequencies.

Active alignment – a very precise alignment process used to attach fibers to die, taking into account 6 degrees of freedom, and often using optical power as the metric to determine proper alignment.

Active devices – devices that generate, amplify, or control light.

Add-drop filter – addition or removal of narrow band wavelengths of light from a broader optical signal being carried along a bus waveguide.

Adiabatic taper – a taper which satisfies the low loss requirement for coupling.

All-pass filter – a filter device which allows all frequencies to pass through it, but changes the phase relationship between some frequencies.

Amplified spontaneous emission (ASE) – background noise in a semiconductor optical amplifier (SOA) caused by photons spontaneously emitting in the active medium.

Arrayed waveguide grating (AWG) – a passive device capable of multiplexing and demultiplexing light with different wavelengths, depending on the direction of the propagation of light through the AWG.

Athermal AWG – AWG devices that do not require external elements to keep the device at a constant temperature.

Attenuation – the gradual loss of optical power due to absorption and scattering of light in the transmission medium.

Back-end process – the assembly and creation of photonic integrated circuit (PIC) devices that takes place in environments with less stringent requirements than clean rooms.

Bar state – when power input and power output occur in waveguides directly across from each other in a multimode interference (MMI) coupler.

Bend waveguides – non-straight waveguides, typically circular arcs.

Birefringence – the difference between the two effective indices of refraction for transverse electric (TE) and transverse magnetic (TM) polarizations.

Bragg grating – a structure with periodic variation in the effective refractive index along the waveguide in the direction of the propagation of light.

Bunny suit – a cleanroom suit, worn in environments with controlled levels of contamination.

Channel waveguide – a type of planar waveguide with comparable width and height, defined by the width and height of the core.

Cladding – a material with a smaller index of refraction than the core; can be one or more layers. Cladding is designed to confine the light to the core via total internal reflection.

Coefficient of variation with temperature – the expression of the change in index of refraction with temperature, represented by $\frac{dn}{dt}$ in units of 1/°C or 1/^{o}K.

Constructive interference – when the result of wave interference and superposition is a wave with the maximum possible amplitude. It occurs when the two waves are completely in phase with each other. This is also called the *phase-matching condition*.

Core – a transparent medium through which light can propagate, usually surrounded by cladding.

Coupling – a method of interconnecting two devices to transfer an optical signal, using light waves.

Coupling coefficient – a non-dimensional, variable characteristic of couplers.

Coupling length – the length of the coupling region for which 100% of light transfers to a second waveguide.

Critical angle – the largest angle of incidence for which refraction can still occur.

Cross state – when power input and power output occur in waveguides diagonally across from each other in an MMI coupler.

Crosstalk – unwanted transfer of light between parallel waveguides.

Demultiplexing – a process that separates signals which have been combined using wavelength division multiplexing (WDM).

Deposition – the process through which layers of materials are added to a silicon wafer.

Destructive interference – when the result of wave interference and superposition is a wave with zero amplitude, which occurs when the two waves are completely out of phase with each other.

Detector – a device that processes an incoming optical signal and converts it to an electrical signal.

Die bonding – attaching the die to the frame of the package.

Diode laser – a laser that uses a semiconductor diode as the active medium.

Direct laser writing – a method of fabricating PICs by using a laser to create 2D or 3D patterns inside a host material.

Directional coupler – a passive device with four ports and two parallel waveguides, used to split or combine light.

Dispersion – pulse spreading during transmission, caused by the variation in index of refraction with wavelength of the transmission medium.

Distributed Bragg reflectors – a light reflecting device (mirror) based on Bragg reflection.

Distributed feedback (DFB) lasers – a type of diode laser where the active region has periodic sections of diffraction grating.

Doping – adding other materials to the core to change properties like refractive index.

Double heterostructure configuration – where a laser diode has a layer of low bandgap material sandwiched between two layers of high bandgap material.

Effective refractive index – a number quantifying the phase delay per unit length in a waveguide, relative to the phase delay in vacuum.

Efficiency – the ratio of total optical (or laser) output power to the pump power.

Electroabsorption – when change in a material's absorption coefficient is caused by a controlling signal, usually electric current.

Electro-absorption modulators (EAM) – modulators that change the absorption of a material when an electric field is applied to it.

Electro-optic effect – a change in refractive index due to an electric field applied to a material.

Electrorefraction – when change in a material's index of refraction is caused by a controlling signal, usually electric current.

Etching – a chemical process used to remove portions of the core layer outside the waveguide patterns.

Evanescent field –an oscillating electric and/or magnetic field which does not propagate as an electromagnetic wave but whose energy is spatially concentrated in the vicinity of the source.

Extinction ratio (ER) – the ratio between the maximum output power (when modulator is on) and the minimum output power (when modulator is off).

Fiber array – a line or array of fibers that have been placed in a grooved substrate and are used for input and/or output to PIC dies.

Flip-chip – when the die at the bottom of a stack is turned upside down and connected to the package using solder, eliminating the need for a wire bond from that die to the package.

Free propagation regions (FPR) – areas of the AWG with planar geometry where light enters the AWG or exits the AWG.

Free spectral range (FSR) – the maximum wavelength range that can pass through an AWG without repeating output waveguides.

Front-end process – the creation of PIC wafers that takes place entirely in a clean room environment.

Fundamental mode – the mode corresponding with the greatest angle of incidence for light traveling in the waveguide.

Gain parameter – the ratio of output power to input power, often used to describe amplification.

III-V semiconductor materials – semiconductor compounds made of elements from group III and group V on the periodic table.

III-V semiconductors – binary compound (two element) semiconductors made by combining elements from Group III and Group V on the periodic table.

Indirect bandgap material – a material where photons cannot be directly emitted by electrons due to the alternate momentum of electrons and holes in the conduction band and valence band.

Insertion loss – the ratio of the total power at the output of the device to the input power.

Interference – when two waves interact and their superposition forms a resultant wave that varies between a minimum and maximum value.

ITU grid – wavelengths and frequencies used in wave division multiplexing that have been standardized by the International Telecommunication Union (ITU).

Known good dies – dies that have been tested and proved functional.

Lateral taper – a taper which changes the waveguide width.

Lower cladding – the cladding layer below the core, also called the substrate.

Mach-Zehnder interferometer (MZI) – a device that uses one source of light split into two waves that travel through different pathways before being brought back together and allowed to interfere.

Metallization – the application of thin film *heaters* over certain regions of an optical waveguide to modulate its refractive index.

Modes – the light waves corresponding to solutions of Maxwell's equations, at which angles of incidence light can propagate. Waveguides have a finite number of modes.

Modulation depth (MD) – a parameter that helps characterize modulators. It is the relationship between minimum and maximum power out, and is equal to 1 in an ideal setting.
$MD = (P_{out}^{max} - P_{out}^{min})/P_{out}^{max}$

Modulators – devices used to control beam power in single or multiple device outputs.

Molecular beam epitaxy – a method of thin-film deposition.

Molecular bonding – when two materials bond at the molecular level, due to sharing of electrons in their outer shell.

Monolithic integration – the integration of all components and devices into a single chip or base semiconductor.

Multimode Waveguide – allows for propagation of more than one mode.

Multimode Interference (MMI) coupler – a passive device that is a wide waveguide which allows the propagation of several modes, and is based on interference between the waveguide modes for coupling.

Multiple quantum well (MQW) laser – a laser where the active region includes thin layers of semiconductor materials with alternating bandgaps, smaller than the bandgaps of the surrounding material. MQWs are used to control the emitted wavelength of the laser.

Multiplexing – combining multiple signals.

N-type semiconductor – a material that has an excess of electron charge carriers, which are free negative charge carriers.

Numerical aperture – a measure of the light-gathering ability of an optical waveguide. It is a function of the refractive indices of the core and cladding.

Optical amplifier – a device that boosts the power of optical signals.

Optical fibers – a type of optical waveguide consisting of a cylindrical core surrounded by cladding.

Optical Switches – devices used to control light going to multiple outputs, capable of being "on" or "off", with an output of either full power or zero power, with no values in between.

Optical waveguide – a physical structure that guides and confines light waves.

Passivation – a process that deposits a protective layer over the surface of a wafer.

Passive optical device – an optical component requiring no external power source, like a fiber or lens that can transmit and/or alter an optical beam (signal).

Phonon – a quantum (or quasiparticle) of vibrational energy.

Photodetectors – devices that detect light.

Photolithography – a process used in microfabrication to pattern parts of a thin film of a substrate, which can define the waveguide core geometry using light to transfer the pattern from a photomask onto the substrate.

Photomask – a geometric pattern placed over a layer of photoresist in photolithography. Light shines through the mask and transfers the geometric pattern to the photoresist layer.

Photonic integrated circuit (PIC) – a device that integrates multiple photonic or optical components.

Photoresist – a material sensitive to light and used to form patterned coatings on a surface.

Planar optical waveguides – waveguides based on a rectangular geometry, with the core having a square or rectangular shape.

Plasma dispersion effect – when the concentration of charge-carriers in a material changes, causing changes in both refractive index and absorption coefficient.

PN junctions – when p-type and n-type semiconductors are joined to make a diode, where the electrons jump from the n-material to the p-material and holes jump from the p-material to the n-material.

Polarization maintaining fiber – a special type of fiber that allows only one polarization (either TM or TE) to propagate.

Propagation loss – loss that light experiences as it travels through the waveguide, typically in units of dB/cm.

P-type semiconductor – a material that has an excess of "hole" charge carriers, which are free charge carriers, the same magnitude as an electron's charge, but with a positive sign.

Receiver – a device that processes an incoming electrical or optical signal.

Refractive index contrast – also called the relative refractive index difference. It is the measure of the relative difference in refractive index of the core and the cladding.

Regenerator – a device that converts an optical signal to an electrical signal and then back (also called repeater).

Resonance – when one object (or wave) vibrating causes another object (or wave) to vibrate (oscillate) at greater amplitudes for a predetermined frequency.

Resonant frequency – the natural frequency of an object at which resonance occurs. This frequency is determined by the physical characteristics of the object.

Resonant wavelengths – wavelengths that satisfy the resonant condition and will be amplified during resonance.

Ridge waveguide – a type of planar waveguide with comparable width and height, described by the width, height, and thickness of the ridge layer of the core.

Ring resonator – a filter device that performs operations based on the wavelength of the input light. The simplest set-ups utilize a ring waveguide and a straight waveguide.

Scattering loss – loss that can occur due to volume scattering, surface scattering, and sidewall loss.

Self-imaging – In an MMI coupler, if the phase differences between all modes at the end of the wide waveguide are multiples of 2π, the modes will interfere constructively and the final distribution of the electric field will reproduce the initial distribution at the start of the wide waveguide.

Semiconductor Optical Amplifier (SOA) – a device that creates gain in the active region of the amplifier.

Silica on silicon – refers to devices fabricated from silica and doped silica, created on a silicon wafer.

Silicon-on-insulator (SOI) – a layered silicon and insulator substrate.

Single-mode – a single-mode waveguide allows for propagation of only the fundamental mode.

Slab waveguide – a type of planar waveguide with a very thin core and a much larger width than height, described by the core thickness.

System-in-Package (SiP) – when multiple chips are included in a single module (package).

Through Silicon via (TSV) – a vertical electrical connection (via) passing completely through a silicon wafer or die. TSV's are high performance interconnect techniques to create 3D ICs with higher density.

Thermal TSVs (TTSVs) – TSVs that are used for heat dissipation and thermal management rather than electrical connection.

Thermo-optic effect – a change in refractive index when heat is applied to a material.

Threshold current – the current in a laser diode at which stimulated emission begins.

Total internal reflection (TIR) – a phenomenon where light strikes a medium boundary at an angle larger than the critical angle, and where the index of refraction of the traveling medium is greater than the index refraction of the adjacent medium.

Transceivers – a device capable of transmitting and receiving electrical signals.

Transmission medium (optical) – the material used to transmit data, in the form of optical signals, over a distance.

Transmitter – a device that impresses data in the form of an electrical signal onto a light source.

Transverse electromagnetic wave (TEM) – a traveling light wave in which the electric field and the magnetic field are perpendicular to each other and to the direction of propagation.

Upper cladding – the cladding layer above the core in an optical waveguide.

V parameter – a normalized frequency parameter used to determine if a fiber is single-mode or multimode. Single-mode fibers have a V parameter less than 2.405.

Variable optical attenuator (VOA) – another name for a PIC modulator.

Vertical taper – a taper which changes the waveguide thickness.

Wavelength division multiplexing (WDM) – a process that combines multiple signals of slightly different wavelengths and launches them in the same optical fiber to increase the amount of information transmitted in an optical communication system. AWGs are an important component for WDM.

Wavenumber – the spatial frequency of a wave, often expressed in radians per unit distance.

Wire bonding – a method using thin metal wires to make electrical connections to the die.

Y-branch coupler – splits an optical signal in one waveguide into two copies in different waveguides.

Index

N

O

P

R